GEORGIA INSTITUTE OF TECHNOLOGY — OFFICE OF CONTRACT ADMINISTRATION

PROJECT ADMINISTRATION DATA SHEET

[X] ORIGINAL [ ] REVISION NO. _____

Project No. E-19-640 R5984-0A0 GTRC/GIT DATE 7 / 22 / 85

Project Director: Dr. A.S. Abhiraman School/Lab Chemistry

Sponsor: Office of Naval Research 800 North Quincy Street

Arlington, VA 22217-5000

Type Agreement: SFRC Contract No. N00014-85-K-0636

Award Period: From 6/1/85 To 5/31/89 (Performance) 7/31/87 (Reports)

Sponsor Amount:	This Change	Total to Date
Estimated:	$	$ 218,372.00
Funded:	$ 97,227.00	$ 97,227.00

Cost Sharing Amount: $ 26,264.00 Cost Sharing No: E-19-333 F5984-0A0

Title: Precursor Structure-Fiber Property Relationships in Polyacrylonitrile-Based Carbon Fibers

ADMINISTRATIVE DATA OCA Contact R. Dennis Farmer X4820

1) Sponsor Technical Contact:

L.H. Peebles, Jr., Code 431
Program Manager Non-Metallic Materials
Office of Naval Research
800 North Quincy Street
Arlington, VA 22217-5000

2) Sponsor Admin/Contractual Matters:

Mr. Thomas A. Bryant
Office of Naval Research
Resident Representative
206 O'Keefe Building
Georgia Institute of Technology
Atlanta, Georgia 30332-0490 (404) 881-4374

Defense Priority Rating: _____ Military Security Classification: _____

(or) Company/Industrial Proprietary: _____

RESTRICTIONS

See Attached Government Supplemental Information Sheet for Additional Requirements.

Travel: Foreign travel must have prior approval – Contact OCA in each case. Domestic travel requires sponsor approval where total will exceed greater of $500 or 125% of approved proposal budget category.

Equipment: Title vests with Georgia Tech if acquisition cost is $1,000.00 or more and equipment is specifically identified in contractor's proposal, unless determination regarding vesting is deferred until after acquisition. Property for which determination is deferred shall be identified in Block 27B of DD Form 2222.

COMMENTS:

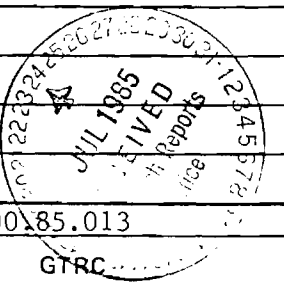

SPONSOR'S I. D. NO. 02.103.000\85.013

COPIES TO:

Project Director
Research Administrative Network
Research Property Management
Accounting
Procurement/GTRI Supply Services
Research Security Services
Reports Coordinator (OCA)
Research Communications (2)
GTRC
Library
Project File
Other Jones

FORM OCA 65.285

GEORGIA INSTITUTE OF TECHNOLOGY
OFFICE OF CONTRACT ADMINISTRATION

NOTICE OF PROJECT CLOSEOUT

Closeout Notice Date 07/18/90

Project No. E-19-640 Center No. R5984-0A0

Project Director ABHIRAMAN A S School/Lab CHEM ENGR

Sponsor NAVY/OFC OF NAVAL RESEARCH

Contract/Grant No. N00014-85-K-0636 Contract Entity GTRC

Prime Contract No. _____

Title PRECURSOR STRUCTURE-FIBER PROPERTY RELATIONSHIP IN POLYACRYLONITRILE-BASE

Effective Completion Date 900615 (Performance) 900830 (Reports)

Closeout Actions Required:	Y/N	Date Submitted
Final Invoice or Copy of Final Invoice	Y	
Final Report of Inventions and/or Subcontracts	Y	
Government Property Inventory & Related Certificate	Y	
Classified Material Certificate	N	
Release and Assignment	Y	
Other _____	N	

Comments _____

Subproject Under Main Project No. _____

Continues Project No. _____

Distribution Required:

Project Director	Y
Administrative Network Representative	Y
GTRI Accounting/Grants and Contracts	Y
Procurement/Supply Services	Y
Research Property Managment	Y
Research Security Services	N
Reports Coordinator (OCA)	Y
GTRC	Y
Project File	Y
Other _____	N
_____	N

NOTE: Final Patent Questionnaire sent to PDPI.

E-19-640

Georgia Institute of Technology
School of Chemical Engineering
Atlanta, Georgia 30332-0100
(404) 894-

DESIGNING TOMORROW TODAY

Reference
3900
Ser 431/85/387
EOY/1131/87/456

"END-OF-THE-FISCAL-YEAR" LETTER

Submitted to

THE OFFICE OF NAVAL RESEARCH

CONTRACT TITLE:	PRECURSOR STRUCTURE - FIBER PROPERTIES RELATIONSHIPS IN PAN-BASED CARBON FIBERS
ONR CONTRACT NUMBER:	N 00014-85-K-0636
ONR WORK UNIT NUMBER:	Y 313177
ONR SCIENTIFIC OFFICER:	DR. L. H. PEEBLES, JR.
PRINCIPAL INVESTIGATOR:	DR. A. S. ABHIRAMAN

SCIENTIFIC RESEARCH GOALS

- To develop a comprehensive knowledge and to provide rational directions for advances in precursor structures and process configurations to extend the range of properties which can be obtained in polyacrylonitrile-based carbon fibers.

- Emphasis is on the chemical and morphological evolution from precursor polymers, through fiber formation, drawing and stabilization, to carbonization. Maximizing the generation and translation of order from precursor fibers to carbon fibers to yield superior mechanical properties (tensile and compressive) is a major goal in this research.

SIGNIFICANT RESULTS OF THE PAST YEAR

(i) High temperature pre-stabilization deformation of precursor fibers which was proposed earlier in this research has been adopted by the industry to yield superior fibers. The maximum temperature in this process is dictated by the onset of rapid reactions and it has been increased significantly by deformation in nitrogen, instead of air.

(ii) The development described in (i) has been extended to multi-step high temperature deformation. The last step in this deformation process has been incorporated in the first zone of a multi-zone stabilization process.

(iii) A detailed mathematical model has been developed for oxidative stabilization. The general model has been modified to yield a workable set of equations. The responses predicted by the modified model are of the same order of magnitude as those observed in practical stabilization processes.

(iv) Two different mechanisms have been identified for the formation of a hollow core in carbonization, one through incomplete stabilization and the other through consolidation of carbonized structure inwards, starting from the skin.

(v) Plasticized melt-spun precursors have been shown to possess the morphological features similar to those of solution-spun precursors. Carbon fibers of at least intermediate properties (400 ksi tensile strength and 35 msi modulus) can be produced from these fibers.

(vi)* The combination of ammonia and air in the stabilization environment has been shown to cause the reactions to occur at lower temperatures and also increase the rate of reactions in the stabilization process.

* Based on Dr. Peeble's earlier studies.

NEXT YEAR'S RESEARCH

1. The computer-controlled multi-zone stabilization line in our laboratories will be used to explore multi-environment, multi-stress stabilization. Stabilization rates and translation of order will be the main aspects of this study.

2. Low concentration polymer blends with polyacrylonitrite will be examined as precursors to yield finer lateral structures in the precursor fibers and carbon fibers. This path will be explored for improving intrinsic compressive properties of carbon fibers.

3. Preliminary experiments in our laboratories have shown that fused multi-filament precursor bundles can be obtained without significant loss of morphological order. This path will be explored for eliminating microbuckling in carbon fibers.

4. Research on multi-stage high temperature deformation in a nitrogen environment will be continued to explore ways for maximizing precursor order.

5. Evolution of structure and properties during carbonization at intermediate temperatures (1400 - 1700°C) will be studied.

PARTICIPANTS

Name	Position
Dr. A. S. Abhiraman	Professor
Dr. W. C. Tincher	Professor
Dr. S. K. Bhattacharya	Post-doctoral Research Fellow
Mr. D. A. Grove	Graduate Student
Ms. T. A. Long	Graduate Student
Mr. G. Bhat	Graduate Student
Mr. P. Desai	Graduate Student

Degrees Granted

Mr. D. A. Grove - M. S.
Ms. T. A. Long - M. S.
MR. G. Bhat - M. S.

ENCLOSURE 2

LIST OF PUBLICATIONS/REPORTS/PRESENTATIONS

1. Papers in Refereed Journals

"Conversion of Acrylonitrile-based Precursors Carbon Fibers - I. Review of the Physical and Morphological Aspects", J. Materials Science, 22, 278 (1987) (with M. K. Jain).

"Conversion of Acrylonitrile-based Precursors to Carbon Fibers - II. Precursor Morphology and Thermooxidative Stabilization", ibid, p. 301 (with M. K. Jain, M. Balasubramanian S. Bhattacharya and M. K. Jain).

"Conversion of Acrylonitrile-based Precursors to Carbon Fibers - III. Thermooxidative Stabilization and Continuous Carbonization", ibid, in press (with M. Balasubramanian and M. K. Jain).

"Exploratory Experiments in the Conversion of Plasticized Melt Spun PAN-based Precursors to Carbon Fibers", Carbon, in Press (with D. A. Grove and P. Desai).

"Mathematical Model of Solid State Thermo-oxidative Stabilization of Acrylic Fibers for Carbon Fibers", ibid, submitted (with D. A. Grove).

2. Presentations

A. Invited

"Evolution of Structure and Properties in the Formation of PAN-based Carbon Fibers", ACS Symposium on Fibers for Composites, Anaheim, CA (1986).

"Processing Influences on Fiber Structure", Fiber Producers Conference, Greenville, SC (1986).

"From PAN-based Precursor Polymers to Carbon Fibers: Evolution of Structure and Properties", SAMPE Symposium on Advanced Fiber Technologies, Anaheim, CA (1987). Published in SAMPE Series, 32, 945 (1987).

"Carbon Fibers - Production and Properties", PIA Conference on Advances in Synthetic Fibers, Atlanta, GA (1987).

"Fundamental Research Needs in Textile Materials: Science, Engineering and Technology", A Focus Paper at the NSF Planning Workshop on Research Needs in Fiber, Textile and Related Industries, Washington, D.C. (1987).

"High Performance Fiber Formation", Spotlight on Research at Georgia Tech: Advanced Materials and Composites, Atlanta, GA (1987).

"Fundamental Aspects of Conversion of PAN-based Precursors to Carbon Fibers". Gordon Research Conference on Fiber Science, New Hampshire (1987).

"Plasticized Melt Spun PAN-based Precursors for Carbon Fibers", Invited Poster, Gordon Research Conference on Fiber Science, New Hampshire (1987).

B. Contributed

"Order Enhancing Deformation of PAN-based Precursors" XVIII Biennial Conference on Carbon, Worcester, Mass. (1987) (Extended Abstracts, p. 13) (With S. K. Bhattacharya, G. Bhat and V. Daga).

"Mathematical Model of Oxidative Stabilization" ibid (Extended Abstracts, p. 34) (With D. A. Grove)

"Plasticized Melt Spun Acrylic Precursors for Carbon Fibers", ibid, Poster Session (With D. A. Grove and S. K. Bhattacharya).

ENCLOSURE 3: LIST OF AWARDS

Name of Person Receiving Award	Recipient Institution	Name of Award	Sponsor of Award
A. S. Abhiraman (Research by D. A. Grove)	Georgia Tech	Thesis Advisor - Outstanding Research Contribution	Sigma Xi - Georgia Tech Chapter
A. S. Abhiraman (Research by U. S. Agarwal)	Georgia Tech	Thesis Advisor - Outstanding Research Contribution	Sigma Xi - Georgia Tech Chapter
P. Desai*	Georgia Tech	Outstanding Student Paper	Fiber Society
P. Desai	Georgia Tech	Best Student Paper	SPE - Southern Section
A. S. Abhiraman*	Georgia Tech	Distinguished Achievements in Fiber Science	Fiber Society

* To be awarded in November, 1987

FY 89 End of Fiscal Year Letter
(01 Oct 1988 - 30 Sep 1989)

3900
SER 1131/260
EOY/1131/89/283

ONR CONTRACT INFORMATION

Contract Title: Precursor Structure - Fiber Property Relationships in Polyacrylonitrile-Based Carbon Fibers

Performing Organization: Georgia Institute of Technology

Principal Investigator: A.S. Abhiraman

Contract Number: 89-J-1855

R & T Project Number: 43131N

ONR Scientific Officer: L.H. Peebles

A. DESCRIPTION OF THE SCIENTIFIC RESEARCH GOALS

To identify appropriate mechanisms for advances in carbon fiber formation through a fundamental study of material and process interactions. Of particular interest: (i) identifying and achieving appropriate morphological features in carbon fibers to realize the optimum combination of tensile and compressive strengths and (ii) effecting more rapid oxidative stabilization while ensuring maximum transfer of order from the precursor fiber to carbon fibers.

B. SIGNIFICANT RESULTS IN THE PAST YEAR

(i) Presence of ammonia in the oxidative stabilization environment has been shown to effect a significantly more rapid stabilization, especially in precursors which do not contain any acid comonomers. The accelerating effect of ammonia also extends to fibers from PAN homopolymer. Extensive morphological and chemical studies suggest this effect to be a combination of *plasticization of the solid state structure of the precursor fibers* and *interaction of NH_3 with the nitrile group of PAN to initiate nitrile polymerization.*

(ii) Although NH_3 has a significant accelerating effect on stabilization, presence of oxygen in the environment is essential for carrying the fiber to the state necessary for cohesive carbonization.

(iii) Plasticized melting and recrystallization studies with NH_4OH indicate the possibility of low temperature plasticized extrusion of PAN-based precursor fibers.

(iv) Preliminary results from a study of the evolution of mechanical properties in a carbonization process (at 1200°C) indicate that, while tensile strength evolves monotonically to an asymptote, the compressive strength might exhibit a maximum as a function of time of carbonization. The validity of this observation is being examined through an extensive evaluation of these properties.

C. PLANS FOR NEXT YEAR'S RESEARCH

(i) Influence of the morphological and chemical effects of NH_3 in stabilization on the corresponding features and the mechanical properties of carbon fibers will be examined.

(ii) The phase diagram for PAN-NH_3-H_2O system will be established to determine if low pressure, i.e., below the boiling point of the mixed solvent, extrusion of acrylic precursor fibers is feasible.

(iii) The evolution of mechanical properties in steady-state carbonization processes will be

examined, especially to determine the location of maximum compressive strength and the corresponding morphological features.

(iv) A major problem in investigations of the conversion of acrylic precursors to carbon fibers arises from the absence of appropriate techniques, or combination of techniques, for a consistent evaluation of orientational and crystalline order at different stages of the process. Application of solid-state NMR techniques, which are being refined at Georgia Tech for other synthetic fibers, will be explored for this purpose.

D. LIST OF PUBLICATIONS/REPORTS/PRESENTATIONS

1. Papers Published in Refereed Journals

   A.S. Abhiraman, Gajanan Bhat, F.L. Cook, L. Peebles, "New Aspects in the Stabilization of Acrylic Fibers for Carbon Fibers," *Carbon*, in press.

2. Non-Refereed Publications and Published Technical Reports

   A.S. Abhiraman, G. Bhat and V. Daga, "Multi-zone Deformation and Stabilization of Acrylic Precursors for Carbon Fibers," *Proceedings of the XIX Biennial Conference on Carbon*, University Park, PA, 258 (1989).

   A.S. Abhiraman, G. Bhat, L.H. Peebles and F.L. Cook, "New Aspects in the Stabilization of PAN-Based Precursors of Carbon Fibers," *Proceedings of the XIX Biennial Conference on Carbon*, University Park, PA 252 (1989).

3. Presentations

   (a) Invited

   "Formation, Structure and Properties of Carbon Fibers," Air Force Materials Lab., Wright Patterson Air Force Base, Dayton, OH, 1988.

   A series of lectures on fundamental aspects of polymerization, rheology, processing and structure-property relations in fiber formation, presented at AKZO Research Center, Arnhem, The Netherlands, 1988.

   "High Performance Carbon and Ceramic Fibers for Composites," Spotlight on Research at Georgia Tech for the Industrial Research Institute, Atlanta, GA, 1988.

   (b) Contributed

   "Random Walks Through Polymers," "What Have We Done Lately in Polymers?" Seminar Series, Georgia Tech, 1989.
   Two papers listed under Non-Refereed Publications were presented at the XIX Biennial Conference on Carbon.

4. Books (and sections thereof)

"Precursor Structure - Fiber Property Relationships in Polyacrylonitrile-based Carbon Fibers," *Advances in Chemistry Series - Composites*, T.L. Vigo (Editor), American Chemical Society (to appear).

E. List of Honors and Awards

Name of Person Receiving Award	Recipient's Institution	Name, Sponsor and Purpose of Award
Bruce Wade	Georgia Tech	Best Paper Award, Student Paper Competition Fiber Society

F. PARTICIPANTS AND THEIR STATUS

Dr. Labone Moeti, post doctoral fellow, left Georgia Tech to join University of Florida in the Fall of 1988.

Dr. N. Venkatasubramanian, post doctoral fellow.

Vijay Daga, received Master's of Science in Chemical Engineering in June, 1988; now working for Raychem, Richmond, CA.

Sundaravel Damodaran, PhD candidate, Multidisciplinary Graduate Polymer Program, Georgia Tech.

Gajanan Bhat, PhD candidate, Multidisciplinary Graduate Polymer Program, Georgia Tech, to complete degree early 1990.

Bruce Wade, PhD candidate, Multidisciplinary Graduate Polymer Program, Georgia Tech.

Dr. Steve Warner, Associate Professor, School of Materials Engineering

Dr. Prashant Desai, Assistant Professor, School of Textile and Fiber Engineering

Dr. A.S. Abhiraman, Professor, School of Chemical Engineering

G. OTHER SPONSORED RESEARCH DURING FY89

"Formation, Structure and Properties of Boron Nitride Fibers from Polymer Precursors," sponsored by Office of Naval Research, $99,976 for 1989, start date 3/1/89.

"Fundamental Study of Compressive Strength Development in PAN- Based Carbon Fibers," sponsored by Air Force Office of Scientific Research, $75,000 annually, start date 9/1/88.

H. SUMMARY OF FY89
PUBLICATIONS/PATENTS/PRESENTATIONS/HONORS/PARTICIPANTS

Papers Submitted to Refereed Journals (and not yet published): 1 (accepted)

Papers Published in Refereed Journals:

Books (and sections thereof) Submitted for Publication: 1 (accepted)

Books (and sections thereof) Published:

Patents Filed: 1

Patents Granted:

Invited Presentations at Topical and Scientific/Technical Society Conferences: 2

Contributed Presentations at Topical and Scientific/Technical Society Conferences: 2

Honors/Awards/Prizes: 1

Non-Refereed Publications and Published Technical Reports: 2

Number of Graduate Students: 3

Number of Post Docs: 1

JOURNAL OF MATERIALS SCIENCE 22 (1987) 301–312

Conversion of acrylonitrile-based precursors to carbon fibres

Part 2 *Precursor morphology and thermooxidative stabilization*

MUKESH K. JAIN*, M. BALASUBRAMANIAN, P. DESAI, A. S. ABHIRAMAN‡
Georgia Institute of Technology, Atlanta, Georgia 30332, USA

The progress of stabilization of two compositions of acrylic fibres with various orientations has been followed by a variety of techniques. The thermooxidative treatments for stabilization have been carried out in a continuous process and also in a batch process under free shrinkage, constant length and constant tension conditions. The morphological model of acrylic fibres consists of an alternating sequence of laterally ordered and laterally disordered regions along the fibre direction. This structure is consistent with the observations based on small-angle X-ray scattering of copper-impregnated precursor fibres and thermomechanical response, thermal stress development, calorimetry, wide- and small-angle X-ray scattering and sonic modulus measured at different extents of stabilization. Lateral as well as orientational order in these fibres can be increased markedly through a high-temperature deformation process prior to stabilization. An increase in perfection and extent of order is observed in the early stages of stabilization. There is also a simultaneous decrease in the orientation of the disordered phase at this stage and the extent of this decrease depends on the axial constraints imposed on the fibre. Little difference in the rate of stabilization is observed as measured by density or oxygen uptake for fibres with different extents of orientation, lateral order or restraint. Fibres containing itaconic acid, a stabilization catalyst, did show an increased rate of stabilization. Inferences have been drawn regarding additional research pertaining to achieving high order in precursor fibres, minimizing orientational relaxation during oxidative stabilization, and the techniques for monitoring the extents of the stabilization treatment and the changes in relevant morphological parameters.

1. Introduction

Thermooxidative stabilization constitutes an important intermediate step in the conversion of acrylonitrile-based precursor fibres to carbon fibres. The precursor fibre is transformed at this stage to yield a structure that can be subjected to the high-temperature carbonization treatment without loss of structural cohesion.

It is well known that the properties of the final carbon fibres are determined by a combination of the nature of the precursor fibres and the physical and morphological rearrangements that occur in the stabilization and carbonization steps. Significant changes in morphology and composition occur at each stage. These changes are much affected by the history of thermal treatments as well as the dimensional constraints stresses imposed during such treatments. Much of the research reported in the literature has been devoted to isolated aspects of the formation of carbon fibres [1] but relatively few attempts have been made to study their development through the stabilization and carbonization stages. Also, the influence of the morphology of the precursor fibres on their stabilization and carbonization behaviour has received little attention. Most of the reported studies involve commercially spun fibres, which restricted them to a limited range of morphology and composition, which were usually unspecified.

A comprehensive experimental facility has been developed in our laboratories to conduct research at all stages of the integrated carbon fibre manufacturing operation. The polymerization and spinning capabilities are an integral part of this research, since they provide the choice of spinning precursor fibres with the desired chemical composition, molecular weight and morphological parameters. We report here the results from a study of the morphology of acrylonitrile-based precursor fibres and the changes introduced in batch and continuous thermooxidative stabilization. The evolution of properties in continuous carbonization is discussed in the third part of this sequence [2]. A comprehensive review of the literature on the physical and morphological changes during the conversion of acrylonitrile-based precursors to carbon fibres is given in Part 1 [1].

2. Experimental procedures

Detailed descriptions of the experimental procedures are given in Jain [3].

*Present address: ALCAN, Arvida Laboratories and Experimental Engineering Center, Jonquiere, Quebec, Canada
‡Author to whom all correspondence should be addressed.

0022–2461/87 $03.00 + .12

TABLE I Conditions for spinning of precursor fibres

Precursor	Polymer solution		Coagulation bath		Drawing conditions		Denier filament
	Concn. (% wt/wt)	Viscosity (P)	Composition (%DMF)	Temperature (° C)	Jet stretch	Draw ratio in boiling H_2O	
I	20	280	60	25	0.7	3	4.1
					0.7	6	2.1
					0.9	3	3.4
					0.7	7.3	1.6
II	17.5	140	60	14	0.7	2.5	3.9
					1.2	3	2.2
					0.7	5	2.2

Spinneret hole diameter was 3 mil (0.003 in.) in all cases.

2.1. Preparation of precursor fibres

Two precursor fibres, I and II, were prepared by solution spinning. For spinning precursor I fibres, a 20% (wt/wt) solution was prepared in dimethyl formamide (DMF) by dissolving commercial acrylic fibres, Orlon 43. For spinning precursor II fibres, a 17.5% (wt/wt) solution of a copolymer of acrylonitrile (AN) and itaconic acid (IA) in the weight ratio of 97/3 (average molecular weight = 131 000 g mol^{-1}, estimated from intrinsic viscosity) was prepared.

The spinning conditions for the two precursors, established to produce fibres of good quality, are given in Table I. The jet stretch and the draw ratio were changed to obtain precursor fibres having different orientations. High-temperature drawing of some of the precursor fibres was performed in order to produce fibres with high orientation and morphological parameters quite different from those produced by drawing in boiling water. Two types of post-spinning high-temperature drawing processes, i.e. hot godet and hot oven, were performed on the hot water (partially) drawn fibres. In the former type of drawing, precursor fibres were drawn directly from the heated feed-godet whereas in the latter type the fibres were first annealed at a relatively low temperature (115 to 130 C) on the feed-godet and then drawn through an oven.

Details of the drawing conditions are given in Table II. The first letter in the sample identification code refers to the precursor type (I for precursor I and II for precursor II). The second and the third terms represent the jet-stretch and the draw ratio (in boiling water), respectively. The last three terms signify the post-spinning, high-temperature plastic drawing conditions such as type of heater (oven or godet), temperature and draw ratio, respectively. The high-temperature draw ratios in these experiments were selected such that the final deniers of the high-temperature drawn fibres matched, within the limits of the experiments, with those of the hot water drawn fibres. This is important if any comparisons in the stabilization and the carbonization behaviour of the two fibres are to be made. The temperatures employed in the hot-oven drawing were the maximum possible for a smooth drawing operation without filament breakages.

2.2. Batch and continuous stabilization

Batch stabilization experiments were carried out in an air circulated oven or in a short tubular furnace, preheated to the desired temperature before the sample was introduced. To determine if dimensional constraints imposed on the fibres influence the changes during this process, experiments were conducted under three different conditions, (i) with free allowance for fibre shrinkage (FL), (ii) by holding the fibre at constant length (CL), and (iii) by hanging suitable weights for constant tension (CT). The batch stabilization treatment was carried out below the temperature at which rapid exothermic stabilization reactions begin.

TABLE II High-temperature drawing conditions

Sample	Draw ratio			Draw godet/oven temp. (° C)	Annealing godet temp. (° C)	Denier filament
	B.W.*	H.T.†	Total			
Precursor I						
I-0.9-3-O-252-1.7	3	1.7	5.1	252, oven	130	2.0
I-0.9-3-O-252-2.3	3	2.3	6.9	252, oven	130	1.4
I-0.7-6-O-240-1.2	6	1.2	7.2	240, oven	120	1.7
I-0.7-6-O-240-1.4	6	1.4	8.4	240, oven	120	1.5
Precursor II						
II-0.7-2.5-O-228-1.8	2.5	1.8	4.5	228, oven	115	2.2
II-0.7-2.5-G-160-1.8	2.5	1.8	4.5	160, godet	160	2.2
II-0.7-2.5-O-224-2.5	2.5	2.5	6.2	224, oven	118	1.6
II-0.7-2.5-G-190-2.7	2.5	2.7	6.7	190, godet‡	190	1.5

Sample notation: Precursor type – jet stretch – hot water draw ratio – oven godet drawing – drawing temperature – draw ratio.
* Draw ratio in boiling water.
† High-temperature draw ratio.
‡ The drawn fibres were yellowish due to partial degradation/stabilization.

The tubular furnace for continuous stabilization was divided into three 6 foot (~183 cm) zones with individual temperature controllers for each zone. Smooth transition from one zone to another and the uniformity of temperature throughout a zone were ensured by a metal tube placed between the heaters and the inner glass tube. The temperature profile inside the furnace was determined with thermocouple probes placed 18 in. (~46 cm) apart. Two air pumps, one at each end of the glass tube provided enough air circulation.

Samples for the study of progression of continuous stabilization were obtained after steady state was reached in a constant length run (identical feed and take-up speeds) by cutting the yarn at the delivery end and rapidly pulling it from the feed end. This was then cut into 1 foot (~30.5 cm) sections for subsequent measurements. An apparent residence time for each section was calculated assuming a constant velocity of the yarn from the feed to the exit of the oven. A flat temperature profile of 265° C and feed and take-up velocities of 1 in. min^{-1} (2.54 cm min^{-1}) were employed for this study.

2.3. Thermal analysis

A DuPont DSC model 990 was employed to determine the temperatures at which the precursor fibres undergo exothermic reactions. The analysis was carried out in a regular sample pan at a heating rate of 10 °C min^{-1}. The fibres were chopped to small pieces (1 to 2 mm long). The temperature range in which the exotherm was observed was employed as a guide in choosing the stabilization temperatures. Fibres stabilized for various periods were further analysed by this method and the changes in the nature and the extent of exotherms were recorded.

A Perkin Elmer DSC-4 instrument was employed to follow the changes in the heat of melting of fibres, plasticized by water, as a function of the time of stabilization of precursor fibres. The pressure capsules employed in this study were supplied by Perkin-Elmer (Part 319-0218). About 10 mg powdered fibre samples were mixed with water (approximately three times the weight of the fibres). The capsules were carefully sealed, weighed and kept at 50° C for at least 24 h. The melting curves at a heating rate of 10 °C min^{-1} were recorded. ΔH_m values per unit mass of fibre samples stabilized for different periods were calculated from the area under the melting curves computed through the Perkin-Elmer data station. The results reported here are to be viewed only for major trends because the degree of reproducibility required for exact quantitative acceptance has not yet been established.

2.4. Wide- and small-angle X-ray scattering

Flat plate wide-angle X-ray diffraction (WAXD) photographs of precursor and batch stabilized fibres were obtained with a Phillips X-ray unit 4100. For quantitative estimation, radial and azimuthal scans were made with a Phillips diffractometer. Samples for equatorial scans were prepared by winding the fibres carefully as a parallel array on the sample holder. The average size of the laterally ordered domains, L_c, also referred to as "crystal size", can be estimated using the Scherrer equation ([4] p. 423):

$$L_c = K\lambda/B_0 \cos\theta \quad (2)$$

where λ is the wavelength of the X-rays, B_0 is the full width at half the maximum intensity (FWHM) in radians and K is a constant commonly assigned a value of unity. The FWHM was estimated from the (1 0 0) peak at $2\theta = 17°$. Corrections to account for inhomogeneous strains and instrumental broadening were neglected in these calculations and so the estimates obtained here are lower bounds for the actual crystal sizes.

Assuming a hexagonal lateral packing of chains in the ordered domains, Herman's orientation function for these segments with respect to the fibre axis, f_c, was calculated from azimuthal intensity scans of the (1 0 0) reflection, $I_{100}(\phi)$. f_c is given by ([4] p. 423)

$$f_c = -2\frac{3\langle\cos^2\phi\rangle_{100} - 1}{2} \quad (3)$$

where

$$\langle\cos^2\phi\rangle_{100} = \frac{\int_0^{\pi/2} I_{100}(\phi)\sin\phi\cos^2\phi\,d\phi}{\int_0^{\pi/2} I_{100}(\phi)\sin\phi\,d\phi} \quad (4)$$

where ϕ is the azimuthal angle with respect to the fibre axis direction.

A limited number of small-angle X-ray scattering (SAXS) flat plate photographs of the precursor and the batch stabilized fibres were taken with a Phillips X-ray unit. The study was included to provide a qualitative insight into the macroscopic arrangement of the ordered and the disordered regions in the pristine and the heat-treated fibres. The appearance of a meridional reflection, according to Hess-Kiessig model ([4] p. 334) can be interpreted as an alternating arrangement of the ordered and disordered phases along the fibre axis.

2.5. Sonic modulus

The measurements of sonic velocity through fibre samples were made with the sonic modulus tester PPM-5 by H. M. Morgan Co. Sonic modulus is calculated from sonic velocity, C, measured along the length of the fibre using the following expression:

$$E = \varrho C^2 \quad (5)$$

where E is the modulus and ϱ is the density. When E is expressed in g/denier and C in km sec^{-1}, we obtain,

$$E(\text{g/denier}) = 11.3\,C^2 \quad (6)$$

2.6. Density

Densities of the precursor fibres and fibre samples at different stages of stabilization were measured using the flotation technique using toluene (density = 0.866 g cm^{-3}) and CCl_4 (density = 1.585 g cm^{-3}) mixed together in various proportions to give solutions of densities ranging from 1.11 to 1.55 in steps of 0.01.

2.7. Elemental analysis

Selected samples from the continuous stabilization

line were analysed for carbon, hydrogen and nitrogen (these measurements were made by Atlantic Microlab, Inc., Atlanta, Georgia). Since the stabilized yarn was hygroscopic, it was dried at 80° C and 1 mm mercury pressure for 8 h before the analysis was performed. The oxygen content was calculated by difference, assuming that the only elements present in the precursor and in the stabilized fibres are carbon, hydrogen, nitrogen and oxygen and was plotted as a function of position in the stabilization furnace.

2.8. Shrinkage and shrinkage force

Shrinkage measurements as a function of heating time in batch stabilization under free length were made using an air circulated oven at 265° C. Per cent shrinkage was calculated from the length change, Δl, as $(\Delta l/l)100$ where l is the initial length of the fibre before shrinkage.

Shrinkage force measurements were carried out at constant length by connecting one end of the precursor fibres to an Instron load cell, passing them through a small oven and tying the other end to a rigid support through a Kevlar yarn. The furnace, heated to a predetermined temperature was kept initially on the Kevlar end and then moved quickly over smooth rails to the precursor end. The tension generated in the fibres was recorded as a function of time.

2.9. Mechanical properties

Tensile properties of the fibres were measured with a mini Instron, model 1130 with rubber-faced pneumatic jaws at 50 psi ($\sim 0.35\,N\,mm^{-2}$) air pressure. A gauge length of 10 in. (25.4 cm) and elongation rate of $5\,in.\,min^{-1}$ ($\sim 12.7\,cm\,min^{-1}$) were employed for testing precursor fibres. Young's moduli of fibres were calculated from the initial slope of the load–elongation curve.

3. Results and discussion

3.1. Summary of results from previous studies in our laboratories

The results from preliminary batch annealing and stabilization experiments with normally drawn precursor I fibres were reported earlier [6]. Significant morphological rearrangements were found to occur both prior to and after the onset of detectable reactions. The degree of changes depended to a large extent on the dimensional constraints imposed during the thermal treatment. The responses indicated clearly the presence of two major phases in the fibres, a laterally ordered phase and a less ordered phase which exhibited a high degree of segmental mobility at temperatures close to those of stabilization. Annealing without dimensional constraints led to a high degree of disorientation in the less ordered phase, with a simultaneous tendency toward increase in both the size and average orientation of the ordered domains. The extent of disorientation in the mobile phase could be reduced significantly by the imposition of dimensional constraints during thermal treatment, indicating that a significant portion of the chain segments in this phase was bridging the ordered domains. The combination of mechanical response and changes in morphological parameters during thermal treatment of these fibres supported the morphological model proposed by Warner *et al.* [6], namely, connected alternating regions of lateral order and disorder (in fibrils), aligned along the fibre direction in oriented acrylic fibres. The results from dimensionally constrained heating also revealed a rapid initial tendency in the precursor fibres toward self ordering, with a significant increase in orientation. This tendency was utilized to improve the orientational and lateral order in the precursor fibres by drawing them at temperatures comparable to those of stabilization.

3.2. Pre-stabilization high-temperature drawing

The properties of high-temperature drawn (HTD) fibres along with the original fibres are given in Tables III and IV. The method of sample designation has been described in the experimental section. The high values of sonic modulus and orientation function, f_c, in HTD fibres suggest a significant increase in the orientation of the ordered phase and in the overall orientation. The average lateral size of the ordered phase (crystal size) increases by more than 100% as a result of this high-temperature drawing. Two samples from precursor I, I-0.9-3-O-252-2.3 (drawn 3 × in hot water followed by an additional 2.3 × in an oven at

TABLE III Properties of precursor I fibres

Sample	Denier/filament	Tenacity (g/denier)	Elong (%)	Young's modulus (g/denier)	Sonic modulus (g/denier)	Orientation function, f_c	Crystal size (nm)
First set for preliminary batch-stabilization studies							
I-0.7-3	4.1	1.8	13	61	95	0.54	5.4
I-0.7-6	2.1	2.8	9.5	73	130	0.63	4.7
I-0.7-6-O-250-1.0	2.1	2.5	12	76	145	0.75	10.7
I-0.7-6-O-250-1.2	1.7	3.1	10	111	176	0.79	11.1
I-0.7-6-O-250-1.4	1.5	3.3	8	124	190	0.81	11.5
Second set for batch and continuous stabilization studies							
I-0.7-7.3*	1.6	3.4	11	78	120	0.70	5.4
I-0.9-3	3.4	1.8	19	59	90	0.57	5.1
I-0.9-3-O-252-1.7	2.0	3.2	10	117	175	0.82	12.4
I-0.9-3-O-252-2.3*	1.4	4.1	8	135	211	0.92	13.0

* Fibres chosen for stabilization studies.

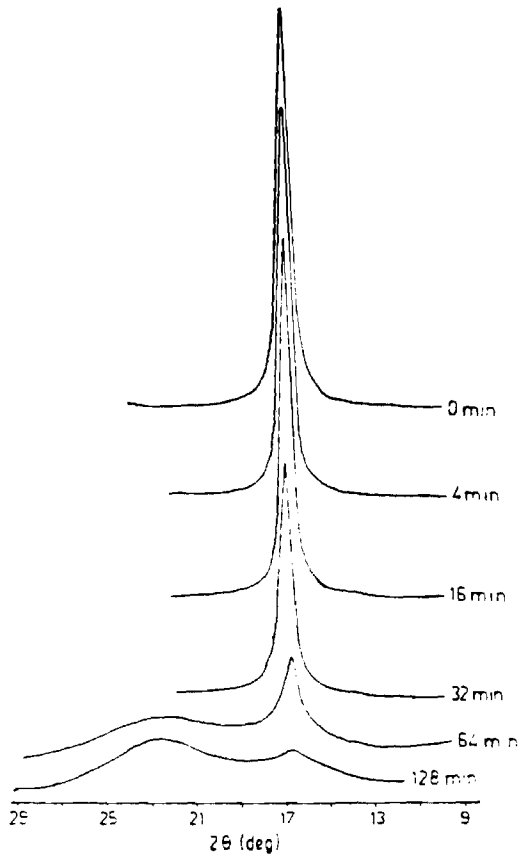

Figure 1 WAXD intensity plots of HTD precursor I fibres heated at 265 C for various durations

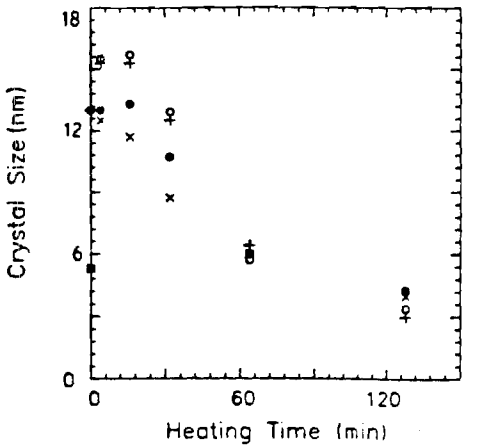

Figure 2 Crystal size of CL and FL batch stabilized fibres. (○) CL, HTD fibres, (●) CL, HWD fibres, (+) FL, HTD fibres, (×) FL, HWD fibres. Heating temperature = 265 C.

252 C) and I-0.7-7.3 (draw ratio = 7.3 in hot water)*, having approximately the same total draw ratio and denier per filament but quite different morphological parameters, were selected to study the influence of orientational and lateral order in the precursor fibres on stabilization.

3.3. Progression of stabilization

3.3.1. Morphological parameters

X-ray diffraction and sonic modulus measurements were made for studying the changes in morphological parameters as a function of stabilization time. Fig. 1 shows a plot of the diffraction intensities against 2θ in a WAXD scan of HTD precursor I fibres heated under constant length conditions at 265 C for various durations. The average size and orientation of the laterally ordered phase in these fibres were estimated as a function of heating time (Figs 2 and 3). The trends are the same as observed before in 3 × and 6 × drawn fibres [5] except that the initial increase in the orientation of the ordered phase is absent in the HTD fibres. Also, the large differences in the crystal size and orientation present in the HTD and HWD fibres diminish as stabilization progresses. The absence of initial increase in orientation of the HTD fibres (Fig. 3) is due to the very high orientation and lateral order that is already present in these precursor fibres.

Orientation of the ordered as well as the disordered phase of the precursor fibres can be inferred from their sonic modulus. High sonic modulus of HTD fibres suggests that there is a high orientation of the ordered and disordered phases along the fibre axis direction. A continuous decrease in this orientation in HTD fibres is observed during their stabilization (Fig. 4), even when no macroscopic shrinkage is allowed. This behaviour is different from the response of the HWD fibres, where an initial increase in sonic modulus at short heating times, followed by a continuous decrease at longer times, is observed. The absence of any further increase in order in HTD fibres could be attributed again to the already high overall orientation present in these fibres. Possible relaxation of some segments in the disordered phase which are

TABLE IV Properties of precursor II fibres

Sample	Denier filament	Tenacity (g denier)	Elong. (%)	Young's modulus (g denier)	Sonic modulus (g denier)	Orientation function, f_c	Crystal size (nm)	Density ($g\,cm^{-3}$)	Moisture content (%)
Boiling water drawn fibres									
II-1.2-3	2.2	2.1	11.1	78	95	0.67	7.3	1.180	2.1
II-0.7-5	2.2	3.1	11.8	90	149	0.78	7.5	1.175	2.0
II-0.7-2.5	3.9	1.8	11.4	64	105	0.61	6.5	-	-
High temperature drawn fibres									
II-0.7-2.5-O-228-1.8	2.2	3.4	9.7	114	150	0.83	11.3	1.175	1.8
II-0.7-2.5-G-160-1.8	2.2	3.5	8.6	117	147	0.77	8.8	1.175	1.7
II-0.7-2.5-O-224-2.5	1.6	4.4	8.7	132	182	0.87	11.0	1.180	2.1
II-0.7-2.5-G-190-2.7	1.5	4.4	7.6	144	207	0.84	12.8	1.185	1.6

*Referred to as HTD and HWD fibres, respectively, in all subsequent discussions.

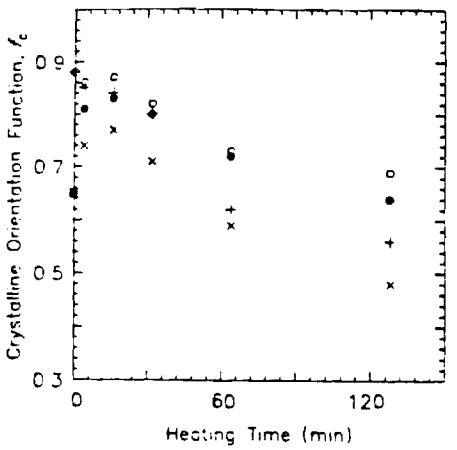

Figure 3 Crystalline orientation function, f_c, of CL and FL batch stabilized fibres. (○) CL, HTD fibres, (●) CL, HWD fibres, (–) FL, HTD fibres, (×) FL, HWD fibres. Heating temperature = 265 C.

not anchored effectively in the ordered phase may contribute to a decrease in the sonic modulus even at short heating times in these fibres. This partial relaxation of orientation in the disordered phase is also suggested by the shrinkage force experiments discussed in Section 3.3.3 (a part of the initial stress developed relaxes almost instantaneously). In HWD fibres, an increase in the sonic modulus is observed at short heating times in spite of probable partial relaxation in the less ordered phase, because of the simultaneous large increase in the crystalline orientation (Fig. 3). The decrease in sonic modulus at longer heating periods is due to the change in the intrinsic properties of the precursor fibres as a result of stabilization reactions. As expected, the free length heated fibres show a pronounced decrease in the sonic modulus in both precursor fibres (Fig. 4), due to the extensive orientational relaxation of even the bridging segments in the disordered phase between the ordered domains. In constant tension experiments, with the applied tension being the maximum that was possible without causing filament rupture, the fibres extended by almost 10 to 12%. This extension caused an increase in orientation in both HTD and HWD fibres, as reflected by the initial increase in sonic modulus (Fig. 4). The rise in sonic modulus, as expected, is more pronounced in the case of the HWD fibres.

The sonic moduli of samples from a continuous stabilization line are plotted in Fig. 5 as a function of residence time in the oven (apparent heating time). The sampling technique has been described in the experimental section. Although continuous stabilization was carried out at the same feed and take-up speeds, it does not prevent local changes in the velocities due to compensating extension and shrinkage of the fibre inside the furnace. The fibre, as soon as it reaches a temperature above its glass transition temperature (T_g), will tend to shrink provided the shrinkage can be compensated by extension in another section of the furnace. Warner *et al.* [7] have explained this phenomenon in detail. The general trends in the sonic moduli of both HWD and HTD fibres observed in continuous stabilization are similar to those in batch stabilization at constant length (Fig. 4). The slower initial increase in the sonic modulus of HWD fibres in continuous stabilization when compared to batch stabilization is due to a slower heating to 265 C in the former as opposed to the instantaneous exposure to 265 C in the latter process.

3.3.2. Calorimetry

The DSC exotherms of samples from a continuous stabilization run, representing various apparent heating periods, are shown in Fig. 6. A simultaneous decrease in the area under the exothermic peak and increase in the peak width are observed. As stabilization progresses, the nitrile groups in the precursor fibre undergo cyclization resulting in a decrease in the extent of the exotherm. A complete disappearance of the exotherm suggests completion of the cyclization reactions. Incorporation of oxygen and cyclization of nitrile groups during the stabilization of precursor fibre alters the chemical structure originally present in these fibres. This new structure formed during the intermediate stages of stabilization modifies the course of further cyclization, as indicated by the broadening of the exothermic peak.

The results from plasticized melting studies are

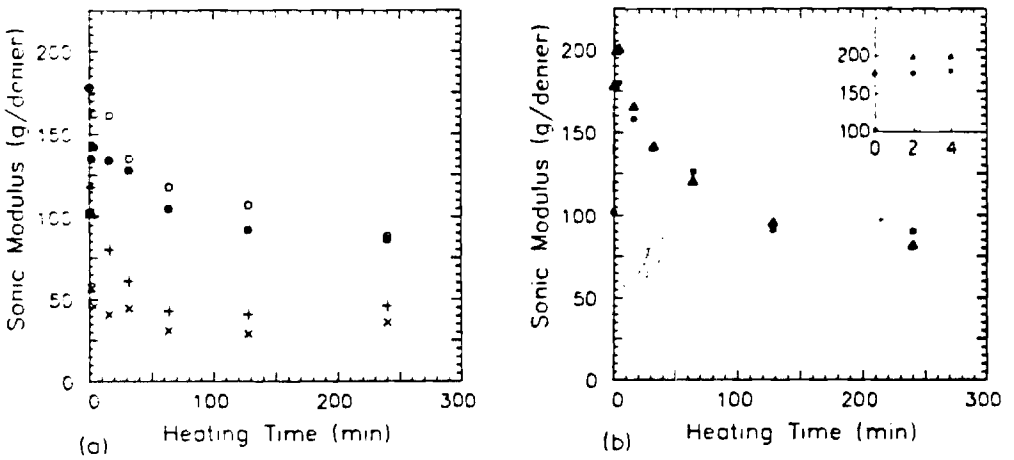

Figure 4 Sonic modulus of CL, FL and CT batch stabilized fibres. (a): (○) CL, HTD fibres, (●) CL, HWD fibres, (+) FL, HTD fibres, (×) FL, HWD fibres. (b) (■) HWD fibres, 0.1 g/denier tension; (▲) HTD fibres, 0.14 g/denier tension. (Inset: the initial response, plotted on an expanded scale.) Heating temperatures = 265 C.

TABLE V Results of plasticized melting studies

Heating time (min)	HTD fibres				HWD fibres			
	Heat of melting ($cal\,g^{-1}$)	$\Delta H_m(t)/\Delta H_m(t=0)$	Heat of crystallization ($cal\,g^{-1}$)	$\Delta H_c(t)/\Delta H_c(t=0)$	Heat of melting ($cal\,g^{-1}$)	$\Delta H_m(t)/\Delta H_m(t=0)$	Heat of crystallization ($cal\,g^{-1}$)	$\Delta H_c(t)/\Delta H_c(t=0)$
0	12.3	1.00	9.51	1.00	12.9	1.00	9.45	1.00
2	12.5	1.02	9.81	1.03	12.0	0.93	9.07	0.96
4	12.3	1.00	9.68	1.02	13.4	1.04	8.96	0.95
16	16.5	1.34	9.46	0.99	10.3	0.80	7.10	0.75
32	9.2	0.75	4.68	0.49	7.6	0.59	4.39	0.46
64	1.9	0.15	–	–	Negl.	–	Negl.	–

Temperature of heating = 265° C.

given in Table V. Depletion of the unreacted ordered phase in the later stages of the process can be seen clearly, consistent with the WAXD results reported earlier. Plasticized recrystallization results show the expected monotonic decrease in the potential of the material to crystallize with increasing time of thermal treatment. The most important aspect of these plasticized melting and recrystallization experiments is the clear observation of the characteristic enthalpy changes associated with first order transitions, establishing the presence of true crystals in the precursor fibres.

3.3.3. Shrinkage and shrinkage force

Shrinkage in acrylic fibres during their stabilization has been employed for the optimization of stabilization by previous researchers [8]. Total shrinkage during stabilization under free conditions can be divided into an almost instantaneous initial shrinkage due to the coiling-up of the oriented chains in the laterally disordered phase and a slow delayed shrinkage, also known as secondary shrinkage, which has been attributed to the chemical reaction associated with stabilization [9–11]. A plot of shrinkage against heating time, with the fibres heated at 265° C in air, is given in Fig. 7. The HTD fibres shrink instantaneously to a lower extent, 12%, compared to HWD fibres which show an instantaneous shrinkage of 17%, the difference being maintained throughout the stabilization process. The lower entropic shrinkage in HTD fibres is due to the presence of a higher fraction of the laterally ordered phase and thus a lower fraction of the oriented but laterally disordered regions which contribute to this shrinkage. The secondary shrinkage which increases with the progression of stabilization is caused by the chemical reactions associated with the stabilization. Melting of the ordered segments which takes place during the course of chemical reactions can result in continued shrinkage with the progression of stabilization. Both HWD and HTD fibres show similar rates and extents of secondary shrinkage.

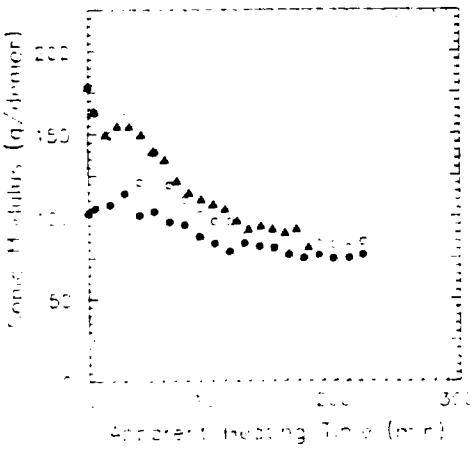

Figure 7 Change in sonic modulus during continuous stabilization at 265° C (●) HWD fibres, 1 in min^{-1}, (○) HTD fibres, 1 in min^{-1}, (▲) HTD fibres, 1.25 in min^{-1}.

When no macroscopic changes in the length of precursor fibres are allowed during heating, stress is developed due to the tendency of chains in the disordered phase to undergo entropic relaxation. This tendency of the chains to coil up is greater when their orientation is higher. Fig. 8 shows the stress or shrinkage force generated in the HTD and HWD fibres as a function of heating time. The HTD fibres have a significantly higher non-crystalline and overall orientation compared to the HWD fibres and therefore show a higher shrinkage force. Much of the initial tension decays in a relatively short period (less than 2 min) due to relaxation of some of the oriented chains in the disordered phase. The decay is slower and to a lower extent in HTD fibres compared to HWD fibres, suggesting higher connectivity between the ordered and the disordered phases. Under a macroscopically constrained state, the chains in the disordered phase of the HTD fibres cannot relax as much as the chains in HWD fibres, in spite of a larger tendency toward it.

The dependence of shrinkage force on the draw ratio is shown in Fig. 9 where the initial stresses generated in three precursor fibres having different draw ratios are plotted. An almost instantaneous and complete decay of the initial stress is observed in fibres with no high-temperature drawing, whereas fibres with high-temperature draw ratios of 1.7 and 2.3 show a larger initial stress and a slower decay, again suggesting a higher connectivity between the ordered and the disordered segments in these highly ordered fibres. The decay of initial stress is followed by a slow development of a secondary stress as a result of chemical reactions propagating to the ordered regions. As discussed earlier, these reactions are accompanied by the melting of the ordered domains which results in the development of a shrinkage force in the later stages of stabilization. Consistent with the extents of lateral order in the precursor fibres, a higher secondary stress is observed in the HTD fibres than in HWD fibres.

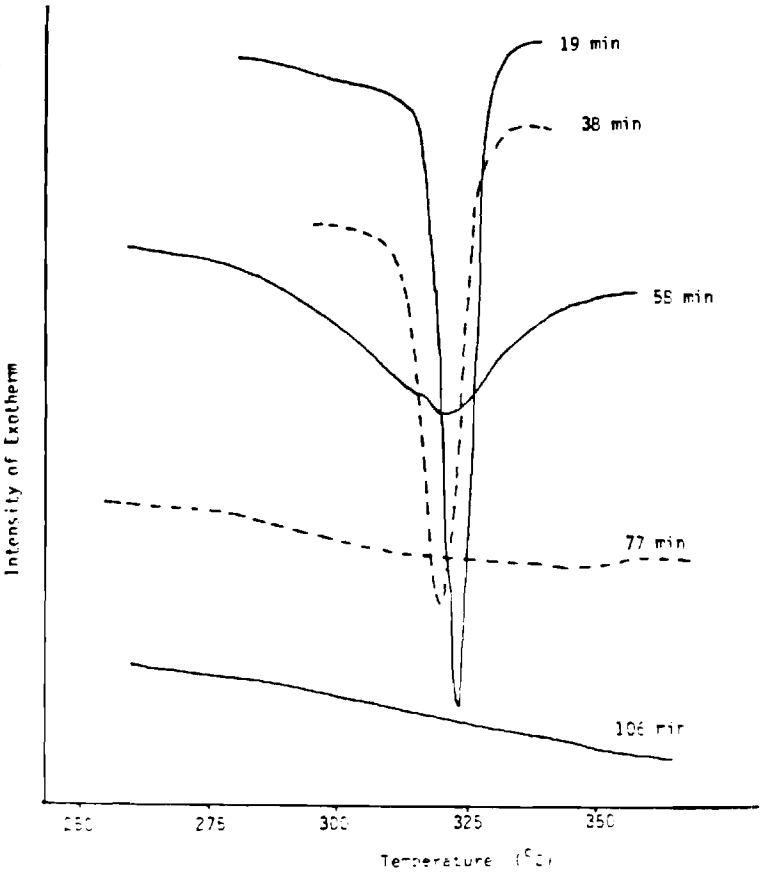

Figure 6 DSC exotherms of samples from continuous stabilization (265 C, flat profile). Various apparent heating times are shown for precursor I-0.9-3-O-252-1.7.

3.3.4. Density and oxygen pick-up

Incorporation of oxygen from the air and the denser packing of the aromatic species created during stabilization contribute to a monotonic increase in density. Both density and oxygen content have been employed in the industry as indicators of the extent of stabilization in acrylic fibres and this aspect is discussed in Part 3 [2]. The progressions of densities of the HTD and HWD precursor I fibres during batch and continuous stabilization are shown in Figs 10 and 11. Under each condition of dimensional constraint imposed during this process (FL, CL, CT or continuous), little difference is seen between the rates of change in HTD or HWD fibres. Although significant differences exist in the morphological parameters of these two precursor fibres (Table III), these differences diminish due to the rearrangements in the early stages of stabilization (Figs 2 to 5). Thus morphological contributions to the rates of solid-state reactions in stabilization, as inferred by density changes, are not likely to be revealed here. The diffusion-controlled incorporation of oxygen (Fig. 12) is also entirely consistent with the progression of density. The rate of stabilization increases with the tension (Fig. 10) in the fibres (tension in free length < in constant length < in constant tension). This, however, can not be attributed unequivocally to the higher orientations obtained at the higher tensions. The filament diameter also decreases with increase in the tension, thus raising the overall rate of diffusion-controlled reactions.

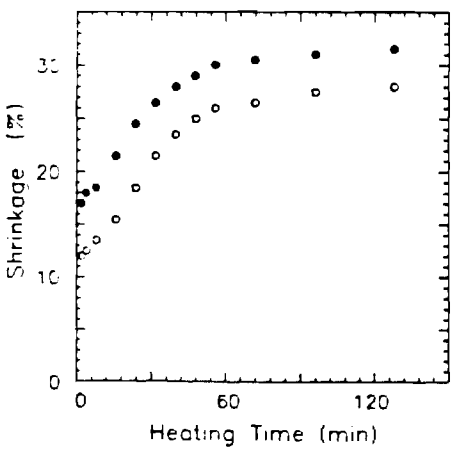

Figure 7 Shrinkage in FL batch stabilized fibres. (○) HTD fibres, (●) HWD fibres. Temperature = 265 C.

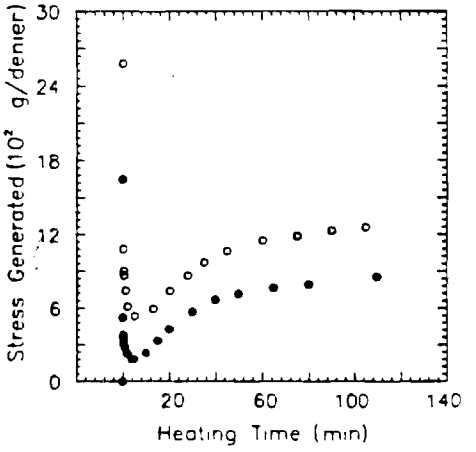

Figure 8 Shrinkage stress generated during CL batch stabilization. (○) HTD fibres, (●) HWD fibres. Temperature = 265 C.

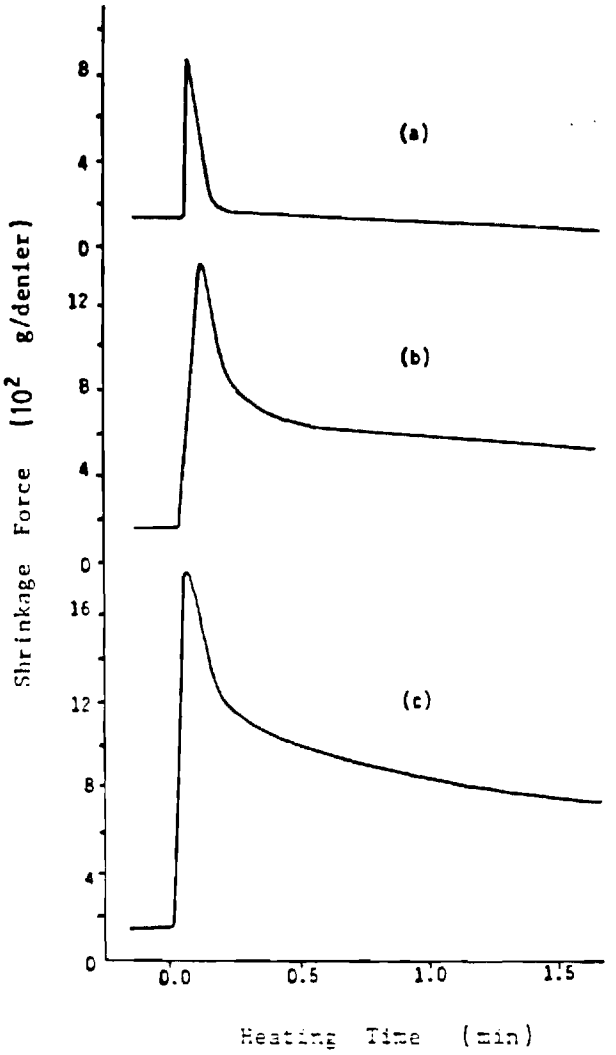

Figure 9 Shrinkage stress generation and decay in precursor I fibres (a) [sic] 9-3-O-252-1.7, (b) [sic] 9-3-O-252-2.3.

3.3.5. Comparison of precursors I and II

The progression of changes observed in batch and continuous stabilization of precursor II fibres, containing itaconic acid comonomer which can initiate the stabilization reactions, has the same general character as those reported here for precursor I fibres. The quantitative differences observed are due to the higher rate of stabilization in precursor II fibres. For example, the density changes (Fig. 13) for two precursor fibres (I-0.7-7.3 and II-0.7-5) show a significantly higher rate of increase in precursor II in spite of the higher denier of these filaments (2.2 denier) when compared with the denier of the precursor I filaments (1.6 denier). When these fibres are heated at constant length, the delayed shrinkage force, which indicates the propagation of stabilization reactions, also rises much faster in precursor II fibres, suggesting a higher rate of stabilization in these fibres (Fig. 14). Additional results from stabilization of this precursor are reported in Part 3 [2].

3.4. Morphology of acrylic precursor fibres

The following observations clearly show that the basic morphological unit in oriented acrylic fibres consists of a repeating sequence of oriented, laterally ordered and oriented but laterally disordered domains with a significant portion of the chain segments in the latter phase bridging the ordered domains. This model has been proposed earlier by Warner *et al.* [6]:

1. clear WAXD evidence for the presence of laterally ordered domains;
2. calorimetric evidence for the "melting of crystals" when the melting temperature is reduced through plasticization to temperatures below those of degradation reactions;
3. spontaneous shrinkage at high temperatures, *without any loss in the extent or the orientation of the ordered domains*, and the large drop in sonic modulus which accompanies this shrinkage process indicating that the ordered and disordered domains are arranged in a connected sequence along the fibre direction;
4. when thermal treatment of oriented acrylic fibres is carried out without allowance for shrinkage, the change in sonic modulus depends on the change in the extent of lateral order in the fibres. An increase in sonic modulus accompanies a significant initial increase in the extent and orientation of the laterally ordered fraction but a measurable decrease is seen when only a slight increase in lateral order occurs in those fibres which possess a high degree of initial order. These responses indicate the presence of *celia* and loose loops in the laterally disordered fraction.

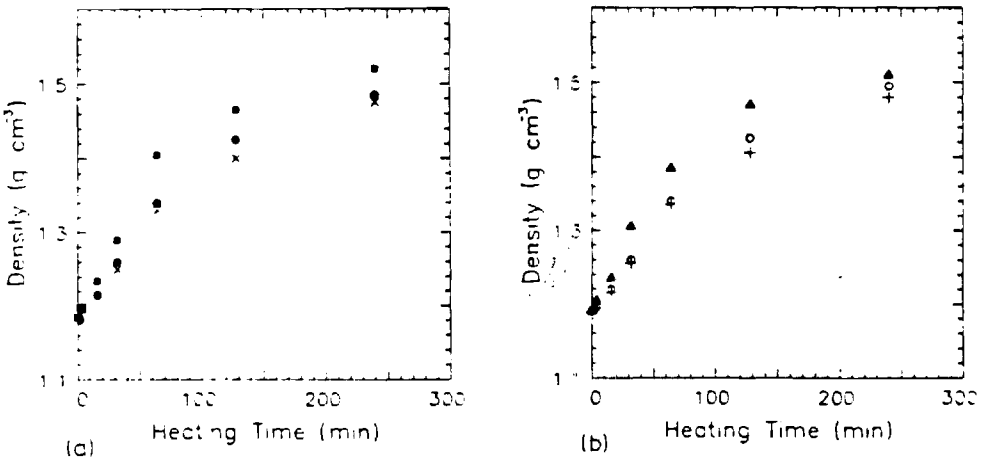

Figure 10 Effect of constraints on the density of batch stabilized HWD and HTD fibres. (a): HWD fibres, (×) FL, (●) CL, (■) 0.1 g denier tension. (b) HTD fibres, (+) FL, (○) CL, (▲) 0.14 g denier tension. Temperatures = 265° C.

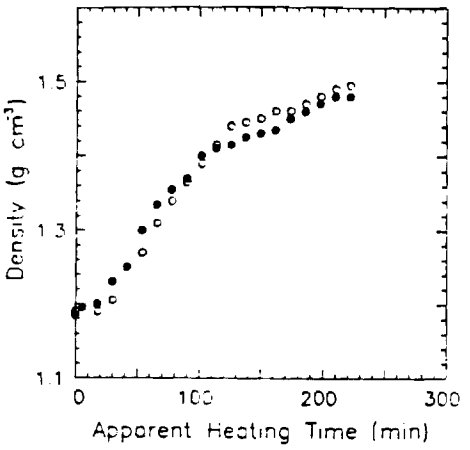

Figure 11 Change in density during continuous stabilization at 265° C. (●) HWD fibres, (○) HTD fibres.

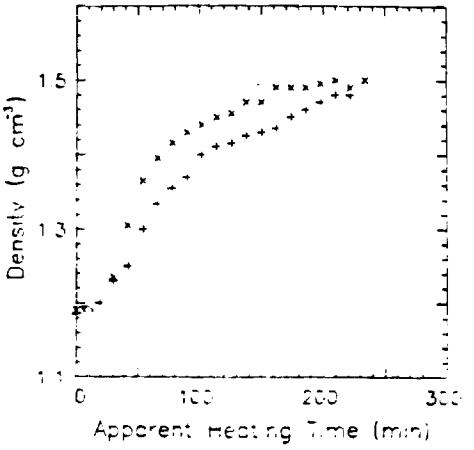

Figure 13 Change in density of precursor I and II fibres during continuous stabilization at 265° C. (+) I-0.7-7.3, (×) II-0.7-5.

The initial decrease in sonic modulus during "constant length" heating of HTD fibres is still much less than the drastic drop which accompanies "free" thermal treatment, indicating that a majority of the segments in the laterally disordered fraction act as tie chains between the laterally ordered domains.

5. acrylic fibres with demonstrably different extents of order show little difference in density, indicating that the packing densities in the laterally ordered crystals and the laterally disordered "noncrystalline" regions are essentially the same. Thus, the meridional reflection in SAXS, characteristic of the proposed two-phase oriented structure, is absent in these fibres (Fig. 15a). After heating the precursor fibres for 16 min in air, a meridional spot is observed in SAXS flat plate photographs, indicating the presence of a long period (Fig. 15b). Appearance of this meridional reflection with the onset of stabilization reactions has been presumed to be the result of their preferential occurrence in one of the two phases, thus providing indirect evidence for the proposed morphology. Confirmation of the existence of a long period in the precursor fibres is obtained by conducting SAXS studies subsequent to impregnation of these fibres with copper ions (Fig. 15c) by refluxing them in a solution of CuCl in HCl for 30 min. The electron density of the disordered phase is increased by the dispersion of copper salt in this phase, resulting in the appearance of the meridional reflection in SAXS studies.

4. Conclusions

A number of significant results have been obtained through the research on oxidative stabilization of acrylic precursors for carbon fibres reported here. These results and the inferences from them, regarding needed additional research are summarized below.

1. Through a combination of evidence from thermomechanical response, thermal stress development, calorimetry, wide-angle and small-angle X-ray scattering, and sonic modulus studies of fibres through the course of an oxidative stabilization process, and small-angle X-ray scattering studies of precursor fibres impregnated with copper, the basic morphological unit in oriented acrylic fibres has been shown to have laterally ordered domains connected along the fibre axis direction through domains in which such order is absent. Our observations confirm this important aspect of the morphological model proposed by Warner *et al.* [6]. The other major aspect of their model, fibrillar geometry of this morphological unit, is being examined through small- and wide-angle X-ray

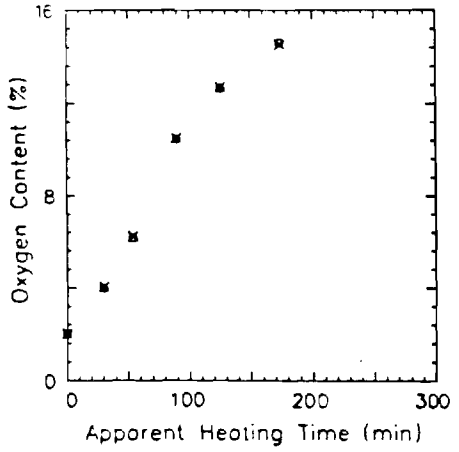

Figure 12 Oxygen incorporation during continuous stabilization of precursor I fibres at 265° C. (×) HWD fibres, (○) HTD fibres.

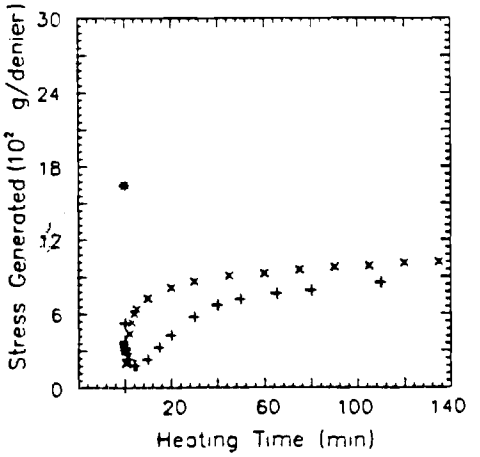

Figure 14 Shrinkage stress developed in precursor I and II fibres at 265° C. (+) I-0.7-7.3, (×) II-0.7-5.

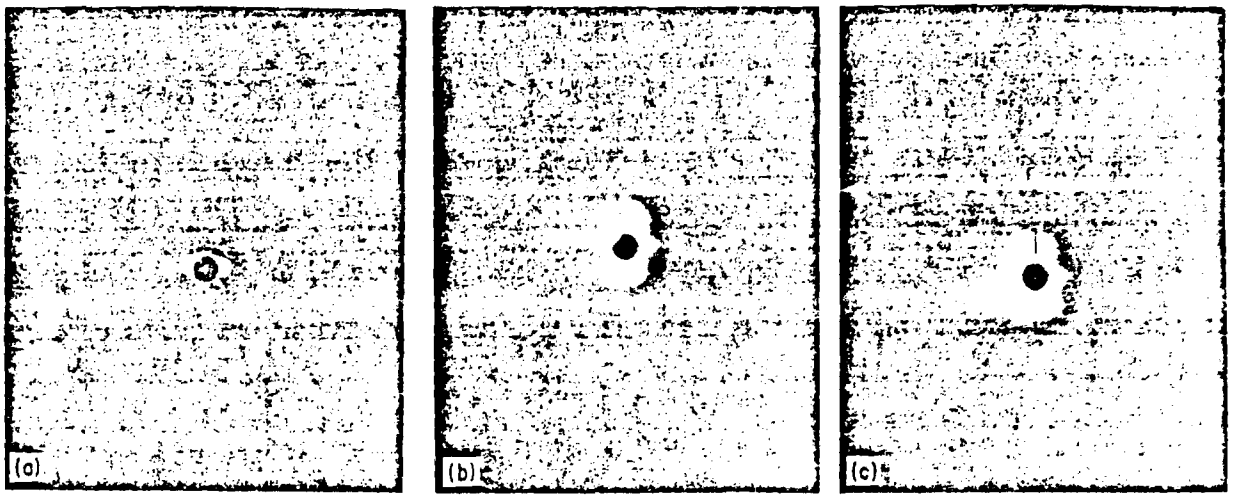

Figure 15 Small-angle flat plate photographs: (a) precursor, (b) 16 min CL stabilized, (c) copper impregnated.

scattering studies of oriented acrylic fibres after swelling them in DMF.

2. The ordered fraction and the overall orientational order in acrylic precursor fibres can be increased markedly through a process which involves plastic stretching at high temperatures of a fibre which has been only partially stretched in a conventional wet spinning process.

3. When acrylic precursor fibres are heated to the temperatures involved in the oxidative stabilization step of the process for carbon fibre formation, the physical changes that precede the onset of a significant level of stabilization reactions depend on the externally imposed dimensional constraints. The present study shows clearly that whether dimensional constraints are imposed or not, a significant tendency for increase in perfection and the extent of the laterally ordered domains occurs in the early stages of this step. The extent of this increase diminishes with increasing order initially present in these fibres. The constraints imposed on the length have a pronounced effect on the relaxation of orientation in the laterally disordered fraction. The decrease in orientation in this phase is dramatic when no constraint against shrinkage is imposed on the fibres. The effect of the degree of orientational relaxation permitted at this stage, which can be controlled by the application of stress, on the ultimate properties of carbon fibres produced from these fibres remains to be studied.

4. The critical stress for failure and the stresses generated at any level of imposed deformation (or, conversely, the deformation at any level of imposed stress) would change throughout the course of stabilization. Since the temperature tension deformation time profile that can be applied during stabilization is limited by the continuously changing critical stress, it is necessary to have the provision to control these through a multistage stabilization process so that the influence of these factors on the structure of the carbon fibres can be established. There is a clear need for separating the stabilization process into at least three independently controlled stages, i.e. an initial zone of rapid morphological rearrangements, a second zone of reactions predominantly in the disordered fraction, and the subsequent zone of reactions propagating into the ordered fraction of the fibres. A multistage stabilization line would also allow the use of different environments in the different zones. In order to realize the maximum potential of a given precursor fibre, it is important to "tailor" the conditions of oxidative stabilization to suit the rates of such reactions and the deformation characteristics of the fibres during this stage. Conducting precisely controlled experiments at this stage will help in establishing the important link between the structure of the precursor fibres and the structure and properties of the carbon fibres that can be obtained from them.

5. When the progression of stabilization is monitored with measurements such as density and oxygen pick-up, little difference is seen in the rates of stabilization with the orientation or the lateral order present initially in the fibres. This appears to be the result of the nature of morphological rearrangements during the early stages of the process, especially the increase in the extent of the ordered fraction to approximately the same levels in these fibres.

6. Among the techniques examined in the present study for the characterization of morphological parameters of the fibres, wide-angle X-ray diffraction (WAXD), sonic modulus, differential scanning calorimetry (DSC), birefringence and infrared dichroic ratio, the combination of sonic modulus, WAXD and DSC was found best suited for obtaining at least semi-quantitative measures of the degree of lateral order and orientation in the precursor fibres and the changes occurring in the early stages of stabilization. Birefringence and infrared dichroic ratio were discarded because of apparently similar polarizabilities parallel and perpendicular to the chains at the precursor stage which render them unsuitable for distinguishing differences in orientational order. The difference in intrinsic polarizabilities parallel and perpendicular to the chain direction is known to become significant when these fibres are subjected to the conditions of a stabilization process. Infrared dichroism and birefringence may prove suitable for inferring the orientational order in stabilized fibres.

7. During the early stages of a stabilization process,

at least partial relaxation of orientation occurs in the occurs in the fraction in which lateral order is absent, even when a macroscopic constraint against shrinkage is present. These disorienting segments to which macroscopic constraints are not transmitted could be one of the sources of sites of low orientational order and structural defects in carbon fibres. The degree to which it can be eliminated through increase in order in the precursor fibres and through a significant increase in the molecular weight of the precursor polymer remains to be explored.

8. Aspects related to the extent to which the stabilization reactions need to be carried out before the fibres would become suitable for carbonization are discussed in Part 3 [2].

Acknowledgements

We wish to thank Dr L. H. Peebles for many useful suggestions during the course of this work and in the inferences drawn from experimental data. Discussions with Dr W. C. Tincher and Dr F. L. Cook are gratefully acknowledged. This study was supported by the United States Office of Naval Research.

References

1. M. K. JAIN and A. S. ABHIRAMAN, *J. Mater. Sci.* 2: (1987) 278.
2. M. K. JAIN, M. BALASUBRAMANIAN and A. S. ABHIRAMAN, submitted for publication.
3. M. K. JAIN, PhD thesis, Georgia Institute of Technology, Atlanta, Georgia (1985).
4. L. E. ALEXANDER, "X-ray Diffraction Methods in Polymer Science," (Wiley-Interscience, New York, 1969).
5. M. K. JAIN and A. S. ABHIRAMAN, *J. Mater. Sci.* 18 (1983) 179.
6. S. B. WARNER, D. R. UHLMANN and L. H. PEEBLES Jr, *ibid* 14 (1979) 1893.
7. S. B. WARNER, L. H. PEEBLES Jr and D. R. UHLMANN, *ibid* 14 (1979) 565.
8. O. P. BAHL and L. M. MANOCHA, *Fibre Sci. Technol* 9 (1976) 77.
9. D. J. MÜLLER, E. FITZER and A. K. FIEDLER, Proceedings of the International Conference on Carbon Fibres, their composites and applications, (Plastics Institute, London 1971) paper 2.
10. E. FITZER and D. J. MÜLLER, *Die Makromol. Chemie* 144 (1971) 117.
11. E. FITZER and M. HEYN, *Chem. Ind.* 16 (1976) 663.

Received 8 October 1985
and accepted 22 May 1986

Conversion of acrylonitrile-based precursor fibres to carbon fibres

Part 1 *A review of the physical and morphological aspects*

MUKESH K. JAIN*, A. S. ABHIRAMAN‡
Georgia Institute of Technology, Atlanta, Georgia 30332, USA

The physical and morphological aspects of the conversion of acrylonitrile-based precursors to carbon fibres are reviewed. The development of structure through the different stages of the process, namely precursor fibre formation, oxidative stabilization and carbonization, is described. The interactive contributions of process conditions and the precursor structures to the morphology and the properties of carbon fibres are discussed.

1. Introduction

Carbon or graphite fibre composites are emerging as important construction materials in applications where light weight and high strength and modulus are the prime requirements. Basal planes of graphite crystal possess enormous mechanical strength but the resistance to shear between the planes is poor, causing most ordinary carbons and graphites to exhibit low stiffness and strength. A possible solution to this problem was discovered in one-dimensional form whereby the strong bonds are preferentially oriented along the axis of a whisker or fibre. Experimental whiskers produced in the laboratory [1, 2] have displayed excellent properties close to the theoretical limits of crystal properties, but it has not been possible to develop an industrially useful process for their production. The line of attack that has yielded results of more practical value is through the carbonization of fibres such as rayon, pitch and acrylic fibres.

Although large quantities of carbon fibre and cloth made from cellulose-based precursors are produced for various industrial applications, generally their mechanical properties are poor. Improvements in the mechanical properties of rayon-based carbon fibres are possible by stretching such fibres during high-temperature carbonization [3, 4]. Nevertheless, the hot-stretching process remains intrinsically difficult and expensive and appropriate precursor materials are no longer commercially produced to the extent necessary. Shindo of Japan [5–8] discovered about 20 years ago that carbonization of air-oxidized polyacrylonitrile (PAN) fibre produces a material with appreciable crystalline orientation. Later, British investigators discovered that if PAN fibres were suitably stressed during a carefully controlled process of oxidative stabilization, the resultant fibres obtained after carbonization using temperatures in excess of 1000° C were highly oriented and possessed good tensile strength and modulus [9]. Since then, a great deal of work had been published on the production, structure and physical properties of these fibres. There have been several excellent reviews [10–16] and doctoral theses [17–24] dealing with the study of PAN-based carbon fibres. The industrial efforts have been to produce a consistently high performance product at low cost. The approaches to this include modifications, chemical as well as physical, of the precursor and new innovative methods for stabilization and carbonization. Advances in the technology of the fibre manufacturing process have made it possible to produce carbon fibres with improved quality at much lower cost. Mesophase pitch is the latest raw material for producing high strength and high modulus carbon fibres (up to 120×10^6 psi modulus, $\sim 8.27 \times 10^5$ N mm^{-2}) without high-temperature stretching. In this report, however, the discussion will be confined to PAN-based carbon fibres.

2. Carbon fibre manufacturing processes

The manufacture of carbon fibres from PAN-based precursors, as disclosed in various patents, consists of a low-temperature oxidative stabilization in air followed by a high-temperature carbonization in an inert atmosphere. The PAN copolymer used for spinning precursor fibres usually contains about 2 to 10% of a comonomer such as methyl acrylate (MA) or methyl methacrylate (MMA). A small amount of a third comonomer which initiates the stabilization reactions at lower temperatures is often present in the precursor fibres. Both dry and wet spinning techniques using organic solvents such as dimethyl formamide (DMF) and sodium thiocyanate have been employed for spinning precursor fibres. In some instances, use of inorganic solvents involving ionic salts is found to have a detrimental effect on the thermal stability of the carbon fibres [25, 26]. PAN fibres spun by a melt spinning process have been developed recently by American Cyanamid Co. [27], which are also being explored for carbon fibre production. Fine filaments,

**Present address*: ALCAN, Arvida Laboratories and Experimental Engineering Center, Jonquiere, Quebec, Canada.
‡Author to whom all correspondence should be addressed.

0022–2461/87 $03.00 + .12

usually 1 to 3 denier/filament, are employed in the form of a continuous tow containing 100 to 50 000 filaments for carbon fibre manufacture. The preoxidation or stabilization of these tows is carried out at 200 to 300° C for sufficient time to render them infusible and flameproof. Temperatures below about 200° C are impractical since very long periods are required, while temperatures above about 300° C cause violent exothermic reactions [28, 29] resulting in significant weight loss [30] and formation of tarry substances. Oxidative stabilization is very critical to the production of carbon fibres. Improper stabilization could result in blow out of a core portion during carbonization [31, 32] due to its incomplete oxidation. Proper conditions of rate of heating and time and temperature of heating should, therefore, be established for optimum stabilization for each precursor. In a batch process, heating the precursor in air at 220 to 250° C was employed by early workers, whereas modern practice is to pass the precursor tow continuously through a furnace divided into several zones with increasing temperature profiles. A residence time of several hours is usually required for complete stabilization [33–35], which is generally carried out in air but oxygen or oxidizing gases may be substituted for air [36–39]. The density of precursor fibre increases continuously while the white precursor changes to a shiny black fibre.

In spite of several studies using various analytical tools such as infrared spectroscopy [39–54], thermal analysis [55–64], gas chromatography [57, 64, 65–69], mass spectroscopy [34, 66, 70, 71] and wet chemical techniques [56, 72, 73], the chemistry of stabilization remains complicated and not well understood. The cyclization of nitrile pendant groups of PAN to give polyimine type structure seems to be well accepted as the main reaction during stabilization [30, 70, 74]. These imine sequences are postulated to be three to six units long. The effect of various comonomers in initiating or terminating the cyclization reactions has been studied in detail by Grassie and his colleagues [75–82] using thermal techniques. Some weight loss from chain scission and elimination of hydrogen cyanide and ammonia accompanies the cyclization reactions [34, 55, 83, 84]. Oxygen, which is added during stabilization, is mostly present as –OH and >CO groups [41, 55, 84–87] but some authors, based on infrared spectroscopic and model compound studies, have suggested that oxygen becomes attached to the imine nitrogen atoms to give a nitrone (>N–O) moiety [74, 85–89]. The presence of oxygen promotes cross-linking and is also believed to help in the aromatization of the cyclized sequences by the elmination of water, both being essential for the basal plane formation in carbon fibres. Various mechanisms of thermo-oxidative degradation of PAN polymer have been reviewed by Peebles [90].

The application of tension during the oxidation of precursor fibre is important since it prevents polymer chains from relaxing and losing their orientation, which becomes locked-in through cross-linking. Both physical and chemical [91, 92] changes during stabilization are affected by the presence of tension. The stabilized fibres show an amorphous X-ray pattern, but a high degree of crystalline order and orientation is displayed after their carbonization at temperatures in excess of 2000° C. A detailed discussion of morphological changes in precursor fibre as it undergoes stabilization and carbonization will be given in a later section. The extent of shrinkage or extension allowed during stabilization varies over a wide range depending on the precursor and the manufacturing process. A patent by Johnson *et al.* [9] allows a shrinkage of less than 12% whereas a 40 to 70% shrinkage of Beslon fibres has been suggested in a patent by Toho Beslon Co. [93]. A patent by NRDC [94] allows no shrinkage. Yet another patent by Japan Exlan Co. [95] recommends 0 to 50% extension during stabilization. The influence of various tensions and corresponding length changes during stabilization on the mechanical properties of carbon fibres will be discussed in a separate section.

Various measurements have been suggested for the optimization of conditions for oxidative stabilization. One which is more popular is the measurement of oxygen content as a function of stabilization time or temperature [33, 86, 91, 92, 96–103]. A stabilized fibre is considered suitably stabilized when its oxygen content is in the range of 8 to 12% [93]. An oxygen content of more than 12% results in the deterioration of stabilized fibre quality which gives low-quality carbon fibre, whereas less than 8% oxygen results in low yield of carbon fibres due to excessive weight loss during carbonization [31].

Since stabilization is the speed-limiting step in the production of carbon fibres, variations from the conventional stabilization processes described above have been attempted to speed up this step. One approach has been to modify the chemical composition of the precursor fibre either by using a comonomer [43, 94, 104–106] or an additive [107], or by impregnation with chemicals [108–113], which enhance stabilization. A patent by Japan Exlan Co. [105] describes this approach by using precursor fibres (1.3 denier/filament) spun from a PAN copolymer containing 2% methacrylic acid. These fibres, when passed through a furnace having a temperature gradient from 200 to 280° C, required only 25 min for complete stabilization. A second approach has been to modify the stabilization conditions and apparatus to speed up stabilization. A recent patent by Great Lakes Corp. [114] uses a V-shaped temperature profile instead of the more popular ascending one for continuous stabilization. Precursor fibres are first heated to a temperature 2 to 8° C short of fusion followed by cooling at a predetermined rate until a critical density is reached and then heated again until a density greater than 1.35, capable of sustaining carbonization temperature of at least 800° C, is obtained. A typical stabilization time of 25 min has been reported. Another patent by Toray Industries [32] claims a 2 to 20 min stabilization time by contacting the precursor fibre with a heated surface in the presence of an oxidizing gas. Speeds over 20 m min^{-1} have been claimed making it possible to couple stabilization with precursor spinning. Yet another approach for speeding up the

stabilization has been to use non-air environments [115–118].

The carbonization of preoxidized or stabilized fibres is caried out in an inert atmosphere containing gases such as nitrogen or argon. The temperature of carbonization is usually decided by the type of application of the resulting carbon fibres. For high-strength applications, heating at 1500 to 1600° C is preferred since above this temperature a decrease in the tensile strength has been observed [33, 119–121]. For preparing high modulus carbon fibres, an additional heat treatment at 2500 to 3000° C is required. Nitrogen cannot be used at temperatures above about 2000° C due to its reaction with carbon to form cyanogen. The rate of heating and residence time during carbonization vary depending on the type of precursor and stabilization conditions. There is a large weight loss (up to 50%) during this stage, producing a large volume of volatiles and some tarry substances. The heating rates, therefore, have to be carefully controlled to avoid fibre damage during the release of volatiles. The gases evolved during carbonization consist mainly of H_2O and CO_2 at 300 to 500° C from dehydrogenation and cross-linking [34, 70]. This is followed by the evolution of HCN and N_2 at temperatures higher than 600° C, mainly due to the intermolecular condensation of ladder-type structures (containing ring nitrogen) into large sections, known as basal planes [34, 70, 122]. Other pyrolysis products identified during carbonization are H_2, NH_3, CO, CH_4 and C_4 hydrocarbons [57, 70]. The relative fractions of these gases have been shown by Bromley [57] to vary with the rate of heating. The structure of stabilized fibre changes from essentially amorphous to partly crystalline after heat treatment temperature (HTT) in the 1200 to 1500° C range and highly crystalline after HTT of > 2500° C.

Relatively long times have been reported in early patents for carbonization whereas modern practice is to pass stabilized fibres through an increasing temperature profile giving a total residence time of only a few minutes. In a 1970 patent issued to Great Lakes Corp. [35], the oxidized yarn was placed in a kiln and its temperature was raised to 1000° C in 4 h. For high-modulus fibres, the temperature was further raised to 2500° C in about 90 min and was kept at that level for 30 min. A more recent patent [123], however, described two furnaces, a vertical furnace maintained at 500 to 1000° C and a transverse furnace maintained at 800 to 2000° C, through which preoxidized strands are passed at a rate of 25 m h^{-1}. The furnaces had a length of 2 and 1.8 m, respectively, giving a total residence time of about 9 min. A process described by Ezekeil [124–127] for the preparation of high-modulus carbon fibres uses a short time (1 min) exposure of oxidized yarn directly to 2500 to 2900° C without going through 1200 to 1500° C carbonization. Many variations of conventional carbonization have been reported. Stretching of carbon fibres during the HTT of 2500 to 3000° C has been reported to result in improvement in mechanical properties of the fibre [3, 128, 129]. Other variations include heating by an electric current passing through the fibre where the yarn establishes a temperature of 1800 to 3000° C [130], application of vibrational energy to the fibres while they are held under tension (0.2 to 1.2 g/denier) during carbonization and carbonization under hydrogen [130] and in nitrogen diluted with about 5% acetylene [131]. Catalytic amounts of boron compounds used during carbonization have been reported to improve the mechanical properties of resulting carbon fibres [132]. Similarly, immersion of carbon fibres in liquid bromine followed by its removal with an inert gas was shown to result in an increase in the tensile strength of carbon fibres [133].

3. Shrinkage and shrinkage force during carbon fibre manufacture

In order to minimize the relaxation of molecular orientation during stabilization, the precursor fibres are longitudinally constrained. Two methods have been used widely for constraining the fibres. In one, the fibre is heat treated while constrained to constant length and in the other, the fibre is restrained by a constant force during heat treatment. In a continuous process the stabilization can be carried out by feeding and removing the fibres at the same speed from the heat-treatment zone. Although the same feed and take-up speeds are maintained, the fibres can undergo compensating local shrinkage and extension during this treatment. For stabilization of fibres under constant tension, weights are placed on the thread-line and the feed or take-up speed is adjusted so as to maintain the weight position. When the fibre is heated with both ends fixed, a certain amount of tension or shrinkage force is generated as a result of the tendency of the molecular chains to coil, the extent of which depends on the initial morphology of the precursor. This initial tension could relax even without allowance for any macroscopic shrinkage if the polymer chains are not part of a continuous network between the two fixed ends. When a constant load is applied during stabilization, the fibre could shrink if the applied load is less than the shrinkage force, extend if the load applied is greater than the shrinkage force or maintain the same length if the applied load balances exactly the shrinkage force generated. The response under both constant force and constant length conditions is complicated by the simultaneous occurrence of chemical reactions which can influence the mobility in the system and thus the shrinkage and shrinkage force.

Length changes during the heating of unspecified acrylic fibres at 220° C in air under a constant load have been reported by Watt and Johnson [134]. At low loads the fibres shrank while at higher loads the fibres initially stretched and then shrank. Fitzer and co-workers [135, 136] also observed the latter behaviour upon heating Dralon-T fibres under the highest permissible load short of actual rupture. Contrary to Watt and Johnson, who attribute the shrinkage to molecular relaxation, Fitzer and Heym suggest that the shrinkage, which follows the plastic flow due to tensile loading, is chemical in nature and is caused by dehydrogenation at the points of atacticity [137] and by intermolecular cyclization [135, 136]. The initially parallel chains rotate during cyclization to a position in which they form an angle of 120 degrees with each

other causing macroscopic shrinkage in the precursor. According to them a shrinkage of 13 to about 33% could result, depending on the type of ladder sequences formed. Layden [138] observed a different response from that observed by Watt and Johnson and Fitzer and co-workers during annealing of homopolymer PAN fibres. When small loads were applied, the fibre as it was heated to 270° C shrank initially, then stretched and finally shrank again. At larger loads, the fibre either shrank first and then stretched or just stretched without shrinking, depending on the magnitude of the applied load, and finally broke. Bahl and colleagues [36, 139] have reported a cumulative shrinkage of 27% for unidentified copolymer fibres and 34% for homopolymer fibres at 215° C in an oxygen environment. This shrinkage decreased when load was applied, showing a similar response as observed by Layden. The cumulative shrinkage was shown by them to consist of an instant initial or primary shrinkage of 3 and 10%, respectively, for copolymer and homopolymer fibres, followed by a slow secondary shrinkage. The primary shrinkage was found to be independent of the temperature and the atmosphere, whereas the secondary shrinkage was influenced by the temperature and environment. Both groups believe that the initial shrinkage is due to physical relaxation and that the secondary shrinkage is a result of chemical reactions similar to those suggested by Fitzer and co-workers [135–137]. Studies relating free shrinkage with the rates of heating have been reported by Fitzer and Heine [140].

The tension generated in a homopolymer PAN fibre during its heating to 270° C while held under constant length had been described by Layden [138]. Considerable tension was generated during heating to about 150° C, but it fell rapidly between 150 and 250° C and then rose again at 270° C, before levelling off finally with time. Warner *et al.* [141], using four different precursor fibres, observed an initial instantaneous shrinkage force and a delayed secondary shrinkage force when fibres were heated under constant length. The initial shrinkage force or tension depended upon the precursor processing history whereas the secondary shrinkage force was found to be related to stabilization kinetics. The increase of secondary shrinkage force with heating time was found to be parabolic in the case where the stabilized fibre cross-section was characterized by a two-zone morphology and linear when the fibre changed colour uniformly over the entire cross-sectional area. It was possible to define a temperature range for each type (and denier) of fibre, with the secondary shrinkage force increasing linearly with time in the lower temperature range and parabolically in the higher temperature range. The rate of increase in secondary shrinkage force was found higher for fibres drawn to higher draw ratios (lower denier), showing a linear relationship with the inverse of the square root of denier of the fibre. When the precursor fibre was passed continuously through a furnace with a temperature gradient from 230 to 290° C, different local velocities were observed throughout the hot zone in spite of the same feed and take-up velocities. The fibre shrank first, causing an increase in its denier, then it drew and finally it shrank again. This behaviour has been explained with the help of a model of fibre response. An oriented semi-crystalline fibre, when subjected to a temperature gradient between the feed and take-up rolls rotating at the same speeds, will first decelerate in the vicinity of the glass transition temperature (T_g) owing to entropic recovery and then accelerate to compensate for the decrease in its velocity. Chemical reactions produce a secondary shrinkage requiring a compensating amount of additional draw which occurs at the region in the threadline where the fibre offers the least amount of resistance (i.e., in the unreacted acrylic material after entropic shrinkage and not in the stabilized material). Recent papers by Takaku *et al.* [142, 143], where they have reported contractive stresses at different temperatures, show behaviour similar to that observed by others [36, 138, 141] at short times, but at longer times the stress due to secondary shrinkage reaches a maximum and shows a decrease on further heating. The peak position shifted to shorter times at higher temperatures, disappearing completely when the temperatures employed were as high as 280 to 290° C.

During carbonization of fully stabilized fibres a small (4 to 6%) shrinkage is observed. A higher shrinkage is seen if the fibres are incompletely stabilized. The additional shrinkage due to the continuation of stabilization reactions can, however, be controlled by the application of suitable loads during carbonization. Bromley [57] has shown the effect of rate of heating during carbonization on the length changes under various loads. Pyrolysis (up to 1000° C) of oxidized Courtelle fibres by heating at the rate of 40° C min^{-1} resulted in shrinkage under low loads but in extension under high loads over the temperature range 300 to 500° C. On slower pyrolysis, i.e. by heating for 30 min at a given temperature before it was raised a further 30° C, only shrinkage was observed even under high loads. Manocha *et al.* [37] observed that understabilized 6% methyl acrylate copolymer fibres shrank about 12% during carbonization which was reduced to 5% when the time of oxidation was increased and to 2% by the application of load during carbonization. Whether the precursor was allowed to shrink or was stretched during preoxidation had no effect on carbonization shrinkage. However, the same authors have reported, in a later publication, a large dependence of carbonization shrinkage on the amount of shrinkage allowed during the preoxidation of Beslon fibres [139]. High shrinkage during oxidation resulted in low carbonization shrinkage but when shrinkage during oxidation was suppressed by the application of load, a large shrinkage was observed during carbonization.

4. Development of carbon fibre structure

4.1. Structure of PAN fibres

The literature contains several references [144–156] to X-ray diffraction studies of PAN but few definite conclusions have been reached as to the crystal structure of this polymer. Typical wide-angle X-ray diffraction (WAXD) photographs of oriented fibre display an

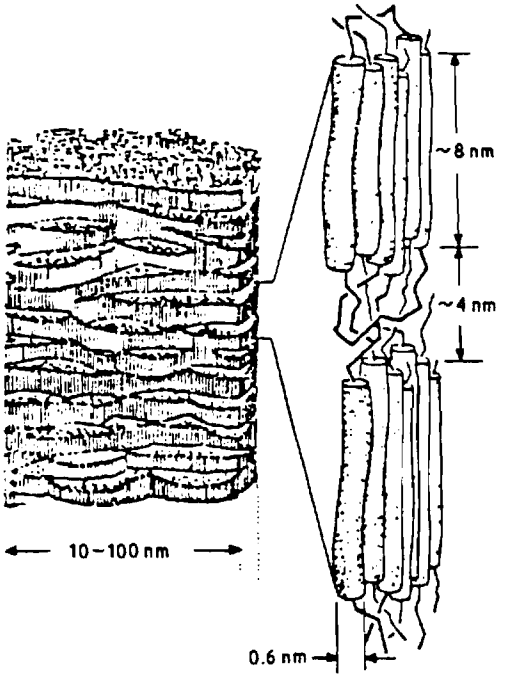

Figure 1 Morphological model of PAN fibre by Warner *et al.* [158], showing ordered and disordered regions.

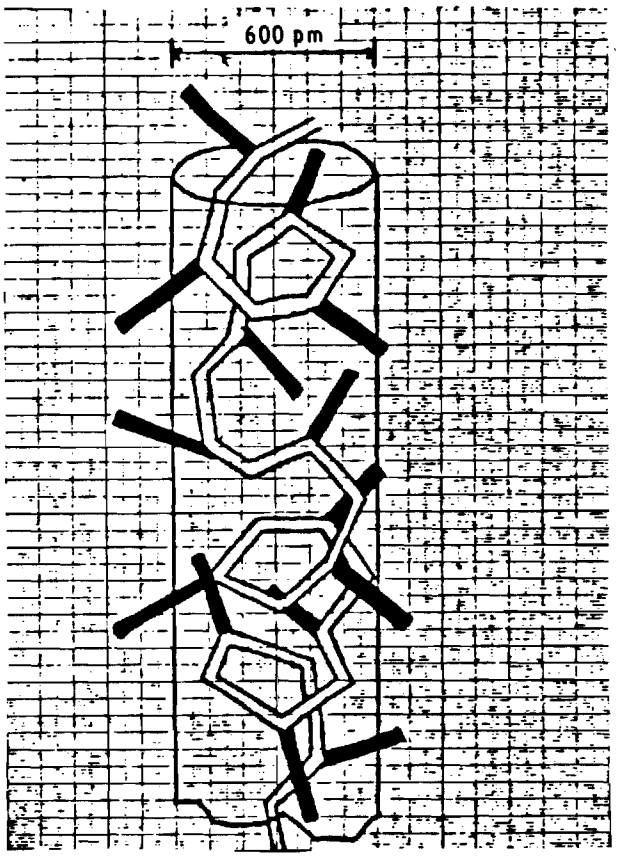

Figure 2 Irregular helix structure of PAN chains suggested by Olive and Olive [168].

intense and a faint arc at the equator which correspond to lattice spacings of approximately 0.52 and 0.3 nm, respectively [157, 158]. Off-equatorial reflections are usually absent, indicating the presence of only lateral order. Nevertheless, two types of unit cells, hexagonal [159] and orthorhombic [144, 148], have ben proposed by early workers. Holland *et al.* [154] were the first to grow single crystals of PAN, of platelike texture, from a propylene carbonate solution. A stack of these gave only equatorial reflections on X-ray and electron diffraction [155]. The absence of off-equatorial reflections has been attributed by Lindenmeyer and Hosemann to the paracrystalline nature of these single crystals [146]. Recent X-ray studies by Kumamaru *et al.* [153] on single crystals grown during solution polymerization of acrylonitrile (AN) have, however, shown equatorial as well as meridional reflections. This three-dimensional order has also been reported in highly oriented films and fibres by others [144, 149, 160]. The unit cell proposed in some of the recent studies is orthorhombic, but different lattice parameters have been suggested by different researchers. A three-dimensional orthorhombic unit cell with a = 2.148, b = 1.155 and c = 0.710 nm, has been proposed by Colvin and Storr [149] from their X-ray studies of PAN fibres. Based on this unit cell, the calculated crystalline density of PAN is 1.19 g cm^{-3}, which agrees quite well with the values quoted in the literature [161, 162].

Spherulites have been observed by Holland [163] and by Gohil *et al.* [164] in thin films of PAN, whereas fibres have been shown to possess a fibrillar structure. Precipitation of fibres from solution generates a spongy network which collapses and is drawn out during the stretching operation to produce a fibrillar morphology in PAN fibres [165]. Small-angle X-ray scattering studies reveal the presence of elongated micropores in these fibres. The fibrils, 10 to 100 nm diameter [166], and the micropores are aligned parallel to the fibre axis. A model proposed recently by Warner *et al.* [158] describes the fine structure within a typical fibril, where the ordered and disordered regions are connected along the fibre axis. The parallel rods constitute the major part of the ordered phase in a fibril. The rods are not in perfect alignment with respect to the rod ends, but rather exhibit some misalignment as depicted in Fig. 1. The disordered regions connecting the rods consist of loops, folds, entangled chains, defects, comonomer sequences, tie chains etc. The lateral dimensions of the ordered domains as estimated from WAXD data are in the range of 5 to 20 nm, depending on the thermal history of the precursor fibres. The length of these domains is of the other of 8 to 10 nm, roughly twice that of the disordered regions. The rod diameter is proposed to be approximately 0.6 nm based on WAXD [158, 167] and molecular model studies [158]. The large dipole moment of the nitrile groups, together with their close proximity in space, leads to very large intramolecular dipolar and steric repulsions which compel the individual macromolecules into a somewhat helical conformation [168]. As indicated in Fig. 2, the twisted, kinked molecule may be thought of as a more or less rigid structure, fitting within a cylinder, which is not appreciably deformed on drawing. The random orientation of nitrile groups in space in this model explains the observed low infrared dichroic ratios [156, 169, 170] and optical birefringence [156–170].

Commercial PAN precursor fibres are rarely

pure but contain up to 10% comonomer. X-ray scattering peaks are broader [150, 151] and the extents of crystallization lower [150] in copolymers than in pure PAN. The accuracy of extents of crystallization as estimated from the area under the diffraction peak is, however, debatable in PAN polymer and fibres. Amorphous PAN polymer, prepared by using organometallic catalysts, gives rise to diffuse X-ray diffraction peaks [152] which overlap with the crystalline peaks, making the measurement of crystallinity highly unreliable in PAN polymer and fibres. The calculation of crystallinity using density measurements, frequently used in semi-crystalline polymers, fails in the case of PAN due to similar densities of the crystallized and uncrystallized samples [172, 173]. Differential scanning calorimetry (DSC) has often been used to estimate the extent of crystallization in semi-crystalline polymers from the area under the melting curve. This technique is also not suitable for PAN fibres due to their degradation before melting. A novel method has, however, been employed recently by Frushour [174, 175] where the melting behaviour of PAN copolymers is studied by DSC in a pressure cell containing water, which depresses the melting point of PAN by over 100° C [174], shifting it to well below the degradation temperature. This technique has been claimed to be very sensitive to even small differences in crystallinity. Even though absolute measurements of the extents of crystallization are still not possible, this technique may prove useful for relative measures of the extent of crystallization through a comparison of plasticized heat of melting values in PAN fibres.

4.2. Transformation of structure during carbon fibre manufacture

During oxidative stabilization and subsequent carbonization of PAN-based precursor fibres, the linear chain structure is transformed to a planar structure. Rings are formed due to the cyclization of nitrile groups of PAN during stabilization, followed by their aromatization and condensation during carbonization to give planar sections oriented along the fibre axis. The new structure is a consequence of chemical as well as morphological transformations.

4.2.1. Transformation during stabilization

Wide- and small-angle X-ray and electron diffraction have been employed to study the morphological changes during stabilization. The intensity of the main equatorial reflection at $2\theta = 17°$ from the (1 0 0) planes of PAN lattice shows an initial increase followed by a continuous decrease during stabilization [17, 158]. The spreads of the (1 0 0) reflection in the radial and azimuthal directions have been used to estimate the size and the orientation, respectively, of the laterally ordered phase in the precursor. Subsequent changes in them during stabilization of the precursor have been measured as a function of stabilization time or stabilization temperature. The method, however, is limited to the early part of stabilization due to complete disappearance of this reflection towards the end of stabilization. Rose [17] observed an initial increase followed by a continuous decrease in the orientation of the ordered phase as a function of heat-treatment temperature during stabilization in air. Thorne and Majoram [176] observed similar trends as a function of extent of reaction carried out in a nitrogen atmosphere, estimated by the amount of reacted nitrile groups from infrared spectroscopic measurements. They also studied the changes in the birefringence of precursor fibres during their heat treatment. A high birefringence of the new species formed as a result of chemical reactions would result in the high birefringence values of the annealed fibres even when the overall orientation remains unchanged. The data of Thorne and Marjoram, when replotted to give the birefringence of the species appearing in stabilization, indicate that the orientation of the new species appearing throughout the conversion is significant and that this orientation lies within a narrow range (Fig. 3).

Use of small-angle X-ray scattering (SAXS) has also been described in the literature for characterizing the morphological changes during stabilization. Such studies, although useful in identifying the superstructure which exists in the precursor fibres, reveal very little in terms of the morphology of the stabilized fibres. SAXS studies with wet-spun acrylic fibres show scattering from microvoids that is typical of wet-spun fibres [177, 178]. The characteristic long period reflecting a periodic density fluctuation which one normally observes in oriented synthetic fibres is, however, absent in these fibres. If the difference between the densities of the laterally ordered domains and the regions where such order is absent is very small [172, 173], SAXS would fail to differentiate between the presence and absence of any ordered sequence of these domains. Upon heat treatment of acrylic fibres in air or in an inert atmosphere, a meridional reflection appears which corresponds to a length of 8 to 16 nm of the scattering unit [158, 178–181]. The lateral dimensions of this scattering unit, calculated from the breadth of the reflection using the Scherrer equation, was found to be of the order of 6 nm [178, 179]. The intensity of this reflection goes through a maximum with time or temperature of heating.

According to Fillery and Goodhew [178], the spacing corresponding to the meridional streak varied with the precursor type, being 9.8 and 16.3 nm in the case of Courtelle and Dralon-T fibres, respectively. A size of 8 nm has been reported by Tyson [179] when unspecified commercial fibres were employed. Hinrichsen [180] also studied a number of commercial fibres and found apparent long periods ranging from 11 to 16 nm. When Dralon-N fibres drawn at 100° C were employed, the shape and size of the meridional reflections varied with the precursor draw-ratio, suggesting that the precursor morphology plays an important role in the development of long period. Warner *et al.* [158] studied the SAXS from two commercial fibres, coded fibre M containing 7% vinyl acetate and fibre C containing a small amount of an acid comonomer. The maximum intensity of meridional reflection was observed after 90 min in fibre M as opposed to 20 min in fibre C when heated at 220° C in air. The corresponding spacings in the two cases were 13.9 and

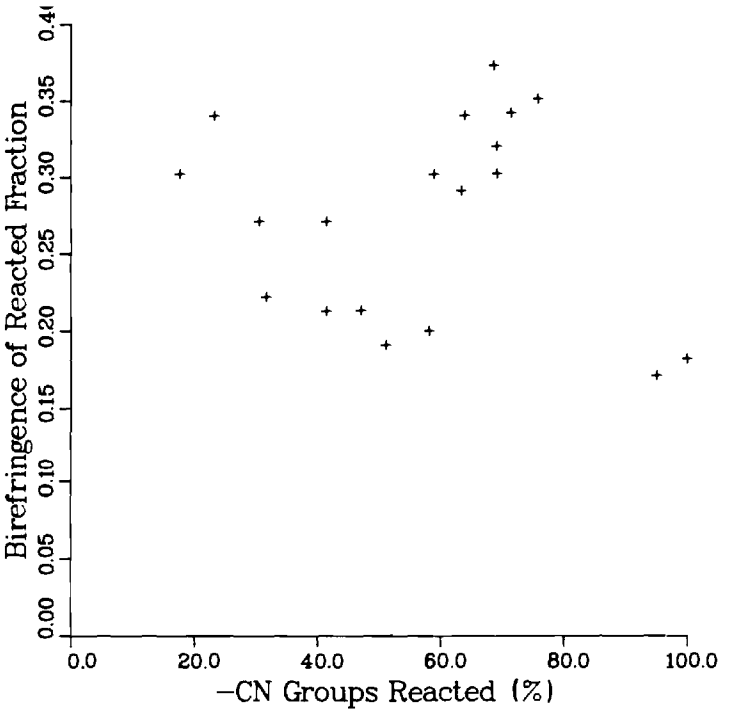

Figure 3 Replotted data of Thorne and Majoram [176] showing the birefringence of species appearing in stabilization.

8.8 nm, respectively. They explain the observed differences in intensity and spacing of the meridional reflections in the two commercial fibres in terms of both the differences in the stabilization mechanisms due to the different comonomers present in them and the possibly different starting morphologies of the two precursors.

The origin of the apparent long period observed in the above studies has not been shown precisely. Tyson suggests recrystallization and chain folding as the cause for the appearance of long period during pyrolysis. Fillery and Goodhew believe that the scattering intensity is controlled by the unreacted inner core and is influenced by the fibre diameter. Hinrichsen [180] proposes the intensification of the two-phase structure as a result of annealing close to the melting point and/or a change in the density of one of the phases due to selective reaction, either within the more ordered or in the less ordered regions, as the cause for the long period. As the chemical reactions proceed in the other phase, the density difference will diminish resulting in the disappearance of the long period in the later stages of stabilization. This explanation seems to be consistent with the appearance and disappearance of the long period.

4.2.2. Transformation during carbonization

During the carbonization stage, basal planes oriented along the fibre axis are formed, giving rise to the appearance of diffuse low intensity peaks at $2\theta = 26°$ and 44°. These reflections are indicative of relatively low lattice order and may be regarded as incipient (0 0 2) and (1 0 0) reflections of the graphite-like structure. The layer planes possess an interplanar distance of approximately 0.34 nm in carbon fibres (see Table I), slightly more than in pure graphite. This distance between the layer planes is indicated by $c_0/2$ based on the terminology used in X-ray studies of

TABLE I Wide-angle structural parameters for carbon fibres

C-fibre type	HTT* (°C)	Young's modulus (GPa)	L_c (nm)	$c_0/2$ (nm)	Z	$-q$	$L_{a\parallel}$ (nm)	$L_{a\perp}$ (nm)	Reference
GY-70	–	530	9.0	0.342	–	–	–	–	[218]
Type I	2500	390	5.3	0.350	20	0.78	9.8	8.0	[188]
Type II	1500	250	1.7	0.360	41	0.55	3.9	2.7	
Type III	1000	210	1.2	0.370	41	0.51	3.2	1.9	
Type I	2700	–	–	–	–	–	11.9	6.4	[199]
Type II	1250	–	–	–	–	–	3.5	3.4	
RR	2800	434	6.0	–	–	–	7.0	–	[189]
	2400	386	4.0	–	–	–	6.2	–	
	2400	338	3.4	–	–	–	5.4	–	
	1400	248	1.8	–	–	–	3.5	–	
	1000	214	1.0	–	–	–	2.0	–	
C	3000	483	11.2	0.3397	–	–	14.2	13.9	[170]
B	2750	434	9.3	0.3408	–	–	13.0	12.2	
A	2500	400	7.0	0.3414	–	–	8.8	8.1	

*Final heat-treatment temperature during their manufacture.

fibres lacks three-dimensional order and is termed "turbostratic graphite". The layer planes in a turbostratic structure are randomly rotated with respect to each other, as shown in Fig. 4b. The stack height of the layer planes, L_c, has been estimated from the radial spread of the (0 0 2) reflections by substituting the full width at half maximum (FWHM) intensity, B_{002}, in the Scherrer equation [178],

$$L_c = K\lambda/(B_{002} \cos \theta)$$

where λ is the wavelength of X-rays and θ is the Bragg angle. K, the Scherrer parameter, can be considered as a factor by which the apparent size must be multiplied to obtain the true size. For (0 0 l) type reflections, K is generally given the value of 0.9 for FWHM or 1.0 for integral breadth. The (1 0 0) reflection is spread into a ring because of the turbostratic packing of graphitic layers. The layer plane length, L_a, parallel to the fibre axis is given by substituting the meridional width B_{100}(m) in the Scherrer equation. Similarly, the equatorial width B_{100}(e) is used to obtain the layer-plane dimension, $L_{a\perp}$, perpendicular to the fibre axis. K values for (h k 0) reflections vary with preferred orientation and have been evaluated by Johnson [183] and by Ruland and Tompa [184, 185]. The azimuthal spread of the (0 0 2) reflection is caused by the presence of the azimuthal direction can be converted to a parameter, q, which varies from + 1 for perfect orientation perpendicular to the fibre axis, through 0 for random orientation, to − 1 for perfect orientation parallel to the fibre axis [186]. A simpler and more commonly used parameter for preferred orientation is Z, the FWHM in degrees, which is a measure of the average misalignment of the basal planes with respect to the fibre axis. The average tilt angle of the basal planes from the fibre axis is approximately $Z/2$.

Both L_c and L_a have been found to be low, of the order of 1 to 1.5 nm and 1.5 to 2.5 nm, respectively, up to a carbonization temperature of 800° C [34, 187]. A slight tendency towards increase in L_a from 1.9 to 2.5 nm during pyrolysis between 320 and 800° C has been reported by Watt *et al.* [34]. The dimensions of L_c and L_a, however, increase significantly upon graphitization. Table I lists various WAXD parameters for PAN-based carbon fibres obtained by different researchers. A general trend of increase in stack height and orientation of basal planes with increase in the heat-treatment temperature is quite evident [188, 189].

A relationship between the Young's modulus of carbon fibres, corrected for porosity using the assumption that the effect of pores on the modulus is essentially only an increase in the fibre cross-section,

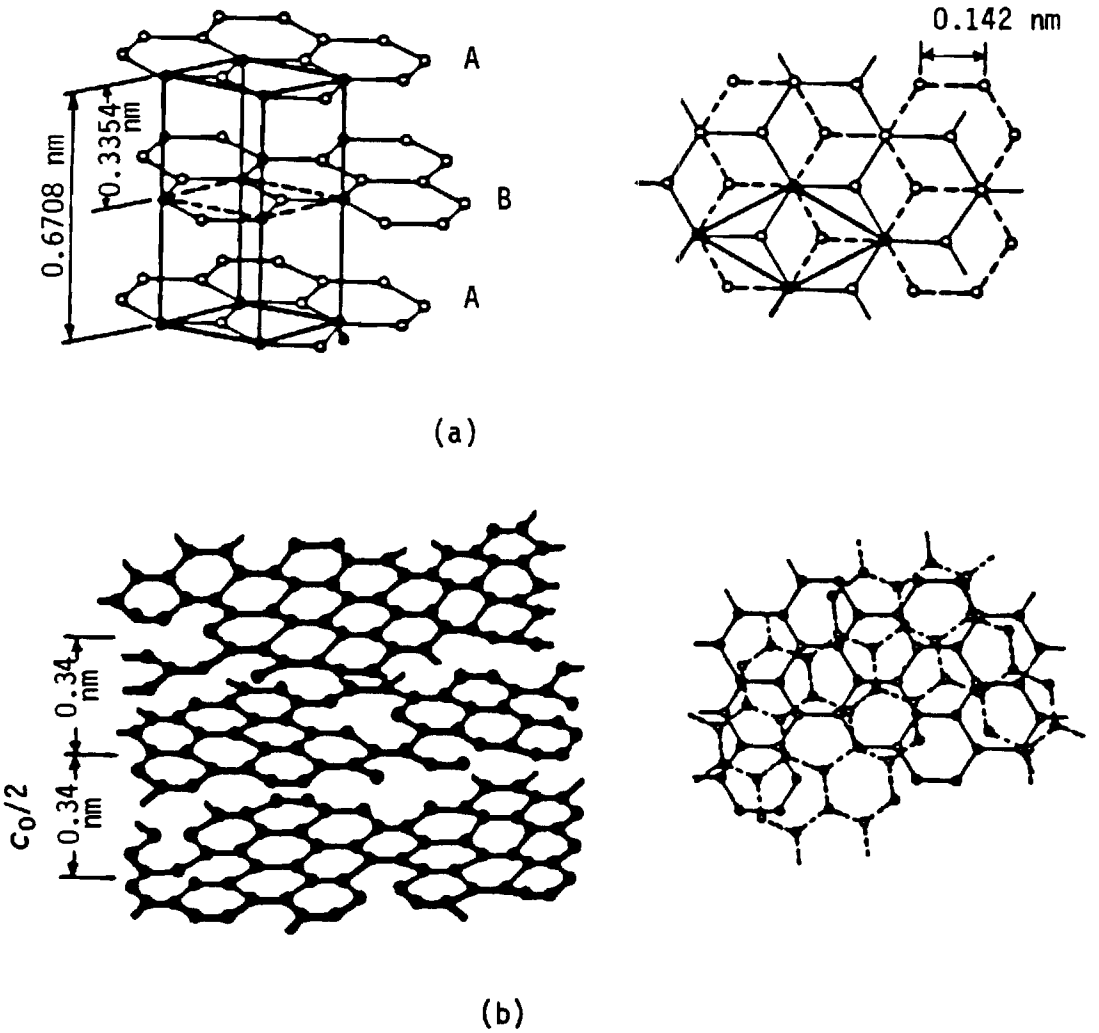

Figure 4 Arrangement of basal planes in carbon. (a) Graphitic carbon, (b) turbostratic carbon.

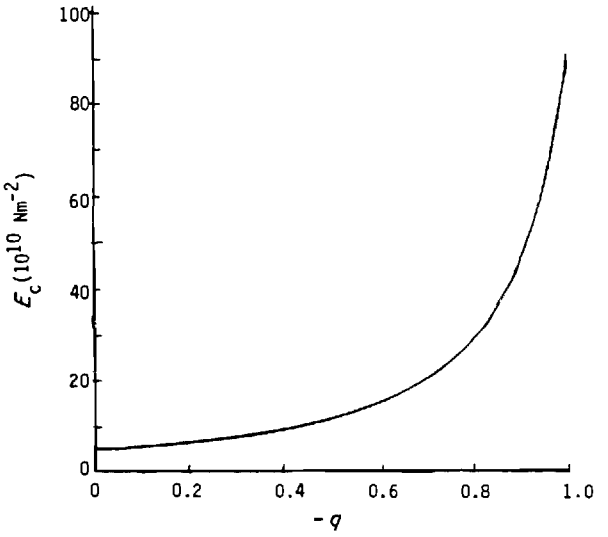

Figure 5 Plot of Young's modulus against orientation parameter of carbon fibres (Ruland [191]).

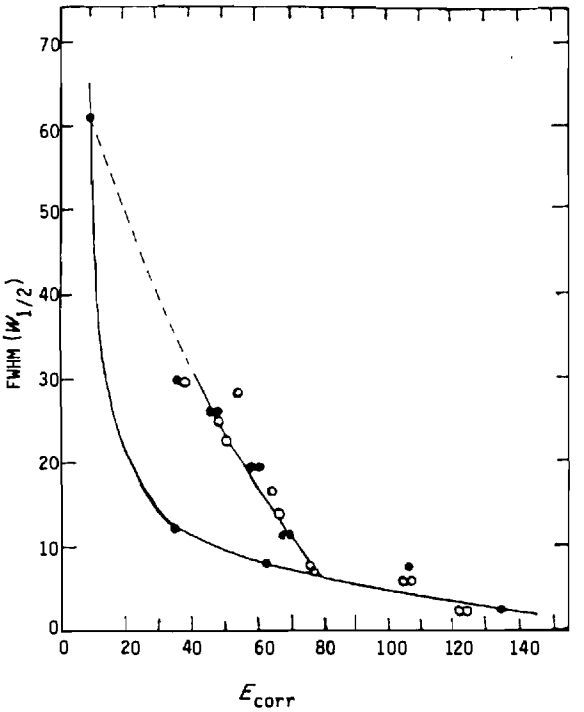

Figure 6 Plot of FWHM ($w_{1/2}$) against Young's modulus of carbon fibres. (Diefendorf and Tokarsky [192]). (●) Rayon base, (○) Courtelle PAN, (●●) Orlon PAN, (○○) experimental PAN.

and the orientation parameters has been observed by Fischer and Ruland [190, 191] (Fig. 5). This relationship, according to their observations, holds for carbon fibres of various precursors, heat treatments and preferred orientations. Diefendorf and Tokarsky [192], on the contrary, observed that only cellulose-based carbon fibres adhere to the Ruland-type relationship, while PAN-based fibres show a significant deviation (Fig. 6). This difference, they suggest, is caused by a gradient in preferred axial orientation present in PAN-based carbon fibres.

Skin-core heterogeneity in high modulus carbon fibres has been studied by Johnson's group [193–195] by measuring structural parameters in the interior and the surface from selected-area electron diffraction patterns after the application of peak resolution procedures. The crystallites in the skin (about 5% of the radius of the fibre) were found to be larger and more highly oriented than those in the core. Wicks and Coyle [196, 197] studied the size and the orientation of layer planes at various depths in single carbon fibres thinned to a "pencil point" taper using a flame-polishing technique. The results using X-ray and electron diffraction techniques suggest an inner region or core characterized by a relatively low axial alignment and large crystallite size and an outer sleeve or sheath of material of high preferred axial orientation and low average crystallite size. The larger crystallite size in the core compared to the sheath, however, is in total contradiction to the observations by Bennett and Johnson [193] where the crystallites in the core region were found smaller than in the sheath.

The presence of micropores in carbon fibres is indicated by an intense lobe-shaped scattering in the small-angle X-ray scattering (SAXS) photograph. These pores are shown to thin and needle-like, being longer in general than the crystallites which bound them [198–201]. From small-angle powder diagrams, three small-angle parameters have been calculated by Johnson and Tyson [198, 200] using the methods of Debye and Porod [202–205]. Porod has defined a "distance of heterogeneity", l_p, in terms of the integral width of the correlation function $C(r)$ (which is related to the probability that a line of length r will have both ends situated in pores) as

$$l_p = 2\int_0^\infty C(r)\,dr \quad \text{where } C(r) = \exp(-r/a)$$

a is a correlation length which can be determined from the slope to intercept ratio of the $I^{1/2}$ against θ^2 straight-line relationship (Fig. 7). The average chord lengths of the pore and the carbon region, l_p and l_c, respectively, and the surface area per unit mass inside the fibres, S_v, can then be calculated by using the relationships

$$l_p = 2a, \quad l_c = a/(1 - D)$$
$$\text{and} \quad S_v = 4D(1 - D)/a$$

where D is the fraction of fibre occupied by carbon, usually approximated by the ratio of the fibre density to the bulk graphite density. More rigourous methods which make use of the small-angle fibre diagrams have been described by Perret and Ruland [199, 201]. Table II lists the values of the above small-angle structural parameters in PAN-based carbon fibres reported by various authors. No comparisons between different data are possible due to lack of details about the precursors and the conditions for their conversion to carbon fibres. In general, the results give an idea about the relative sizes of the pores and the crystallites, which have also been confirmed by electron microscopic measurements [134, 188, 190, 198, 206–208]. An increasing trend in l_p and l_c parameters and a decrease in pore surface area with increase in treatment temperature is quite evident from Johnson and Tyson's results [188, 189, 200]. Ruland [199, 209] has attributed the increase in l_p and l_c at high temperatures

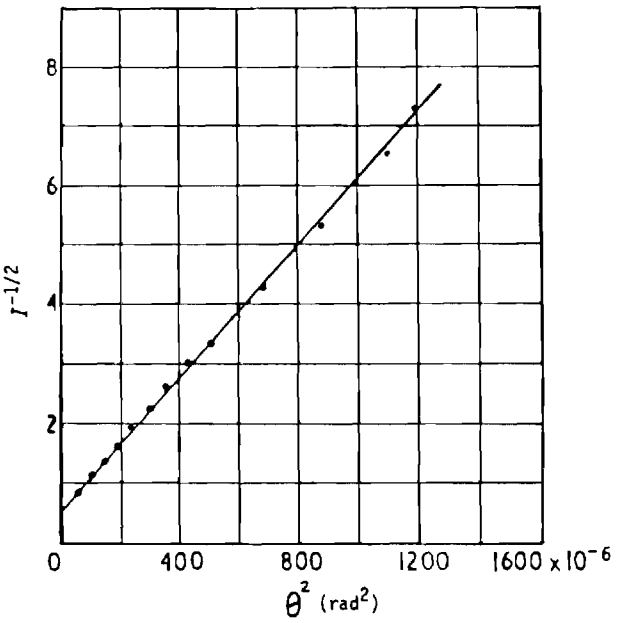

Figure 7 Plot of $I^{-0.5}$ against θ^2 for low-angle powder-type diffraction from graphitized fibres Type A [198].

to the elimination of smaller pores, with a simultaneous increase in the crystal size through "elastic unwrinkling". The fraction of pores is about 10% of the total volume of fibres, which is of the same order as the value (15%) of internal porosity closed to helium gas reported by Spencer *et al.* [210].

4.3. Structure of carbon fibres

The structure and properties of carbon fibres depend on several factors, the most important of which are the heat-treatment temperature (HTT) and the type of precursor used. Among polyacrylonitrile (PAN)-based carbon fibres, two types, i.e. high modulus or type I (2500 to 3000° C) and high strength or type II (1200 to 1600° C), have been widely employed for detailed structural studies. The development of structure in carbon fibres, which also decides their properties, depends on the process conditions employed during their manufacture. A knowledge of fibre structure in three dimensions, from the scale of the fibre diameter to at least the ultra-structural level, is therefore essential if the process is to be optimized for desired fibre properties. The moduli of individual fibres will depend on the details of the preferred axial orientation in each fibre structure, while the strength will be a function not only of preferred orientation but also of the flaws and the textures and the gradients in structure present. The techniques employed for structure determination in carbon fibres include electron spin resonance [207, 208], neutron [213], electron and X-ray diffraction and optical and electron microscopic examinations.

Optical microscopy of thin transverse sections of carbon fibres from fully stabilized Courtelle and Orlon fibres displayed extinction crosses when viewed under polarized light which, according to LeMaistre and Diefendorf [214], suggest an onion-skin type cross-section with the basal plane showing a preferred orientation parallel to the fibre surface. Commercially produced carbon fibre, on the other hand, displayed a radial texture in the core while a circumferential orientation of basal planes was present in the sheath. Wicks and Coyle [197] have reported at least four types of layer plane arrangements in various filaments of a commercially produced tow of high modulus PAN-based carbon fibres. Knibbs [215], however, has claimed that by varying the process conditions, the type of texture can be altered, varying from a circumferentially arranged sheath with an isotropic or radially oriented core to a circumferential orientation throughout the cross-section. The skin–core heterogeneity in high modulus carbon fibres has been confirmed by others with scanning electron microscopy (SEM) of fractured [192, 193, 197, 216, 217] and oxygen plasma etched [217, 220] specimens. Johnson [221], on the contrary, discounts the presence of radial heterogeneity and has proposed a random arrangement of crystallites. According to his experiments, similar amounts of erosions were observed in the sheath and core upon etching with argon ions for short erosion times (less than 60 min) and they appeared uniform in electron microscopical observations. He suggests that the Maltese cross pattern observed in the polished cross-sections of carbon fibres is caused not by structural anisotropy but by strain birefringence. The radial stresses in the fibre cross-section which lead to strain birefringence are probably caused by the differential shrinkage, during

TABLE II Structural parameters for carbon fibres from SAXS studies

C-fibre type	HTT* (° C)	Young's modulus (GPa)	l_p (nm)	S_v (m^2 cm^{-3})	l_c (nm)	Reference
GY-70	–	530	1.6	490	7.3	[218]
Type I	2500	390	2.5	–	–	[188]
Type II	1500	250	1.4	–	–	
Type III	1000	210	0.9	–	–	
Type I	2700	–	1.5	226	12.4	[199]
Type II	1250	–	0.7	454	6.4	
RR	2800	434	2.8	340	10.0	[189, 200]
	2400	386	2.9	363	8.6	
	2000	338	2.5	485	6.7	
	1400	248	1.2	1100	3.4	
	1000	214	0.9	1450	2.6	

*Final heat-treatment temperature during their manufacture.

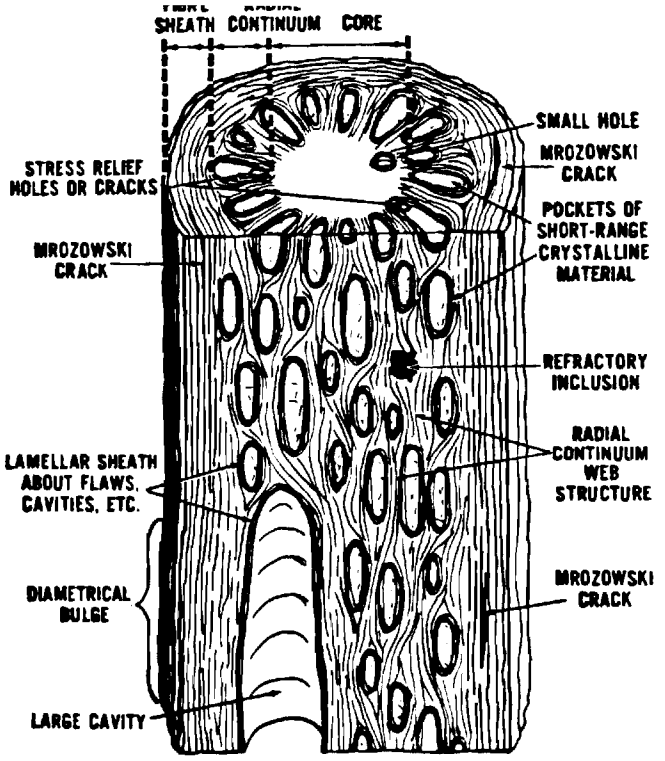

Norr [220].

carbonization and subsequent cool down, between the oxygen-rich surface and the partially oxidized core. A three-dimensional structural model for high modulus PAN-based carbon fibres was proposed by Barnet and Norr [219, 220] based on electron microscopical observations of oxygen plasma-etched fibres. The artefacts produced by etching were interpreted as originating from a highly crystalline sheath surrounding a radial structure of crystalline webs separated by large voids (Fig. 8).

Several other structural models of carbon fibres have been proposed by various researchers [198, 199, 214, 222–225]. These models are based on X-ray and electron microscopical examinations of carbon fibres. A schematic illutration of the model proposed by Johnson and Tyson [198, 200], based on the wide- and low-angle X-ray scattering of high modulus carbon fibres is shown in Fig. 9. The idealized tetragonal-shaped crystals, approximately 7 nm in size, enclose sharp-edged voids, about 1 nm wide. Extinction bands orthogonal to the crystal direction were observed in phase contrast microscopy which suggest the presence of subgrain boundaries between the crystals with both tilt and twist components. Perret and Ruland [199], however, disagree with this model and propose, based on their X-ray and electron microscopical observations, a ribbon-type structure for PAN-based carbon fibres. The basic unit of Ruland's model is a ribbon of sp^2 type carbon with an average width of 5 to 7 nm. The ribbons are slowly undulating and contain straight parts with lengths in the 6 to 13 nm range depending on the preferred orientation. An extensive parallel stacking of these ribbons, which has also been observed by others [134, 198, 206, 207, 218], is suggested. These ribbons pass smoothly from one domain of stacking to the other, as shown in Fig. 10. The space between the contours of these parallel stacks gives rise to needle-shaped pores or voids which are considerably longer than the average straight parts of the ribbons. Similar models have been suggested by Hugo *et al.* [213] and by Diefendorf and Tokarsky [192]. The structural units of the model proposed by the latter authors are microfibrils which are made of 10 to 30 basal planes in the form of ribbons (Fig. 11). For low

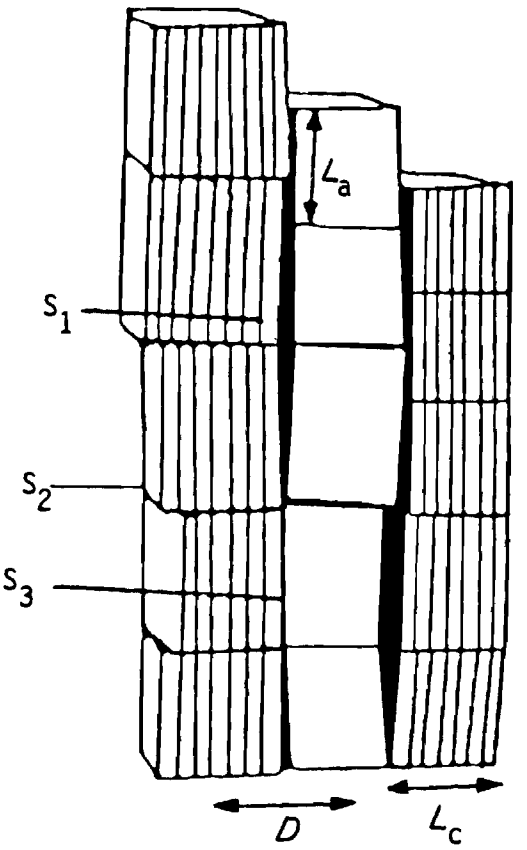

Figure 9 Model of carbon fibres; tetragonal crystals and sharp-edged voids [198].

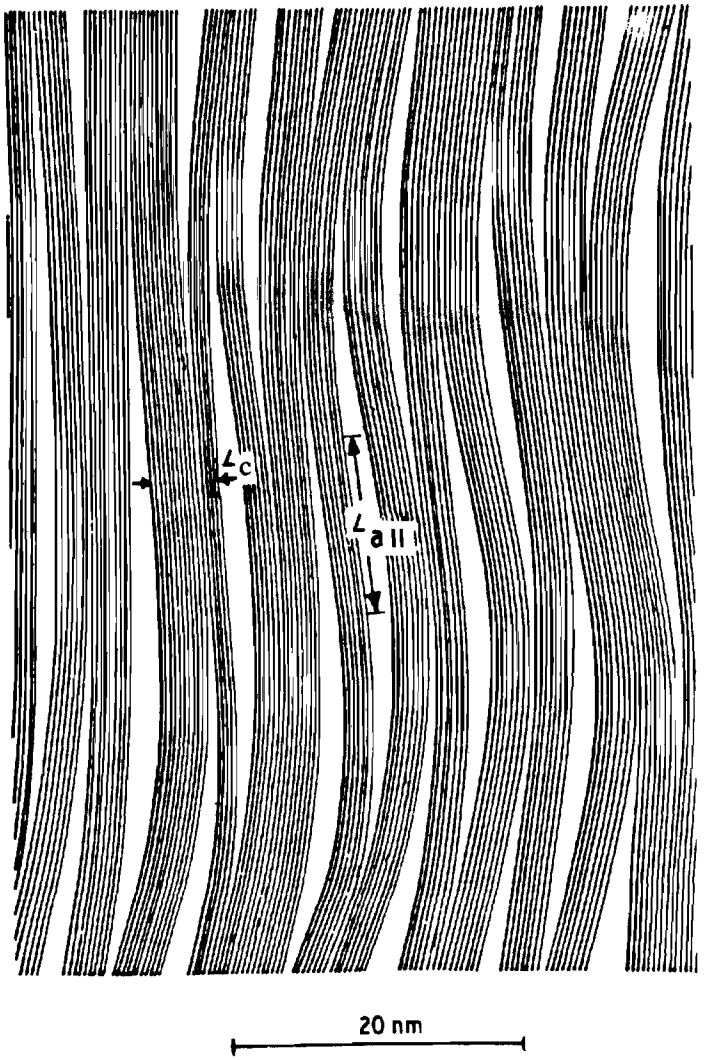

Figure 10 Ribbon model of carbon fibres suggested by Perret and Ruland [199].

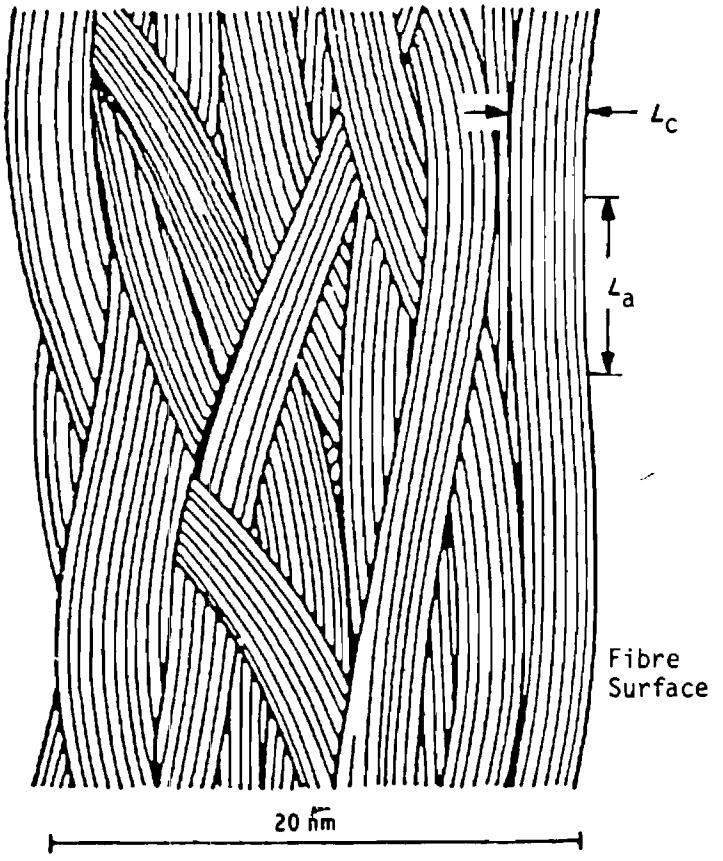

Figure 11 Structural model of carbon fibres suggested by Diefendorf and Tokarsky [192] showing microfibrils.

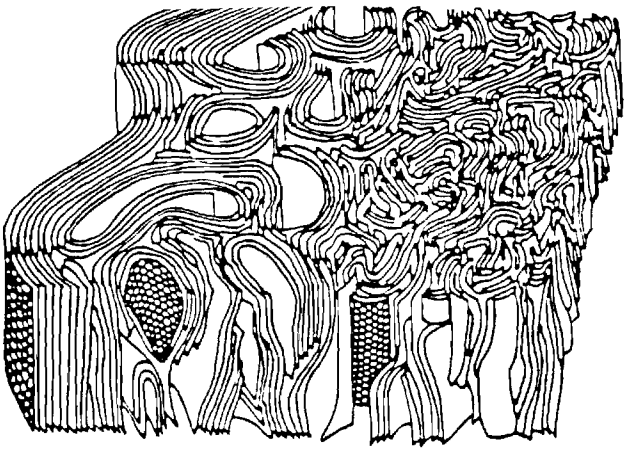

Figure 12 Schematic illustration of model derived by Bennett and Johnson from electron microscopic observations [194].

modulus (40×10^6 psi, $\sim 2.76 \times 10^5$ N mm^{-2}) fibres, the ribbons are typically 13 layer planes thick and 4 nm wide, whereas the corresponding dimensions increase to 30 layers and 9 nm for high modulus (100×10^6 psi, $\sim 6.89 \times 10^5$ N mm^{-2}) fibres. The microfibrils undulate, the amplitude of undulation being greater than the wavelength in high strength fibres, becoming smaller in high modulus fibres due to dewrinkling of the ribbons [224]. An increase in the orientation of (0 0 2) planes with increase in the fibre treatment temperature [186, 188, 208] supports this hypothesis. Based on their bright- and dark-field transmission electron microscopy (TEM) of high modulus fibres, Diefendorf and Tokarsky [192] and Oberlin *et al.* [225] proposed that wrinkled sheets rather than ribbons describe better the structure in these fibres. A schematic model, as shown in Fig. 12, was drawn by Bennett and Johnson [194] after combining the observations from high-resolution electron microscopy which included dark- and bright-field image analysis and specimen tilting procedures. The layer planes in crystallites, oriented along the fibre axis, are shown to interlink in a highly complex manner, giving a range of crystallite sizes enclosing an intricate void system.

In addition to the microfibrillar structure discussed in the preceding paragraphs, morphological features with dimensions much larger than those of the microfibrils have been observed in microtomed sections of carbon fibres of various origins and degrees of graphitization [134, 206, 207, 226]. They are usually referred to as secondary fibrils and their dimensions are estimated to be in the range 20 to 100 nm. Mencik *et al.* [227], however, based on their low-resolution TEM studies, suggest that secondary features larger than the graphite fibrils [1.5 to 15 nm) are artefacts created by the interaction of the knife with the fibres during microtoming.

The observations of carbon fibre structure by various researchers are contradictory at times. In most cases, the type of precursor fibres, their structure and conditions for converting them to carbon fibres are not disclosed. It is known that these parameters have substantial influence on the development of structure in carbon fibres. The concept of basal planes forming ribbons or sheets, arranged parallel to the fibre axis direction in some fashion, has been well substantiated from X-ray and electron microscopic studies by several workers. A sheath–core structure having different arrangements of these basal planes in the skin and the inside seems possible with certain precursors and processing conditions, while some other precursor and conditions could as well result in an isotropic cross-section of the carbon fibres. It would be erroneous to presume that the morphologies of all the carbon fibres produced from different precursors and under different conditions would correspond to any one of the proposed morphological models.

5. Tensile properties of carbon fibres

5.1. Methods of testing

For comparing the tensile strengths of various carbon fibres, it is important to understand the test methods involved and the test specimen used. The tensile testing of single filaments is laborious because of the fragile nature of the fine filaments (typically 6 to 10 μm diameter). The method has, however, been used extensively in testing experimental fibres in research and development. There is a standard ASTM specification (ASTM-3379-75) for the preparation, mounting and testing of high modulus single filament materials of over 20 GPa (3×10^6 psi) Young's modulus. In testing yarns and tows comprising many hundreds or thousands of filaments, a portion of the tow is selected which is passed through a resin bath, dried and cured. The cured specimens in the form of rods are then tested using a tensile tester with rubber-faced clamps for tight grasping of these composite rods without crushing. Alternatively, a large diameter collar of liquid resin, fitting within a smaller receptacle on the testing machine, is cast on the exposed fibre ends for a good grip while testing [228–229]. Dry strand testing of fibres was pursued by McMahon [230], who compared the test data of the impregnated strands of carbon fibres with dry strand techniques. Good correlation of test results was reported by him for the tensile strengths in the two cases. In continuous manufacture of carbon fibres it is useful to be able to measure mechanical properties continuously since this will give an immediate indication of any change in the process. Methods for on-line measurement of Young's modulus of carbon fibres include measurement of the electrical resistivity [231] and determination of transit time for short ultrasonic pulses along the fibre bundle [232], which are then converted to elastic modulus through the use of predetermined correlations.

5.2. Development through stabilization and carbonization

The tensile properties of the precursor fibres change continuously during stabilization and carbonization. The stress–strain plot of a precursor fibre shows an initial elastic portion with a definite yield point followed by a regime of plastic deformation with increasing resistance to deformation until fracture occurs. The initial elastic region has been explained by Rosenbaum [233] to be due to reversible straightening of twisted molecules against intra-molecular repulsion of

each other at the yield point because the cohesive energy between the chains is overcome. According to Watt [55], the flow and straightening of non-aligned chains causes a more equal distribution of load between the chains so that the cohesive energy of more dipoles have to be overcome which accounts for the increasing resistance to flow until the fibre finally breaks.

Unidentified precursor fibres, when oxidized at 220° C for 5 h, showed the same initial elastic portion as the original fibre followed by a steep plastic deformation region, which has been attributed by Watt [55] to a decrease in the cohesive energy between the chains. The decrease in cohesive energy results from the conversion of highly polar nitrile groups to the less polar >C=N– groups upon oxidation. Bahl and Manocha [39, 234] observed a continuous decrease in the tensile strength of acrylic fibres upon heating in oxygen which they have attributed to the chemical changes as suggested by Watt. The primary or initial modulus of the precursor fibre decreased suddenly after 9 h heating at 205° C and continued to decrease thereafter. A continuous decrease in the tensile strength, tensile modulus and extension at break with increase in temperature of Courtelle fibres above 200° C in argon has been reported by Turner and Johnson [30]. Similar experiments by Ferguson and Mahapatro [235, 236] on some experimental fibres showed quite different results as a function of pyrolysis time. The initial modulus as well as tenacity went through a maximum whereas extension at break fell rapidly to low values upon pyrolysis at 220° C under a slight tension. A similar trend was observed by Russian workers [237] as a function of the temperature of heating between 150 and 200° C in air. These changes have been associated with chemical changes by Ferguson and Mahapatro. In support, they have shown that the ratio of the absorbances at 6.29 μm due to >C=C< and at 3.12 μm due to end groups such as –COOH and –CONH in infrared spectroscopy, which is a measure of the ratio of cyclization to degradation, also goes through a maximum with pyrolysis time. The same fibres, when drawn 700% at 100° C and pyrolysed, showed different trends [236]. The changes in initial modulus were dependent upon the form of constraints imposed during pyrolysis, an initial increase followed by a decrease under constant load conditions (0.35 g tension was applied on filaments of unspecified denier) and a sharp decrease under constant length pyrolysis. Breaking strength showed a continuous decrease while elongation at break first increased and then decreased under both conditions. The different behaviour of the drawn fibres has been attributed by Ferguson and Mahapatro to the occurrence of different degrees of molecular relaxation processes along with the chemical changes during pyrolysis. The effect of molecular weight of the original polymer on the changes in the tensile properties of fibres with pyrolysis at constant load has also been shown by them. Takaku *et al.* [142, 143] measured tensile modulus during air heating at various temperatures, by extending the specimen to a small elongation, measuring the stress and immediately releasing it. This measurement, when carried out on a specimen which was heated at the rate of 1° C min^{-1} showed a decrease in tensile modulus up to a temperature of approximately 200° C after which it increased. Isothermal heating in excess of 200° C showed an increase in modulus with increasing heat-treatment time, with a tendency to level off at longer times. The curves shifted towards shorter times with increasing temperature. Rate constants at various temperatures were calculated by Takaku *et al.* from the above curves which gave an apparent activation energy of 98.3 kJ mol^{-1}.

With the exception of Takuku *et al.*'s experiment where the initial modulus was measured during heating of the precursor [142, 143], the tensile strength, Young's modulus and elongation at break of the stabilized fibres have been found to be less than those of the starting precursor fibres. Except for the elongation at break, these properties start improving when the stabilized fibres are subjected to high temperatures in an inert environment during carbonization. According to Watt [55] and Watt and Green [70], strength and modulus were found to increase on pyrolysis around 300° C and continued to increase monotonically up to 1000° C. Heat treatment at temperatures higher than about 1500° C usually results in a decrease in tensile strength [33, 119–123] whereas the Young's modulus continues to increase up to 3000° C. This decrease in tensile strength has been attributed by Reynolds and Moreton [238] to the surface flaws originated from dust particles on the fibre surface by their reaction with the fibre surface itself at these high temperatures. When precursor fibres spun in clean room conditions were used, the tensile strength of carbon fibres was found to increase continuously up to a heat-treatment temperature of 2500° C [239].

5.3. Dependence on precursor properties

The quality of the ultimate carbon fibre depends on the precursor properties and on the stabilization and carbonization conditions. For a given chemical composition of the precursor, the properties of carbon fibres are decided by the properties of the precursor, provided the same stabilization and carbonization conditions are employed. The spinning and the drawing history of the precursor fibres plays an important role. Moreton [240], from his studies of carbon fibres made from copolymer fibres, which were wet spun from an inorganic system and drawn 5 to 13 times in steam, concluded that the tensile strength and modulus of carbon fibres are directly related to the stretch ratio of the precursor (Table III). When glycerol at 130 and 150° C was substituted for steam as the drawing medium, a significant improvement in the tensile properties of the precursor fibres was observed. These fibres possessed larger crystals and on conversion to carbon fibres showed better tensile strength and modulus than those from steam-drawn fibres [241]. Increasing the glycerol bath temperature to 160° C resulted in a deterioration in the properties of the precursor as well as the carbon fibres made from them. Similarly the properties of carbon fibres made from very highly drawn (22× in glycerol) fibres were

TABLE III Results of Moreton's studies – 6% methacrylate copolymer

Draw ratio	Drawing temperature (° C)/medium	Precursor fibres		Fibres carbonized at 1000° C		Fibres carbonized at 2500° C		Reference
		Tensile strength (GPa)	Young's modulus (GPa)	Tensile strength (GPa)	Young's modulus (GPa)	Tensile strength (GPa)	Young's modulus (GPa)	
5	100/steam	0.18	3.78	0.84	101	0.68	213	[240]
6	100/steam	0.20	4.20	0.78	105	0.55	248	
8	100/steam	0.27	5.51	0.92	130	0.83	282	
9	100/steam	0.30	5.64	0.94	124	0.83	283	
13	100/steam	0.59	9.64	1.14	154	1.22	345	
14	100/steam	0.61	15.20	1.50	227	1.32	427	[241]
14	130/glycerol	0.63	16.50	1.51	241	1.78	461	
14	150/glycerol	0.85	18.60	2.19	255	1.98	448	
14	160/glycerol	0.83	17.90	1.71	255	1.52	448	
22	150/glycerol	1.14	19.30	1.86	241	1.41	448	
14/clean*	100/steam	0.55	10.40	2.19	186	2.75	380	[239]
14/control	100/steam	0.65	13.00	1.95	172	1.51	366	

*Specified clean-room conditions (less than 100 particles/ft^3 at 0.5 μm and above, none > 5 μm).

inferior to that from 14× drawn fibres even though the former possessed better tensile strength and modulus than the latter in the precursor form. Moreton has explained it in terms of overstretching of precursor which leads to the generation of defects upon carbonization. This discrepancy could also be explained in terms of the overstabilization of the 22× drawn fibres. Since the same stabilization conditions were used by them for various precursor fibres which had different deniers, it is quite possible that the 22× drawn fibre of much lower filament denier was overstabilized, thus giving inferior properties on carbonization when compared with the 14× drawn fibre.

Ishikawa *et al.* [242, 243] stretched precursor fibres up to 280% in steam before converting them to carbon fibres and found that the strength and modulus of carbon fibres prepared by carbonization at 2500 to 3000° C increase with increase in the draw ratio of the precursor. Similar results have also been reported recently in 1100 to 1350° C treated carbon fibres by Fitzer and Muller [244], Radhakrishnan *et al.* [245] and Nagabhushanam *et al.* [246] from precursor fibres drawn to different draw ratios. Fitzer and Muller emphasize the fact that each stretch ratio needs an individual optimization of the stabilization time. This aspect has been ignored by most previous workers trying to correlate precursor properties with carbon fibre properties. Other attempts to study the effect of precursor composition [104, 247, 248] and the type of spinning (wet compared to dry) [249] on carbon fibre properties have been made by various workers. A direct relationship between the Young's moduli of various PAN-based commercial precursors and the carbon fibres produced from them were observed by Chari *et al.* [250]. The ratio of carbon fibre to precursor fibre modulus was found to be approximately 20. Based on the WAXD patterns of three commercial precursor fibres, Beslon, Courtelle and Toray, they also recommend that the longitudinal order, as seen in the Beslon fibres should be avoided since it hinders the process of molecular chain orientation during the preoxidation stage, thus giving carbon fibres with inferior properties [251]. Their conclusion, however, is based only on the fact that slightly lower modulus is obtained in carbon fibres from Beslon fibres than that from Courtelle fibres. They have unjustifiably ignored the chemical composition and the spinning history of these precursors, which could significantly influence the properties of carbon fibres.

5.4. Dependence on process conditions

In addition to the dependence on precursor properties, the stabilization and carbonization conditions such as the time, temperature and rate of heating and the dimensional constraints imposed during these processes have a significant influence on the final carbon fibre properties. Influence of the air flow rate during stabilization of commercial acrylic fibres from Courtaulds on the Young's modulus of carbon fibres has been reported recently by Nagabhushanam *et al.* [246]. A decrease in the Young's modulus of the carbon fibres, prepared by carbonization at 1100° C, was observed when the air flow was increased from zero to 35 l min^{-1} during stabilization. This decrease was negligible when the above precursor was drawn by 15% at 190° C before converting it to carbon fibre. The effect of stabilization temperature on the carbon fibre properties was studied by Bahl and Manocha [39] where they employed stabilization temperatures of 205 and 215° C in oxygen, while a constant load of 0.1 g/denier was applied which caused extensions of 12 and 16%, respectively, in the two cases. The 20% higher strength of carbon fibres reported by them when a higher stabilization temperature was employed could have resulted from increased orientation due to tensile deformation during stabilization.

Time of oxidative stabilization should be optimized for a given temperature and precursor, since under- or over-stabilization could result in loss of properties of the final carbon fibres [33, 234]. The observations by Bahl and Manocha [39] and by Watt and Johnson [33], where the tensile strength of carbon fibres went through a maximum with stabilization time, show this very clearly. Various chemical and physical methods

have been employed to ascertain optimum stabilization. In addition to the measurements of unreacted nitrile groups [53, 252], density [30, 114, 176, 253], oxygen pick-up [33, 91, 92, 96, 97, 99] moisture pick-up [32, 85] and per cent shrinkage [93, 140, 254] have also been employed frequently as quality control measures. Layden [99] has defined an optimum time for stabilization at a given temperature as the time when the oxygen pick-up of the fibre approaches 10%. Based on experimental data, he has suggested empirical relationships to calculate the time for optimum stabilization for homopolymer fibres in air. Bahl and Manocha [38] have supplemented these equations by additional equations to include the copolymer fibres and oxygen environment. Their optimization is, however, based on a free shrinkage of 24% in precursor fibre.

The load and elongation during stabilization of precursor fibres have been shown to affect the final carbon fibre properties. A continuous increase in tensile strength and modulus of carbon fibres was observed by Ishikawa *et al.* [242] when increasing tensions up to 0.16 g/denier were applied during stabilization. Watt and Johnson [33, 134] also witnessed an improvement in the properties of carbon fibres with increase in load during stabilization of Courtelle fibres. Extensions of up to 40% were observed during this stage upon application of up to 0.15 g/denier tension. The changes in properties were more dramatic for carbon fibres treated at 2500° C than for the fibres produced at 1000° C. Since the extent of stretching is more when a higher load is applied [33, 134, 242] or when a higher temperature is used [39] during stabilization, the stabilized fibre will posses a higher orientation which will ultimately lead to carbon fibres with higher orientation and thus superior tensile properties. Contrary to the observations by other workers, Bahl and Manocha [139], from their experiments with Beslon fibres, showed that both the tensile strength and modulus of carbon fibres go through a maximum when plotted against load applied during preoxidation. The best properties were obtained at a tension of approximately 0.1 g/denier corresponding to about 7% shrinkage during oxidation. The decrease in properties at loads higher than an optimum load results, according to them, from bond rupture during the preoxidation stage. A further improvement in carbon fibre properties was obtained by applying a low (0.015 g/denier) tension during a programmed heating of the precursor fibres to 240° C followed by 0.1 g/denier tension during a 100 min soak-up period at this temperature. The properties of carbon fibres are also influenced by the application of load or stretching during carbonization. When an unspecified load corresponding to a shrinkage of 3 to 8% was applied during carbonization of a fully stabilized precursor fibre at 1000° C, a small increase of about 10% in strength and modulus of carbon fibres was observed by Manocha *et al.* [37]. Experiments by Ezekiel [126], where different tensions were applied during carbonization at 2500 to 2900° C, showed only minor changes in tensile properties of carbon fibres, whereas stretching of the fibres during carbonization resulted in significant improvement in their properties. W. Johnson [129] observed more than a 30% increase, from 60 to about 90 $\times$ 10^6 psi, in the ($\sim$ 4.14 to 6.2 $\times$ 10^5 N mm^{-2}) Young's modulus of carbon fibres when stretched up to 28.6% during carbonization at 2500 to 2800° C. Similar results have also been reported by J. W. Johnson's group [128] where they observed a 20 to 30% increase in the tensile strength and modulus by stretching in the temperature range 2000 to 3000° C. The strength of the stretched carbon fibres showed a linear dependence on modulus while the unstretched fibres suggested no such relationship.

5.5. Flaw or defect dependency

Studies show that the tensile fracture in carbon fibres mainly originates at points of internal and surface irregularities or flaws. The tensile strength of PAN-based carbon fibres increases with decreasing gauge length due to the reduction of available flaws in the gauge length. Diefendorf [255] extrapolated such data and concluded that zero flaw carbon fibres would display tensile strengths in the range of 1.5 $\times$ 10^6 psi ($\sim$ 1.03 $\times$ 10^4 N mm^{-2}). Values of 10^6 psi ($\sim$ 6.89 $\times$ 10^3 N mm^{-2}) have also been predicted by Jones and Johnson [256]. This is still only about half the tensile strength obtained by Bacon [1, 2] in the case of carbon whiskers, which possess a high degree of crystalline perfection with no grain boundaries and very low dislocation density, void content and surface imperfections. The theoretically estimated tensile strength of these whiskers, using the modulus of elasticity obtained from vibrational measurements is 15 $\times$ 10^6 psi ($\sim$ 1.03 $\times$ 10^5 N mm^{-2}), approximately one-tenth of their modulus [257].

A number of studies were made in the early seventies of flaws or defects, their nature and their influence on the fracture behaviour of carbon fibres. The technology has advanced since then and the commercial carbon fibres currently in the market are more uniform and possess superior tensile properties (Table IV). Earlier work on the nature of defects or flaws in carbon fibres may not, therefore, relate fully to the carbon fibres produced today. A review by Reynolds [258] on the physical properties of carbon fibres describes the earlier research (up to 1973) on the dependence of tensile properties on surface and internal flaws.

Fracture mechanisms based on the shear stresses in the misoriented crystallites have been suggested by Stewart and Feughelman [259]. When the fibre is loaded to typical tensile loads, there is a high concentration of shear strain energy in the regions of enhanced misorientation of crystallites, which is believed to initiate cracks. Increased crystallization is also produced around the flaws making the initial crack propagation easier. In a recent paper by Bennett and Johnson [260], the emphasis is placed on the failure due to misoriented crystallites in the fibre rather than the flaw itself. Internal flaws which did not initiate failure were seen to have walls containing crystallites arranged mostly parallel to the fibre axis but the flaws which did initiate failure showed evidence of large misoriented crystallites in the walls of

Fibre type/ manufacturer	Year	Tensile strength (10^3 psi)*	Young's modulus (10^6 psi)	Comments	Reference
Data obtained from early publications					
Acrilan-based	1969	180	20	–	[262]
R.A.E. process	1969	309	24.9	HS/1500	[266]
		266	53.4	HM/2500	
Le Carbone Lorraine	1971	312	26.7	HS	[280]
		232	55.7	HM	
Watt, Philips and Johnson	1971	250	50	HM	[277]
Courtauld	1974	363	37.7	HTS/1500	[264]
		160	59.5	HMS/3000	
Recent data from various manufacturers					
Magnamite by Hercules Corp.	1984	635	40.4	Type IM6	
		600	35.3	AS6	
		320	50.0	HMS	
		400	55.0	HMU	
Celion by Celanese Corp.	1984	630	34.4	Type ST	
		515	34.0	C-6	
		270	75.0	GY-70	
Thornel by Union Carbide	1984	660	36.0	Type T-700	
		530	35.0	T-500	
		350	57.0	T-50	
		325	120.0	P-120†	
		325	105.0	P-100†	

* 10^3 psi $\equiv$ 6.89 N mm^{-2}.
† Pitch-based carbon fibres.

the flaws. They conclude that the presence of misoriented crystallites in the walls of the flaws rather than the flaw itself determines whether or not tensile failure will occur. In the absence of gross flaws, they have predicted breaking strains of 1 to 1.3% in high modulus and greater than 2% in high-strength PAN-based carbon fibres. Similar predictions have also been made by Jones and Johnson [256].

5.6. Nature and origin of flaws

Tensile test data on carbon fibres show variations in the Young's modulus and breaking strength values but the typical coefficient of variation for breaking strength is higher, about 25%, when compared with the variation in modulus which is only about 10% [261]. This large scatter in the breaking strength of carbon fibres has been associated with the surface and internal irregularities or flaws. In carbon fibres from Courtelle and Acrilan precursors, both surface and internal flaws were found responsible for premature brittle failure [262]. The majority of internal flaws were identified as elongated voids or cavities, 1 to 4 μm in width. The flaws were found distributed extremely unevenly in the fibre sample, with an average flaw concentration of approximately 8 per cm in Acrilan-based carbon fibres. A cathodic etching technique which employed argon ion bombardment was used by Johnson [119] to remove some of the fibre surface, thus producing a longitudinal section exposing the fibre interior. The voids responsible for failure were diconic in shape with the long axes parallel to the fibre length. These internal voids, it is believed, are produced by impurities in the precursor fibre, since PAN fibres spun with deliberately included particulate matter [263] also showed the diconic-shaped structures. According to Sharp *et al.* [264], the diconic-shaped flaws produce local misorientation due to the tendency of the basal planes to follow the contours of the flaws. These regions of enhanced misorientation are believed to be sources of weakness in the fibre.

The origin of surface flaws in carbon fibres has also been traced to the precursor fibre formation process by Murphy and Jones [265]. As the viscous polymer solution emerges from the spinneret during precursor spinning, they believe that some filaments stick together and also that droplets of polymer solution are deposited on the surface of the individual filaments. When the precursor tow is subsequently heat treated, both these can lead to defects on the surface. Scanning electron microscopy (SEM) of some commercial carbon fibres demonstrated the presence of surface deposits and joined fibres. Oxidation of these fibres at 680° C in air for 45 min changed the surface deposits to pits due to more rapid oxidation of these sites compared to the surface. Some of the fibres were found to have circumferential defects with shapes very similar to the shapes one would expect if the joined fibres were separated. It is difficult, however, to generalize from these isolated observations regarding universal sources of defects in carbon fibres. It was proposed by Johnson and Thorne that the surface flaws can be modified by argon-ion etching [119] or air oxidation [262] to improve the tensile strength of carbon fibres.

TABLE V Gauge length and tensile strength of carbon fibres

Source	Gauge length (cm)	No. of tests	Tensile strength (10^3 psi)*	S.D. (%)	Comments	Reference
Manufactured by	10.0	50	266	21.0	HM/2500	[266]
R.A.E.	5.0	50	300	28.0		
(1968)	0.5	50	400	23.0		
	10.0	50	309	23.0	HS/1500	
	5.0	50	346	21.0		
	0.5	50	450	22.0		
Morganite	5.0	173	238	21.8	Type IS	[268]
Modmor Inc.	0.5	136	324	18.0	(HM)	
(1972)	0.2	120	352	19.1		
	0.1	86	371	16.1		
	5.0	206	334	22.9	Type IIS	
	0.5	136	444	18.3	(HS)	
	0.2	133	480	20.3		
	0.1	123	494	16.9		
Commercial	3.0 in.	–	215	27.0	GY-70, HM	[269]
C-fibres	1.0 in.	–	240	25.0	Celanese	
(1974)	0.25 in.	–	310	23.0		
	3.0 in.	–	363	20.0	Type-AS, HS	
	1.0 in.	–	441	20.0	Hercules	
	0.25 in.	–	549	18.0		
	0.1 in.	–	636	11.0		
	3.0 in.	–	311	22.0	Thornel 300	
	1.0 in.	–	392	27.0	Union-Carb.	
	0.25 in.	–	482	18.0		
	0.1 in.	–	488	23.0		
Courtaulds	5.0 in.	24	359	17.4	Type HMS	
(1979)	0.5	10	428	24.0		
	0.05	10	550	15.7		
	5.0	25	400	13.4	Type HTS	
	0.5	10	528	14.4		
	0.25	10	503	25.3		

*10^3 psi $\equiv$ 6.89 N mm^{-2}.

5.7. Variations with gauge length and fibre diameter

In addition to direct observations of defects by optical and electron microscopy, other experimental observations, e.g. variation of average tensile strength with fibre diameter and gauge length, also point to the importance of defects in the tensile failure of various carbon fibres. Moreton [266] measured the breaking strengths of carbon fibres heat treated over a range of temperatures between 1000 and 3000° C using gauge lengths of 0.5, 5 and 10 cm. Some typical results are included in Table IV, along with the results obtained by others. The average tensile strength values were found to decrease exponentially with increase in the gauge length. Detailed histograms also showed that the range of the strengths was displaced downward by the use of longer gauge lengths. The actual distribution of strengths was ascribed to the presence of randomly occurring defects. Comparison was therefore made with the weak-link theory of Tippett [267] and a reasonable correspondance was observed. Barry [268] has reported single filament testing of Modmor fibres, manufactured in early 1972 measured at four different gauge lengths (see Table V). A logarithmic plot of breaking strength against gauge length suggested a linear relationship. McMahon [269] extrapolated the tensile strength data from a similar study on various commercial fibres to a gauge length of 0.025 in. and used it to predict the tensile strength of unidirectional composites through an empirical relationship. Hitchon and Phillips [270] measured breaking strengths of Courtaulds HMS and HTS fibres using gauge lengths of 0.05, 0.5 and 5 cm and observed that the strengths at shorter lengths were less than predicted from the 5 cm strength using the Weibull theory [271]. They explained it in terms of a bimodal or a combination of two unimodal flaw size distributions instead of a homogeneous unimodal distribution required by the Weibull theory. Two recent papers by Beetz [272, 273] also describe a bimodal distribution of strength in Thornel-P fibres. He has extended the Weibull theory to include a bimodal distribution which allowed more accurate estimates of mean fibre strength at short gauge lengths.

The effect of fibre diameter on the tensile properties of carbon fibre was studied by Lamotte and Perry [274, 275], Diefendorf *et al.* [276] and by Jones and Duncan [277]. Lamotte and Perry found that the strength of Grafil-HT fibres diminished by about 20% as their diameter rose from 7 to 12 μm, whereas the modulus decreased from 290 GPa at 7.5 μm to 250 GPa at 10.5 μm. Grafil-A fibres, which represent the intermediate product (starting from PAN) from which type HT fibres are made by a thermal treatment, did not show any dependence on fibre diameter. They have associated the decrease in tensile strength and modulus to a non-typical outer surface layer in thick fibres. Since different diameters are a result of

different degrees of stretching of the precursor filaments in a tow during their manufacture or during their conversion to carbon fibres, an additional contribution could be from the different orientations, higher in smaller diameter fibres, introduced during these processes. A similar decrease in tensile strength and modulus was observed by Jones and Duncan [277] in experimental PAN-based carbon fibres. They attribute the variations in Young's modulus to the differences in the relative amounts of sheath and core structures in fibres of different diameters. According to them, thin fibres would possess a thicker sheath which shows better basal plane alignment than the core, while a thick fibre would contain a larger fraction of the core. The variations in the breaking strengths have been explained by them in terms of basal plane cracks which result from the anisotropic thermal contraction of the crystallites. More cracks are likely to occur in a thick fibre due to a larger core which would decrease the tensile strength of these fibres.

6. Modification of carbon fibre surface

The outstanding mechanical properties of carbon fibres become of practical interest only if they can be efficiently translated into a usable structural form such as composites, the properties of which depend to a large extent on the interaction between the fibre and the matrix. Composite characteristics which are highly dependent on fibre–resin coupling include flexural and interlaminar shear strength and modes of failure. Early work with carbon fibre–epoxy composites gave disappointingly low values for the interlaminar shear strength, a general measure of the adhesion at the interface. A considerable effort was subsequently devoted to the study of surface properties of carbon fibres [15, 25, 278–284] and possible alteration of the surface [279, 281, 285–288] for good fibre–matrix adhesion. Numerous procedures for altering the carbon fibre surface have been described in the open as well as patented literature. It is beyond the scope of this review to go into the details of these methods. The basis appears to be to change the chemical nature of the surface and to change the smooth surface of high strength and high modulus carbon fibres to a rough or porous surface, through a mild oxidation. Controlled oxidation has been successfully achieved by using both liquid [287, 289–291] and gaseous [292–295] oxidizing agents.

7. Concluding remarks

The structure and properties of carbon fibres depend, in addition to the precursor properties, on the stabilization and carbonization conditions employed during their manufacture. The morphology of the precursor fibres plays an important role. The importance of proper optimization and control of stabilization and carbonization during the conversion of PAN-based precursor fibres to carbon fibres is quite evident from the literature reviewed here. This requires the use of suitable techniques for characterizing the fibre at various stages during these operations. It is clear from published literature that the constraints imposed on many precursor fibres during stabilization and/or carbonization play an important role. The techniques or measurements which are sensitive to the differences in the fibre structure and properties during their heat treatment with different levels of constraints therefore become important.

The morphological order developed during spinning and drawing operations could be considerably different depending on the conditions employed during these processes. These precursors with different morphologies could require, in spite of their same chemical composition and denier/filament, quite different stabilization and carbonization conditions in order to produce carbon fibres with good mechanical properties. This emphasizes the need for studies of initial morphology and the changes in it as a function of the progression of stabilization and carbonization in precursor fibres with significantly different orientations and other morphological parameters.

There is indeed a vast amount of literature on the conversion of acrylonitrile-based precursors to carbon fibres. Much of it, unfortunately, is on isolated aspects of this complex process and so fails to provide a cohesive link between the various material and process aspects. A high degree of empiricism exists still in determining the optimum conditions of processing. It is necessary to conduct comprehensive research on the chemical and morphological aspects of the conversion of precursor polymer to carbon fibres in order to improve our understanding of the evolution of structure and properties of these critical high performance materials. Many successful processes have indeed been designed with only a partial understanding of fundamental aspects. It is our belief, nevertheless, that these can be significantly improved and that new processes for new precursor compositions can be designed with greater ease through improved comprehension at an elementary level.

Acknowledgements

The authors express their appreciation to Mr Prashant Desai and Dr M. Balasubramanian for the numerous ways in which they helped in the preparation of this review. Financial support from the Office of Naval Research for this study is gratefully acknowledged. The authors express their deep gratitude to Dr L. H. Peebles for many valuable suggestions regarding this study.

References

1. R. BACON, *J. Appl. Phys.* **31** (1960) 283.
2. Union Carbide Corp., USA US Patent 2957756 (1960).
3. *Idem*, US Patent 3454362 (1969).
4. *Idem*, US Patent 3503708 (1970).
5. A. SHINDO, *Osaka Kogyo Gijitsu Shikuko Kiko* **12** (1961) 110.
6. *Idem, ibid.* **12** (1961) 119.
7. *Idem, Rep. Gov. Ind. Res. Inst. Osaka* No. 317 (1961).
8. *Idem, Carbon* **1** (1964) 391.
9. W. JOHNSON, L. PHILLIPS and W. WATT, US Patent 3412062 (1968).
10. P. J. GOODHEW, A. J. CLARKE and J. E. BAILEY, *Mater. Sci. Eng.* **17** (1975) 3.
11. D. H. LOGSDAIL, *Appl. Polym. Symp.* **9** (1969) 245.
12. W. WATT, *Carbon* **10** (1972) 121.

ference (Manchester, Textile Institute, 1977) p. 73.
14. P. E. MORGAN, *Textile Prog.* **8** (1976) 69.
15. D. W. McKEE and V. J. MIMEAULT, "Chemistry and Physics of Carbon", Vol. 8, edited by P. A. Thrower and P. L. Walker (Dekker, New York, 1973) p. 151.
16. R. BACON, *Appl. Polym. Symp.* **9** (1969) 213.
17. P. G. ROSE, PhD thesis, University of Aston, UK (1971).
18. C. W. LeMAISTRE, PhD thesis, Rennslaer Polytechnic Institute, New York (1972).
19. P. W. BARRY, PhD thesis, University of Newcastle, Australia (1974).
20. R. MORETON, PhD thesis, University of Surrey UK (1976).
21. S. B. WARNER, ScD thesis, Massachussetts Institute of Technology, USA (1976).
22. O. ZUBZANDA, PhD thesis, University of New South Wales, Australia (1980).
23. Th. MUELLER, PhD thesis, University of Karlsruhe, FRG (1982).
24. M. K. JAIN, PhD thesis, Georgia Institute of Technology, Atlanta, Georgia, USA (1984).
25. H. H. GIBBS, R. C. WENDT and F. C. WILSON, *Polym. Eng. Sci.* **19** (1979) 342.
26. B. H. ECKSTEIN, *Fibre Sci. Technol.* **14** (1981) 139.
27. J. WARD, private communication, American Cyanamid, USA (1983).
28. L. M. MANOCHA and O. P. BHAL, *Die Angew. Makromol. Chemie* **64** (1977) 115.
29. E. V. THOMPSON, *J. Polym. Sci. Polym. Lett.* **4** (1966) 361.
30. W. N. TURNER and F. C. JOHNSON, *J. Appl. Polym. Sci.* **13** (1969) 2073.
31. J. W. JOHNSON, P. G. ROSE and G. SCOTT, in Proceedings of the 3rd Conference on Industrial Carbon and Graphite, London (Soc. Chem. Ind., London, 1970) p. 443.
32. Toray Industries Inc., US Patent 4 065 549 (1977).
33. W. WATT and W. JOHNSON, in Proceedings of the 3rd Conference on Industrial Carbon and Graphite, London (Soc. Chem. Ind., London, 1970) p. 417.
34. W. WATT, D. J. JOHNSON and E. PARKER, in Proceedings of the Plastics and Polymers Conference, Suppl. **6** (Plastics Institute, London, 1974) 3.
35. Great Lakes Carbon Corp., New York, US Patent 3 533 743 (1970).
36. O. P. BAHL and L. M. MANOCHA, *Die Angew. Makromol. Chemie* **48** (1975) 145.
37. L. M. MANOCHA, O. P. BAHL and G. C. JAIN, *ibid.* **67** (1978) 11.
38. O. P. BAHL and L. M. MANOCHA, *Fibre Sci. Technol.* **9** (1976) 77.
39. *Idem, Carbon* **13** (1975) 297.
40. S. P. VARMA, B. B. LAL and N. K. SRIVATSAVA, *ibid.* **14** (1976) 207.
41. J. E. BAILEY and A. J. CLARKE, *Nature* **234** (1971) 529.
42. J. SIMITZIS, *J. Coll. Polym. Sci.* **255** (1977) 1074.
43. J. FERGUSON and N. DEBNATH-RAY, *Fibre Sci. Technol.* **13** (1980) 167.
44. L. I. KOMLYAKOVA, N. V. PISKAREV, N. V. BALYEV, V. A. MIKHAILOVA and N. V. POLYAKOVA, *Khim. Volokna* **2** (1976) 49.
45. M. M. COLEMAN and R. J. PETCAVICH, *J. Polym. Sci. Polym. Phys. Ed.* **16** (1978) 821.
46. M. M. COLEMAN and G. T. SIVY, *Carbon* **19** (1981) 123.
47. *Idem, ibid.* **19** (1981) 127.
48. *Idem, ibid.* **19** (1981) 133.
49. M. M. COLEMAN, G. T. SIVY, P. C. PAINTER, R. W. SNYDER and B. GORDON III, *ibid.* **21** (1983) 255.
50. L. E. WOLFRAM, J. G. GRASSELLI and J. L. KOENIG, *Appl. Polym. Symp.* (1974) 25.
51. *Idem, ibid.* (1974) 27.
52. R. T. CONLEY and J. F. BIERON, *J. Appl. Polym. Sci.*
53. I. NOB and H. YU, *J. Polym. Sci. Polym. Lett.* **B4** (1966) 721.
54. W. J. BURLANT and J. L. PARSONS, *J. Polym. Sci.* **22** (1956) 249.
55. W. WATT, in Proceedings of the 3rd Conference on Industrial Carbon and Graphite, London (Soc. Chem. Ind., London, 1970) p. 431.
56. G. RADHAKRISHNAN, T. NAGABHUSHANAM, K. J. JOSEPH and M. SANTHAPPA, *Makromol. Chem.* **180** (1979) 2923.
57. J. BROMLEY, in Proceedings of the International Conference on Carbon Fibres, their Composites and Applications, Plastic Institute, London (1971) p. 3.
58. M. MINAGAWA and T. IWAMATSU, *J. Polym. Sci. Polym. Chem. Ed.* **18** (1980) 481.
59. E. FITZER and D. J. MULLER, *ACS Polym. Chem. Symp.* (1973) 396.
60. *Idem, Carbon* **13** (1975) 63.
61. Y. N. SAZANOV, N. A. SHIROKOV and B. E. GOLTSIN, *Thermo Chimica Acta* **32** (1979) 73.
62. C. A. GAULIN and W. R. McDONALD, Air Force Report SAMSO-TR-71-61 I (1971).
63. A. GUYOT and M. BERT, *Eur. Polym. J.* **14** (1978) 101.
64. J. SIMITZIS, *Coll. Polym. Sci.* **255** (1977) 948.
65. E. URBAS and E. KULLIK, *J. Chromatography* **137** (1977) 210.
66. Y. TSUCHIYA and K. SUMI, *J. Appl. Polym. Sci.* **21** (1977) 975.
67. S. SATONAKA and J. MATSUI, *Plastics Industry News* **26** (1980) 151.
68. E. I. KAZAKOV, M. A. KOSTAMAROVA, Z. S. SMUTKINA, M. E. KAZAKOV, N. F. KARPOVA, V. I. KASATOCHKIN and N. P. RADIMOV, *Khim Volokna* **6** (1971) 27.
69. R. S. LEHRLE, J. C. ROBB and J. R. SUGGATE, *Eur. Polym. J.* **18** (1982) 443.
70. W. WATT and J. GREEN, in Proceedings of the International Conference on Carbon Fibres, their Composites and Applications (Plastics Institute, London, 1971) p. 23.
71. C. A. GAULIN and W. R. McDONALD, Air Force Report SAMSO-TR-72-304 II (1972).
72. S. S. CHEN, J. HERMS, L. H. PEEBLES Jr and D. R. UHLMANN, *J. Mater. Sci.* **16** (1981) 1490.
73. G. AYREY, S. K. CHADDA and R. C. POLLER, *Eur. Polym. J.* **19** (1983) 313.
74. J. N. HAY, *J. Polym. Sci. A-1* **6** (1968) 2127.
75. N. GRASSIE, "Developments in Polymer Degradation" (Applied Science, London, 1977) p. 133.
76. N. GRASSIE and R. McGUCHAN, *Eur. Polym. J.* **6** (1970) 1277.
77. *Idem, ibid.* **7** (1971) 1091.
78. *Idem, ibid.* **7** (1971) 1357.
79. *Idem, ibid.* **7** (1971) 1503.
80. *Idem, ibid.* **8** (1972) 243.
81. *Idem, ibid.* **8** (1972) 257.
82. *Idem, ibid.* **8** (1972) 865.
83. H. H. G. JELLINEK and A. DAS, *J. Polym. Sci. Polym. Chem. Ed.* **16** (1978) 2715.
84. M. M. KANOVICH and A. P. RUDENKO, *Khim. Volokna* 3 (1982) 19.
85. J. W. JOHNSON, W. D. POTTER, P. G. ROSE and G. SCOTT, *Br. Polym. J.* **4** (1972) 527.
86. A. J. CLARKE and J. E. BAILEY, *Nature* **243** (1973) 146.
87. W. D. POTTER and G. SCOTT, *Nature Phys. Sci.* **236** (1972) 30.
88. L. H. PEEBLES Jr, *J. Polym. Sci. A-1* **5** (1967) 2637.
89. L. H. PEEBLES Jr and J. BRANDRUP, *Makromol. Chem.* **98** (1966) 189.
90. L. H. PEEBLES Jr, "Encyclopedia of Chemical Technology, Suppl"., (Wiley, New York, 1979) p. 1.
91. G. M. KERCH, A. M. TOLKS, G. A. KARLSON and L. A. IRGEM, *Khim Volokna* **2** (1978) 50.
92. R. C. ROWE, NTIS Report, AD-755427 (National

Technical Information Service, Springfield, Virginia, 1972).
93. Toho Beslon Co Ltd, US Patent 4 069 297 (1978).
94. National Research and Development Council, UK, US Patent 4 079 122 (1978).
95. Japan Exlan Co Ltd, US Patent 4 009 991 (1977).
96. W. WATT and W. JOHNSON, *Nature* **257** (1975) 210.
97. S. B. DARNER, L. H. PEEBLES Jr and D. R. UHLMANN, *J. Mater. Sci.* **14** (1979) 556.
98. J. S. PERKINS, R. J. SACHER, R. J. SHUFORD, G. R. THOMAS and S. E. WENTWORTH, NTIS Report AD-750362 (National Technical Information Service, Springfield, Virginia, 1972).
99. G. K. LAYDEN, *Carbon* **10** (1972) 59.
100. B. DANNER and J. MEYBECH, in Proceedings of the International Conference on Carbon Fibres, their Composites and Applications (Plastics Institute, London, 1971) p. 36.
101. M. V. G. I. STANCHENKO, M. V. ABRAMOV, B. P. MORIN and M. V. SHABLYGIN, *Khim. Volokna* **1** (1981) 20.
102. D. BRAUN and R. DISSELHOFF, *Die Angew. Makromol. Chemie* **74** (1978) 225.
103. E. FITZER and A. K. FIELDER, *ACS Polym. Chem. Symp.* **14** (1973) 401.
104. V. C. McLOUGHLIN and R. MORETON, NTIS Report AD-A026-743 (National Technical Information Service, Springfield, Virginia, 1974).
105. Japan Exlan Co Ltd, British Patent 1 500 675 (1978).
106. *Idem*, US Patent 4 154 807 (1979).
107. Celanese Corp., New York, US Patent 4 002 426 (1977).
108. D. E. CAGLIOSTRO, *Text. Res. J.* **50** (1980) 632.
109. I. L. KALNIN, A. H. DiEDWARDO, E. W. CHOE and J. M. RHODES, *Org. Coat. Plast. Chem.* **38** (1978) 685.
110. Monsanto Co., St. Louis, US Patent 3 814 577, (1974).
111. Celanese Corp., New York, US Patent 4 004 053 (1977).
112. *Idem*, US Patent 4 364 916 (1982).
113. *Idem*, US Patent 3 850 876 (1974).
114. Great Lakes Carbon Corp., New York, US Patent 4 279 612 (1981).
115. A. H. DiEDWARDO, *Org. Coat. Plast. Chem.* **38** (1978) 692.
116. K. MORITA, H. MIYACHI and T. HIRAMTSU, *Carbon* **19** (1981) 11.
117. O. P. BAHL, R. B. MATHUR and K. D. KUNDRA, *Fibre Sci. Technol.* **13** (1980) 155.
118. Nippon Carbon Co., Japan, US Patent 3 529 934 (1970).
119. J. W. JOHNSON, *Appl. Polym. Symp.* **9** (1969) 229.
120. G. A. COOPER and R. M. MAYER, *J. Mater. Sci.* **6** (1971) 60.
121. R. MORETON, W. WATT and W. JOHNSON, *Nature* **213** (1967) 690.
122. D. A. BRANDRETH, W. M. RIGGS and R. E. JOHNSON, *Nature Phys. Sci.* **236** (1972) 10.
123. Toho Beslon Co Ltd, Japan US Patent 4 073 870 (1978).
124. H. B. EZEKIEL, US Patent 3 635 675 (1972).
125. *Idem*, US Patent 3 671 192 (1972).
126. *Idem, Appl. Polym. Symp.* **21** (1973) 167.
127. *Idem, ibid.* **21** (1973) 153.
128. J. W. JOHNSON, J. R. MARJORAM and P. G. ROSE, *Nature* **221** (1969) 357.
129. W. JOHNSON, in Proceedings of the 3rd Conference on Industrial Carbon and Graphite, London (Soc. Chem. Ind., London, 1970) p. 447.
130. Union Carbide Corp., USA, US Patent 3 454 362 (1969).
131. Ames Research Center, California, NASA Tech. Briefs, Spring (1983).
132. Celanese Corp., USA, US Patent 3 723 605 (1973).
133. V. DIETZ, US Patent 3 931 392 (1976).
134. W. WATT and W. JOHNSON, *Appl. Polym. Symp.* **9** (1969) 215.
135. D. J. MULLER, E. FITZER and A. K. FIEDLER, in Proceedings of the International Conference on Carbon Fibres, their Composites and Applications (Plastics Institute, London, 1971) paper 2.
136. E. FITZER and D. J. MULLER, *Die Makromol. Chemie* **144** (1971) 117.
137. E. FITZER and M. HEYM, *Chem. Ind.* **16** (1976) 663.
138. G. IK. LAYDEN, *J. Appl. Polym. Sci.* **15** (1971) 1709.
139. O. P. BAHL and R. B. MATHUR, *Fibre Sci. Technol.* **12** (1979) 31.
140. E. FITZER and M. HEINE, in Proceedings of the 16th Biennial Conference on Carbon, San Diego, California 1983 (American Carbon Society, 1983) p. 501.
141. S. B. WARNER, L. H. PEEBLES Jr and D. R. UHLMANN, *J. Mater. Sci.* **14** (1979) 565.
142. A. TAKAKU, S. TERUI, C. SUZUKI and J. SHIMIZU, *Fibre Sci. Technol.* **16** (1981) 237.
143. A. TAKAKU, S. KOBAYASHI, *et al., ibid.* **15** (1981) 87.
144. V. G. HINRICHSEN and H. ORTH, *Kolloid Z. Z. Polymere* **247** (1971) 844.
145. L. G. WALLNER and K. RIGGERT, *J. Polym. Sci. Polym. Lett.* **1** (1963) 111.
146. P. H. LINDENMEYER and R. HOSEMANN, *J. Appl. Phys.* **34** (1963) 42.
147. R. STEFANI, M. CHEVRETON, M. GARNIER and M. C. EYRAUD, *Acad. des Sciences* (1960) 2147.
148. *Idem, ibid.* (1959) 2006.
149. B. G. COLVIN and P. STORR, *Eur. Polym. J.* **10** (1974) 337.
150. A. K. GUPTA and N. CHAND, *ibid.* **15** (1979) 899.
151. R. B. BEEVERS, E. F. WHITE and L. BROWN, *Farad. Trans.* (1960) 1535.
152. Y. IMAI, S. MINAMI, T. YOSHIHARA, Y. JOH and H. SATO, *J. Polym. Sci. Polym. Lett.* **8** (1970) 281.
153. F. KUMAMARU, T. KAJIYAMA and M. TAKAYANAGI, *J. Crystal Growth* **48** (1980) 202.
154. V. F. HOLLAND, S. B. MITCHELL, W. L. HUNTER and P. H. LINDENMEYER, *J. Polym. Sci.* **62** (1962) 145.
155. J. J. KLEMENT and P. H. GEIL, *ibid. A2* **6** (1968) 1381.
156. C. R. BOHN, J. R. SCHAEFGEN and W. O. STATTON, *ibid.* **55** (1961) 531.
157. R. C. HOUTZ, *Text. Res. J.* (1950) 786.
158. S. B. WARNER, D. R. UHLMANN and L. H. PEEBLES Jr, *J. Mater. Sci.* **14** (1979) 1893.
159. H. A. STUART, *Physik der Hochpolymeren* **3** (1955) 167.
160. G. HINRICHSEN and H. ORTH, *J. Polym. Sci. Polym. Lett.* **9** (1971) 529.
161. R. B. HURLEY and L. S. TZENTIS, *ibid.* **1** (1963) 423.
162. M. TAKAHASHI and Y. NUKUSHINA, *J. Polym. Sci. S19* **163** (1962) 56.
163. V. F. HOLLAND, *ibid.* **142** (1960) 572.
164. R. M. GOHIL, K. C. PATEL and R. D. PATEL, *Die Angew. Makromol. Chemie* **25** (1972) 83.
165. J. P. CRAIG, J. P. KNUDSEN and V. F. HOLLAND, *Text. Res. J.* **32** (1962) 435.
166. P. TUCKER and W. GEORGE, *Polym. Eng. Sci.* **12** (1972) 364.
167. G. NATTA and G. DALL'ASTA, Italian Patent 570 434 (1959).
168. G. H. OLIVE and S. OLIVE, *Adv. Polym. Sci.* **32** (1979) 123.
169. J. L. KOENIG, L. E. WOLFRAM and J. G. GRASSELLI, *J. Macromol. Sci. Phys. Ed. B4* **3** (1970) 491.
170. I. M. FOUDA and K. A. ELFARHATY, *Acta Physica Polonica* **A61** (1982) 137.
171. I. B. KLIMENKO and L. V. SMIRNOV, *Vsokomol. Soyed.* **5** (1963) 1520.
172. R. CHIANG, *J. Polym. Sci.* **A1** (1963) 2765.
173. W. R. KRIGBAUM and N. TOKITA, *ibid.* **XLIII** (1960) 467.
174. B. G. FRUSHOUR, *Polym. Bull.* **4** (1981) 305.
175. *Idem, ibid.* **7** (1982) 1.
176. D. J. THORNE and J. R. MARJORAM, *J. Appl. Polym. Sci.* **16** (1972) 1357.
177. L. E. ALEXANDER, "X-Ray Diffraction Methods in Polymer Science", (Wiley, New York, 1969).
178. M. E. FILLERY and P. J. GOODHEW, *Nature Phys. Sci.* **233** (1971) 118.
179. C. N. TYSON, *ibid.* **229** (1971) 121.
180. G. HINRICHSEN, *J. Appl. Polym. Sci.* **17** (1973) 3305.

181. S. B. WARNER, *J. Polym. Sci. Polym. Lett. Ed.* **16** (1978) 287.
182. L. E. ALEXANDER, "X-ray Diffraction Methods in Polymer Science", (Wiley, New York, 1969) p. 423.
183. D. J. JOHNSON, Extended Abstracts of the 15th Biennial Conference on Carbon, Philadelphia (American Carbon Society, 1981) p. 304.
184. W. RULAND and H. TOMPA, *Acta. Crystallogr.* **A24** (1968) 93.
185. *Idem, J. Appl. Cryst.* **5** (1972) 225.
186. W. RULAND, *J. Appl. Phys.* **38** (1967) 3585.
187. V. I. KASATOCHKIN, Z. S. SMUTKINA, M. A. KAZAKOV, M. A. CHUBAROVA and N. P. RADIMOV, *Khim Volokna* **4** (1972) 10.
188. D. J. JOHNSON, *Phil. Trans. R. Soc. Lond.* **A294** (1980) 443.
189. D. J. JOHNSON, in Proceedings of the International Conference on Carbon Fibres, their Composites and Applications, Vol. 4 (Plastics Institute, London, 1971) paper 8.
190. L. FISCHER and W. RULAND, *Coll. Polym. Sci.* **258** (1980) 917.
191. W. RULAND, *Appl. Polym. Symp.* **9** (1969) 293.
192. R. J. DIEFENDORF and E. TOKARSKY, *Polym. Eng. Sci.* **15** (1975) 150.
193. S. C. BENNETT and D. J. JOHNSON, *Carbon* **17** (1979) 25.
194. *Idem*, in Proceedings of the Fifth International Conference on Carbon and Graphite, London (Soc. Chem. Ind., London, 1978) p. 377.
195. D. J. JOHNSON, D. CRAWFORD and B. F. JONES, *J. Mater. Sci.* **8** (1973) 286.
196. B. J. WICKS, *ibid.* **6** (1971) 173.
197. B. J. WICKS and R. A. COYLE, *ibid.* **11** (1976) 376.
198. D. J. JOHNSON and C. N. TYSON, *Brit. J. Appl. Phys. J. Phys. D* **2** (1969) 787.
199. R. PERRET and W. RULAND, *J. Appl. Cryst.* **3** (1970) 525.
200. D. J. JOHNSON and C. N. TYSON, *J. Phys. D Appl. Phys.* **3** (1970) 527.
201. R. PERRET and W. RULAND, *J. Appl. Cryst.* **2** (1969) 209.
202. P. DEBYE and A. M. BEUCHE, *J. Appl. Phys.* **20** (1949) 1518.
203. G. POROD, *Kolloidzeit* **124** (1951) 83.
204. *Idem, ibid.* **125** (1951) 51, 108.
205. P. DEBYE, H. R. ANDERSON and H. BRUMBERGER, *J. Appl. Phys.* **28** (1957) 679.
206. W. JOHNSON and W. WATT, *Nature* **215** (1967) 384.
207. D. V. BADAMI, J. C. JOINER and G. A. JONES, *ibid.* **215** (1967) 387.
208. B. J. WICKS, *J. Mater. Sci.* **6** (1971) 173.
209. W. RULAND, *Polym. Preprints* **9** (1968) 1368.
210. D. H. SPENCER, M. A. HOOKER, A. C. THOMAS and B. A. NAPIER, in Proceedings of the International Carbon Conference, London (Soc. Chem. Ind., London, 1970) p. 467.
211. J. B. JONES and L. S. SINGER, *Carbon* **20** (1982) 379.
212. D. ROBSON, F. Y. I. ASSABGHY, D. J. E. INGRAM and P. G. ROSE, in Proceedings of the 3rd Conference on Industrial Carbon and Graphite, London (Soc. Chem. Ind., London, 1970) p. 453.
213. D. H. SAUNDERSON and C. G. WINDSOR, *ibid.*, p. 438.
214. C. W. LeMAISTRE and R. J. DIEFENDORF, *SAMPE Q.* **4**(4) (1973) 1.
215. R. H. KNIBBS, *J. Microscopy* **94** (1971) 273.
216. C. W. LeMAISTRE and R. J. DIEFENDORF, Proceedings of the Advances in Material Composites and Carbon, Symposia of the American Ceramic Society (American Ceramic Society, Columbus, Ohio, 1972) p. 77.
217. J. A. GRIFFOTHS and H. MARSH, Extended Abstracts of the 12th Biennial Conference on Carbon (American Carbon Society, St Marys, Pennsylvania, 1981) p. 316.
218. P. KWIZERA, M. S. DRESSELHAUS, D R. UHLMANN, J. S. PERKINS and C. R. DESPER, *Carbon* **20** (1982) 387.
219. F. R. BARNET and M. K. NORR, *ibid.* **11** (1973) 281.
220. *Idem*, in Proceedings of the International Conference on Carbon Fibres, their Composites and Applications (Plastics Institute, London, 1974) p. 32.
221. W. JOHNSON, *Nature* **279** (1979) 142.
222. D. CRAWFORD and D. J. JOHNSON, *J. Micros.* **94** (1971) 51.
223. J. A. HUGO, V. A. PHILLOPS and B. W. ROBERTS, *Nature* **226** (1970) 144.
224. W. RULAND, *ACS Polym. Preprints* **9** (1968) 1368.
225. A. OBERLIN, F. MOLLEYRE and M. BASTICK, Extended Abstracts of the 13th Biennial Conference on Carbon (American Carbon Society, St Marys, Pennsylvania, 1977) p. 371.
226. R. BACON and A. F. SILVAGGI, *Carbon* **9** (1971) 321.
227. Z. MENCIK, H. K. PLUMMER Jr and L. BARTOSIEWICZ, *ibid.* **13** (1975) 417.
228. E. FITZER and J. SIMITZIS, Extended Abstracts of the 12th Biennial Conference on Carbon (American Carbon Society, St Marys, Pennsylvania, 1975) p. 291.
229. ASTM D 3039-76, "Annual Book of ASTM Standards", Vol. **36** (1978) 721.
230. P. E. McMAHON, in Proceedings of the Symposium by ASTM D30 Committee, STP-521 (1973) 367.
231. Rolls-Royce Ltd, French Patent 1 590 257 (1970).
232. W. N. REYNOLDS, in Proceedings of the 3rd Conference on Industrial Carbon and Graphite, London (1970) p. 472.
233. S. ROSENBAUM, *J. Appl. Polym. Sci.* **9** (1965) 2071.
234. O. P. BAHL and L. M. MANOCHA, *Carbon* **12** (1974) 417.
235. J. FERGUSON and B. MAHAPATRO, *Fibre Sci. Technol.* **9** (1976) 161.
236. *Idem, ibid.* **11** (1978) 55.
237. S. D. FEDOSEEV, T. V. KOMAROVA and A. K. ZAKHAROV, *Khim. Volokna* **6** (1976) 24.
238. W. N. REYNOLDS and R. MORETON, *Phil. Trans. R. Soc. Lond.* **A294** (1980) 451.
239. R. MORETON and W. WATT, *Carbon* **12** (1974) 543.
240. R. MORETON, in Proceedings of the 3rd Conference on Industrial Carbon and Graphite, London (Society of Chemical Industries, London, 1970) p. 472.
241. *Idem*, in Proceedings of the International Conference on Carbon Fibres, their Composites and Applications, Plastic Institute, London, (1971) paper 12.
242. T. ISHIKAWA, R. MAKI and M. MORISHITA, in Proceedings of the ACS 161st National Meeting, Los Angeles (ACS, Washington, DC, 1971) p. 400.
243. *Idem*, ACS 161st National Meeting, Division of Cellulose Wood and Fibre Chemistry (ACS, Washington, DC, 1971) paper 26.
244. E. FITZER and T. MULLER, Extended Abstracts of the 15th Biennial Conference on Carbon (1981) p. 312.
245. G. RADHAKRISHNAN, K. T. JODHEP and M. SANTAPPA, *Leather Sci.* **28** (American Carbon Society, St Marys, Pennsylvania, 1981) p. 27.
246. T. NAGABHUSHANAM, Th. MULLER, A. E. SIMIONATA and J. L. GOMES DE SILVA, Extended Abstracts of the 16th Biennial Conference on Carbon (American Carbon Society, St Marys, Pennsylvania, 1983) p. 509.
247. E. FITZER and J. SIMITZIS, Extended Abstracts of the 12th Biennial Conference on Carbon (American Carbon Society, St Marys, Pennsylvania, 1983) p. 291.
248. National Research and Development Council, UK, Canadian Patent 1 132 297 (1982).
249. D GOLDEN and P. ROSE, in Proceedings of the 5th International Conference on Carbon and Graphite, London (American Carbon Society, St Marys, Pennsylvania, 1978) p. 388.
250. S. S. CHARI, O. P. BAHL and R. B. MATHUR, *Fibre Sci. Technol.* **15** (1981) 153.
251. O. P. BAHL, R. B. MATHUR and K. D. KUNDRA, *ibid.* **15** (1981) 147.
252. J. P. KENNEDY and C. M. FONTANA, *J. Polym. Sci.*

39 (1959) 501.
253. V. O. GORBACHEVA and E. AV. KHLEBNIKOVA, *Khim. Volokna* **6** (1976) 42.
254. Y. KOBAYASHI, S. OKAJIMA and H. KOSUDA, *J. Appl. Polym. Sci.* **11** (1967) 2525.
255. F. J. DIEFENDORF, *Div. Petroleum Chem. Preprints* **20** (1975) 447.
256. W. R. JONES and J. W. JOHNSON, *Carbon* **9** (1971) 645.
257. J. P. STERRY and W. L. LACHMAN, *Chem. Eng. Progr.* **58** (1962) 37.
258. W. N. REYNOLDS, "Chemistry and Physics of Carbon", edited by P. A. Thrower and P. L. Walker, Vol. **11** (1973) p. 1.
259. M. STEWART and M. FEUGHELMAN, *J. Mater. Sci.* **8** (1973) 1119.
260. S. C. BENNETT and D. J. JOHNSON, *ibid.* **18** (1983) 3337.
261. W. WATT and W. JOHNSON, in Proceedings of the 3rd Conference on Industrial Carbon and Graphite, London (Society of Chemical Industries, London, 1970) p. 417.
262. J. W. JOHNSON and D. J. THORNE, *Carbon* **7** (1969) 659.
263. D. J. THORNE, V. J. GOUGH and G. HIPKISS, *Fibre Sci. Technol.* **3** (1970) 119.
264. J. V. SHARP, S. G. BURNAY, J. R. MATHEWS and E. A. HARPER, in Proceedings of the International Conference on Carbon Fibres, their Composites and Applications (Plastics Institute, London, 1974) paper 5.
265. E. V. MURPHY and B. F. JONES, *Carbon* **9** (1971) 91.
266. R. MORETON, *Fibre Sci. Technol.* **1** (1968) 271.
267. L. H. C. TIPPETT, *Biometrika* **17** (1925) 364 (from [254]).
268. P. W. BARRY, *Fibre Sci. Technol.* **11** (1978) 245.
269. P. E. McMAHON, *SAMPE Q.* October (1974) 7.
270. J. W. HITCHON and D. C. PHILLIPS, *Fibre Sci. Technol.* **12** (1979) 217.
271. W. WEIBULL, *J. Appl. Mech.* **18** (1951) 293 (from [258]).
272. C. P. BEETZ Jr, *Fibre Sci. Technol.* **16** (1982) 45.
273. *Idem*, Extended Abstracts of the 15th Biennial Conference on Carbon (American Carbon Society, St Marys, Pennsylvania, 1981) p. 300.
274. A. J. PERRY, K. PHILLIPS and E. De LAMOTTE, *Fibre Sci. Technol.* **3** (1971) 317.
275. E. De LAMOTTE and A. J. PERRY, *ibid.* **3** (1970) 157.
276. R. J. DIEFENDORF, R. J. CHEN, W. P. SUH, GROVES and J. J.-H. WANG, Tech. Report AD A096473 (Rensselaer Polytechnic Institute, Troy, New York, 1981).
277. B. F. JONES and R. G. DUNCAN, *J. Mater. Sci.* **6** (1971) 289.
278. P. BLESS and J. B. LANDO, *J. Polym. Sci. Polym. Lett.* **13** (1975) 153.
279. L. T. DRZAL, J. A. MESCHER and D. L. HALL, *Carbon* **17** (1979) 375.
280. J. B. DONNET and H. DAUKSCH, in Proceedings of the International Conference on Carbon Fibres, their Composites and Applications (Plastics Institute, London, 1971) paper 7.
281. B. RAND and R. ROBINSON, *Carbon* **15** (1977) 257.
282. F. HOPFGARTEN, *Fibre Sci. Technol.* **11** (1978) 67.
283. E. FITZER, K. H. GEIGL and L. M. MANOCHA, *Man Made Text. India* **21** (1978) 193.
284. O. P. BAHL and L. M. MANOCHA, *Die Angew. Makromol. Chemie* **75** (1979) 137.
285. J. H. CRANMER, G. C. TESORO and D. R. UHLMANN, *Ind. Eng. Chem. Prod. Res. Dev.* **21** (1982) 185.
286. E. FITZER, K. H. GEIGL and W. HUTTNER, *Carbon* **18** (1980) 265.
287. United Aircraft Corp., US Patent 3660140 (1972).
288. *Idem*, US Patent 3720536 (1973).
289. Union Carbide Corp., US Patent 3791840 (1974).
290. R. DAUKSYS, US Patent 3801350 (1974).
291. V. DIETZ, US Patent 3931392, (1976).
292. National Research and Development Council, UK, US Patent 3476703 (1969).
293. United Aircraft Corp., US Patent 3720536 (1973).
294. F. MOLLEYEYRE and M. BASTICK, in Proceedings of the International Conference on Carbon. BadHonnef, FRG. (1976) 500, from J. Delmonte, "Technology of Carbon and Graphite Fibre Composites" (Van Nostrand Reinhold, New York) p. 33.
295. L. P. KOBETS, N. V. POLYAKOVA, M. A. KUZETSOVA, O. B. KOLYASINSKAYA, V. S. SAMOILOV and N. V. BONDARENKO, *Polymer Mech.* **4** (1979) 4.

Received 8 October 1985
and accepted 22 May 1986

Journal of Materials Science

CHAPMAN AND HALL

Journal of Materials Science is an international publication reporting recent advances in all the major fields of investigation into the properties of materials. Papers and letters on metallurgy, ceramics, polymers, electrical materials, biomaterials, composites, and fibres appear regularly.

Papers for submission to the *Journal of Materials Science* should be sent to Professor W. Bonfield, Dept. of Materials, Queen Mary College, Mile End Road, London E1 4NS.

Journal of Materials Science is published monthly by Chapman and Hall Ltd., 11 New Fetter Lane, London EC4P 4EE, from whom subscription details are available.

JOURNAL OF MATERIALS SCIENCE 22 (1987) 3864–3872

Conversion of acrylonitrile-based precursors to carbon fibres

Part 3 *Thermooxidative stabilization and continuous, low temperature carbonization*

M. BALASUBRAMANIAN, M. K. JAIN, S. K. BHATTACHARYA, A. S. ABHIRAMAN*
School of Chemical Engineering, Georgia Institute of Technology, Atlanta, Georgia 30332, USA

The effects of stabilization conditions on the formation of a consolidated carbon fibre structure from two acrylonitrile-based precursor fibres, one containing itaconic acid as comonomer and the other a commercial precursor, have been studied. The progression of changes in elemental composition and properties such as sonic modulus, electrical resistance and density in a continuous, low temperature (1200° C) carbonization process are reported for the first time. A criterion based on attaining a composition dependent critical density in stabilization is proposed for avoiding the formation of a hollow core in carbon fibres processed continuously at reasonably rapid rates. Aspects related to the development of open and closed micropores in the carbon fibre structure and the possible mechanisms for the formation of a hollow core in carbonization are also discussed.

1. Introduction

Manufacture of carbon fibres from acrylonitrile-based precursor copolymers involves

(a) formation of oriented fibres, usually through solution spinning and a combination of drawing in the gel state and plastic deformation of dried fibre,

(b) low temperature (200–350° C) thermooxidative stabilization of the oriented precursor fibre to yield a structure that can maintain its cohesion during subsequent carbonization,

(c) carbonizing heat treatment (800–1600° C) in an inert atmosphere to drive off non-carbon elements, and

(d) an optional high temperature (> 2000° C) treatment to improve the mechanical properties, especially the stiffness of the fibres.

The nature of the fibres at every stage in the formation of carbon fibres depends on the conditions of processing at that stage as well as the chemical composition and the geometrical and morphological features of the material produced at the previous stage. As described in our review of the literature on the production of carbon fibres [1], numerous studies of isolated aspects have yielded extensive empirical knowledge but only a partial understanding of this complex process. We have undertaken a comprehensive experimental study in our laboratories to help expand our knowledge of the material and process contributions to the properties of the ultimate carbon fibres. The results from experiments in precursor fibre formation and batch stabilization, and from an extensive study of the rearrangements in continuous thermooxidative stabilization have been reported earlier [2, 3]. We report here additional results from continuous stabilization and initial experiments on the evolution of properties in low temperature (1200° C) continuous carbonization. The progression of carbonization was monitored through measurements of density, linear density, elemental composition, electrical resistance and sonic modulus.

2. Experimental details

2.1. Precursor fibres

Detailed descriptions of the experimental procedures are given in [3]. Two acrylic precursor fibres, II and III, were used in this study. Precursor III is a commercial precursor for carbon fibres. Precursor II fibres were produced in our laboratories from a 17.5% (w/w) solution of a copolymer of acrylonitrile (AN) and itaconic acid (IA) in the weight ratio of 97/3 (average molecular weight = 131 000 g mol^{-1}, estimated from intrinsic viscosity). The spinning conditions for precursor II, established to produced fibres of good quality, are given in Table I. The jet stretch and the draw ratio were changed to obtain fibres having different orientations. High-temperature drawing of some of the precursor fibres was performed in order to produce fibres with high orientation and morphological parameters different from those produced by drawing in boiling water. Two types of post-spinning high temperature drawing processes, i.e. over a hot godet and through a hot oven, were performed on the hot water (partially) drawn fibres. In the former type of drawing, precursor fibres were drawn directly from the heated feed-godet, whereas

*Author to whom all correspondence should be addressed.

0022–2461/87 $03.00 + .12

TABLE I Conditions of formation of precursor II fibres

	Precursor II		
Polymer solution:			
Solution concentration, % (w/w)	17.5		
Solution viscosity, poise	140		
Coagulation bath			
Coagulation bath composition, % DMF	60		
Coagulation bath temp., °C	14		
Drawing conditions:			
Jet Stretch	0.7	1.2	0.7
Draw Ratio, in boiling water	2.5	3	5
Denier/filament (dpf)	3.9	2.2	2.2

in the latter type the fibres were first annealed at a relatively low temperature (115 to 130° C) on the feed-godet and then drawn through an oven. Details of the drawing conditions are given in Table II. The first letter in the sample identification code refers to the precursor type. The second and the third terms represent the jet-stretch and the draw-ratio (in boiling water), respectively. The last three terms signify the post-spinning, high temperature plastic drawing conditions, such as type of heater (oven or godet), temperature and draw-ratio, respectively. The temperatures employed in the hot-oven drawing were the maximum possible for a smooth drawing operation without filament breakages. The mechanical properties and morphological parameters of the precursor fibres are given in Table III. It can be seen clearly that a broad range of precursor fibre properties has been achieved through the different drawing processes.

2.2. Continuous stabilization and carbonization

The fibres were stabilized in air in a continuous process with an 18-ft long linear, tubular oven. The furnace was divided into three, 6-ft zones, with each zone controlled by individual temperature controllers. Various ascending temperature profiles (Table III) were used in this process. Precursor II was processed at an input and output linear velocity of 1 inch min^{-1}. When processed at constant input and output velocities, precursor III fibres developed excessive shrinkage forces, leading to breakage of filaments and so these were run with the minimum net shrinkage (9%)

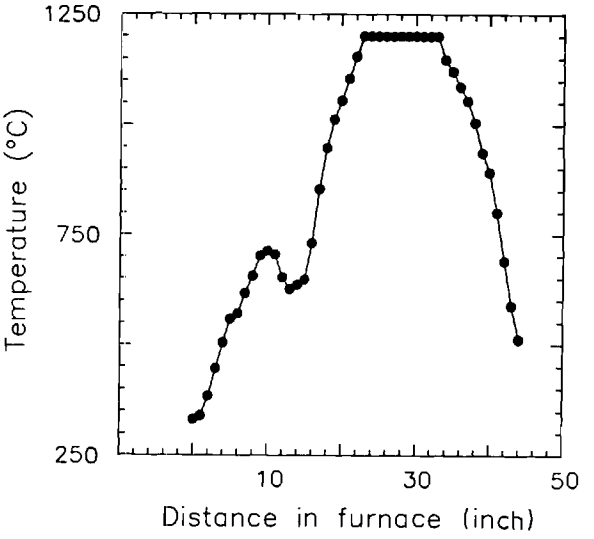

Figure 1 Temperature profile in carbonization.

required for good processing. The finer filaments in this precursor required lower residence times for stabilization when compared with Precursor II fibres and so these were processed at input and output velocities of 2.75 and 2.5 inch min^{-1}, respectively.

Carbonization of the stabilized fibres was carried out by passing them through a Lindberg furnace at 1200° C. To avoid thermal shock and allow for a gradual increase in the temperature of the filaments, two heaters were installed at the entrance to the furnace which provided two 6-inch precarbonization zones of 500 and 700° C. The temperature profile obtained in this set-up is shown in Fig. 1. The dip in the temperature profile is caused by the separation between the second preheater and the heater in the Lindberg furnace. Nitrogen was passed through both ends of the furnace to maintain an inert atmosphere.

Samples for studies of the progression of carbonization in a steady state process were obtained by cutting the fibre bundle at the delivery end and rapidly winding it on a spool at the feed end.

2.3. Properties of fibres

Measurement of velocity of sonic pulse propagation through the fibre samples was made with the sonic modulus tester PPM-5 with a refractory mount,

TABLE II Precursor II drawing conditions

Sample	Draw-ratio			Drawing godet/oven temp. (°C)	Annealing godet temp. (°C)	Denier/filament
	B.W.*	H.T.†	Total			
II-1.2-3	3.0	–	3.0	– –	–	2.3
II-0.7-5	5.0	–	5.0	– –	–	2.2
II-0.7-2.5-O-228-1.8	2.5	1.8	4.5	228, oven	115	2.2
II-0.7-2.5-G-160-1.8	2.5	1.8	4.5	160, godet	160	2.2
II-0.7-2.5-O-224-2.5	2.5	2.5	6.2	224, oven	118	1.6
II-0.7-2.5-G-190-2.7	2.5	2.7	6.7	190, godet§	190	1.5

*Draw-ratio in boiling water.
† High-temperature draw-ratio.
§ The drawn fibres were yellowish due to partial degradation/stabilization.
Sample notation: Precursor type-jet stretch-hot water draw ratio-oven/godet drawing-drawing temperature-draw ratio. e.g., II-0.7-2.5-O-228-1.8 refers to a sample with precursor II, jet stretch = 0.7, hot water draw ratio = 2.5, drawing through the oven at 228° C with draw ratio of 1.8.

TABLE III Mechanical properties and morphological parameters of precursor fibres.

Sample	Denier/ filament	Tenacity (g denier^{-1})	Elong. (%)	Young's modulus (g denier^{-1})	Sonic modulus (g denier^{-1})	Orientn. function f_c	Crystal size (nm)

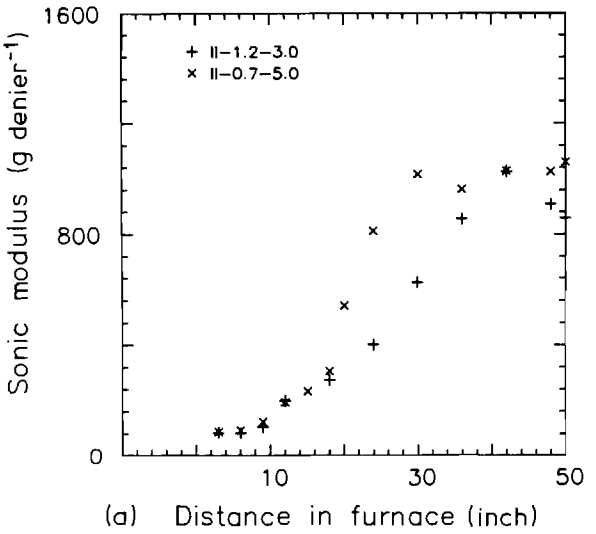

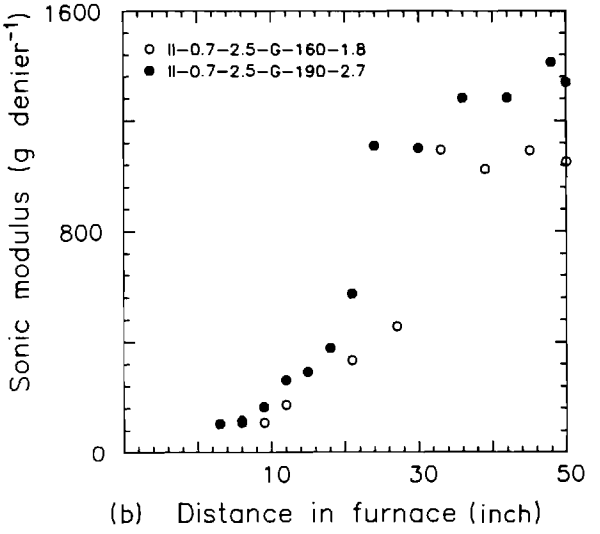

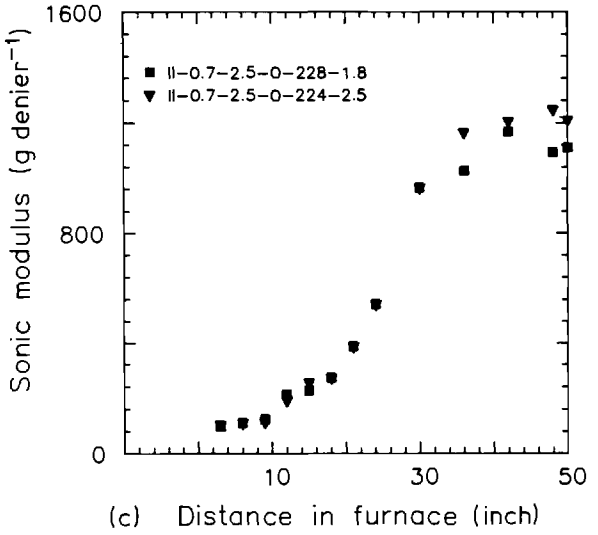

Figure 2 Change in sonic modulus during carbonization of precursor II. The fibres are drawn in (a) hot water; (b) hot water and over a hot godet; (c) hot water and through a hot oven. (The conditions of formation of the precursor fibres are given in the sample designations.)

same trend of rapid change in the 700 to 1200° C zone (Fig. 4). The resistance falls from about $10^{14}\,\Omega\,cm^{-1}$ to less than $10\,\Omega\,cm^{-1}$ when the temperature is raised to its maximum of 1200° C, after which it remains constant upon continued heating at this temperature.

The progression of density changes is plotted as a function of distance in the furnace in Fig. 5. Density increases very rapidly during the 700 to 1200° C heating, suggesting significant rearrangements leading to consolidation of structure in the fibres, but it is followed by a sharp drop before levelling off upon continued heating at 1200° C. This decrease in the measured density of the carbonized fibres is quite significant and is observed in all fibres. A plot of densities of three samples from carbonization, using II-0.7-5 fibres stabilized at 250–275–300° C, shows that the trend is very reproducible (Fig. 5d). The reason for this drop in apparent density is not very clear at this point and is being explored further. A reason for this drop in apparent density could be the conversion of open pores to closed pores, i.e. some of the pores which are initially accessible to the solvents employed for the density measurement become inaccessible, resulting in a decrease in the measured density. This suggests that consolidation of the structure occurs around the pores during the high temperature

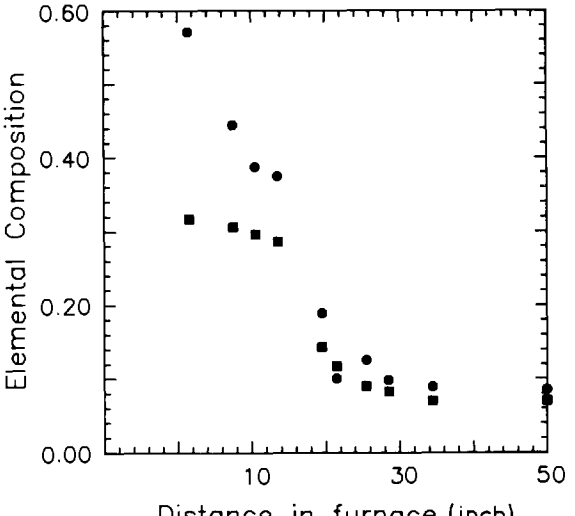

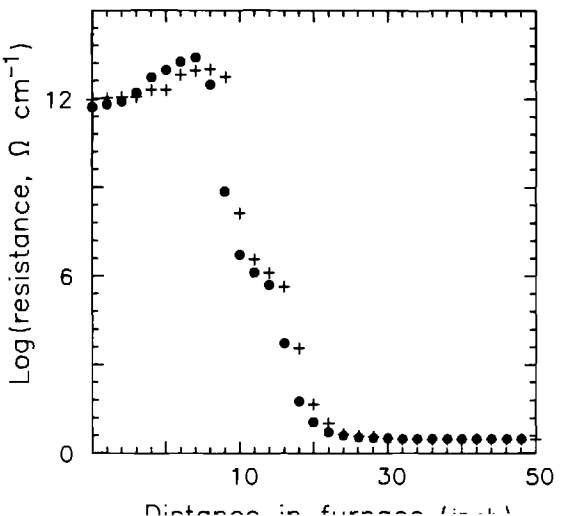

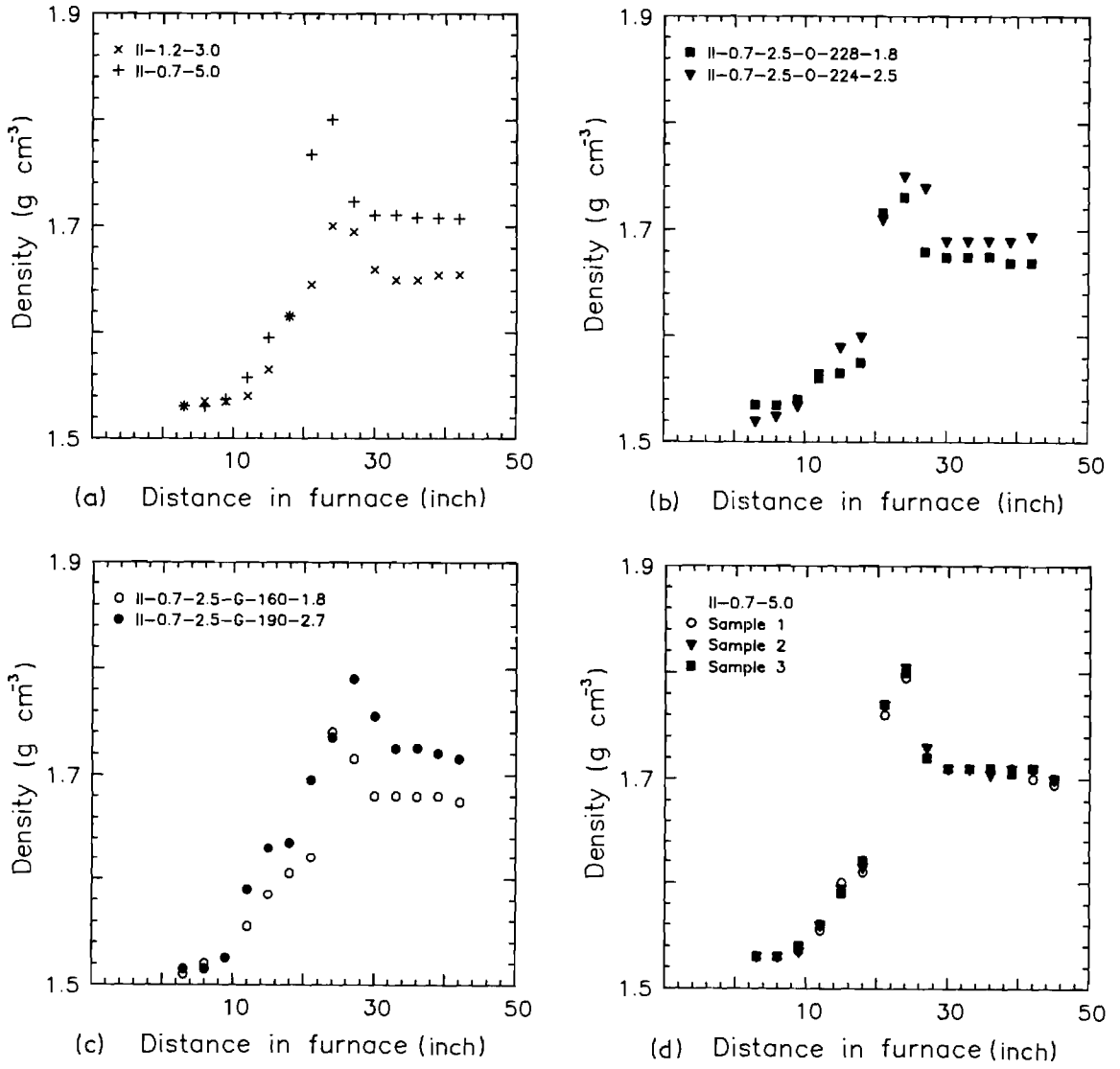

Figure 5 Change in density during carbonization of precursor II. (a) and (d) drawn in hot water; (b) drawn in hot water and hot oven; (c) drawn in hot water and hot godet. (The conditions of formation of the precursor fibres are given in the sample designations, d)

annealing in the latter stages. A similar explanation has been offered earlier by Gibson [6] for the decrease in density observed for carbon fibres produced at increasing temperatures in the range of 1000 to 2000° C.

The effect of continuous carbonization at different speeds was also explored with precursor II fibres. Sample II-0.7-5 was employed for this study and carbonization was carried out at speeds ranging from 0.5 to 3.9 ft min^{-1}, giving a residence time range of 1 to 8 min in the furnace (0.25 to 2 min in the 1200° C zone). At speeds greater than 2 ft min^{-1} very fuzzy bundles with many broken filaments were obtained. Electron microscopic examination of the cross-sections of the carbonized fibres showed holes in the centre of fibres processed at speeds of 2 ft min^{-1} and higher (Table V). From the progression of changes in carbonization discussed earlier, it is apparent that the highest temperature which the fibre experiences during carbonization is important since limits on fibre properties are dictated by this temperature. In the

TABLE V Carbonization at different speeds

Take-up speed (ft min^{-1})	Residence time at 1200° C (min)	Carbon fibres from precursor II			Carbon fibres from precursor III			
		Hollow core	Density (g cm^{-3})	Sonic modulus (g denier^{-1})	Hollow core	Density (g cm^{-3})	Sonic modulus (g denier^{-1})	Denier
0.5	2.00	No	1.715	1061	–	–	–	–
1.0	1.00	No	1.705	1049	No	1.740	1210	1650
2.0	0.50	Yes	1.665	964	Yes	1.715	1195	1761
3.0	0.33	Yes	1.660	918	Yes	1.710	1066	1818
3.9*	0.26	Yes	1.650	908	Yes	1.710	1035	1805

*Maximum speed of the take-up unit.
Temperature profile in stabilization: Precursor II-0.7-5 250-275-300° C.
Precursor III 250-275-275° C.

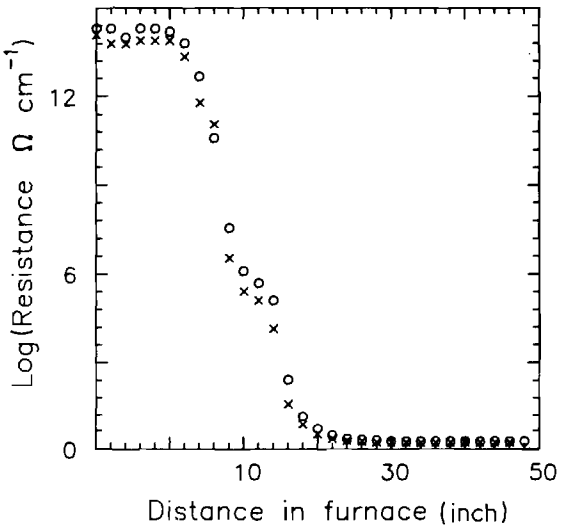

Figure 6 Change in electrical resistance during carbonization of precursor III. (○) 1 ft min^{-1}, (×) 6 inch min^{-1}.

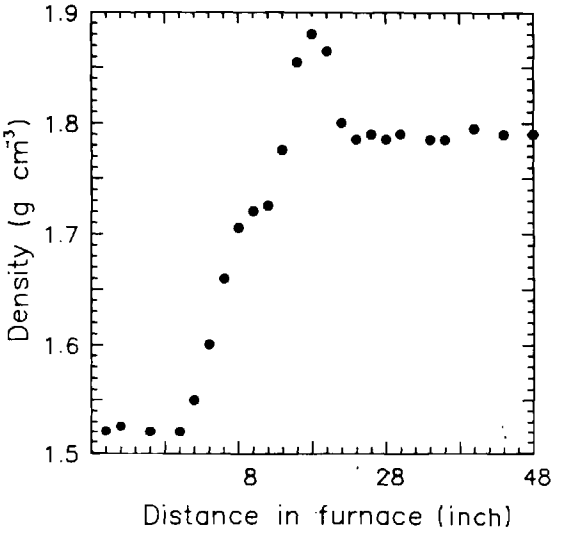

Figure 7 Change in density during carbonization of precursor III.

experiments on carbonization at different speeds, the fibre was always exposed to the maximum temperature of 1200° C, but this temperature was reached at higher rates at the higher processing speeds. The formation of a hollow core when these apparently well stabilized fibres are carbonized at higher rates of heating suggests that more than a single mechanism exists for hole formation in the core. At the higher heating rates, an outer layer of the fibre may be carbonized rapidly, with subsequent consolidation of the structure from the sheath inwards, resulting in a hollow core at the end of the process. The decrease in sonic modulus and in the apparent density of carbon fibres (Table V) produced at higher carbonization speeds reflects also poor consolidation of structure under these conditions.

The progression of changes during continuous carbonization of precursor III fibres show the same features as seen with precursor II fibres (for example, Figs 6, 7). Linear densities were also measured on these samples. These measurements reveal once again Fig. 8) simultaneous rapid loss of material and consolidation of the solid state structure in the initial zone where the temperature is raised to the maximum temperature, with little change beyond this point. When carbonization is carried out at different speeds, the development of a hollow core as well as evidence for incomplete consolidation (Table V) are seen again at processing speeds of 2 ft min^{-1} and higher.

In order to establish the validity of the two different mechanisms that have been proposed to operate under different conditions of formation of a hollow core in carbon fibres, namely,

i. "burning off" of the core material when an incompletely stabilized fibre from a diffusion controlled solid-state stabilization process is carbonized, and,

ii. propagation of the consolidated carbonized structure inwards from the skin when a well stabilized fibre is carbonized rapidly,

additional measurements were carried out in a series of carbonization experiments with incompletely and sufficiently stabilized precursor III fibres. In these experiments, the results of which are reported in Table VI, the linear densities and diameters of these fibres are compared. When the fibres are carbonized at low speeds (0.5 ft min^{-1}), the linear density of the carbon fibres from sufficiently stabilized precursor is significantly higher than that from the incompletely stabilized precursor indicating the expected loss of material in the latter through "burn off". Every filament in the latter bundle also exhibited a hollow core. When these two precursor fibres were carbonized at a higher speed (3.5 ft min^{-1}), a hollow core developed in both cases, but the linear density *and* the diameter of the sufficiently stabilized precursor were higher, consistent with the consolidation mechanism at the higher rates of carbonization proposed here. Comparison of the carbon fibres produced at different speeds from apparently well stabilized fibres shows little difference in linear densities, lending further support to the mechanism of consolidation inwards from the skin. Also, when the sufficiently stabilized precursor is carbonized repeatedly at 1.5 ft min^{-1}, a condition which yields a hollow core in about 60% of the filaments, little change in diameter is observed with

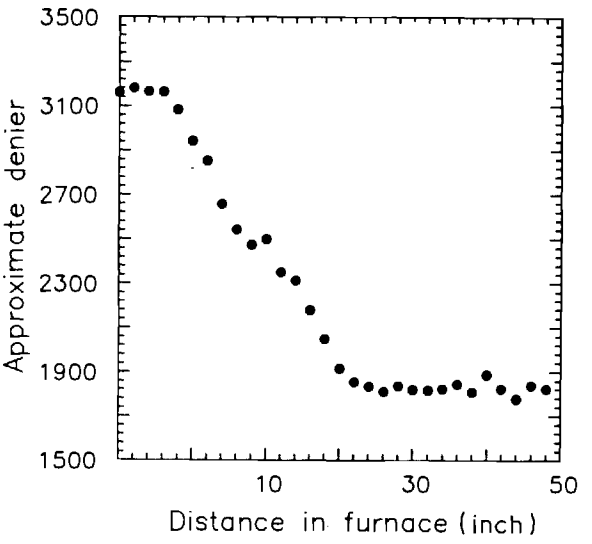

Figure 8 Change in linear density during carbonization of precursor III.

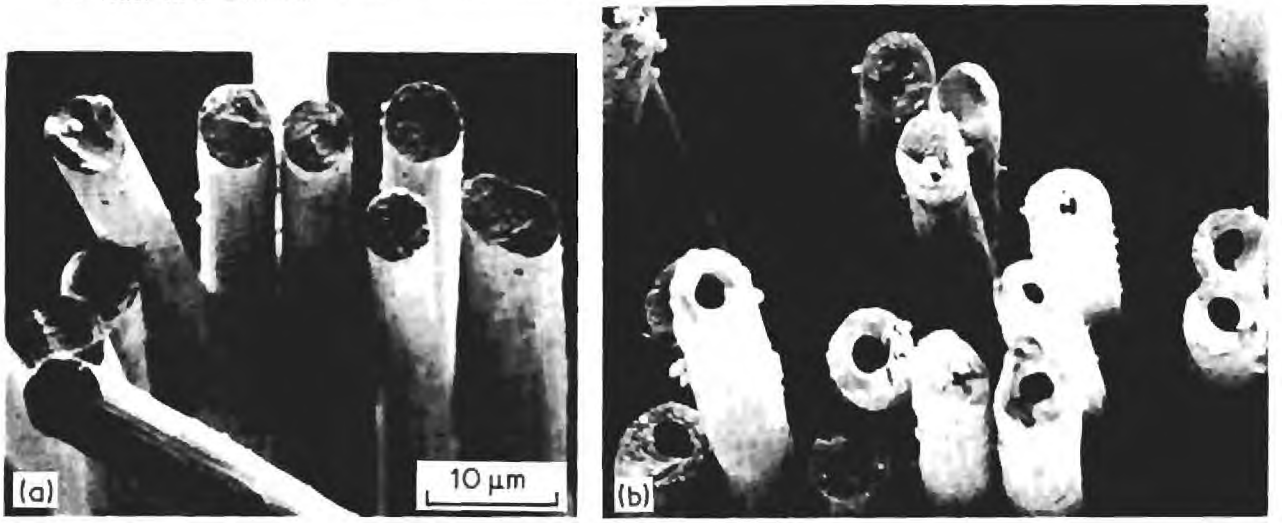

Figure 9 Typical cross-sections of carbonized fibres from precursor III. (a) Stabilized at 250–275–275, carbonized at 0.5 ft min^{-1}. (b) Stabilized at 250–275–275, carbonized at 3.5 ft min^{-1}. (c) Stabilized at 250–265–265, carbonized at 3.5 ft min^{-1}.

reconsolidation. Typical cross-sections from these experiments are shown in Fig. 9.

We see that the qualitative features of the progression of changes during the carbonization are not changed with composition (comonomer with AN) or the extent of orientational and lateral order generated in the formation of precursor fibres. Fundamental aspects of the evolution of properties revealed through the measurements in this study are thus believed to be the general characteristics of the formation of carbon fibres from acrylonitrile-based precursor fibres.

4. Conclusions

A number of significant results have been obtained through the research on continuous low temperature carbonization reported here. These findings and the inferences from them regarding needed additional research are summarized in the following.

i. It is necessary to carry out the stabilization treatment until a critical density is reached in order to avoid the formation of a hollow core in carbon fibres processed under reasonably rapid carbonization conditions. This aspect has been known in commercial practice. The dependence of this critical density on composition remains to be explored.

ii. A hollow core is also formed when apparently well stabilized fibres are carbonized at rates higher than a critical rate. This suggests that more than a single mechanism exists for hole formation in the core and that structural/chemical changes are temperature/time dependent. The influence of low stabilization and slow carbonization against high stabilization and fast carbonization on ultimate properties was not determined. It is possible that, at the higher rates of the carbonization process, an outer layer of the fibre is carbonized rapidly and that subsequent consolidation occurs from the skin inwards, resulting in a hollow core at the end of the process.

iii. Properties such as electrical conductance and sonic modulus, which depend on the extent of formation of ordered basal planes, develop rapidly initially

TABLE VI Carbonization with sufficiently (A) and incompletely (B) stabilized precursor III fibres. Stabilization temperature sequence: A (250-275-275) and B (250-265-265) in °C.

Sample	Carbonization speed (ft min^{-1})	Density (gm cm^{-3})	Denier/filament	Diameter (μm)
A-1	0.5	1.73	0.60	5.6
A-2	3.5	1.71	0.59	6.5
A-3	1.5	1.73	0.60	6.6
A-3-1*	1.5	1.73	0.58	6.5
A-3-2†	1.5	1.76	0.58	6.6
B-1	0.5	1.71	0.54	5.3
B-2	3.5	1.71	0.53	5.5

* Re-carbonization of A-3.
† Re-carbonization of A-3-1.

in the carbonization process, with a slower asymptotic increase with continued heating at the highest temperature. Both the rate and the extent of increase in sonic modulus during carbonization increase with the extent of lateral and orientational order present in the precursor fibres which should promote the ordering process during carbonization. These trends are also reflected in [H]/[C] and [N]/[C] ratios which indicate the degree of aromatization and basal plane formation.

iv. The density of fibres rises in the initial stages of carbonization but reaches a relative maximum beyond which it decreases rapidly to a lower steady value. This apparent decrease is believed to be the result of consolidation of ordered domains around some of the micropores, converting them from "open" pores to "closed" pores, inaccessible to the measuring liquid. This hypothesis needs to be confirmed with a combination of SAXS and measurements based on volume filling of accessible pores and adsorption on accessible surfaces. The combination of density and accessible surface area measurements has been used by Kipling *et al.* [7] to infer open and closed pore structures in graphitizing and non-graphitizing carbons. Additional evidence can also be obtained by combining linear density with measurements of filament diameter along the carbonization line.

v. Procedures developed in this study for monitoring the evolution of carbon fibres in a continuous process can be valuable in optimizing the carbonization set-up. It is necessary to have the provision to alter the temperature profile in carbonization so that measurements of the evolution of properties during the process can be used to advantage in tailoring the appropriate time–temperature profile.

Note

Preliminary results from current research in our laboratories indicate that while the levels of modulus that can be reached in carbonization may be dictated by the orientational order in the precursor fibres, the strength that can be obtained may be affected by both orientational and lateral crystalline order in the precursor fibres. A very high degree of crystalline order in the precursor fibres would diminish the orientational relaxation that can occur during stabilization, especially in the early stages, and thus reduce the concentration of the strength limiting misoriented crystallites in the carbon fibres produced from them. These aspects will be discussed later in this sequence.

Acknowledgements

The authors wish to thank Drs W. C. Tincher and F. L. Cook, and Mr P. Desai for valuable discussions on many aspects of this research. We wish to express our gratitude to Dr L. H. Peebles for many useful suggestions during the course of this work and in the inferences drawn from experimental data. The study was supported by the United States Office of Naval Research.

References

1. M. K. JAIN and A. S. ABHIRAMAN, *J. Mater. Sci.* **22** (1987) 278.
2. *Idem. ibid.* **18** (1983) 179.
3. M. K. JAIN, M. BALASUBRAMANIAN and A. S. ABHIRAMAN, *J. Mater. Sci.* **22** (1987) 301.
4. M. K. JAIN, PhD thesis, Georgia Institute of Technology, Atlanta, Georgia (1985).
5. US Patent 4279612, Great Lakes Carbon Corp., New York (1981).
6. D. W. GIBSON, *18th National SAMPE Symp.*, **18** (1973) 165.
7. J. J. KIPLING, J. N. SHERWOOD, P. V. SHOOTER and N. R. THOMPSON, *Carbon* **1** (1964) 321.

Received 8 October 1985
and accepted 15 January 1987

PRECURSOR STRUCTURE – FIBER PROPERTY RELATIONSHIPS IN POLYACRYLONITRILE-BASED CARBON FIBERS

By

A. S. ABHIRAMAN

PRINCIPAL INVESTIGATOR

FINAL REPORT

JULY 11, 1990

Contract Number N00014–85–K–0636

Sponsored by: THE OFFICE OF NAVAL RESEARCH

School of Chemical Engineering
GEORGIA INSTITUTE OF TECHNOLOGY
A Unit of the University System of Georgia
Atlanta, Georgia 30332

SECURITY CLASSIFICATION OF THIS PAGE

REPORT DOCUMENTATION PAGE

1a. REPORT SECURITY CLASSIFICATION Unclassified	1b. RESTRICTIVE MARKINGS
2a. SECURITY CLASSIFICATION AUTHORITY	3. DISTRIBUTION / AVAILABILITY OF REPORT Unlimited
2b. DECLASSIFICATION / DOWNGRADING SCHEDULE	
4. PERFORMING ORGANIZATION REPORT NUMBER(S) E-19-640-1	5. MONITORING ORGANIZATION REPORT NUMBER(S)
6a. NAME OF PERFORMING ORGANIZATION Ga.Tech Research Corp. — 6b. OFFICE SYMBOL (*If applicable*)	7a. NAME OF MONITORING ORGANIZATION ONR
6c. ADDRESS (*City, State, and ZIP Code*) Ga.Tech Research Corp. Georgia Institute of Technology Centennial Res.Bldg., Rm. 24, Atlanta, GA 30332-0420	7b. ADDRESS (*City, State, and ZIP Code*) Delores H. Perdue Code 1513: GFT, Office of Naval Research 800 N. Quincey St., Arlington, VA 22212-5000
8a. NAME OF FUNDING / SPONSORING ORGANIZATION — 8b. OFFICE SYMBOL (*If applicable*)	9. PROCUREMENT INSTRUMENT IDENTIFICATION NUMBER N00014-85-K0636
8c. ADDRESS (*City, State, and ZIP Code*) Office of Naval Research 800 N. Quincy St. Arlington, VA 22212-5000	10. SOURCE OF FUNDING NUMBERS PROGRAM ELEMENT NO. — PROJECT NO. — TASK NO. — WORK UNIT ACCESSION NO.

11. TITLE (*Include Security Classification*)
'Precursor Structure - Fiber Property Relationships in Polyacrylonitrile-Based Carbon Fibers" U

12. PERSONAL AUTHOR(S)
A.S. Abhiraman

13a. TYPE OF REPORT	13b. TIME COVERED	14. DATE OF REPORT (*Year, Month, Day*)	15. PAGE COUNT
Final Report	FROM 850601 TO 900615	900712	117

16. SUPPLEMENTARY NOTATION

17. COSATI CODES			18. SUBJECT TERMS (*Continue on reverse if necessary and identify by block number*)
FIELD	GROUP	SUB-GROUP	Polyacrylonitrile; Stabilization;Carbonization; Carbon Fibers; PAN-based Carbon Fibers

19. ABSTRACT (*Continue on reverse if necessary and identify by block number*)

This report describes a research effort which was aimed to strengthen the fundamental knowledge base and to provide rational directions for advances in precursor fiber structures and process routes to generate new morphologies and superior mechanical properties in PAN-based carbon fibers. Critical aspects pertaining to each of the three interactive stages of carbon fiber production, viz., precursor fiber formation, oxidative stabilization and carbonization, were studied. Important new results pertaining to morphology of oriented precursor fibers, morphological rearrangements during stabilization, mathematical modeling of the solid-state reactions in stabilization,critical criteria for evaluating the suitability of oxidized fibers for carbonization, and evolution of morphology, chemical structure and properties in carboni-zation were obtained. Mechanisms for obtaining high morphological order in precursor fibers and for maximizing transfer of this order from the precursor to the carbon fiber were identified.

Recommendations have been made regarding future research to explore mechanisms by which the following may be accomplished: (i) new carbon fiber morphologies with improved compressive properties; (ii)new routes for precursor fibers which would eliminate current (continued)

20. DISTRIBUTION / AVAILABILITY OF ABSTRACT	21. ABSTRACT SECURITY CLASSIFICATION
☒ UNCLASSIFIED/UNLIMITED ☐ SAME AS RPT. ☐ DTIC USERS	Unclassified
22a. NAME OF RESPONSIBLE INDIVIDUAL	22b. TELEPHONE (*Include Area Code*) — 22c. OFFICE SYMBOL

DD FORM 1473, 84 MAR — 83 APR edition may be used until exhausted. All other editions are obsolete.

SECURITY CLASSIFICATION OF THIS PAGE

PRECURSOR STRUCTURE – FIBER PROPERTY RELATIONSHIPS IN POLYACRYLONITRILE-BASED CARBON FIBERS

By

A. S. ABHIRAMAN

PRINCIPAL INVESTIGATOR

FINAL REPORT

JULY 11, 1990

Contract Number N00014-85-K-0636

Sponsored by: THE OFFICE OF NAVAL RESEARCH

School of Chemical Engineering
GEORGIA INSTITUTE OF TECHNOLOGY
A Unit of the University System of Georgia
Atlanta, Georgia 30332

Contents

PRECURSOR STRUCTURE – FIBER PROPERTY RELATIONSHIPS IN POLYACRYLONITRILE-BASED CARBON FIBERS* [1]

I. Introduction and Objectives

Carbon fibers occupy a premier position among high performance fiber structures, with a combination of physical and mechanical properties, in tension and in compression, that makes them uniquely suitable for application in many advanced fiber-reinforced composites. Fundamental investigations pertaining to precursor fibers and conversion processes in the last decade have paved the way for significant improvements in mechanical properties, especially in the tensile properties of polyacrylonitrile- (PAN) based fibers. Much of the empiricism which existed in the early phases of carbon fiber development has been replaced by fundamental knowledge of the evolution of structure and properties. Georgia Tech has been a significant contributor to this global effort, with important contributions and current research spanning the range from acrylic precursor fiber formation, through oxidative stabilization, to carbonization.

The primary objectives of the research reported here have been to strengthen the fundamental knowledge base and to provide rational directions for advances in precursor fiber structures and process routes to generate new morphologies and superior mechanical properties in PAN-based carbon fibers. Significant progress in this direction has been made through a general emphasis on exploration of the fundamental aspects of the chemical and morphological evolution from PAN-based precursors to carbon fibers. "Material–Process–Morphology–Property" relations have been explored at each of the three major stages in the conversion of PAN-based polymers to carbon fibers [2–12, 14, 15]. The major emphasis has been on the following aspects

1. Morphology and relevant morphological parameters in PAN-based precursor fibers.

[1]* Substantial portions of the material in this report will be published as a chapter in *"Composites: Chemical and Physicochemical Aspects,"* eds. Tyrone L. Vigo and Barbara J. Kinzig, Advances in Chemistry, ACS. (Authors:Dale Grove, Vijay Daga, Prashant Desai and A. S. Abhiraman)

2. Stress-Environment-Material interactions during oxidative stabilization.

3. Evolution of structure and properties in carbonization.

Significant results have been obtained in every component of this investigation. The procedures for – and the results from – these investigations are summarized in Section II. Additional information pertaining to the summary are given in Appendix II via reproduction of some of the critical publications from this research.

II. Summary of Procedures and Results

II.1 Morphology of Acrylic Precursor Fibers

A prerequisite to our ability to describe structure development during the various stages in the formation of carbon fibers is an understanding of the morphology of the PAN-based precursor fibers. Through an exhaustive study of structure and thermorheological behavior of oriented acrylic fibers, the fibrillar model with alternating laterally ordered and disordered regions, proposed by Warner, Uhlmann and Peebles [1], has been determined to be the most appropriate morphological model for these fibers [2-5]. The salient features are summarized in Table 1. The data in the table and the accompanying figures are for a commercial acrylic fiber, redissolved and spun in our laboratories (Table 2) [5]. One fiber, HWD, was obtained by drawing to a draw ratio of 7.3 in boiling water to yield precursor fibers. The other precursor fiber, HTD, was obtained by drawing to a draw ratio of 3.0 in boiling water followed by drawing in a hot oven at 252°Cto a draw ratio of 2.3.

When PAN fibers are heated in a calorimeter, an exotherm is observed in the heating thermogram. This exotherm corresponds to chemical reactions that contribute to oxidative stabilization. A melting endotherm is not observed. However, if water is used as a plasticization agent in a closed sample cell, the melting point of the crystals can be depressed to temperatures lower than the reaction temperatures (Figure 2). If the cell is cooled subsequent to the heating scan an exothermic transition, due to recrystallization, can be observed. The reversible first order transition in plasticized calorimetry of PAN-based fibers demonstrates the existence of true crystals.

Spontaneous shrinkage at high temperatures (figure 3), without any loss in the extent or the orientation of the ordered domains (figure 4), and the large drop in

Table 1: Morphological model of drawn, PAN-based precursor fiber

OBSERVATIONS	INFERENCES
1. WAXD Pattern (Fig. 1)	Presence of an Oriented, Laterally Ordered Phase
2. Enthalpy Changes in Plasticized Heating (Fig. 2)	The Laterally Ordered Phase consists of "True" Crystals, i.e. products of First Order Transitions
3. Spontaneous Shrinkage upon Free Annealing without Loss of Orientation in the Laterally Ordered Phase (Figs. 3, 4)	Presence of an Oriented but Less Ordered Phase with Chain segments bridging the Laterally Ordered Crystals along the Fiber Direction
4. Development of Thermal Stress upon Constrained Annealing (Fig. 5)	
5. Large Spontaneous drop in Sonic Modulus ONLY when Shrinkage is Allowed during Annealing (Fig. 6)	
6. Constant Density of Fibers with Different extents of Lateral Order	Laterally Ordered and Disordered Phases of Possibly the Same Density
7. SAXS Meridional "Peak" after Diffusion of Electron Dense Molecules (Fig. 7)	Repeating Sequence of Oriented Laterally Ordered (LO) and Laterally Disordered (DO) Phases

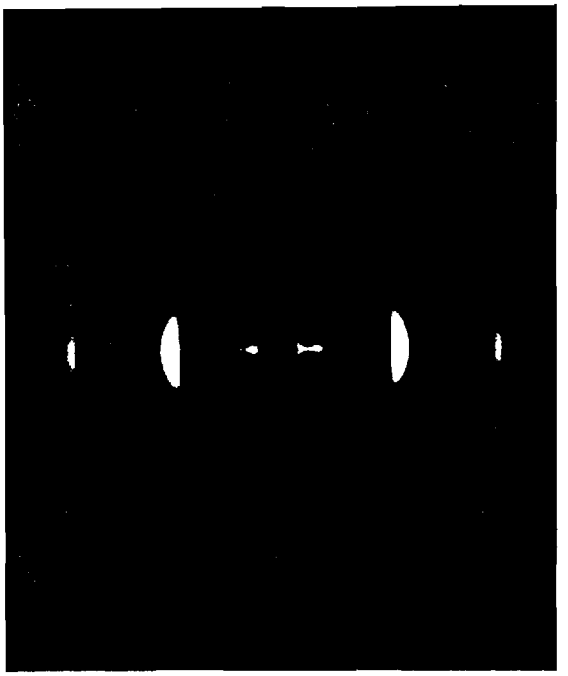

Figure 1: Wide angle x-ray diffraction flat plate photograph of a typical acrylic precursor fiber.

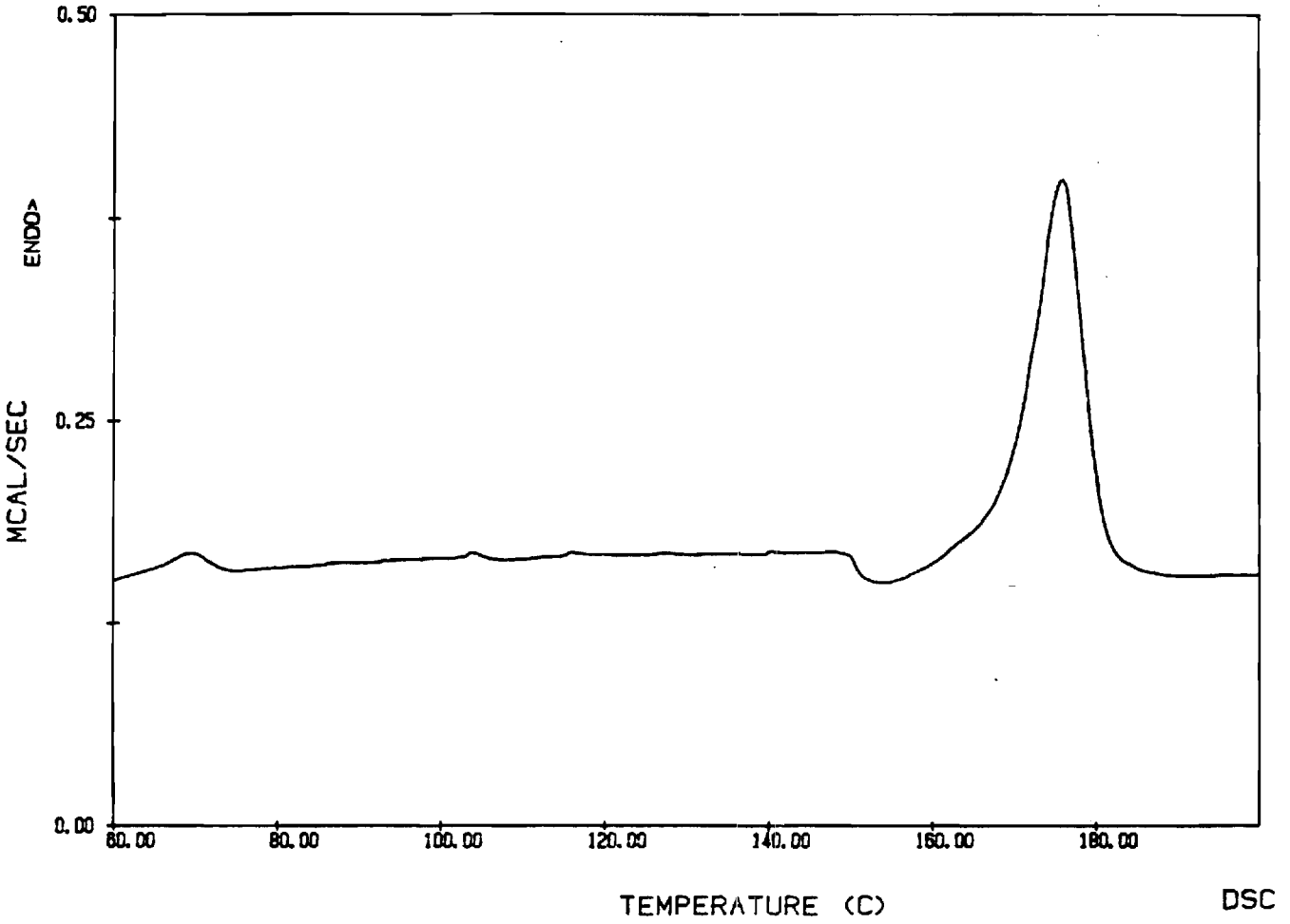

Figure 2: DSC thermogram of PAN-based precursor fiber on plasticized heating.

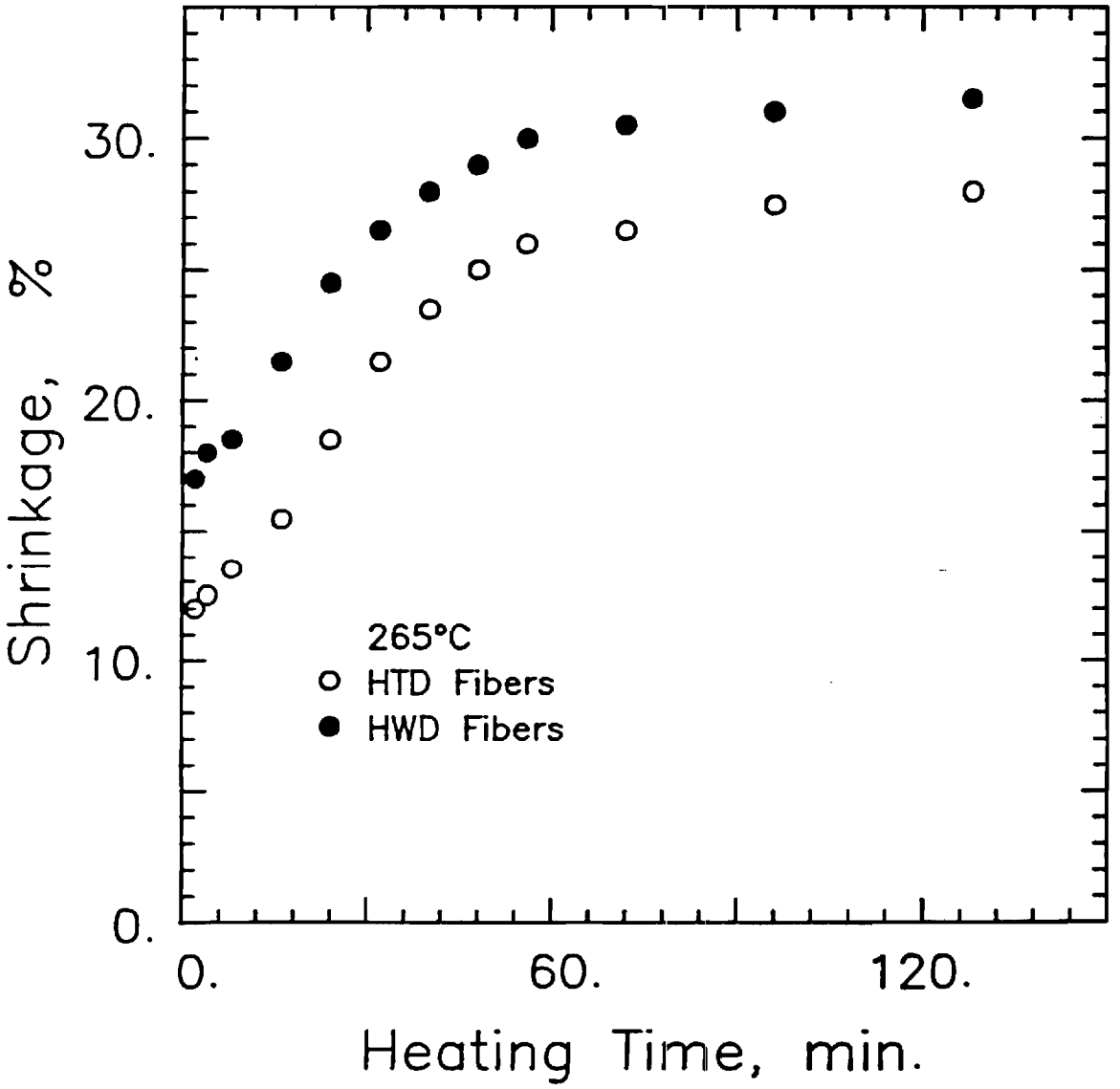

Figure 3: Shrinkage in FL batch stabilized fibers. (O) HTD Fibers (●) HWD Fibers [5].

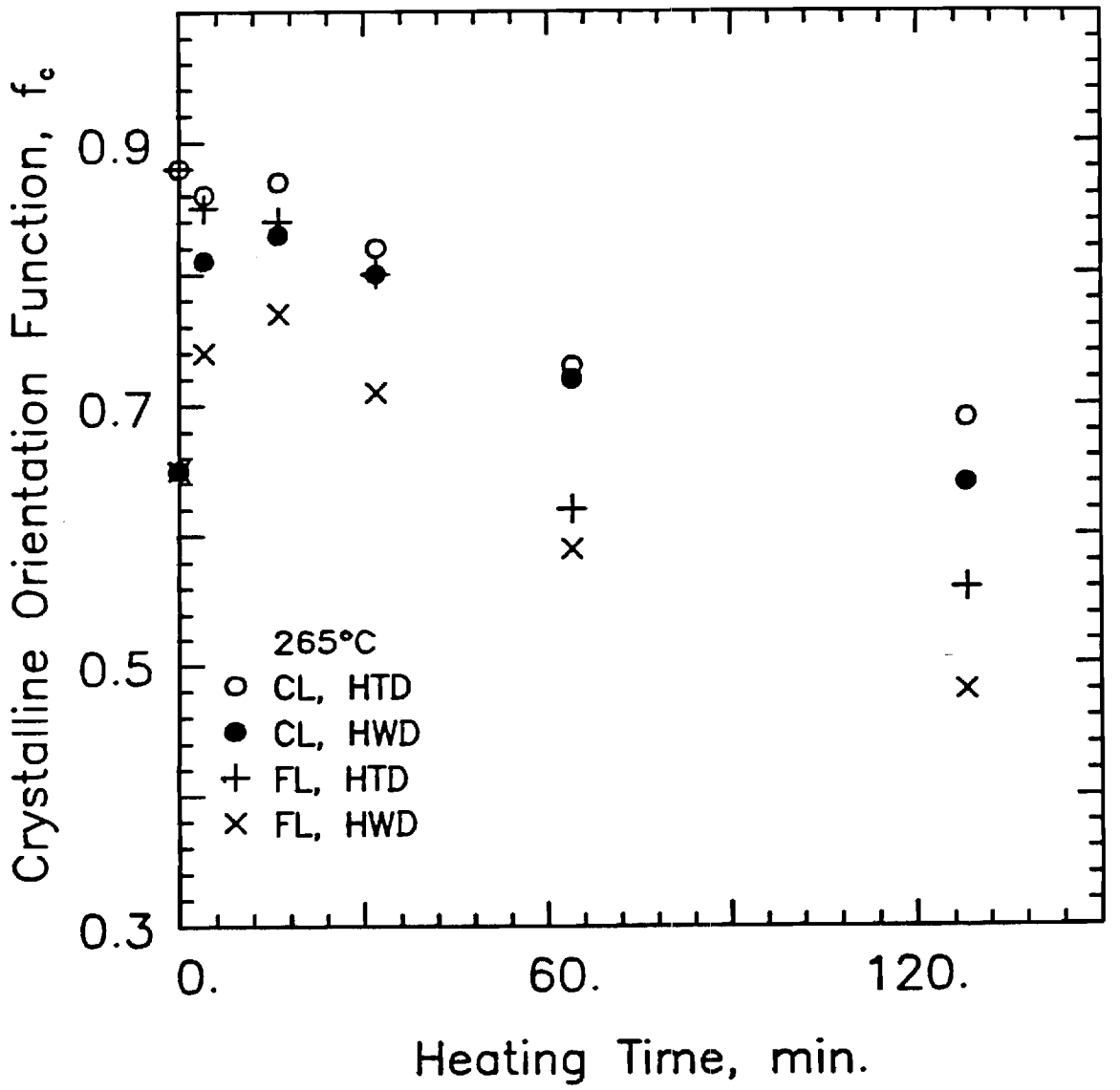

Figure 4: Crystalline orientation function, f_c, of CL and FL batch stabilized fibers. (O) CL, HTD Fibers (●) CL, HWD Fibers (+) FL, HTD Fibers (X) FL, HWD Fibers [5].

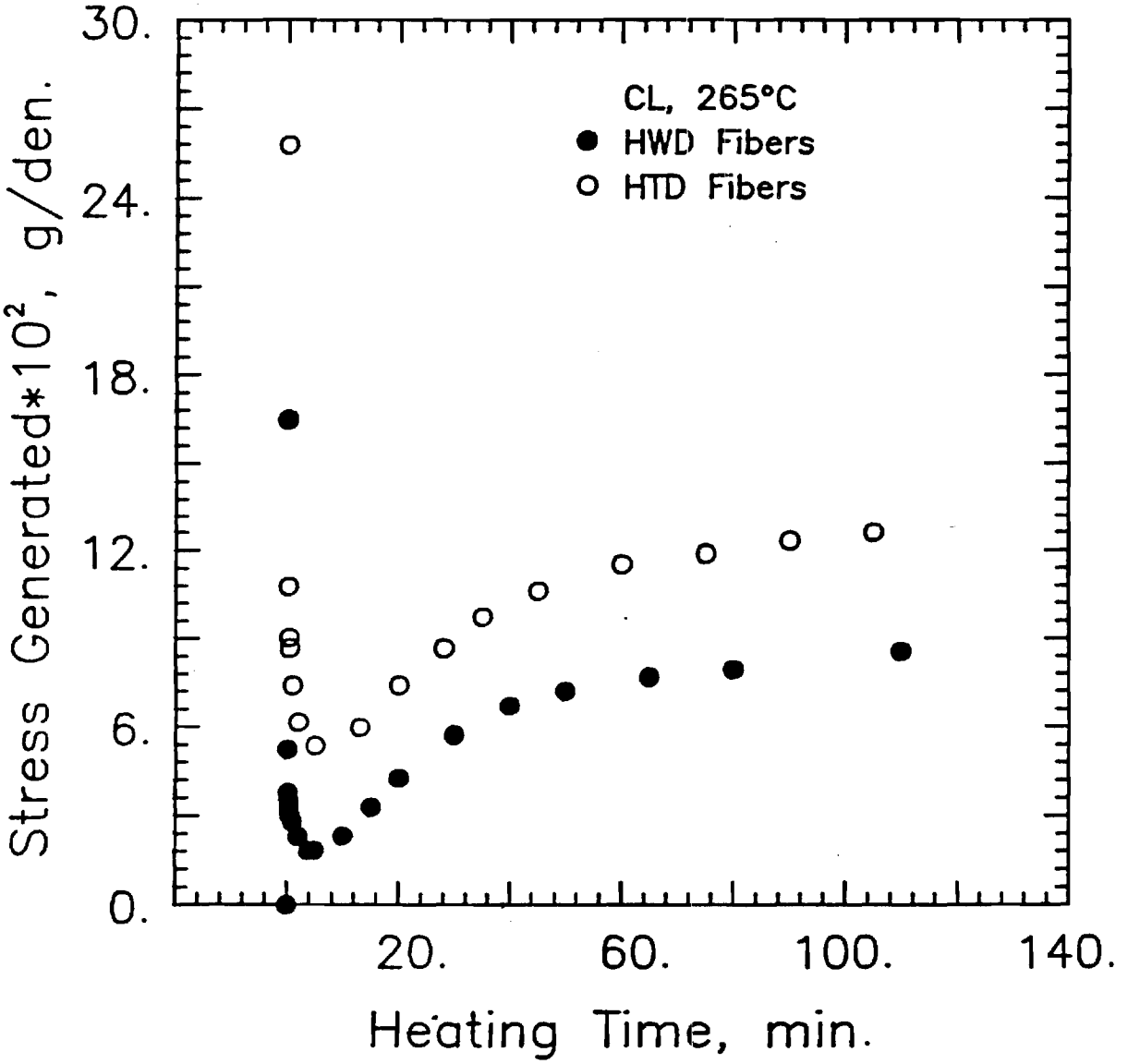

Figure 5: Shrinkage stress generated during CL batch stabilization. (O) HTD Fibers (●) HWD Fibers [5].

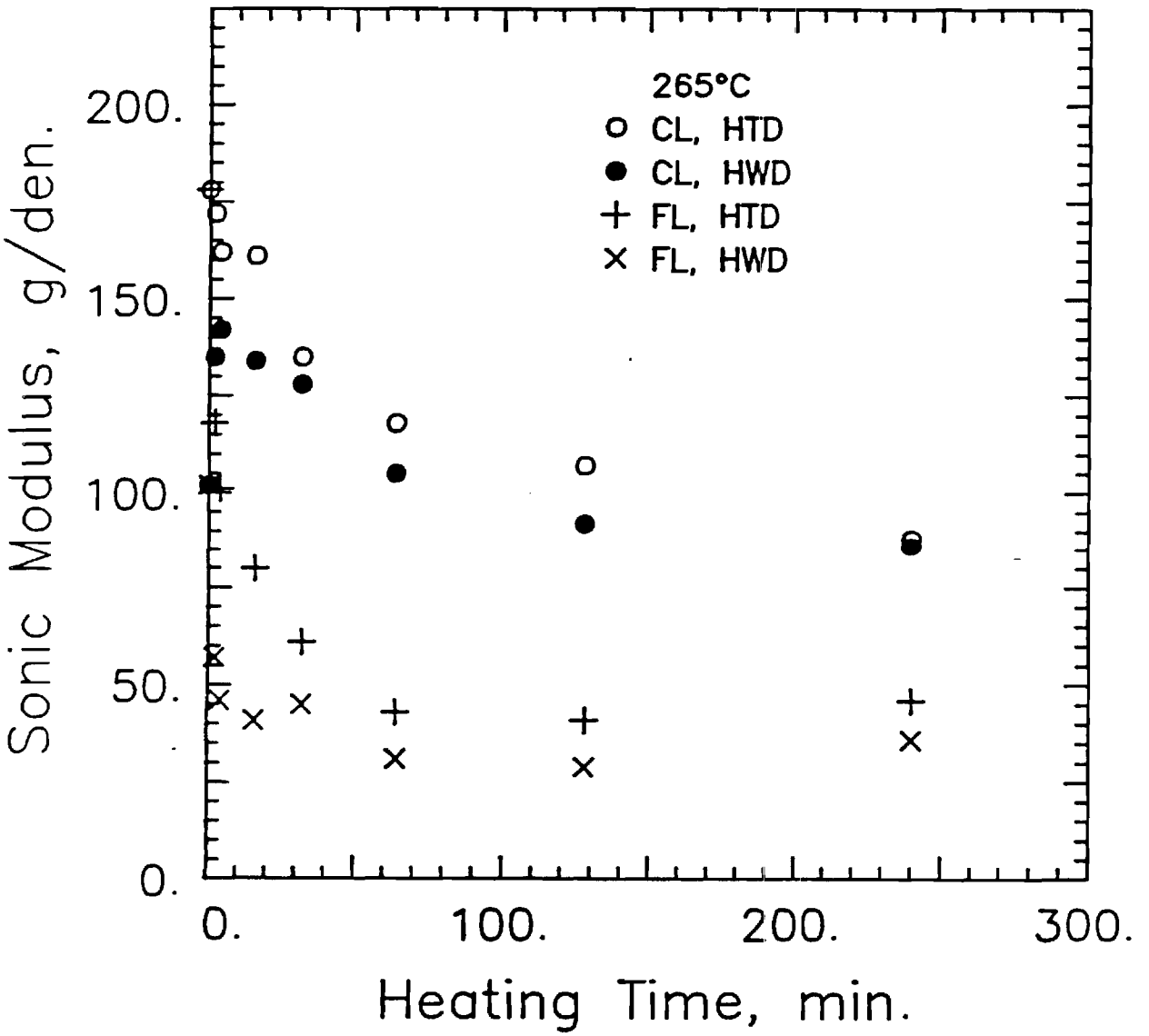

Figure 6: Sonic modulus of CL and FL batch stabilized fibers. (O) CL, HTD Fibers (●) CL, HWD Fibers (+) FL, HTD Fibers (X) FL, HWD Fibers [5].

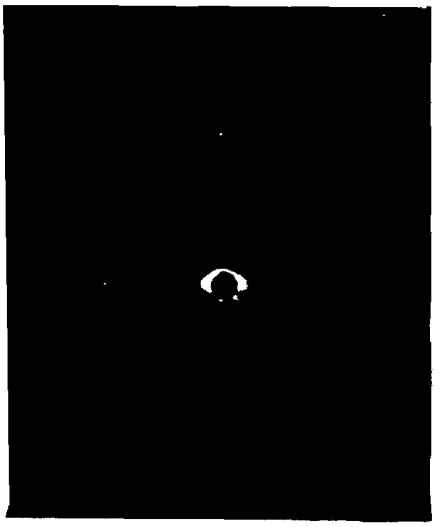

(a)

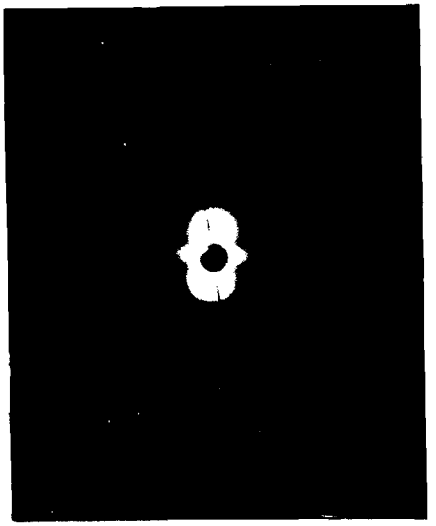

(b)

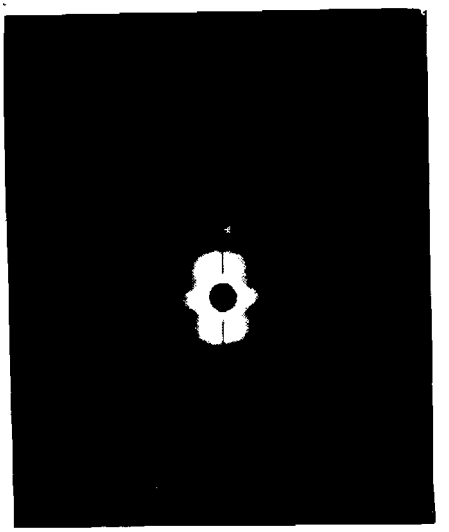

(c)

Figure 7: Small angle flat plate photographs a) precursor, b) 16 min. CL stabilized, c) Cu impregnated [5].

Table 2: Properties of a High Temperature Drawn (HTD) Precursor Fiber compared to a Hot Water Drawn (HWD) Precursor Fiber [6].

	HWD	HTD
Jet Stretch	0.7	0.9
Draw Ratio (Hot Water)	7.1	3.0
Draw Ratio (High Temperature)	—	2.3
Oven Temperature (°C)	—	252
Denier/Filament	1.6	1.4
Sonic Modulus	120	211
Crystal Orientation function	0.7	0.92
Average Crystal Size (nm)	5.4	13.0

sonic modulus which accompanies this shrinkage process (figure 6) indicate that the ordered and disordered domains are arranged in a sequence along the fiber direction.

When thermal treatment of oriented acrylic fibers is carried out without allowance for shrinkage, the change in sonic modulus depends on the change in the extent of lateral order in the fibers (figure 6). An increase in sonic modulus accompanies a significant increase in the extent and orientation of the laterally ordered fraction but a measurable decrease is seen when only a slight change occurs in those fibers which possess a high degree of initial order, indicating the presence of cilia and loose loops in the laterally disordered fraction. The initial decrease in sonic modulus during "constant length" heating of HTD fibers is still much less than the drastic drop which accompanies "free" thermal treatment, indicating that a majority of the segments in the laterally disordered fraction act as tie chains between the laterally ordered domains.

Acrylic fibers with demonstrably different extents of order show little difference in density, indicating that the packing densities in the laterally ordered crystals and the laterally disordered "noncrystalline" regions are essentially the same. Thus, the long period in SAXS, characteristic of the proposed two phase oriented structure, is absent in these fibers (figure 7a). After heating the precursor fibers for 16 minutes in air, a meridional spot is observed in SAXS flat plate photographs, indicating the presence of a long period (figure 7b). The appearance of this long period with the onset of stabilization reactions has been presumed to be the result of their preferential occurrence in one of the two phases, thus providing an indirect evidence for the proposed morphology. Confirmation of the existence of a long period in the precursor fibers is obtained by conducting SAXS studies subsequent to impregnation of these fibers with copper ions (figure 7c) by refluxing them in a solution of CuCl in HCl for 30 minutes. The electron density of the disordered phase is increased by the dispersion of Cu salt in this phase, resulting in the appearance of the long period in SAXS studies.

Thus one can clearly see through the cumulative evidence from thermal, thermorheological and morphological measurements that the predominant structural unit in oriented acrylic fiber consists of an alternating sequence of laterally ordered and

laterally disordered regions along the fiber direction, with a majority of the segments in the disordered bridging the laterally ordered domains.

II.2 Highly Ordered Precursor Fibers

PAN-based fibers have been found to undergo rapid morphological rearrangements at temperatures in the range of practical oxidative stabilization, well before the onset of the chemical reactions. The physical changes that precede the onset of a significant level of chemical reactions depend on the externally imposed constraints. Whether dimensional constraints are imposed or not, a significant tendency for increase in perfection and in the extent of the laterally ordered domains occurs in the early stages of this step, but these constraints have a pronounced effect on the relaxation of orientation in the laterally disordered phase. The decrease in orientation is dramatic, as seen by reduction in sonic modulus, when no constraint against shrinkage is imposed on the fibers. A higher level of orientational order and mechanical properties could be retained with higher levels of tensile stress in stabilization. An example of this aspect can be seen in figure 8 which shows the progression of sonic modulus in isothermal batch stabilization of an acrylic precursor in air under three conditions: (i) FL – free length, (ii) CL – constant length, and, (iii) CT – constant tension of 0.1 g/denier.

Based on these observations of a spontaneous tendency towards increase in lateral order and the ductility of the fibers under these conditions, a high temperature deformation process was proposed to generate highly ordered precursor fibers [2,5-7]. An example of this is illustrated in Table 2. The high temperature drawing process was conducted through an oven at a temperature (252 °C) close to stabilization temperatures at a takeup speed of approximately 15 ft/min (corresponding to a residence time of ca. 4 seconds in the oven). The high temperature drawn (HTD) fiber has been drawn to a similar overall draw ratio as the hot water drawn (HWD) fiber, but possesses clearly superior properties as well as orientational and lateral order. The high lateral order achieved in the precursor fibers could reduce orientational relaxations in subsequent processes, especially in the early stages of oxidative stabilization, thus minimizing a source for the formation of strength-limiting misoriented crystals in carbon fibers.

The extent to which deformation can be effected in a precursor fiber is a function of the rate for deformation, the temperature, and the order which exists prior to the

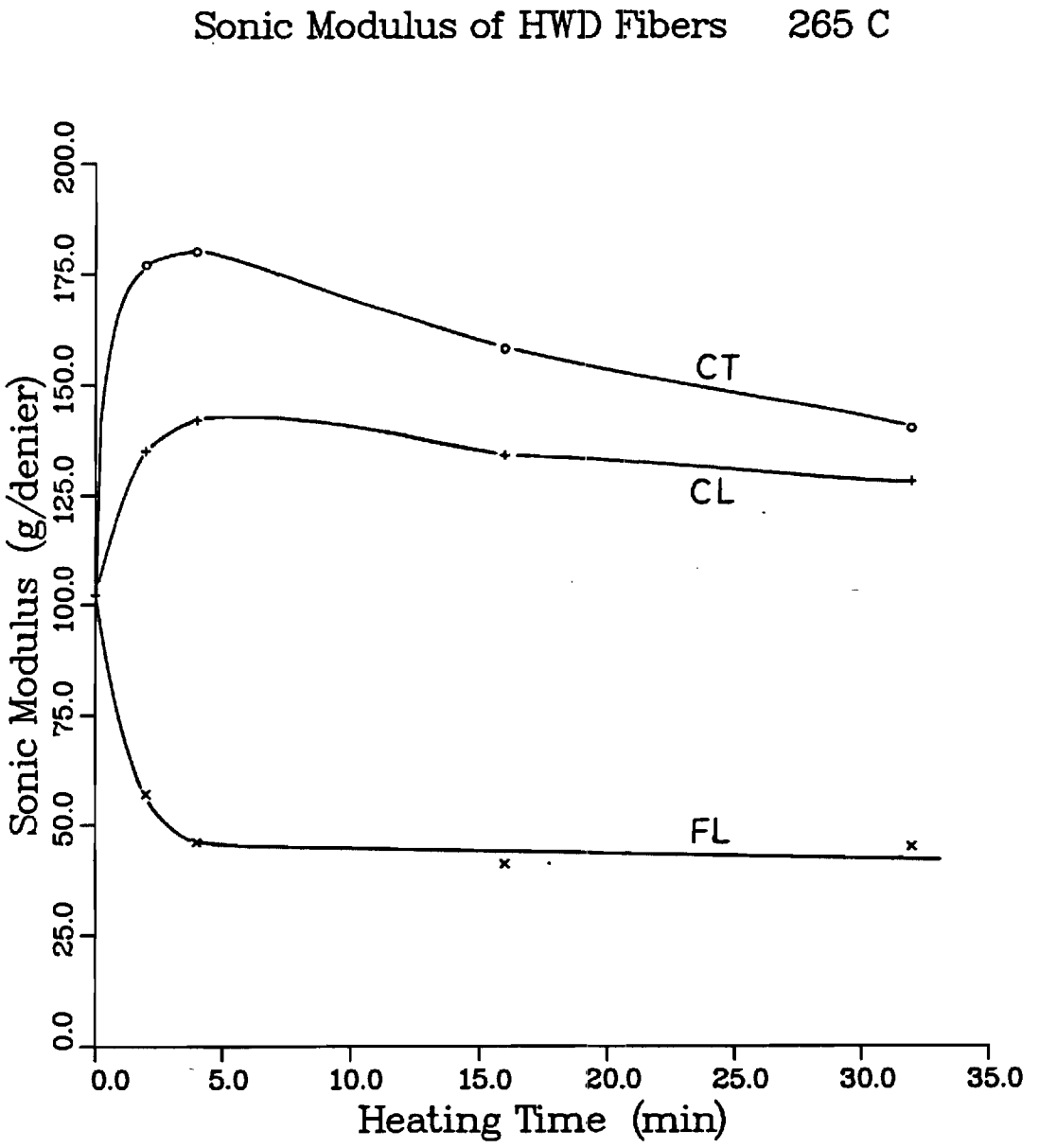

Figure 8: Progression of sonic modulus during stabilization at 265°C. FL – Free length; CL – Constant length; CT – Constant tension of 0.1 g/denier [9].

deformation process. High levels of drawing can be achieved through slow deformation or sequential drawing at successively higher temperatures. This aspect is discussed in the next section.

II.3 Multi-zone Stabilization

The critical stress for failure and the stress generated at any level of imposed deformation (or, conversely, the deformation at any level of imposed stress) would change throughout the course of stabilization. Since the temperature–tension/deformation–time profile that can be applied during the course of stabilization is limited by the continuously changing critical stress level, it may be necessary to have the provision to control these through a multi-stage stabilization process, so that the influence of these factors on the carbon fibers can be established. The stabilization process may be separated into at least three independently controlled stages, viz., an initial zone of rapid morphological rearrangements, a second zone of reactions predominantly in the disordered phase, and a third zone of reactions propagating into the ordered phase of the fibers [8,9].

A computer controlled four-zone line has been built for conducting optimization experiments pertaining to these factors (figure 9). One aspect of these experiments involves the feasibility of coupling the high temperature drawing process with stabilization in a continuous manner. While deforming during stabilization in air, the combination of internally initiated reactions and those initiated by species arising from diffusion controlled incorporation of oxygen is expected to result in an inhomogeneous stress distribution across the fiber cross section. It is believed that the inhomogeneities may be reduced through stabilization in an inert atmosphere to promote (effect) nitrile polymerization in the initial stages, followed by thermooxidative stabilization in air. In order to explore these aspects, deformation in an inert atmosphere (nitrogen) has been studied, in conjunction with the initial stages of stabilization. An experimental precursor with methyl acrylate and itaconic acid as comonomers, supplied by a commercial producer, was used in these studies [7]. It was observed that the fibers could be drawn to a considerable extent both in air (Table 3) and in nitrogen (Table 4). The data in the tables is a comparison between the fibers that were drawn with those which experienced the same thermal history without being drawn. It is evident from the data that drawing results in increased orientation and

improved mechanical properties of the partially stabilized fibers. The extent to which these fibers could be drawn depends on the temperature, increasing with increasing drawing temperature. However, since orientational relaxation also occurs at higher rates with increase in temperature, the increase in maximum draw ratio does not translate into better results in the drawn fibers.

Fibers which gave the best properties after stage I drawing were drawn at a higher temperature in a second stage. These fibers could be drawn again to a considerable extent, showing a definite increase in orientational order [6,7].

Although the differences in properties of drawn and undrawn stabilized fibers are not significant, final carbon fiber properties distinctly show the effect of drawing during the early stages of stabilization (Table 5). It is evident that one can combine deformation with stabilization with a resulting improvement in carbon fiber properties. Care must be exercised to avoid excess drawing which can lead to surface defects, such as cracks, which in turn can reduce the strength of these fibers in spite of increase in modulus due to the higher orientation achieved by drawing.

II.4 Mathematical Model of Oxidative Stabilization

Solid state thermooxidative stabilization, a necessary step before acrylic fibers can be carbonized cohesively, causes a complex combination of a large number of chemical reactions with diffusion of some of the reaction species in a morphology which changes with the progress of these reactions [10]. Developing a mathematical model of this step is extremely complex because of the multitude of events that occur. Among the factors to be considered are (i) initiation reactions by different species in the precursor polymer, such as comonomers and defect structures, (ii) reaction of oxygen with the backbone and the reactions initiated by the species which arise from it, (iii) multiple options for reaction paths, (iv) intra- and inter-molecular reactions between similar species, (v) transport of species such as O_2, *OH, etc., and (vi) morphological changes and constraints on molecular mobility accompanying the reactions, which should alter the rate constants for diffusion and the reactions. If all of the possibilities are considered, it leads to a large number (>30) of coupled partial differential equations, with the associated boundary conditions and material constants [10]. We have reduced this general set of equations to five equations by lumping similar reactions together and developed a procedure for solving them. The

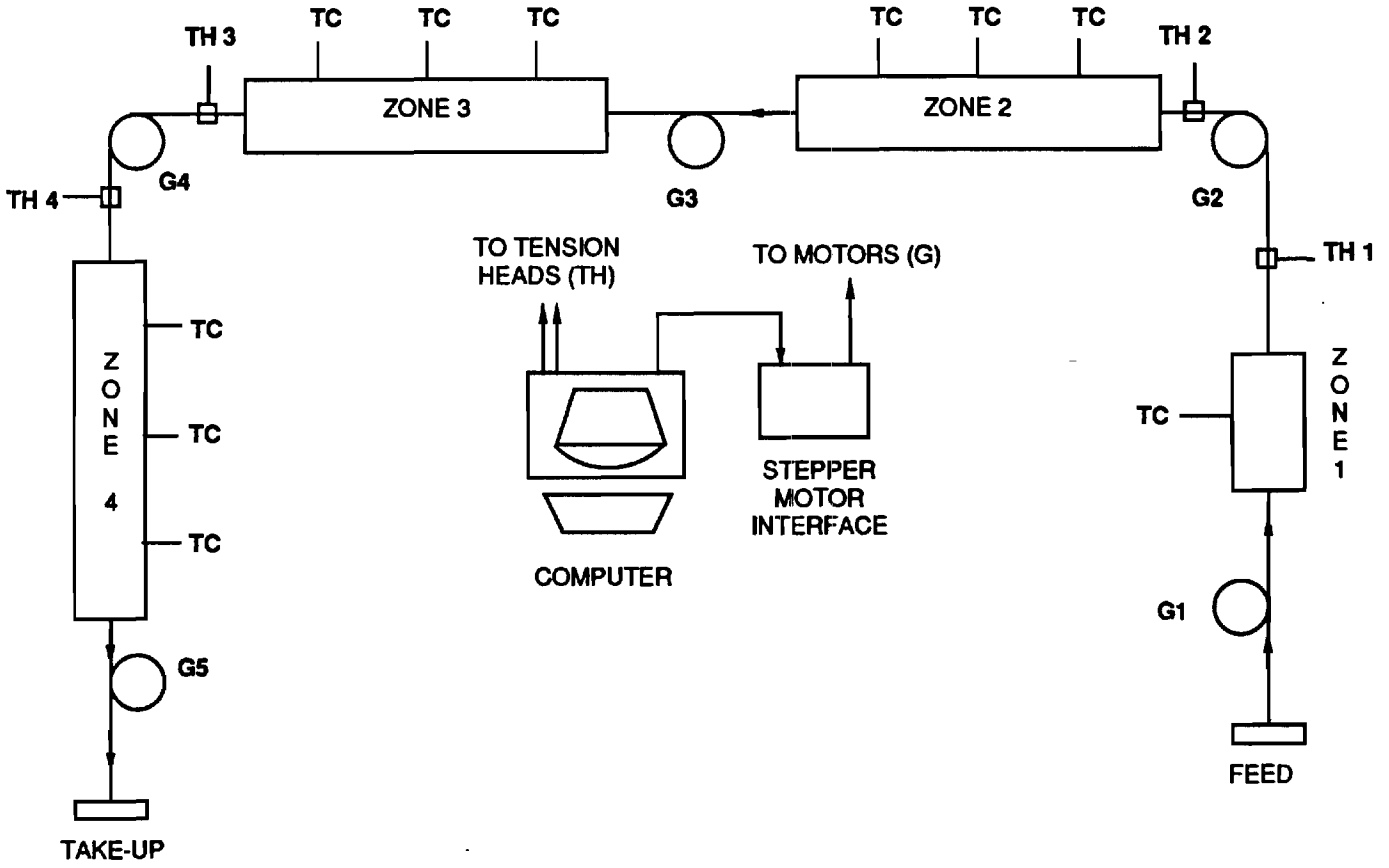

Figure 9: Schematic of Multistage stabilization line. TC – thermocouples connected to temperature controllers; TH – tension measuring heads; G – drive godets.

Table 3: High Temperature Drawing in Air (Stage I) [7].

Temperature of Drawing (°C)	Draw Ratio	Sonic Modulus (cN/dtex)	Tenacity (cN/dtex)	f_c
220	1.00	177	3.5	0.79
220	1.13	193	3.8	0.83
240	1.00	146	2.7	0.89
240	1.46	193	3.5	0.79

Table 4: High Temperature Drawing in Nitrogen (Stage I) [7].

Temperature of Drawing (°C)	Draw Ratio	Sonic Modulus (cN/dtex)	Tenacity (cN/dtex)	f_c
200	1.00	157	3.8	0.83
200	1.11	210	4.0	0.85
240	1.00	176	3.6	0.86
240	1.25	191	4.1	0.88

Table 5: Properties of Carbon Fibers [7].

Sample	Tenacity (cN/dtex)	Initial Modulus (cN/dtex)	Sonic Modulus (cN/dtex)
Control (DR=1.0)	12.0	1250	1356
Drawn in Air*	21.1	2043	1495
Drawn in Nitrogen #	12.1	1685	1897

All Fibers carbonized at 1525 °Cat 1 ft/min

Drawing Conditions:

$*$ – 220°C, DR = 1.13; 250°C, DR = 1.44

– 200°C, DR = 1.11; 260°C, DR = 1.33

mathematical model developed is for batch stabilization occurring in an inert or oxidizing environment based on low temperature processing of PAN-based precursor fibers. Low temperature stabilization, which eliminates rapid exothermic reactions, permits the assumptions of constant temperature across the filament cross section and negligible evolution of HCN and NH_3. The model monitors the concentration of chemical groups such as –CN, oxygen reacted onto the backbone (which is known to be an important process parameter), comonomer concentration, etc. Although certain reaction orders and rate constants are assumed in obtaining sample solutions, the mathematical description and the computer simulation are general enough to allow refinements in rate constants and reaction orders. Preliminary predictions, based on material and reaction constants estimated from the literature, have been found to be consistent with the known trends in practical stabilization processes [10,11]. Examples of the results are shown in figures 10–13. Calculated oxygen content in precursor fibers as a function of stabilization time is shown in figure 10 for two sets of assumed conditions. In Set 2, the ratio of the rate of reaction of oxygen with the polymer to the rate of diffusion of oxygen through the polymer is higher than in Set 1. The predicted trend is quite similar to the trends found experimentally (figure 14). The model, which requires precise information regarding the composition of the initial material and estimates of rate constants from experiments in inert and oxidizing environments, can be used to develop a numerical method for optimizing stabilization.

Experiments can be conducted to compare model predictions with global and, if possible, local concentrations of major reaction species. Experimental studies of local concentration of various species (such as –CN, bonded oxygen, etc.) as a function of temperature, time and environment are necessary to establish the material constants in the simplified model. With such information the model may be used to predict the responses with changes in material composition and process parameters. It is hoped that this approach can lead ultimately to elimination of the trial and error methods used currently for establishing stabilization conditions.

II.5 Criterion for Fully Stabilized Fibers

It is important to carry out the stabilization treatment until a critical extent of the reactions occurs throughout the fiber cross section, so that "burn off" of the core

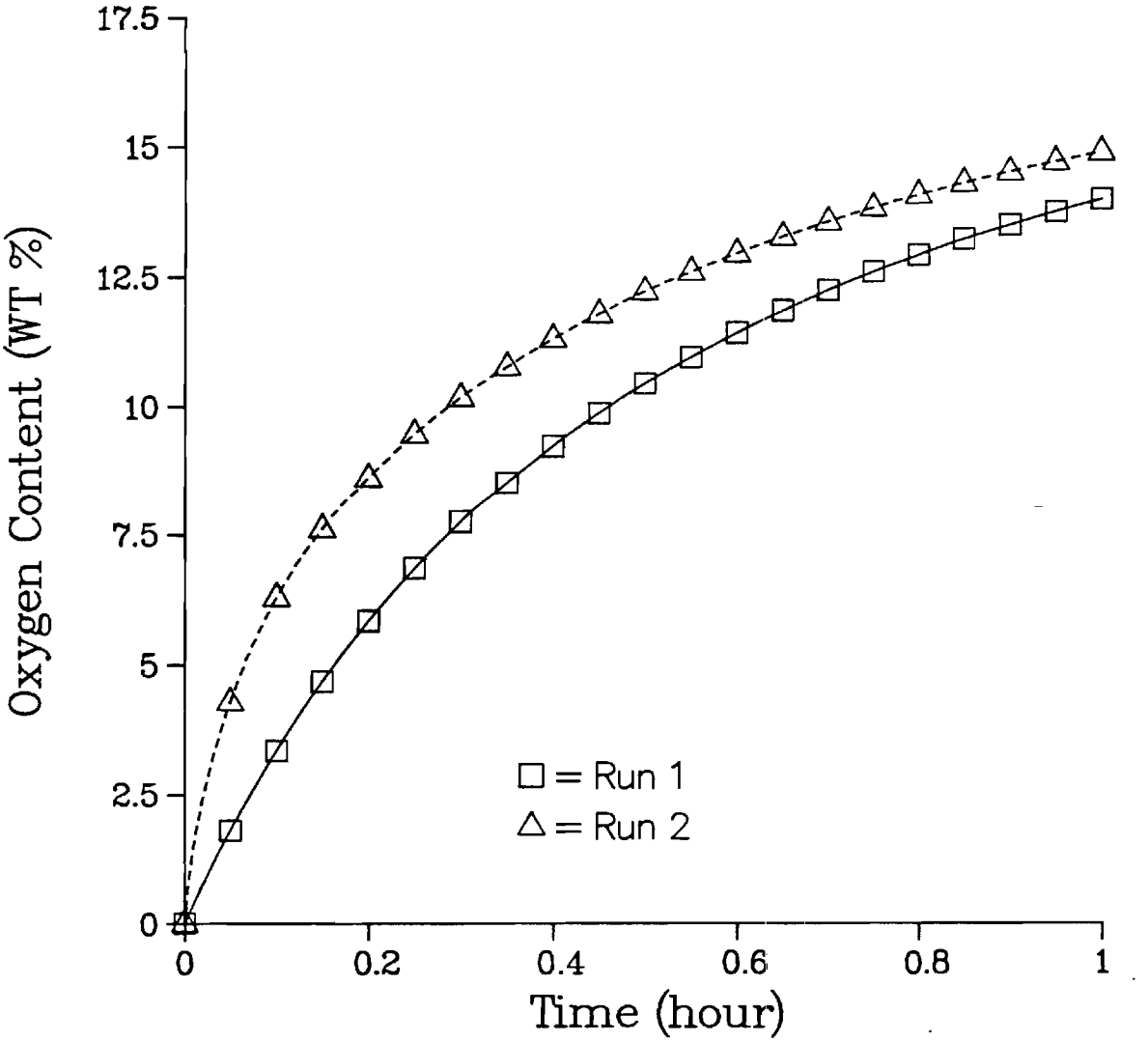

Figure 10: Calculated oxygen content of precursor fibers as a function of stabilization time for two sets of conditions [11].

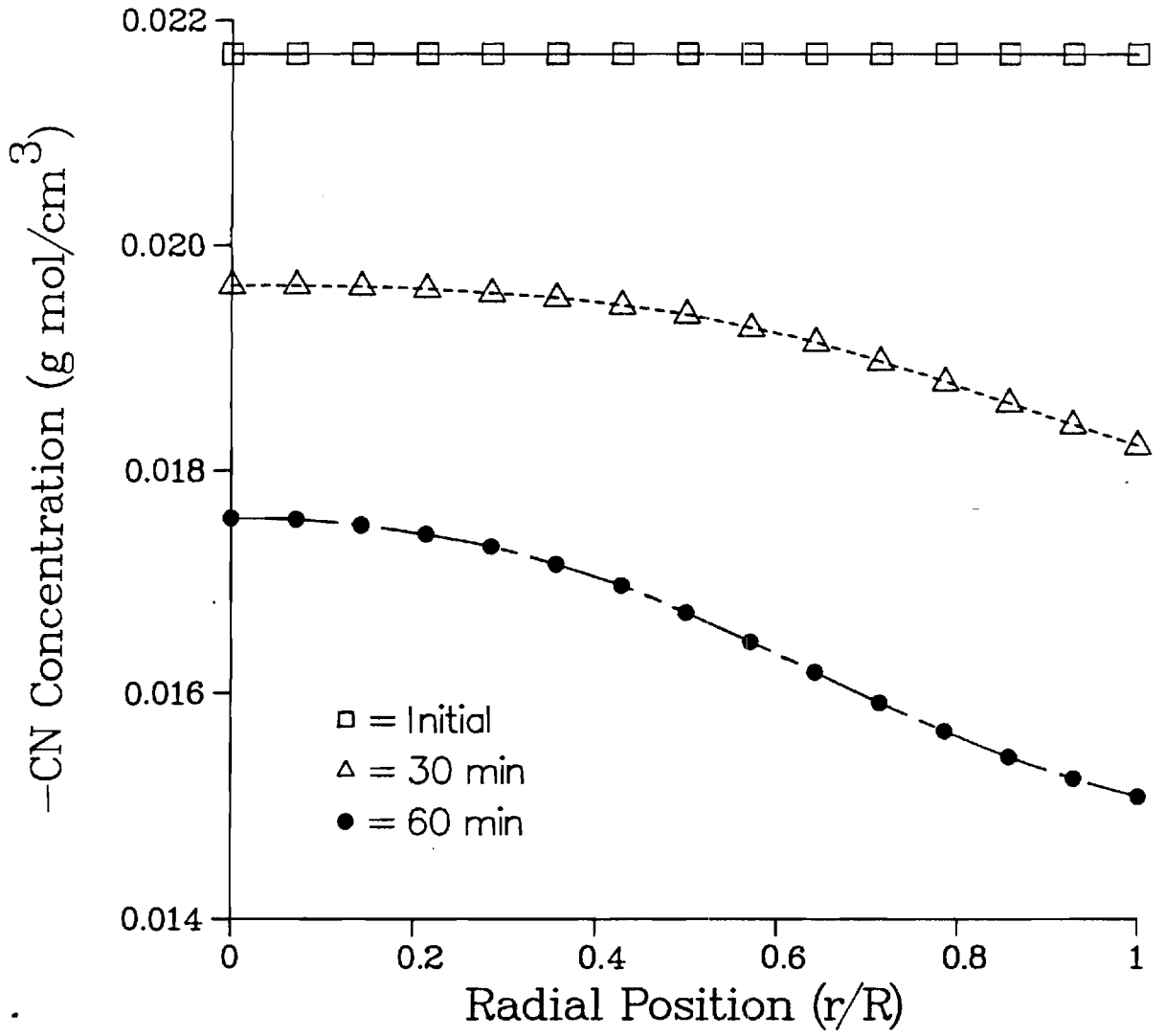

Figure 11: Nitrile (–CN) concentration profiles for an isothermal stabilization example [11].

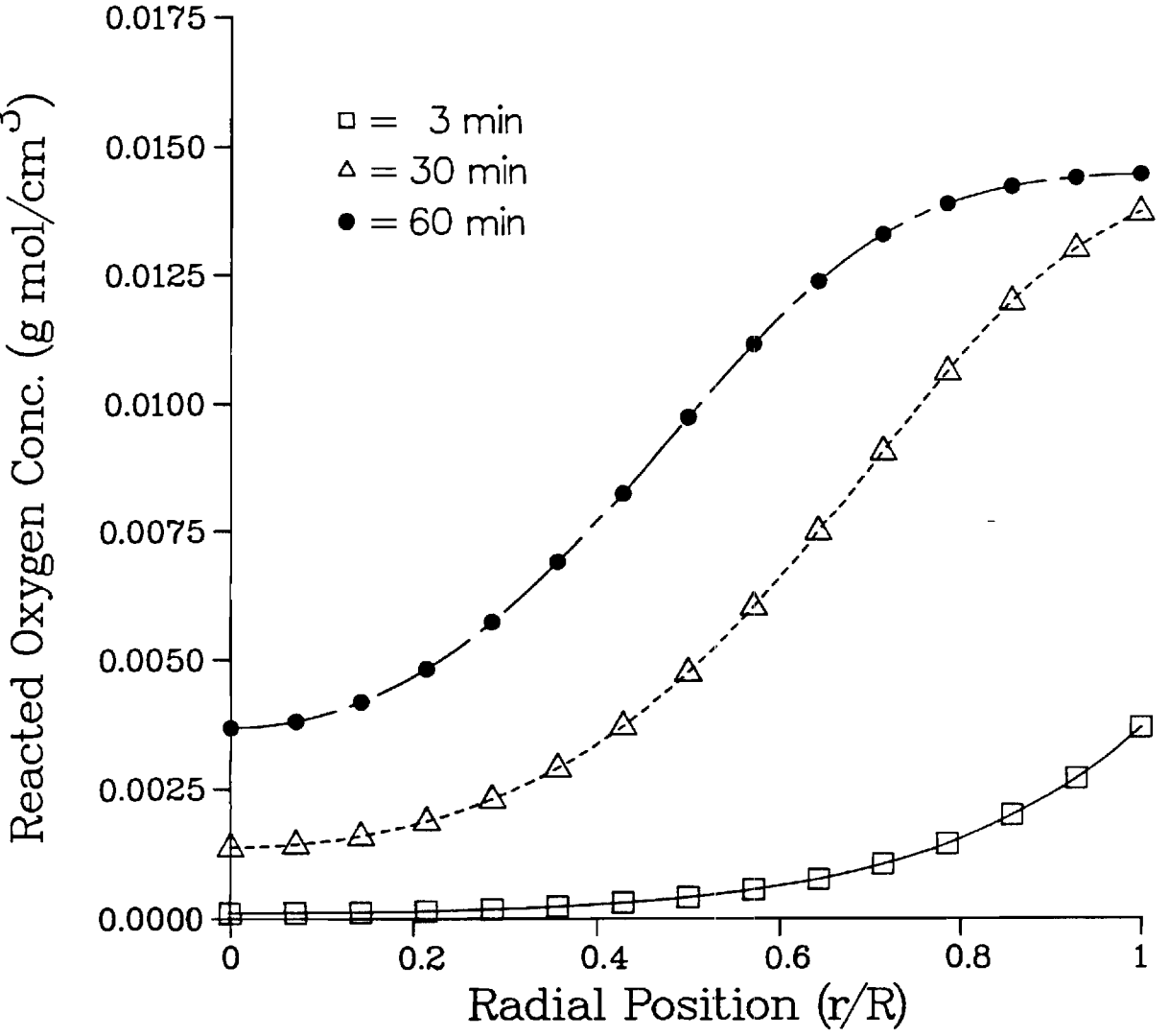

Figure 12: Reacted Oxygen concentration profiles for an isothermal stabilization example [11].

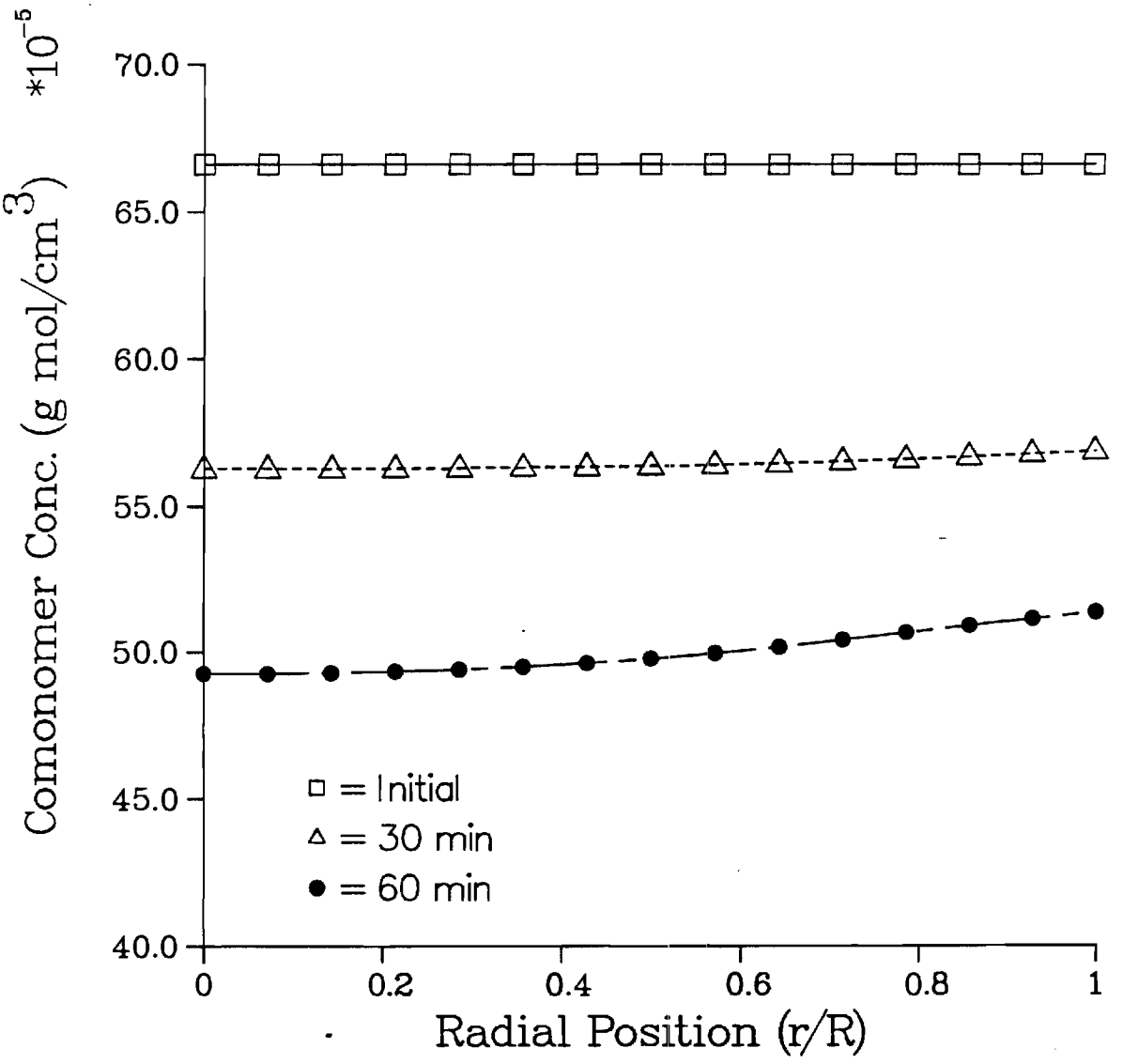

Figure 13: Comonomer concentration profiles for an isothermal stabilization example [11].

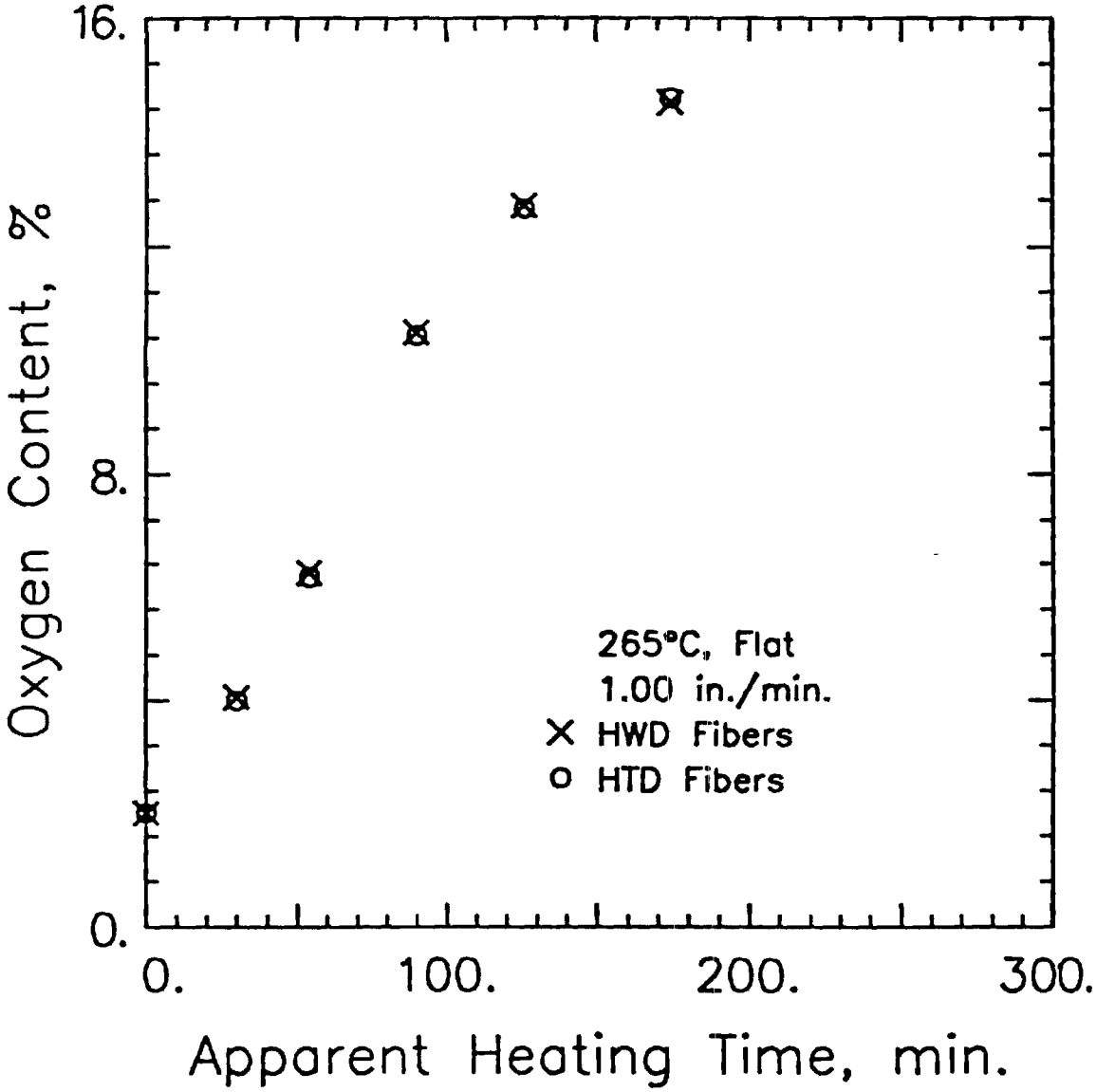

Figure 14: Oxygen incorporation during continuous stabilization of precursor I fibers at 265°C. (X) HWD Fibers (O) HTD Fibers [5].

(core blowout) can be prevented in carbonization. Among the commonly measured parameters (oxygen content, moisture regain, density, etc.), attaining a precursor composition-dependent critical density in stabilization has been found to be the most consistent criterion for avoiding core blow out under normal rates of carbonization [12]. As an illustration, consider the data for a PAN precursor containing 3 % itaconic acid (average molecular weight 138,000 g/mole) produced in our laboratories (Precursor II). Stabilization under different conditions yielded densities in the range from 1.455 to 1.535 g/cm^3 depending on the precursor draw ratio and the temperature profile employed for its stabilization [12]. When the stabilized fibers possessed densities of 1.52 g/cm^3 or greater, the carbonized fibers did not show holes due to core blowout, irrespective of the precursor fiber formation conditions and the temperature profile employed in stabilization. The fact that narrow density ranges are required for optimum stabilization has also been disclosed in the patent literature [13]. Moisture content of stabilized fibers do not show any specific trends with either the draw ratio or the temperature profile during stabilization. The majority of values, however, fall in the narrow range of 9 to 10 %. It should be mentioned that under different conditions of carbonization, holes in the core of the carbonized fibers can result even with apparently well stabilized fibers. This aspect is discussed further in the next section.

II.6 Hollow Core in Carbon Fibers

Two different mechanisms which could lead to a hollow core in carbon fibers have been identified. These are

(1) "burning off" of the core material when an incompletely stabilized fiber from a diffusion-controlled solid-state stabilization process is carbonized.

(2) propagation of the consolidated carbonized structure inward from the skin when a well stabilized fiber is raised rapidly to carbonization temperatures.

To examine the validity of the two proposed mechanisms, linear densities and fiber diameters were measured for carbon fibers from incompletely as well as sufficiently stabilized fibers (Table 6). The data are for a commercial precursor for carbon fibers (Precursor III). The precursor fibers were stabilized in a linear oven consisting of three 6-foot zones with individual temperature control. The stabilization time was approximately 80 minutes. The stabilized fibers were carbonized at 1200°Cin a furnace whose temperature profile is shown in Figure 15. When the fibers are carbonized

at low speeds (0.5 ft/min), the linear density of the carbon fibers from sufficiently stabilized precursors is significantly higher than from the incompletely stabilized precursors indicating the expected loss of material through "burn off". Every filament in the latter bundle also exhibited a hollow core. When these two stabilized fibers were carbonized at a higher speed (3.5 ft/min), a hollow core developed in both cases, but the linear density *and* the diameter of the sufficiently stabilized fibers were higher, consistent with the consolidation mechanism at higher carbonization rates. Comparison of the carbon fibers produced at different speeds (rates) from apparently well stabilized fibers shows little difference in linear densities, lending further support to the mechanism of consolidation from the skin inward. Also, when the sufficiently stabilized fiber is carbonized repeatedly at 1.5 ft/min, a condition which yields hollow core in about 60% of the filaments, little change in diameter is observed with consolidation. Thus it is clear that, at higher rates of heating to the carbonization temperature, an outer layer of the filaments is carbonized rapidly and that subsequent consolidation occurs from the skin inward, resulting in a hollow core in the densified fibers [12].

II.7 Evolution of Structure in Carbonization

A number of interesting features pertaining to the progression of changes in physical properties and elemental composition during continuous low temperature (1200°C) carbonization have been observed.

Carbonization of the precursor II stabilized fibers was carried out by passing them through a Lindberg furnace at 1200°C. To avoid thermal shock and allow for a gradual increase in the temperature of the filaments, two heaters were installed at the entrance to the furnace which provided two 6-inch precarbonization zones. The temperature profile obtained in this set-up is shown in figure 15. The dip in the temperature profile is caused by the separation between the second preheater and the heater in the furnace. Nitrogen was passed through both ends of the furnace to maintain an inert atmosphere. Samples for studies were obtained by cutting the fiber bundle at the delivery end and rapidly winding it on a spool at the feed end.

Progression of carbonization using stabilized precursor II fibers (stabilized under conditions that would prevent core blow out) was followed with density, [H]/[C] and [N]/[C] ratios, electrical resistance and sonic modulus measurements.

Table 6: Carbonization with sufficiently (A) and incompletely (B) stabilized precursor III fibers. Stabilization temperature sequence in °C– A: 250-275-275 and B: 250-265-265. [12].

Sample	Carbonization speed (ft/min)	Density (g/cm^3)	Denier/filament	Diameter (μm)
A-1	0.5	1.73	0.60	5.6
A-2	3.5	1.71	0.59	6.5
A-3	1.5	1.73	0.60	6.6
A-3-1	1.5	1.73	0.58	6.5
A-3-2	1.5	1.76	0.58	6.6
B-1	0.5	1.71	0.54	5.3
B-2	3.5	1.71	0.53	5.5

$*$ – Recarbonization of A-3

$^{\#}$ – Recarbonization of A-3-1

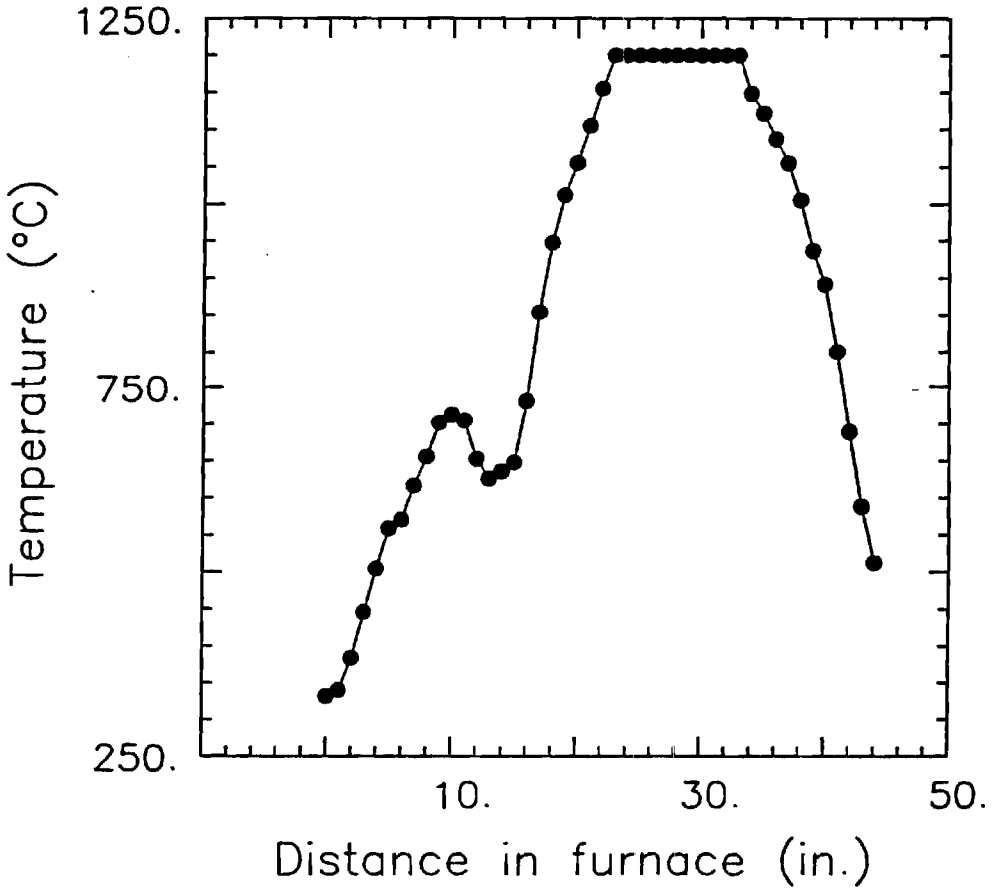

Figure 15: Temperature profile in carbonization furnace [12].

When the plots in Figure 16 are compared with the temperature profile in the carbonization furnace, a sharp increase in sonic modulus during heating from 700°Cto 1200°Ccan be observed. Once the fiber temperature reaches 1200°C, a slower asymptotic increase in sonic modulus occurs with time at this temperature. The sonic moduli of the carbon fibers after 1200°Ccarbonization are higher with precursor fibers of higher draw ratios. Also, the carbon fibers from the high temperature drawn precursor fibers of higher order show an increase to a higher sonic modulus compared to those from boiling water drawn precursor fibers which had a comparatively lower orientational and lateral order. The development of modulus is determined by the orientational order in the basal planes achieved during carbonization. The rate and the extent to which this ordering process occurs should increase with initial order in the precursor fibers.

The results from elemental analysis on samples removed from the carbonization furnace are plotted in Figure 17. The [H]/[C] and the [N]/[C] ratios also change sharply during heating between the temperatures 700°Cand 1200°C, showing that both aromatization and basal plane formation occur rapidly in this temperature range. The requirement that a certain degree of aromatization has to precede the formation of basal planes is reflected clearly in the more rapid change in the [H]/[C] ratio in the early stages when compared with the [N]/[C] ratio. The progression of changes in electrical resistance through carbonization follows the same trend of rapid change in the 700°C–1200°Czone (Figure 18). The resistance, measured at room temperature, falls from about 10^{14} ohms/cm to less than 10 ohms/cm when the temperature reaches its maximum of 1200°C.

Properties such as electrical conductance and sonic modulus, which depend on the extent of formation of ordered basal planes, develop rapidly initially in the carbonization process, with a slower asymptotic increase with continued heating at the highest temperature. Both the rate and the extent of increase in sonic modulus during carbonization increase with the extent of lateral and orientational order present in the precursor fibers which should promote the ordering process during carbonization. These trends are also reflected in [H]/[C] and [N]/[C] ratios which indicate the degree of aromatization and basal plane formation. Elemental changes occur in concert with increase in temperature, with morphological changes lagging behind them [9,12,14].

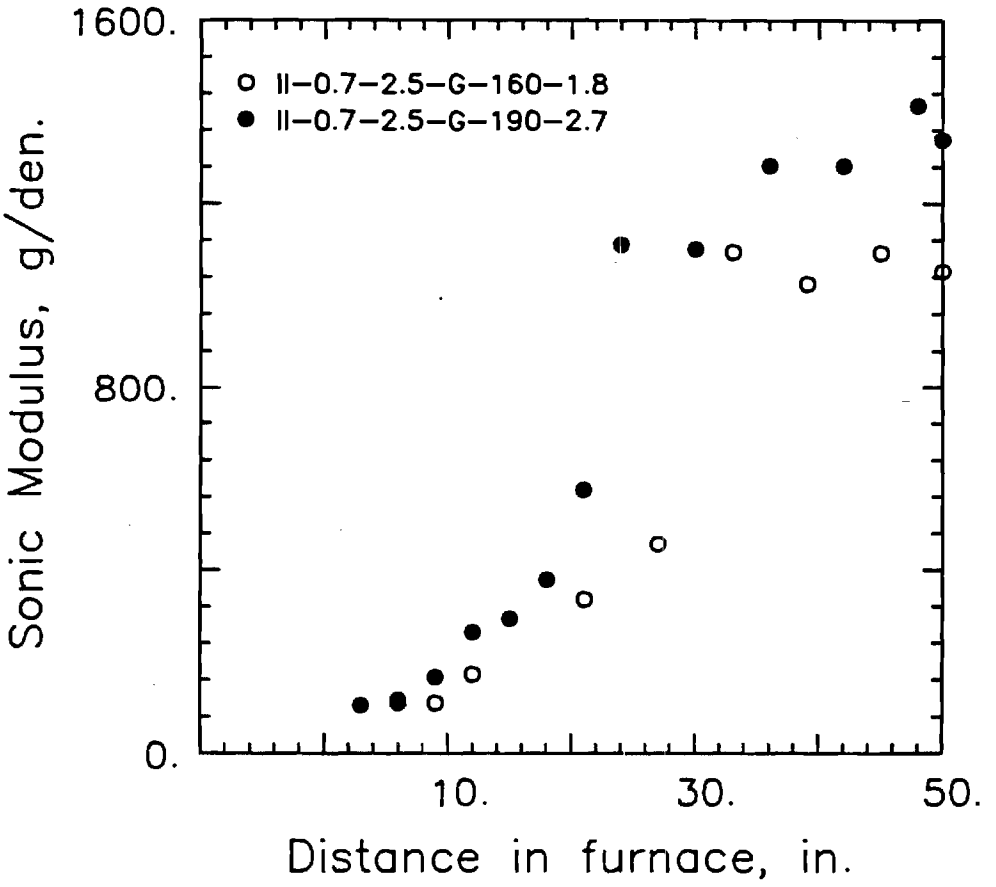

Figure 16: Change in sonic modulus during carbonization of precursor II. The fibers are drawn in hot water (DR= 2.5) and over a hot godet [12]. (O) II-0.7-2.5-G-160-1.8, (O) II-0.7-2.5-G-190-2.7.

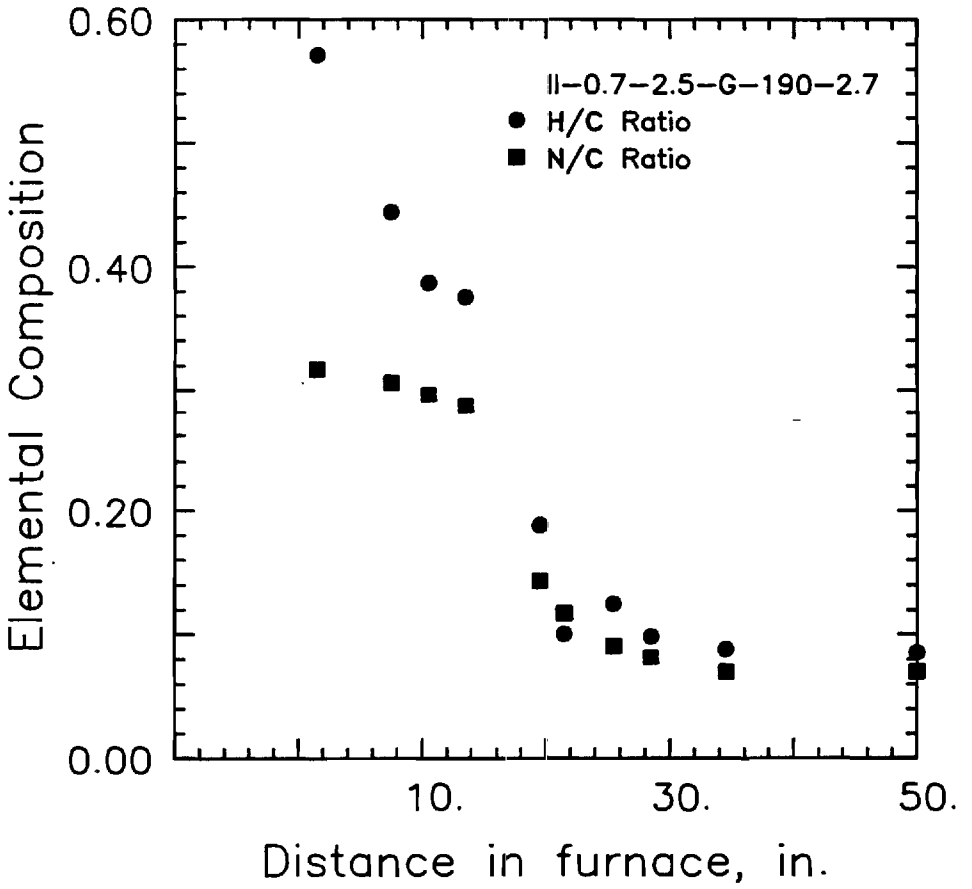

Figure 17: Change in elemental composition during carbonization of II-0.7-2.5-G-190-2.7 fiber. (O) [H]/[C] ratio, ( ) [N]/[C] ratio [12].

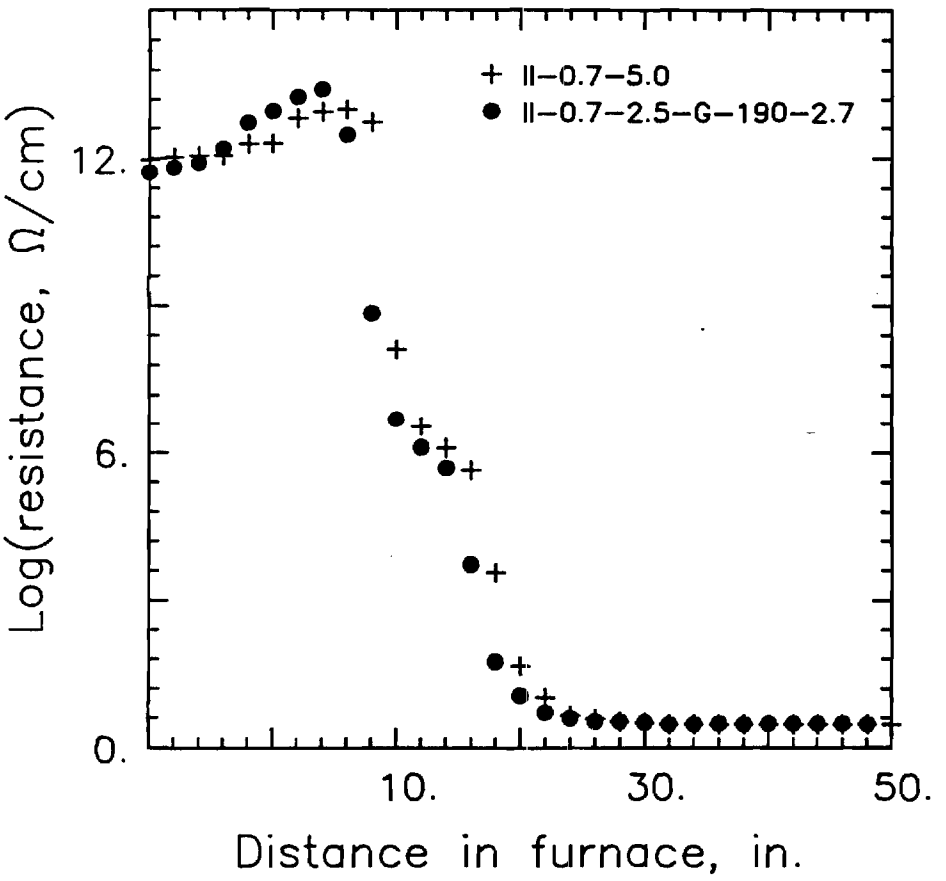

Figure 18: Change in electrical resistance during carbonization of precursor II. (+) II-0.7-5. (●) II-0.7-2.5-G-190-2.7 [12].

The progression of density, measured by a liquid immersion technique, is plotted as a function of distance in the furnace in Figure 19. The density increases very sharply during 700–1200°Cheating suggesting significant rearrangements leading to consolidation of structure in the fibers, but it is followed by an apparently sharp drop before leveling off upon continued heating at 1200°C. This decrease in the measured density of the carbonized fibers is quite significant, reproducible and is observed in all fibers. The reason for this drop in apparent density appears to be the conversion of open pores to closed pores, i.e. some of the pores which are initially accessible to the solvents employed for the density measurement become inaccessible, resulting in a decrease in the measured density. This suggests that consolidation of the structure occurs around the pores during the high temperature annealing in the latter stages. A similar explanation has been offered earlier by Gibson [16] for the decrease in density observed for carbon fibers produced at increasing temperatures in the range of 1000 to 2000°C. This hypothesis needs to be confirmed with a combination of SAXS and measurements based on volume filling of accessible pores and adsorption on accessible surfaces. The combination of density and accessible surface area measurements has been used by Kipling *et al.* to infer open and closed pore structures in graphitizing and non-graphitizing carbons [17]. Additional evidence can also be obtained by combining linear density with measurements of filament diameter along the carbonization line.

We have observed in our studies that the qualitative features of changes during the carbonization are not changed with composition (comonomer with AN) or the extent of orientational and lateral order generated in the formation of precursor fibers. Fundamental aspects of the evolution of properties revealed through these studies are thus believed to be the general characteristics of the formation of carbon fibers from PAN-based precursors.

Procedures developed in this study for "offline" monitoring of the evolution of carbon fibers in a continuous process can be valuable in optimizing the carbonization set-up. It is necessary to have the provision to alter the temperature profile in carbonization so that the appropriate time-temperature profile can be determined through measurements of the evolution of properties during the process.

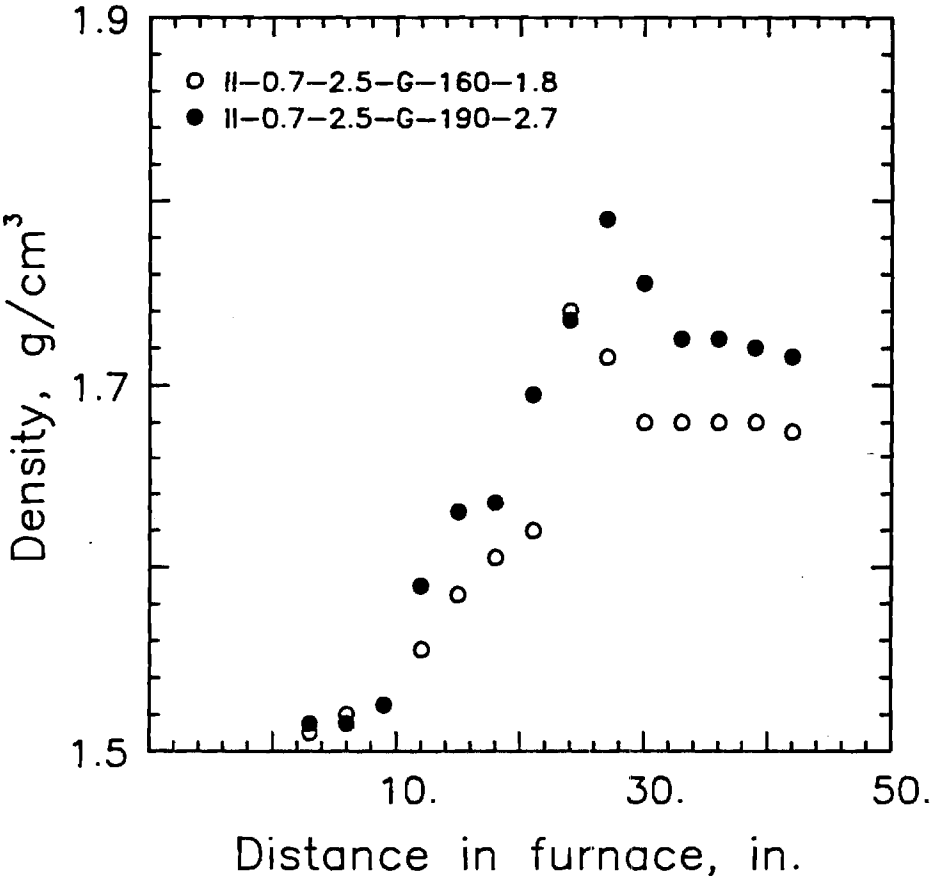

Figure 19: Change in density during carbonization of precursor II. (O) II-0.7-2.5-G-160-1.8, (●) II-0.7-2.5-G-190-2.7 [12].

II.8 Plasticized Melt Spun Precursors

Current carbon fiber production from PAN-based copolymers employ wet or dry spun precursor fibers that require expensive solvents and costly solvent recovery methods. It has been discovered recently that melt spun PAN-based fibers can be prepared by using water as a plasticizer to lower the viscosity and the melting point of PAN [18-20].

A preliminary investigation of plasticized melt spun acrylic fibers has revealed their morphology to be similar to those of solution spun fibers. However, the precursor fibers have broken filaments as well as surface and internal voids, all of which hinder the development of superior properties. Possible sources for the microvoids are impurities (including regions of high water concentration) in the precursor fiber. Porosity in these precursor fibers is indicated by a strong equatorial streak in small angle x-ray scattering photographs [10,15]. Stabilized fibers etched with dimethyl formamide (DMF) contained microvoids indicating that some of the impurities leave the structure during the stabilization process itself. Examination with SEM also revealed small pits along the surface of the carbon fibers.

Reasonable strengths, up to an average of 15 cN/dtex (2.5 GN/m^2), and modulus, 1080 – 1310 cN/dtex (173 – 214 GN/m^2), can be produced in low temperature carbonized carbon fibers. These fibers, with anticipated engineering developments to eliminate gross defects and optimization of stabilization and carbonization processes for these precursors, have been shown to be entirely suitable for producing useful carbon fibers [10,15].

III. Research Facilities Established

Both bench-scale and pilot-scale equipment have been set up to conduct polymerization of polyacrylonitrile homopolymer and copolymers, solution formation, wet solution spinning of PAN precursor fibers, controlled thermo-oxidative stabilization of the precursor fibers, and conversion of "stabilized" fibers to carbon fibers at low, intermediate and high temperatures. This has resulted in the most complete university-based research facility to examine formation of high performance fibers, not necessarily limited to carbon fiber formation. Facilities established for material production, fiber formation and thermal treatments, including consolidation, are outlined below.

- A continuous polymerization unit for emulsion/suspension/solution polymerization to produce homopolymers and copolymers of required compositions and molecular weights. The CSTR unit, with viscosity independent stirrers and tight controls of temperature, composition and residence time, has been used to generate as much as 20 lbs of polymer for the preparation of precursor fibers for carbon fibers.

- A batch polymerization unit, consisting of a two liter Parr autoclave. The polymer yield from this unit is approximately 1/2 lb.

- Two mixing units (1 liter and 2 gallon capacities) for the preparation of polymer solutions under controlled temperature and environment.

- A wet solution spinning line with a temperature controlled coagulation bath, circulation pump for maintaining the composition of the coagulation solution, deionized water source for washing the coagulated fibers, and provision for stretching the coagulated filaments under various conditions (hot water, hot godet, steam). This line has the capacity to spin filament bundles with as many as 500 filaments.

- Exploratory spinning units for dry and wet spinning with up to 0.5 liter of solution.

- An auxiliary drawing unit for high temperature drawing of precursor filaments through a tubular oven (max. temperature = 400°C).

- A linear 18 foot over for thermal treatments, made up of three sections with independent temperature controls (max. temperature = 450°C). This line can be run at a set tension in the line or at a controlled net deformation/shrinkage of the filaments between the input and the output.

- A multi-stage thermal treatment line with programmable computer control of temperature profiles, tension/deformation and environment in four independent zones.

- Batch tubular furnaces for monitoring the development of stress in precursor filaments at constant length or changes in length under constant tensile force at elevated temperatures (max. temperatures = 450°C, 1200°C) in any desired atmosphere.

- Two programmable Lindberg tube furnaces for continuous tension- and temperature- controlled high temperature (1200°C and 1700°C maximum temperatures) conversion of precursor filaments to high performance structures.

- Two 15 kW TOCCO tubular induction furnaces, one with a heated zone of approximately 18 inches and maximum temperature capability of approximately 2000°C, and the other with a heated zone of approximately 12 inches, and a maximum temperature capability of 2500°C. Both furnaces are equipped with either nitrogen or inert gas blanketing, systems for removal of decomposition gases, and a fiber handling system for continuous processing with controlled tension and residence time.

IV. Conclusions

Our research on fundamental aspects of the conversion of PAN-based precursors to carbon fibers has led to the following significant results and conclusions:

1. The two-phase fibrillar morphology, originally proposed by Warner, *et al.*, is the most appropriate model of the structure of oriented acrylic precursors for carbon fibers. Knowledge of the morphology is valuable in establishing process and material variants which govern the ultimate properties of carbon fibers.

2. The tendency in oriented acrylic fibers to undergo rapid morphological rearrangements at high temperatures (>220°C) can be used in a deformation process to yield precursor fibers of significantly higher order. This deformation would lead to a significant reduction in morphological flaws of the carbon fibers which can arise in the form of misoriented crystals. Such a high temperature deformation, combined with minimizing extrinsic sources of flaws (impurities) have been largely responsible for the recent dramatic improvements in tensile properties of commercial carbon fibers.

3. A multi-zone stabilization process, with the computer-assisted control of the stress field in each zone, can be used to effect maximum transfer of order from the oriented precursor to the carbon fibers. It can also be used to combine desirable high temperature deformation with stabilization.

4. In spite of the enormous complexity of the numerous reactions and the transport of resulting species which occur in stabilization, a mathematical model which judiciously groups similar reactions together has been developed. This model represents the first promising effort to examine theoretically the gradients which evolve within the filaments in a stabilization process.

5. Among the many criteria which have been proposed to identify the state of stabilization which is appropriate for carbonization, obtaining a precursor-dependent critical density has been shown to be the most consistent for this purpose.

6. Two mechanisms can produce a hollow core in carbonization, viz., (a) "burning off" of the core material when an incompletely stabilized fiber from a diffusion-controlled solid-state stabilization process is carbonized, and (b) propagation of the consolidated carbonized structure inward from the skin when a well stabilized fiber is raised rapidly to carbonization temperatures. The latter mechanism might be used to produce well consolidated hollow carbon fibers.

7. In order to establish the optimum conditions for carbonization, of any precursor, it is necessary to establish the evolution of chemical structure and morphology *within* a carbonization process. Morphological evolution follows the chemical changes to the carbonized structure which occurs rapidly in this process. The key to obtaining the best combination of properties in tension *and* compression is likely to be in reaching the appropriate combination of lateral order (or disorder) and orientational order.

8. Plasticized melt spinning of precursor acrylic polymer yields a morphology which is entirely appropriate for high performance carbon fibers. This approach can offer a better solvent system for precursor fiber formation in the future.

V. Suggestions and Recommendations

Research efforts in the last decade at Georgia Tech and in other industrial and academic laboratories have indeed led to substantial advances in the properties which can be achieved in PAN-based carbon fibers. A two-fold increase in modulus as well as tensile strength has been achieved primarily through the combination of increased morphological order and reduced levels of contaminants. Significant progress has also been made in reducing processing times, in fiber uniformity at each stage and in physical and analytical monitoring of the evolution of structure in the conversion processes. Such progress notwithstanding, several significant aspects of carbon fiber formation demand continued research. These include

1. *Generation of precursor fiber structures which can lead to new carbon fiber morphologies with improved compressive properties.* The recent advances in achieving superior tensile performance have, unfortunately, not been accompanied by any progress vis-a-vis behavior in compression. Many critical structural applications have been limited by the fact that the compressive strength is only a fraction of the tensile strength of carbon fibers. Among the approaches one might follow here are synthesis of new precursors to form dense carbon network which would still be oriented, and use of precursor polymer alloys to create a higher level of lateral disorder. Both these efforts are aimed at increasing lateral disorder while maintaining orientation of the carbon fibers. It is also necessary to identify the morphological state during the evolution of carbonized structure which would yield the best combination of properties in tension and compression.

2. *New routes for precursor fiber formation.* It is clear that plasticized extrusion of acrylic precursors with water does produce the required morphology. Significant problems remain, however, in relation to control of morphology and the transport processes in fiber extrusion. It is necessary to identify solvent systems in which plasticized recrystallization would occur above ambient temperatures but below the boiling point of the solvent.

3. *Highly ordered precursors.* The next generation of high performance carbon fibers is likely to be obtained from ultrahigh molecular weight precursors which can be ordered through "gel spinning → drawing" to a higher extent than any of the current precursors.

4. *Lower cost material - process options.* Large scale application of high performance carbon fibers is feasible only if its cost can be significantly reduced. New, lower cost precursor materials (eg., lignin, chitin) and simplified, rapid conversion to carbon fibers should be explored for this purpose.

Much progress has been made during the last decade in establishing the fundamental material and process interactions in the formation of high performance carbon fibers. A significant degree of empiricism exists still in this regard. It is necessary to continue current comprehensive research efforts on the chemical and morphological aspects of the conversion of precursor polymers to carbon fibers in order to improve significantly our understanding of the evolution of structure, and thereby the properties, of these critical materials.

Acknowledgments

The following have made significant contributions to the ideas, experimental procedures, theoretical models and the discussion of results contained in this study: Dr. M. Balasubramanian, Dr. G. Bhat, Dr. F. L. Cook, Mr. V. Daga, Mr. S. Damodaran, Mr. C. Daley, Dr. P. Desai, Mr. D. Grove, Dr. M. K. Jain, Ms. T. Long, Mr. J. R. Morgan, Dr. L. H. Peebles, Jr. (ONR), Dr. W. C. Tincher and Dr. S. B. Warner. The author (Dr. A. S. Abhiraman) expresses his appreciation to them for giving him the privilege of collaborating with them in this research.

Bibliography

1. S.B. Warner, S.R. Uhlmann and L.H. Peebles, Jr., J. Mater. Sci., 14, 1893 (1979).

2. M. K. Jain and A. S. Abhiraman, *J. Mater. Sci.*, **18**, 179 (1983).

3. M. K. Jain, P. Desai and A. S. Abhiraman, *Extended Abstracts, 16th Biennial Conference on Carbon*, San Diego, CA, 517 (1983).

4. M. K. Jain, M. Balasubramanian, P. Desai and A. S. Abhiraman, *Extended Abstracts, 17th Biennial Conference on Carbon*, 310 (1985).

5. M. K. Jain, M. Balasubramanian, P. Desai and A. S. Abhiraman, *J. Mater. Sci.*, **22**, 301 (1987).

6. S. K. Bhattacharya, G. Bhat, V. Daga and A. S. Abhiraman, *Extended Abstracts, 18th Biennial Conference on Carbon*, Worcester, MA, 13 (1987)

7. Vijay Daga, M.S. Thesis, Georgia Institute of Technology, June 1988.

8. G. Bhat, P. Desai and A. S. Abhiraman, *Extended Abstracts, 18th Biennial Conference on Carbon*, Worcester, MA, 217 (1987).

9. A. S. Abhiraman, *Proc. 32nd Intl. SAMPE Symp. Exhib.*, Anaheim, CA, 945 (1987).

10. D. A. Grove, M.S. Thesis, Georgia Institute of Technology, 1986.

11. D. A. Grove and A. S. Abhiraman, *Extended Abstracts, 18th Biennial Conference on Carbon*, Worcester, MA, 34 (1987).

12. M. Balasubramanian, M. K. Jain, S. Bhattacharya and A. S. Abhiraman, *J. Mater. Sci.*, **22**, 3864 (1987)

13. US Patent 4 279 612, Great Lakes Carbon Corp., New York (1981).

14. M. Balasubramanian, M. K. Jain and A. S. Abhiraman, *Extended Abstracts, 17th Biennial Conference on Carbon*, 312 (1985).

15. D. A. Grove, P. Desai and A. S. Abhiraman, *Carbon*, **26**, 403 (1988).

16. D. W. Gibson, *18th National SAMPE Symp.*, **18**, 165 (1973).

17. J. J. Kipling, J. N. Sherwood, P. V. Shooter and N. R. Thompson, *Carbon*, **1**, 321 (1964).

18. U.S. Patent 4,163,770, American Cyanamid Company (1979).

19. U.S. Patent 4,301,107, American Cyanamid Company (1981).

20. U.S. Patent 4,461,739, American Cyanamid Company (1983).

APPENDIX I.
PAPERS AND PRESENTATIONS RESULTING FROM:

"PRECURSOR STRUCTURE – FIBER PROPERTY RELATIONSHIPS IN POLYACRYLONITRILE-BASED CARBON FIBERS"

PUBLICATIONS AND INVITED PRESENTATIONS

Refereed Publications

- "Oxidative Stabilization of Oriented Acrylic Fibers - Morphological Rearrangements," M. K. Jain and A. S. Abhiraman, *J. Mater. Sci.*, **18**, 179 (1983).
- "Conversion of Acrylonitrile-based Precursors Carbon Fibers - I. Review of the Physical and Morphological Aspects," M. K. Jain and A. S. Abhiraman, *J. Mater. Sci.*, **22**, 278 (1987).
- "Conversion of Acrylonitrile-based Precursors to Carbon Fibers - II. Precursor Morphology and Thermooxidative Stabilization," M. K. Jain, M. Balasubramanian, P. Desai and A. S. Abhiraman, *J. Mater. Sci.*, **22**, 301 (1987).
- "Conversion of Acrylonitrile-based Precursors to Carbon Fibers - III. Thermooxidative Stabilization and Continuous Carbonization," M. Balasubramanian, M. K. Jain, S. Bhattacharya and A. S. Abhiraman, *J. Mater. Sci.*, **22**, 3864 (1987).
- "Exploratory Experiments in the Conversion of Plasticized Melt Spun PAN-based Precursors to Carbon Fibers," D. A. Grove, P. Desai and A. S. Abhiraman, *Carbon*, **26**, 403 (1988).
- "Evolution of Structure in the Conversion of PAN-Based Carbon Fibers," D. Grove, V. Daga, P. Desai and A. S. Abhiraman, *Composites: Advances in Chemistry Series, ACS* (to appear).

Publications (Proceeding/Preprints/Abstracts of Conferences)

- "High Temperature Deformation in the Conversion of Acrylic Fibers to Carbon Fibers," M. Balasubramanian, W. C. Tincher and A. S. Abhiraman, *Proceedings of the XVI Biennial Conference on Carbon*, San Diego, CA, p. 517 (1983).

- "Morphological Rearrangements in the Conversion of Acrylic Fibers to Carbon Fibers," M.K. Jain, P. Desai and A. S. Abhiraman, *ibid*, p. 497 (1983).

- "Morphology and Oxidative Stabilization of Acrylic Precursor Fibers," M. Balasubramanian, M. K. Jain and P. Desai and A. S. Abhiraman, *Proceedings of the XVII Biennial Conference on Carbon*, Lexington, KY, p. 310 (1985).

- "Evolution of Structure and Properties in Continuous Carbon Fiber Formation," M. K. Jain, M. Balasubramanian and A. S. Abhiraman, *ibid*, p. 312 (1985).

- "From PAN-based Precursor Polymers to Carbon Fibers: Evolution of Structure and Properties," A. S. Abhiraman, *SAMPE Series*, **32**, p. 945 (1987).

- "Order-Enhancing Deformation of PAN-based Precursors," S. K. Bhattacharya, G. Bhat, V. Daga and A. S. Abhiraman, *Proceedings of XVIII Biennial Conf. on Carbon*, Worcester, MA, p. 13 (1987).

- "Mathematical Model of Oxidative Stabilization," D. A. Grove and A. S. Abhiraman, *ibid*, p. 34 (1987).

- "Continuous, Multi-zone Stabilization in PAN-based Carbon Fiber Process," G. Bhat, P. Desai and A. S. Abhiraman, *ibid*, Worcester, MA, p. 217 (1987).

- "Multi-zone Deformation and Stabilization of Acrylic Precursors for Carbon Fibers," G. Bhat, V. Daga and A. S. Abhiraman, *Proceedings of the XIX Biennial Conference on Carbon*, p. 258 (1989).

- "New Aspects in the Conversion of Acrylic Precursors to High Performance Carbon Fibers," G. Bhat, S. Damodaran, P. Desai, L. Peebles, Jr., and A. S. Abhiraman, Second Topical Conference on Emerging Technologies in Materials, "Processing of High Performance Composites - I," AIChE Meeting, San Francisco, CA, p. 277 (1989).

PRESENTATIONS BY A. S. ABHIRAMAN
(• Invited; ⋆ Other)

- "Survey and Analysis of High Performance Fiber Formation Processes," Owens Corning Technical Center, Cleveland, OH (1983).

- "Survey of Current Research on Carbon Fibers at Georgia Tech," Union Carbide Technical Center, Cleveland, OH (1983).

- "Some Aspects of the Formation of Acrylonitrile-Based Carbon Fibers," AKZO Research Center, Arnhem, The Netherlands (1983).

- "High Performance Fibers and Their Composites," ALCAN Research Center, Arvida, Canada (1986).
- "Mathematical Model of Oxidative Stabilization of Acrylic Precursors for Carbon Fibers," Gordon Research Conference Poster Session, NH (1986), with D. Grove.
- "Carbon Fibers - Production and Properties," PIA Conference on Advances in Synthetic Fibers, Atlanta, GA (1986).
- "From PAN-based Precursor Polymers to Carbon Fibers: Evolution of Structure and Properties," SAMPE Symposium on Advanced Fiber Technologies, Anaheim, CA (1987).
- "Carbon Fiber - Its Manufacture and Uses," PIA Conference on Advances in Synthetic Fibers - Processing and Properties, Atlanta, GA (1987).
- "Fundamental Aspects of the Conversion of PAN-based Precursors to Carbon Fibers," Gordon Research Conference on Fiber Science, NH (1987).
- "Evolution of Structure and Properties in a PAN-based Carbon Fiber Process," NASA Fiber-Tex Conference, Greenville, SC (1987).
- "High Performance Fiber Formation," Spotlight on Advanced Materials and Composites, Georgia Tech, Atlanta, GA (1987).
- "Polymer Based High Performance Carbon and Ceramic Fiber Structure," PEC Seminar, DuPont, Kinston, NC (1988).
- "Formation and Properties of PAN-based Carbon Fibers," Fiber Producers Conference, Greenville, SC (1988).
- "Formation, Structure and Properties of Carbon Fibers," Air Force Materials Lab., Wright Patterson Air Force Base, Dayton, OH (1988).
- "High Performance Carbon and Ceramic Fibers for Composites," Spotlight on Research at Georgia Tech for the Industrial Research Institute, Atlanta, GA 1988.
- ⋆ "New Aspects in the Conversion of Acrylic Precursors to High Performance Carbon Fibers," Second Topical Conference on Emerging Technologies in Materials, "Processing of High Performance Composites - I," AIChE Meeting, San Francisco, CA, p. 277-8 (1989), with G. Bhat, S. Damodaran, P. Desai and L. H. Peebles, Jr.

APPENDIX II.
REPRINTS OF PAPERS RESULTING FROM:

"PRECURSOR STRUCTURE – FIBER PROPERTY RELATIONSHIPS IN POLYACRYLONITRILE-BASED CARBON FIBERS"

JOURNAL OF MATERIALS SCIENCE 18 (1983) 179–188

Oxidative stabilization of oriented acrylic fibres—morphological rearrangements

MUKESH K. JAIN, A. S. ABHIRAMAN
Georgia Institute of Technology, School of Textile Engineering, Atlanta, Georgia 30332, USA

Changes in orientational and lateral order when an acrylic fibre is treated thermally at temperatures just below where stabilization reactions occur rapidly are characterized experimentally. Significant morphological rearrangements are shown to precede the onset of these reactions and also during these reactions. These changes are found to depend on the dimensional constraints imposed during thermal annealing. If shrinkage is allowed, the orientation of the ordered phase in the fibres increases but only at the expense of significant orientational relaxation in the less ordered fraction. Imposing dimensional constraints during annealing leads to a rapid increase in the overall order of the precursor. Possible ways of taking advantage of this tendency in a high-temperature drawing are discussed.

1. Introduction

Manufacture of carbon fibres from polyacrylonitrile-based precursor fibres involves:

(a) a thermo-oxidative stabilization stage which converts the precursor to an infusible structure;

(b) a carbonizing heat-treatment to drive off the non-carbon elements; and

(c) an optional high-temperature treatment to improve the mechanical properties of carbon fibres.

The properties of the final carbon fibre are affected by the chemical composition and morphology of the acrylic fibre and the chemical and morphological changes occurring during stabilization and carbonization. Many studies on isolated aspects of these different stages in carbon fibre manufacture have been reported [1–40]*. A comprehensive experimental study has been initiated in our laboratories to establish the material and process interactions with the properties of the ultimate carbon fibre. This study includes both chemical (e.g., comonomer and end group compositions) and morphological aspects of the precursor and the subsequent changes in them during stabilization and carbonization. The initial activity has concentrated primarily on the role of polymer composition in the kinetics of stabilization [41] and on identifying a set of parameters for characterizing morphological order and their interpretation. We report here the results of our initial efforts on the latter aspect, especially in relation to the stabilization stage.

1.1. Morphology

Information from wide-angle X-ray diffraction (WAXD) and electron microscopy studies on acrylic fibres shows clearly the existence of a basic morphological unit with a lateral dimension of the order of 5 to 10 nm in which the molecules are arranged in a laterally ordered hexagonal array [42]. Orientation of these laterally ordered units has also been determined from WAXD studies. The chemical changes that occur during stabilization can alter this lateral order and WAXD measurements with fibres at different stages of stabilization would reflect the nature of only the "surviving" ordered fraction. Studies have been conducted by Hinrichsen [9] with WAXD and by Thorne and Marjoram [10], with a combination of WAXD and birefringence measurements, to

*[1–3] Reviews; [4–13] heat-treatment and morphology of acrylic fibres; [14–30] reactions and kinetics of stabilization; [31–40] carbon fibre formation, structure and properties.

0022–2461/83/010179–10$03.70/0

identify the changes that occur in orientational and lateral order in the precursor as it goes through stabilization. The latter found that birefringence increased monotonically with the extent of disappearance of nitrile groups while the orientation from WAXD showed a slight increase initially followed by a steady decrease. The birefringence data of Thorne and Marjoram can be replotted to reflect the birefringence of the new species appearing in stabilization by using the following equation:

$$\Delta n = f_s \Delta n_s + (1 - f_s)\,\Delta n_p + \Delta n_f,$$

where Δn, Δn_s and Δn_p are, respectively, the birefringences of the fibre at any stage of stabilization, the new species and the unconverted fraction of the original material. Δn_f is the contribution from form birefringence and f_s is the fraction of new species in the fibre. The negligibly small birefringence of oriented acrylic fibres indicates that $(1 - f_s)\Delta n_p + \Delta n_f$ can be neglected. Thus, one gets

$$\Delta n \simeq f_s \Delta n_s$$

or

$$\Delta n_s \simeq \frac{\Delta n}{f_s}.$$

The data of Thorne and Marjoram [10], when replotted to give the birefringence of the species appearing in stabilization, indicate that the orientation of the new species appearing throughout the conversion is significant and that this orientation lies within a narrow range.

Rose [7] and Warner *et al.* [13] have observed an initial sharpening, followed by a gradual broadening of the equatorial peak in WAXD when an acrylic fibre is annealed at 230° C. This indicates an association of laterally ordered domains prior to the depletion of order in them through chemical conversion. Based on X-ray diffraction and electron microscopical studies, the latter have also presented a morphological model of acrylic fibres consisting of fibrils in which connected regions of disordered and partially ordered regions alternate.

Small-angle X-ray scattering (SAXS) studies with wet-spun acrylic fibres show scattering from microvoids that is typical of wet-spun fibres [43]. The characteristic "long period" reflecting density fluctuations which one observes normally in oriented synthetic fibres, however, is absent in these fibres. If the difference between the densities of the laterally ordered domains and the regions where such order is absent is very small, SAXS would fail to differentiate between the presence and absence of such order. Scattering from fibres that have been thermally annealed shows a pronounced long period [5, 13], indicating the possible existence of periodic order in the precursor.

The work reported in the literature shows clearly the existence of significant repetitive and orientational order in the acrylic precursors and at least a partial persistence of the orientational order through the stabilization process. It would be safe to say that the morphology of the precursor, including possible distribution of defects, would influence greatly the morphology of the carbon fibre produced from it. It is our aim to identify the relevant, measurable morphological parameters and to keep an account of the changes in them as a precursor is taken through the different stages of the carbon fibre process. We report here the results of our initial efforts to characterize the changes in an acrylic precursor fibre when it is treated thermally at temperatures just below where the stabilization reactions occur rapidly. Significant morphological rearrangements are shown to precede the onset of these reactions and also during these reactions. These changes are found to depend on the constraints imposed on the fibre during thermal annealing. These annealing experiments show a tendency towards rapid "self ordering" of the precursor. Possible ways of taking advantage of this tendency are discussed.

2. Experimentation

2.1. Wet-spinning of precursor fibres

All the experiments were done on fibres spun in our laboratory by redissolving commercial acrylic fibres (type 43 Orlon; Merge No. 630 N43) supplied by Du Pont. The spinning conditions are given in Table I.

2.2. Thermal analysis

A Du Pont 990 thermal analyser was used to determine the range of temperatures where the

TABLE I Spinning conditions

Dope concentration	20% wt/wt in DMF
Spinneret	100 holes, 3 mil* diameter
Coagulation bath composition	60:40::DMF:H_2O
Coagulation bath temperature	25° C
Jet stretch	0.7
Draw ratio	3 or 6 in boiling H_2O
Drying temperature	110° C

*1 mil ≡ 1/1000 in.

stabilization reactions occur rapidly in the precursor used in this study. At a heating rate of 5° C min^{-1} the exotherm associated with these reactions was observed at temperatures above 285° C.

2.3. Thermal annealing

The annealing experiments were carried out in an air-circulated oven, preheated to the required temperature before the sample is introduced. To determine if constraints imposed on the fibres influence the changes during this process, experiments were conducted with free allowance for fibre shrinkage and under conditions where such shrinkage is prevented by holding the fibre at constant length. For free length annealing (FLA) the fibres were suspended from clips in the oven and for constant length annealing (CLA) the filaments were wound on rigid frames with just enough tension to remove any natural crimp in them. The temperature chosen for these experiments were below that of the onset of rapid reactions determined from thermal analysis.

2.4. X-ray experiments

Phillips X-ray units 4100 and 12215 (Norelco) at 40 kV and 25 mA were used to obtain flat plate diffraction photographs and equatorial intensity scans, used for estimates of the average lateral dimension of laterally ordered morphological units. A G.E. goniometer with a 2 mm square beam was used to measure azimuthal intensity profiles. The fibres were wound carefully by hand at a minimum tension as a parallel array on the sample holder (a frame with a central circular opening). In the case of constant length annealing, the precursor fibre was wound on the X-ray diffraction sample holder and the annealing was carried out with these pre-mounted samples. Sample preparation from free annealed fibres was difficult because of the entanglements and crimp caused by annealing in the air-circulated oven.

Size of the laterally ordered domains were estimated with the width at half the maximum intensity of the 100 peak at $2\theta = 17°$ obtained from the equatorial scan using the Scherer equation [44]. Corrections to account for crystal imperfections and instrument broadening were neglected. The estimated average lateral size is also referred to as the "crystal size" in this report.

Assuming a hexagonal lateral packing, Hermans' orientation function for the orientation with respect to the fibre axis of the chain segments in the laterally ordered regions was calculated from azimuthal intensity scans of the 100 reflection.

Hermans' orientation function of chains in the crystal, f_c, is given by [44],

$$f_c = -2\left[\frac{3\langle\cos^2\phi\rangle_{100}^{-1}}{2}\right],$$

where

$$\langle\cos^2\phi\rangle = \frac{\int_0^{\pi/2} I_{100}(\phi)\sin\phi\cos^2\phi\,d\phi}{\int_0^{\pi/2} I_{100}(\phi)\sin\phi\,d\phi}.$$

2.5. Sonic modulus

A dynamic modulus tester PPM-5, made by H. M. Morgan Company, was used for measurement of sonic velocity. The sonic modulus, E, was calculated in g $denier^{-1}$ * by using the equation [45]

$$E = 11.3C^2$$

where C is the sonic velocity in km sec^{-1}.

The following semi-empirical equation can be used for estimating the Hermans' orientation function, f_s, of the sample with respect to the fibre direction [46]

$$f_s = 1 - \frac{E_{us}}{E_s},\dagger$$

where E_s = sonic modulus of the sample and E_{us} = the sonic modulus of an isotropic sample of the same material. Since we could not make isotropic samples differing from the annealed precursor fibres only in orientation distribution, the orientation functions of the constant length annealed samples were estimated using the sonic moduli of the corresponding free annealed fibres in the place of the isotropic reference. The free annealed samples do show a preferred orientation and so their sonic moduli would be higher than those of the fully isotropic ones. Thus the orientation functions computed here would be lower bounds for the actual values, i.e.,

$$f_{CLA}(t,T) = 1 - \frac{E_{us}(t,T)}{E_{CLA}(t,T)} > 1 - \frac{E_{FLA}(t,T)}{E_{CLA}(t,T)}$$

where $f_{CLA}(t,T)$ is the orientation function of constant length samples annealed for time t at

*Denier = weight (g) of 9000 m.

†This semi-empirical equation assumes a single-phase material. It is used here only for the purpose of comparison.

TABLE II Short-time annealing experiments. Total annealing time 2 min; temperature of annealing 230° C; no evidence of chemical reactions

Precursor D.R.	Treatment condition	Shrinkage (%)	Initial modulus (g denier^{-1})	Breaking elongation (%)	Sonic modulus (g denier^{-1})	f_c	Crystal size (nm)
3	Orig.	–	61	13	95	0.54	5.4
3	CLA	–	70	16	120	0.69	8.9
3	FLA	16	43	23	57	0.59	8.9
3	CFLA	Negligible	67	17	120	0.69	9.9
6	Orig.	–	73	9	130	0.63	4.7
6	CLA		85	13	145	0.75	8.1
6	FLA	16	57	14	78	0.63	8.5
6	CFLA	Negligible	78	12	142	0.75	9.4

temperature T, E_{us} is the sonic modulus of unoriented sample; E_{CLA} is the sonic modulus of constant length annealed sample; and E_{FLA} is the sonic modulus of free annealed sample.

2.6. Mechanical properties

A mini Instron model 1130 was used with a 5000 g load cell. The gauge length and the elongation rates were 10 and 5 in. min^{-1} (25.4 and 12.7 cm min^{-1}) respectively. Since the fibres annealed for more than an hour were extremely brittle, they were tested at an elongation rate of 2 in. min^{-1} (5.08 cm min^{-1}).

3. Results and discussion

3.1. Short-time annealing

The annealing experiments in the present study were carried out at temperatures below 285° C so that the morphological rearrangements occurring in a short time before the onset of the chemical reactions can be separated from those occurring at longer times as a consequence of them.

Exploratory short-time (2 min) annealing experiments were conducted at 230° C. These were carried out under free (FLA) and constant length (CLA) conditions as well as a combination of constant length followed by free annealing (CFLA). The last experiment was included to determine if any changes introduced initially in the presence of the constraint are erased to a significant extent by subsequent treatment without constraint. The results are given in Table II and show clearly that the orientation of the ordered fraction in the material as well as the overall orientation (inferred from sonic modulus) show a significant increase when a constraint against shrinkage is imposed on the fibres. Annealing the precursor under free conditions, however, results in considerable decrease in the overall orientation but shows simultaneously an increase in the orientation of the ordered phase. This indicates clearly the presence of a significant fraction in the material other than the ordered phase. The connections provided by the ordered phase do transfer macroscopic constraints to the rest of the material, thus preventing significant relaxation of orientation. The results from the CFLA experiments (1 min CLA + 1 min FLA) show that the order induced in constrained annealing is likely to be retained in the subsequent treatment under free conditions.

Significant shrinkage in fibres annealed under free conditions without decrease in the orientation of the ordered phase implies that the less ordered morphological units link successive oriented crystals along the fibre direction. The average lateral dimension of the oriented laterally ordered crystals is estimated to be around 5 nm in the unannealed fibres, in agreement with the estimate provided by Warner *et al.* [13]. Since the calculations neglect line broadening from possible imperfections in lateral order, it tends to underestimate the average size.

Increase in the orientation of the ordered phase can be attributed to lateral and longitudinal association in ordered bundles during annealing. The estimated average lateral size of these bundles increases significantly as a consequence of this association.

3.2. Time-scale annealing

In order to follow the progressive changes in morphology brought about by high-temperature treatment, the precursor fibres were treated for varying lengths of time at 270° C. This temperature was chosen to provide a reasonable period before

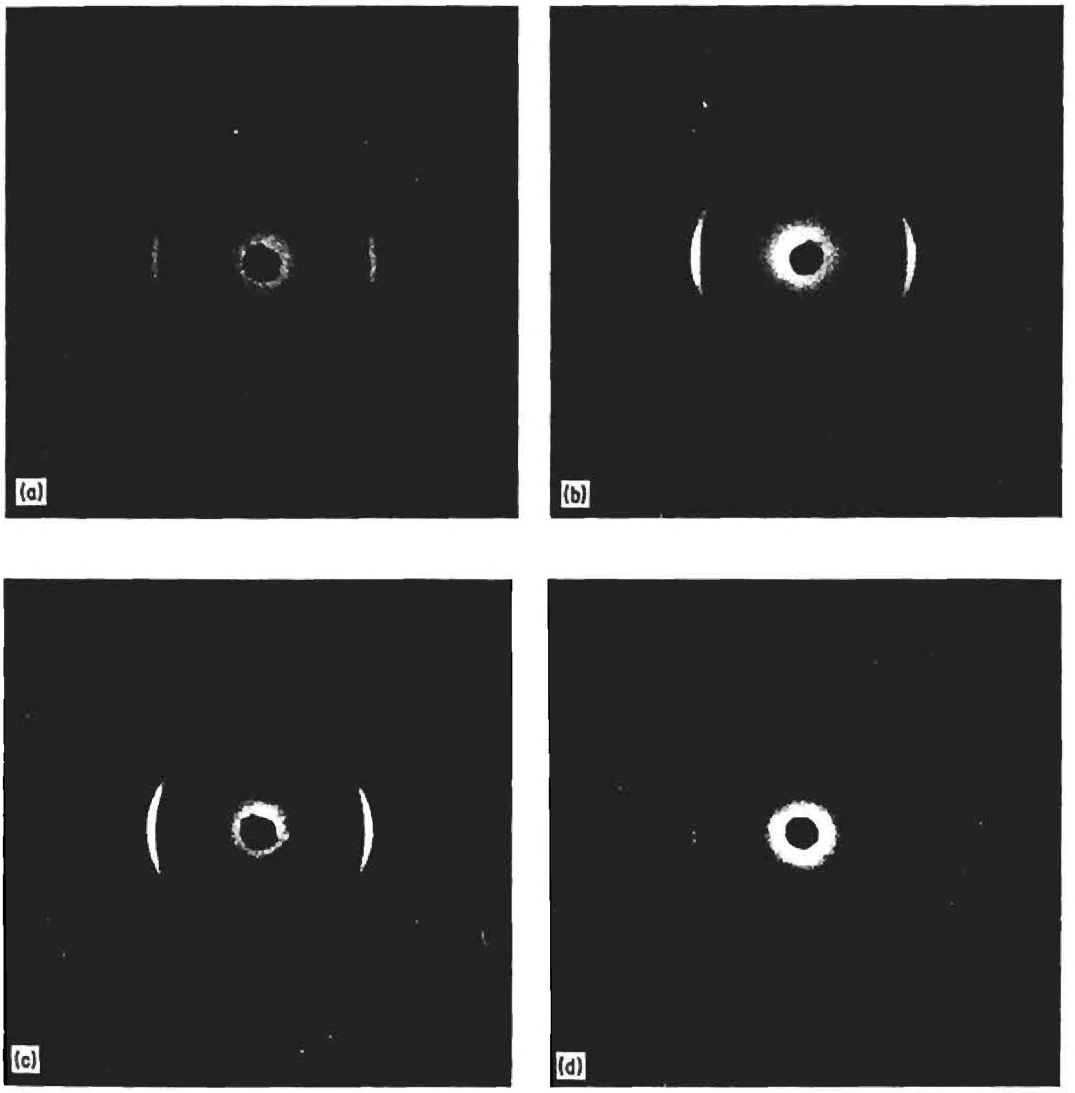

Figure 1 Flat-plate WAXD photographs of fibres (precursor draw ratio = 6) annealed at 270° C in air. (a) Precursor, (b) CLA for 4 min, (c) FLA for 4 min, (d) CLA for 48 min, (e) CLA for 128 min. Exposure time: (a) to (d) 2 h; (e) 4 h.

the onset of significant stabilization reactions in the material. Figs 1a to e show flat-plate WAXD photographs of samples exposed to 270° C in air for various durations. The initial significant increase in the orientation and the size of the ordered phase can be seen here. Quantitative measures of these at different stages of heat-treatments are shown in Fig. 2 (CLA) and Fig. 3 (FLA). The data show clearly that the orientational changes of the ordered phase measured here are a direct consequence of the initial association of segments into these domains followed by

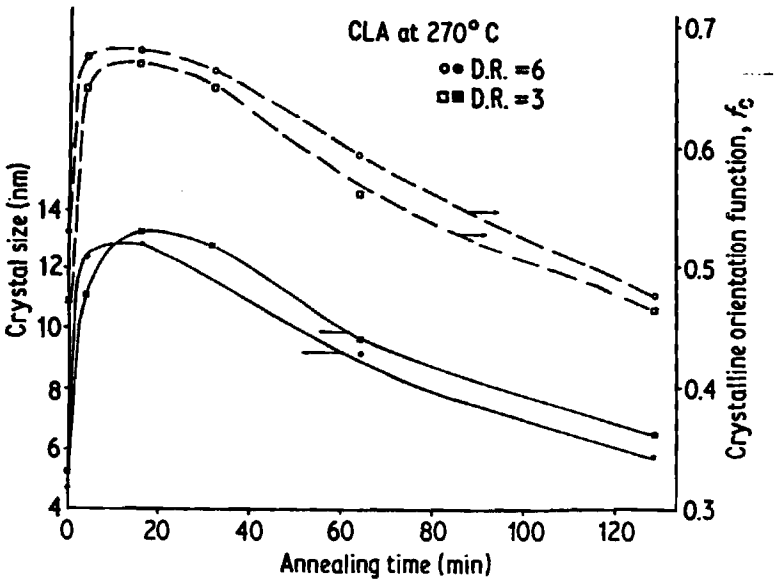

Figure 2 Average lateral size and Hermans' chain orientation function of the ordered phase in CLA fibres. Annealing temperature 270° C; precusor draw ratio: ○, ● 6 and □, ■ 3.

the "lateral order → lateral disorder" transformation caused by the stabilization reactions. The latter proceeds, by necessity, inwards from the boundaries of ordered domains, leading to a decrease in the average size of these domains.

The sonic modulus data of these fibres are shown in Fig. 4. One is tempted, at first glance, to interpret the data as indicating a decrease in the overall orientation at long annealing times. The change in the chemical nature resulting from the stabilization reactions would be expected to change the intrinsic physical properties of the material. The estimation of Hermans' orientation functions from the sonic moduli of the thermally treated fibres should take into account the changes in the sonic moduli of the reference isotropic sample. As discussed earlier, lower bounds for the orientation functions of CLA samples can be obtained using the equation

$$f_{CLA} = 1 - \frac{E_{FLA}}{E_{CLA}}.$$

Typical values of these are given in Table III, which shows that the overall orientation of the material does not change significantly with the occurrence of stabilization reactions.

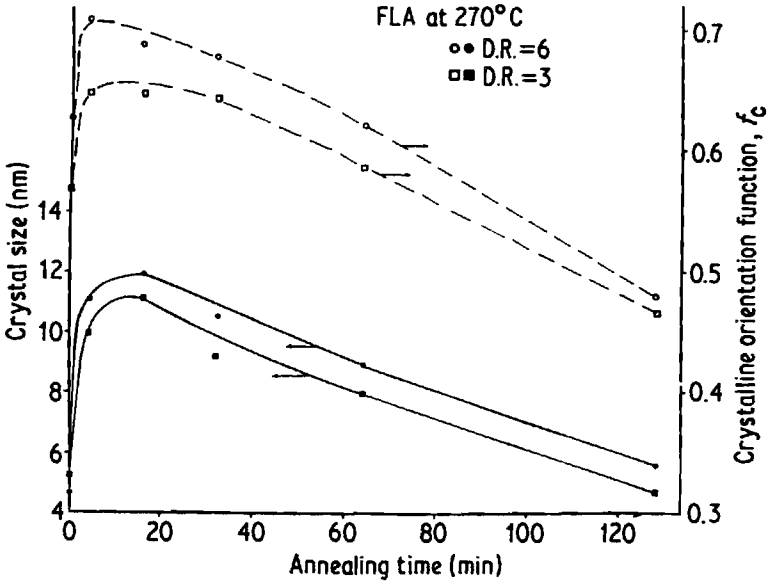

Figure 3 As in Fig. 2 but for FLA fibres.

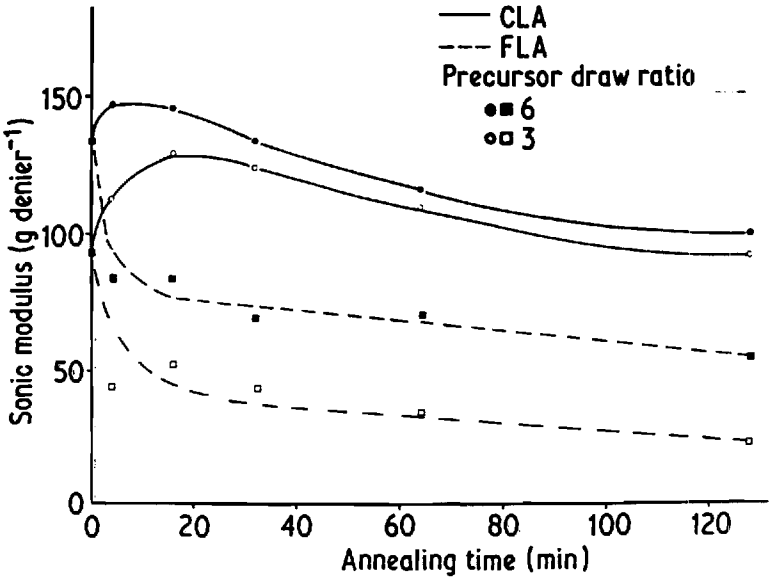

Figure 4 Sonic modulus of fibres annealed at 270° C.

The data from the FLA experiments (Figs 3 and 4) provide clear evidence for the existence of a phase of lower order than the ordered phase. In the absence of macroscopic constraints which prevent shrinkage, this phase can undergo significant orientational relaxation at high temperatures on a time scale that is much shorter than that in which detectable extent of reactions can take place in the material.

3.3. Pre-stabilization high-temperature drawing

The results from constant length annealing revealed a tendency in the precursor fibres towards self ordering with a significant increase in orientation. We have conducted exploratory experiments to determine if this tendency can be utilized to significantly improve the orientational and lateral order in the precursor. The results from a drawing experiment, where the fibre is drawn through a one-foot oven, are given in Table IV and typical flat-plate WAXD photographs are shown in Fig. 5. In the case where the fibre is passed through the oven without any drawing (draw ratio = 1.0), the morphological rearrangements are seen to occur on a very short time scale (the residence time in the oven here is 4 sec). The overall orientation can be increased significantly by drawing under these conditions where considerable mobility exists for allowing rearrangements along with a natural tendency toward ordering.

4. Conclusions

Significant morphological rearrangements take place in acrylic precursor fibres at temperatures comparable to those in a stabilization process. These changes, which occur both prior to and after the onset of detectable chemical reactions, depend to a large extent on the dimensional constraints imposed during annealing. Annealing in the absence of dimensional constraints causes a significant shrinkage and a decrease in overall orientation, but the orientation of the ordered phase increases. If fibre shrinkage is not allowed,

TABLE III Sonic modulus-based overall orientation of constant length annealed fibres. Temperature = 270° C

D.R.	Annealing time (min)	Sonic modulus (g dernier^{-1})		Lower bound for sonic modulus-based orientation function, f_{CLA}
		CLA	FLA	
6	4	147	79	0.46
6	16	145	79	0.45
6	32	133	68	0.49
6	64	115	69	0.40
6	128	99	54	0.45

TABLE IV High-temperature drawing experiments. Precursor D.R. = 6, drawing speed = 15 ft min^{-1} (457 cm min^{-1}), oven temperature = 240° C, length of oven = 1 ft

Sample	Elongation (%)	Initial modulus (g $denier^{-1}$)	Sonic modulus – (g $denier^{-1}$)	f_c	Crystal size (nm)
Original	9	73	133	0.63	4.7
D.R. = 1.0	12	76	145	0.75	10.7
D.R. = 1.2	10	111	176	0.79	11.1
D.R. = 1.4	8	124	190	0.81	11.5

the overall orientation increases and this orientation is retained in subsequent annealing under free conditions.

It is well known that such morphological changes occur during thermal annealing of oriented synthetic fibres. Significant orientational relaxation of uncrystallized segments can occur without decrease in the crystalline orientation when drawn fibres are annealed under free conditions [47, 48]. The connectivity which exists along the axial direction in the oriented fibres necessitates the allowance for macroscopic shrinkage if orientational relaxation is to occur in the uncrystallized segments. Thus, annealing with dimensional constraints leads to a significant increase in overall orientational order brought about by increase in the orientation of the ordered phase without orientational relaxation in the less ordered phase.

The responses to thermal treatments of the acrylic fibres in the present study confirm the presence of at least two phases, one laterally ordered and the other a less ordered phase which contains segments that tend to be mobile at high temperatures. The latter segments are anchored in the ordered phase and macroscopic constraints are transmitted via the ordered phase to these segments, preventing significant orientational relaxation in them. The well established fibrillar morphology of drawn acrylic fibres, coupled with the mechanical response and changes in morphological parameters during annealing support the morphological model proposed by Warner *et al.* [13], namely connected alternating regions of lateral order and disorder along the fibrils. Relaxation of orientation in the disordered regions of such a morphology should lead to a significant decrease in the sonic modulus but without decrease in the orientation of the ordered regions. The results from free length annealing experiments (Figs 3 and 4) support clearly this contention.

The combination of sonic modulus and average orientation and lateral size of the ordered phase is useful in characterization of orientational changes during thermal treatment of acrylic fibres in which both morphological and chemical transformations take place. Trends in both crystalline and overall orientation, which are not always the same can be

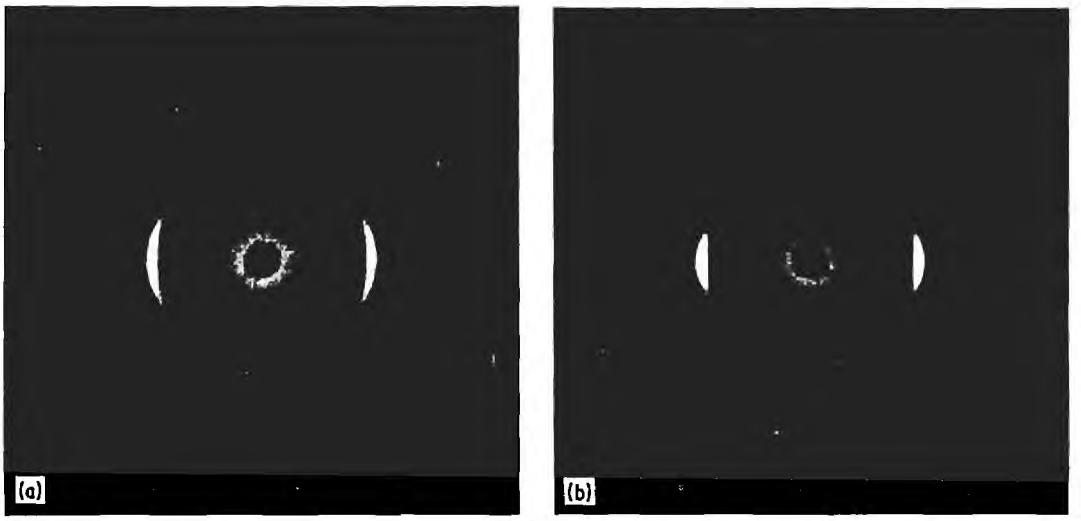

Figure 5 Flat-plate WAXD photographs (exposure time = 2 h) of fibres drawn at 240° C. Draw ratio: (a) 1.0 and (b) 1.4.

inferred from this combination. The favourable role of dimensional constraints during thermal treatment is especially made clear by this combination of techniques.

There is a tendency towards self ordering at high temperature in the presence of dimensional constraints. This has been shown to be advantageous in a high-temperature drawing that produces fibres with improved orientational and lateral order. This improvement occurs without loss of breaking elongation which suggests that the overall perfection also increases simultaneously. The importance of preventing shrinkage and the significant improvement in carbon fibre properties that result from stretching in the early stages of oxidizing acrylic fibres were shown by Watt and Johnson [33]. These effects were attributed by them to increased polymer chain orientation that is reflected ultimately in the carbon fibre. These favourable changes in morphological order may be obtained in a short-time high-temperature drawing process. The significance of these and possible reduction in microvoids induced by such high-temperature drawing in the manufacture of carbon fibres is being investigated.

Acknowledgements

We wish to express our gratitude to Dr Larry Peebles for many useful suggestions during the course of this work and in the inferences drawn from experimental data. We are thankful to Dr Wayne Tincher for inviting us to participate in this project and to Dr Steve Spooner for offering us his helpful advice and X-ray diffraction facilities. Discussions with Dr Tincher and help from Karen Rodriguez in the preparation of the manuscript are gratefully acknowledged. The study was supported by the United States Office of Naval Research.

References

1. W. WATT, *Carbon* 10 (1972) 121.
2. P. J. GOODHEW, A. J. CLARKE and J. E. BAILEY, *Mater. Sci. Eng.* 17 (1975) 3.
3. P. E. MORGAN, *Textile Prog.* 8 (1976) 69.
4. C. N. TYSON, *Nature Phys. Sci.* 229 (1971) 121.
5. M. E. FILLERY and P. J. GOODHEW, *ibid.* 233 (1971) 118.
6. G. K. LAYDEN, *J. Appl. Polymer Sci.* 15 (1971) 1709.
7. P. G. ROSE, PhD thesis, University of Aston in Birmingham (1971).
8. E. A. BOUCHER, D. J. LANGDON and R. J. MANNING, *J. Polymer Sci. A-2* 10 (1972) 1285.
9. G. HINRICHSEN, *J. Polymer Sci. Part C* 38 (1972) 303.
10. D. J. THORNE and J. R. MARJORAM, *J. Appl. Polymer Sci.* 16 (1972) 1357.
11. G. HINRICHSEN, *ibid.* 17 (1973) 3305.
12. S. B. WARNER, *J. Polymer Sci. Polymer Lett. Ed.* 16 (1978) 287.
13. S. B. WARNER, D. R. UHLMANN and L. H. PEEBLES Jr, *J. Mater. Sci.* 14 (1979) 1893.
14. J. N. HAY, *J. Polymer. Sci. A-1* 6 (1968) 2127.
15. N. GRASSIE and R. McGUCHAN, *Europ. Polymer. J.* 6 (1970) 1277.
16. W. WATT, in "Third Conference on Industrial Carbons and Graphite", edited by J. G. Gregory (Society of Chemical Industry, London, 1971) p. 431.
17. W. WATT and J. GREEN, in "Proceedings of the International Conference on Carbon Fibres: Their Composites and Applications", Suppl. No. 5 (The Plastics Institute, London, 1971) p. 23.
18. A. J. CLARKE and J. E. BAILEY, *Nature* 234 (1971) 529.
19. N. GRASSIE and R. McGUCHAN, *Europ. Polymer J.* 7 (1971) 1091.
20. *Idem, ibid.* 7 (1971) 1357.
21. *Idem, ibid.* 7 (1971) 1503.
22. A. J. CLARKE and J. E. BAILEY, *Nature* 243 (1973) 146.
23. E. FITZER and D. J. MULLER, *Carbon* 13 (1975) 63.
24. S. P. VARMA, B. B. LAL and N. K. SHRIVASTAVA, *ibid.* 14 (1976) 207.
25. J. FERGUSON and B. MAHAPATRO, *Fibre Sci. Technol.* 11 (1978) 55.
26. M. M. COLEMAN and R. J. PETCAVICH, *J. Polymer Sci. Polymer Phys. Ed.* 16 (1978) 821.
27. S. B. WARNER, L. H. PEEBLES Jr and D. R. UHLMANN, *J. Mater. Sci.* 14 (1979) 565.
28. L. M. MANOCHA and O. P. BAHL, *Fibre Sci Technol.* 13 (1980) 199.
29. J. FERGUSON and N. DEBNATH-RAY, *ibid.* 13 (1980) 167.
30. M. M. COLEMAN and G. T. SIVY, *Carbon* 19 (1981) 123.
31. W. WATT and W. JOHNSON, *Appl. Polymer Symp.* 9 (1969) 215.
32. R. MORETON, in "Third Conference on Industrial Carbons and Graphites", edited by J. G. Gregory (Society of Chemical Industry, London, 1971) p. 472.
33. W. WATT and W. JOHNSON, *ibid.* p. 417.
34. W. WATT, D. J. JOHNSON and E. PARKER, *Plast. Polym. Conf. Suppl.* 6 (1974) 3.
35. O. P. BAHL and L. M. MANOCHA, *Carbon* 13 (1975) 297.
36. L. M. MANOCHA, O. P. BAHL and G. C. JAIN, *Angew. Makromol. Chemie* 67 (1978) 11.
37. W. N. REYNOLDS and R. MORETON, *Phil. Trans. Roy. Soc. Lond.* A294 (1980) 451.
38. D. J. JOHNSON, *ibid.* A294 (1980) 443.
39. S. S. CHARI, O. P. BAHL and R. B. MATHUR, *Fibre Sci. Technol.* 15 (1981) 153.

40. O. P. BAHL, R. B. MATHUR and K. D. KUNDRA, *ibid.* 15 (1981) 147.
41. F. L. COOK and D. HARTMAN, Paper No. 41, 182nd ACS National Meeting – Cellulose, Paper and Textile Division, New York (1981).
42. L. E. ALEXANDER, "X-ray Diffraction Methods in Polymer Science" (Wiley Interscience, New York, 1969) p. 482.
43. W. O. STATTON, *J. Polymer. Sci.* 58 (1962) 205.
44. L. E. ALEXANDER, "X-ray Diffraction Methods in Polymer Science" (Wiley Interscience, New York, 1969).
45. "Operational Manual of Sonic Modulus Equipment PPM-5" (H. M. Morgan Co., Inc., Norwood, Mass., 1980).
46. A. L. McPETERS and D. R. PAUL, *Appl. Polymer. Symp.* 25 (1974) 159.
47. W. O. STATTON, in "The Setting of Fibers and Fabrics", edited by J. W. S. Hearle and L. W. C. Miles (Merrow, Herts, 1971).
48. R. J. SAMUELS, "Structured Polymer Properties" (Wiley, New York, 1974).

Received 31 March
and accepted 24 June 1982

JOURNAL OF MATERIALS SCIENCE 22 (1987) 301–312

Conversion of acrylonitrile-based precursors to carbon fibres

Part 2 *Precursor morphology and thermooxidative stabilization*

MUKESH K. JAIN*, M. BALASUBRAMANIAN, P. DESAI, A. S. ABHIRAMAN‡
Georgia Institute of Technology, Atlanta, Georgia 30332, USA

The progress of stabilization of two compositions of acrylic fibres with various orientations has been followed by a variety of techniques. The thermooxidative treatments for stabilization have been carried out in a continuous process and also in a batch process under free shrinkage, constant length and constant tension conditions. The morphological model of acrylic fibres consists of an alternating sequence of laterally ordered and laterally disordered regions along the fibre direction. This structure is consistent with the observations based on small-angle X-ray scattering of copper-impregnated precursor fibres and thermomechanical response, thermal stress development, calorimetry, wide- and small-angle X-ray scattering and sonic modulus measured at different extents of stabilization. Lateral as well as orientational order in these fibres can be increased markedly through a high-temperature deformation process prior to stabilization. An increase in perfection and extent of order is observed in the early stages of stabilization. There is also a simultaneous decrease in the orientation of the disordered phase at this stage and the extent of this decrease depends on the axial constraints imposed on the fibre. Little difference in the rate of stabilization is observed as measured by density or oxygen uptake for fibres with different extents of orientation, lateral order or restraint. Fibres containing itaconic acid, a stabilization catalyst, did show an increased rate of stabilization. Inferences have been drawn regarding additional research pertaining to achieving high order in precursor fibres, minimizing orientational relaxation during oxidative stabilization, and the techniques for monitoring the extents of the stabilization treatment and the changes in relevant morphological parameters.

1. Introduction

Thermooxidative stabilization constitutes an important intermediate step in the conversion of acrylonitrile-based precursor fibres to carbon fibres. The precursor fibre is transformed at this stage to yield a structure that can be subjected to the high-temperature carbonization treatment without loss of structural cohesion.

It is well known that the properties of the final carbon fibres are determined by a combination of the nature of the precursor fibres and the physical and morphological rearrangements that occur in the stabilization and carbonization steps. Significant changes in morphology and composition occur at each stage. These changes are much affected by the history of thermal treatments as well as the dimensional constraints/stresses imposed during such treatments. Much of the research reported in the literature has been devoted to isolated aspects of the formation of carbon fibres [1] but relatively few attempts have been made to study their development through the stabilization and carbonization stages. Also, the influence of the morphology of the precursor fibres on their stabilization and carbonization behaviour has received little attention. Most of the reported studies involve commercially spun fibres, which restricted them to a limited range of morphology and composition, which were usually unspecified.

A comprehensive experimental facility has been developed in our laboratories to conduct research at all stages of the integrated carbon fibre manufacturing operation. The polymerization and spinning capabilities are an integral part of this research, since they provide the choice of spinning precursor fibres with the desired chemical composition, molecular weight and morphological parameters. We report here the results from a study of the morphology of acrylonitrile-based precursor fibres and the changes introduced in batch and continuous thermooxidative stabilization. The evolution of properties in continuous carbonization is discussed in the third part of this sequence [2]. A comprehensive review of the literature on the physical and morphological changes during the conversion of acrylonitrile-based precursors to carbon fibres is given in Part 1 [1].

2. Experimental procedures

Detailed descriptions of the experimental procedures are given in Jain [3].

*Present address: ALCAN, Arvida Laboratories and Experimental Engineering Center, Jonquiere, Quebec, Canada.
‡Author to whom all correspondence should be addressed.

0022–2461/87 $03.00 + .12

TABLE I Conditions for spinning of precursor fibres

Precursor	Polymer solution		Coagulation bath		Drawing conditions		Denier/filament
	Concn. (% wt/wt)	Viscosity (P)	Composition (%DMF)	Temperature (° C)	Jet stretch	Draw ratio in boiling H_2O	
I	20	280	60	25	0.7	3	4.1
					0.7	6	2.1
					0.9	3	3.4
					0.7	7.3	1.6
II	17.5	140	60	14	0.7	2.5	3.9
					1.2	3	2.2
					0.7	5	2.2

Spinneret hole diameter was 3 mil (0.003 in.) in all cases.

2.1. Preparation of precursor fibres

Two precursor fibres, I and II, were prepared by solution spinning. For spinning precursor I fibres, a 20% (wt/wt) solution was prepared in dimethyl formamide (DMF) by dissolving commercial acrylic fibres, Orlon 43. For spinning precursor II fibres, a 17.5% (wt/wt) solution of a copolymer of acrylonitrile (AN) and itaconic acid (IA) in the weight ratio of 97/3 (average molecular weight = 131 000 g mol^{-1}, estimated from intrinsic viscosity) was prepared.

The spinning conditions for the two precursors, established to produce fibres of good quality, are given in Table I. The jet stretch and the draw ratio were changed to obtain precursor fibres having different orientations. High-temperature drawing of some of the precursor fibres was performed in order to produce fibres with high orientation and morphological parameters quite different from those produced by drawing in boiling water. Two types of post-spinning high-temperature drawing processes, i.e. hot godet and hot oven, were performed on the hot water (partially) drawn fibres. In the former type of drawing, precursor fibres were drawn directly from the heated feed-godet whereas in the latter type the fibres were first annealed at a relatively low temperature (115 to 130° C) on the feed-godet and then drawn through an oven.

Details of the drawing conditions are given in Table II. The first letter in the sample identification code refers to the precursor type (I for precursor I and II for precursor II). The second and the third terms represent the jet-stretch and the draw ratio (in boiling water), respectively. The last three terms signify the post-spinning, high-temperature plastic drawing conditions such as type of heater (oven or godet), temperature and draw ratio, respectively. The high-temperature draw ratios in these experiments were selected such that the final deniers of the high-temperature drawn fibres matched, within the limits of the experiments, with those of the hot water drawn fibres. This is important if any comparisons in the stabilization and the carbonization behaviour of the two fibres are to be made. The temperatures employed in the hot-oven drawing were the maximum possible for a smooth drawing operation without filament breakages.

2.2. Batch and continuous stabilization

Batch stabilization experiments were carried out in an air circulated oven or in a short tubular furnace, preheated to the desired temperature before the sample was introduced. To determine if dimensional constraints imposed on the fibres influence the changes during this process, experiments were conducted under three different conditions, (i) with free allowance for fibre shrinkage (FL), (ii) by holding the fibre at constant length (CL), and (iii) by hanging suitable weights for constant tension (CT). The batch stabilization treatment was carried out below the temperature at which rapid exothermic stabilization reactions begin.

TABLE II High-temperature drawing conditions

Sample	Draw ratio			Draw godet/ oven temp. (° C)	Annealing godet temp. (° C)	Denier/filament
	B.W.*	H.T.†	Total			
Precursor I						
I-0.9-3-O-252-1.7	3	1.7	5.1	252, oven	130	2.0
I-0.9-3-O-252-2.3	3	2.3	6.9	252, oven	130	1.4
I-0.7-6-O-240-1.2	6	1.2	7.2	240, oven	120	1.7
I-0.7-6-O-240-1.4	6	1.4	8.4	240, oven	120	1.5
Precursor II						
II-0.7-2.5-O-228-1.8	2.5	1.8	4.5	228, oven	115	2.2
II-0.7-2.5-G-160-1.8	2.5	1.8	4.5	160, godet	160	2.2
II-0.7-2.5-O-224-2.5	2.5	2.5	6.2	224, oven	118	1.6
II-0.7-2.5-G-190-2.7	2.5	2.7	6.7	190, godet‡	190	1.5

Sample notation: Precursor type – jet stretch – hot water draw ratio – oven/godet drawing – drawing temperature – draw ratio.
*Draw ratio in boiling water.
†High-temperature draw ratio.
‡The drawn fibres were yellowish due to partial degradation/stabilization.

The tubular furnace for continuous stabilization was divided into three 6 foot (~183 cm) zones with individual temperature controllers for each zone. Smooth transition from one zone to another and the uniformity of temperature throughout a zone were ensured by a metal tube placed between the heaters and the inner glass tube. The temperature profile inside the furnace was determined with thermocouple probes placed 18 in. (~46 cm) apart. Two air pumps, one at each end of the glass tube provided enough air circulation.

Samples for the study of progression of continuous stabilization were obtained after steady state was reached in a constant length run (identical feed and take-up speeds) by cutting the yarn at the delivery end and rapidly pulling it from the feed end. This was then cut into 1 foot (~30.5 cm) sections for subsequent measurements. An apparent residence time for each section was calculated assuming a constant velocity of the yarn from the feed to the exit of the oven. A flat temperature profile of 265° C and feed and take-up velocities of 1 in. min^{-1} (2.54 cm min^{-1}) were employed for this study.

2.3. Thermal analysis

A DuPont DSC model 990 was employed to determine the temperatures at which the precursor fibres undergo exothermic reactions. The analysis was carried out in a regular sample pan at a heating rate of 10° C min^{-1}. The fibres were chopped to small pieces (1 to 2 mm long). The temperature range in which the exotherm was observed was employed as a guide in choosing the stabilization temperatures. Fibres stabilized for various periods were further analysed by this method and the changes in the nature and the extent of exotherms were recorded.

A Perkin Elmer DSC-4 instrument was employed to follow the changes in the heat of melting of fibres, plasticized by water, as a function of the time of stabilization of precursor fibres. The pressure capsules employed in this study were supplied by Perkin-Elmer (Part 319–0218). About 10 mg powdered fibre samples were mixed with water (approximately three times the weight of the fibres). The capsules were carefully sealed, weighed and kept at 50° C for at least 24 h. The melting curves at a heating rate of 10° C min^{-1} were recorded. ΔH_m values per unit mass of fibre samples stabilized for different periods were calculated from the area under the melting curves computed through the Perkin-Elmer data station. The results reported here are to be viewed only for major trends because the degree of reproducibility required for exact quantitative acceptance has not yet been established.

2.4. Wide- and small-angle X-ray scattering

Flat plate wide-angle X-ray diffraction (WAXD) photographs of precursor and batch stabilized fibres were obtained with a Phillips X-ray unit 4100. For quantitative estimation, radial and azimuthal scans were made with a Phillips diffractometer. Samples for equatorial scans were prepared by winding the fibres carefully as a parallel array on the sample holder. The average size of the laterally ordered domains, L_c, also referred to as "crystal size", can be estimated using the Scherrer equation ([4] p. 423):

$$L_c = K\lambda/B_0 \cos\theta \tag{2}$$

where λ is the wavelength of the X-rays, B_0 is the full width at half the maximum intensity (FWHM) in radians and K is a constant commonly assigned a value of unity. The FWHM was estimated from the (1 0 0) peak at $2\theta = 17°$. Corrections to account for inhomogeneous strains and instrumental broadening were neglected in these calculations and so the estimates obtained here are lower bounds for the actual crystal sizes.

Assuming a hexagonal lateral packing of chains in the ordered domains, Herman's orientation function for these segments with respect to the fibre axis, f_c, was calculated from azimuthal intensity scans of the (1 0 0) reflection, $I_{100}(\phi)$. f_c is given by ([4] p. 423)

$$f_c = -2\,\frac{3\langle\cos^2\phi\rangle_{100} - 1}{2} \tag{3}$$

where

$$\langle\cos^2\phi\rangle_{100} = \frac{\int_0^{\pi/2} I_{100}(\phi)\sin\phi\cos^2\phi\,d\phi}{\int_0^{\pi/2} I_{100}(\phi)\sin\phi\,d\phi} \tag{4}$$

where ϕ is the azimuthal angle with respect to the fibre axis direction.

A limited number of small-angle X-ray scattering (SAXS) flat plate photographs of the precursor and the batch stabilized fibres were taken with a Phillips X-ray unit. The study was included to provide a qualitative insight into the macroscopic arrangement of the ordered and the disordered regions in the pristine and the heat-treated fibres. The appearance of a meridional reflection, according to Hess-Kiessig model ([4] p. 334) can be interpreted as an alternating arrangement of the ordered and disordered phases along the fibre axis.

2.5. Sonic modulus

The measurements of sonic velocity through fibre samples were made with the sonic modulus tester PPM-5 by H. M. Morgan Co. Sonic modulus is calculated from sonic velocity, C, measured along the length of the fibre using the following expression:

$$E = \varrho C^2 \tag{5}$$

where E is the modulus and ϱ is the density. When E is expressed in g/denier and C in km sec^{-1}, we obtain,

$$E(\text{g/denier}) = 11.3\,C^2 \tag{6}$$

2.6. Density

Densities of the precursor fibres and fibre samples at different stages of stabilization were measured using the flotation technique using toluene (density = 0.866 g cm^{-3}) and CCl_4 (density = 1.585 g cm^{-3}) mixed together in various proportions to give solutions of densities ranging from 1.11 to 1.55 in steps of 0.01.

2.7. Elemental analysis

Selected samples from the continuous stabilization

line were analysed for carbon, hydrogen and nitrogen (these measurements were made by Atlantic Microlab, Inc., Atlanta, Georgia). Since the stabilized yarn was hygroscopic, it was dried at 80° C and 1 mm mercury pressure for 8 h before the analysis was performed. The oxygen content was calculated by difference, assuming that the only elements present in the precursor and in the stabilized fibres are carbon, hydrogen, nitrogen and oxygen and was plotted as a function of position in the stabilization furnace.

2.8. Shrinkage and shrinkage force

Shrinkage measurements as a function of heating time in batch stabilization under free length were made using an air circulated oven at 265° C. Per cent shrinkage was calculated from the length change, Δl, as $(\Delta l/l)100$ where l is the initial length of the fibre before shrinkage.

Shrinkage force measurements were carried out at constant length by connecting one end of the precursor fibres to an Instron load cell, passing them through a small oven and tying the other end to a rigid support through a Kevlar yarn. The furnace, heated to a predetermined temperature was kept initially on the Kevlar end and then moved quickly over smooth rails to the precursor end. The tension generated in the fibres was recorded as a function of time.

2.9. Mechanical properties

Tensile properties of the fibres were measured with a mini Instron, model 1130 with rubber-faced pneumatic jaws at 50 psi ($\sim 0.35\,N\,mm^{-2}$) air pressure. A gauge length of 10 in. (25.4 cm) and elongation rate of 5 in. min^{-1} (~ 12.7 cm min^{-1}) were employed for testing precursor fibres. Young's moduli of fibres were calculated from the initial slope of the load–elongation curve.

3. Results and discussion

3.1. Summary of results from previous studies in our laboratories

The results from preliminary batch annealing and stabilization experiments with normally drawn precursor I fibres were reported earlier [6]. Significant morphological rearrangements were found to occur both prior to and after the onset of detectable reactions. The degree of changes depended to a large extent on the dimensional constraints imposed during the thermal treatment. The responses indicated clearly the presence of two major phases in the fibres, a laterally ordered phase and a less ordered phase which exhibited a high degree of segmental mobility at temperatures close to those of stabilization. Annealing without dimensional constraints led to a high degree of disorientation in the less ordered phase, with a simultaneous tendency toward increase in both the size and average orientation of the ordered domains. The extent of disorientation in the mobile phase could be reduced significantly by the imposition of dimensional constraints during thermal treatment, indicating that a significant portion of the chain segments in this phase was bridging the ordered domains. The combination of mechanical response and changes in morphological parameters during thermal treatment of these fibres supported the morphological model proposed by Warner *et al.* [6], namely, connected alternating regions of lateral order and disorder (in fibrils), aligned along the fibre direction in oriented acrylic fibres. The results from dimensionally constrained heating also revealed a rapid initial tendency in the precursor fibres toward self ordering, with a significant increase in orientation. This tendency was utilized to improve the orientational and lateral order in the precursor fibres by drawing them at temperatures comparable to those of stabilization.

3.2. Pre-stabilization high-temperature drawing

The properties of high-temperature drawn (HTD) fibres along with the original fibres are given in Tables III and IV. The method of sample designation has been described in the experimental section. The high values of sonic modulus and orientation function, f_c, in HTD fibres suggest a significant increase in the orientation of the ordered phase and in the overall orientation. The average lateral size of the ordered phase (crystal size) increases by more than 100% as a result of this high-temperature drawing. Two samples from precursor I, I-0.9-3-O-252-2.3 (drawn 3 × in hot water followed by an additional 2.3 × in an oven at

TABLE III Properties of precursor I fibres

Sample	Denier/ filament	Tenacity (g/denier)	Elong. (%)	Young's modulus (g/denier)	Sonic modulus (g/denier)	Orientation function, f_c	Crystal size (nm)
First set for preliminary batch-stabilization studies							
I-0.7-3	4.1	1.8	13	61	95	0.54	5.4
I-0.7-6	2.1	2.8	9.5	73	130	0.63	4.7
I-0.7-6-O-250-1.0	2.1	2.5	12	76	145	0.75	10.7
I-0.7-6-O-250-1.2	1.7	3.1	10	111	176	0.79	11.1
I-0.7-6-O-250-1.4	1.5	3.3	8	124	190	0.81	11.5
Second set for batch and continuous stabilization studies							
I-0.7-7.3*	1.6	3.4	11	78	120	0.70	5.4
I-0.9-3	3.4	1.8	19	59	90	0.57	5.1
I-0.9-3-O-252-1.7	2.0	3.2	10	117	175	0.82	12.4
I-0.9-3-O-252-2.3*	1.4	4.1	8	135	211	0.92	13.0

*Fibres chosen for stabilization studies.

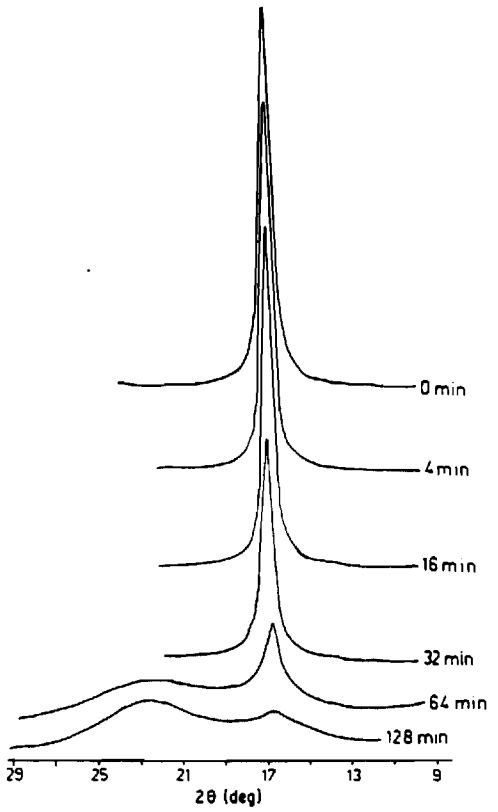

Figure 1 WAXD intensity plots of HTD precursor I fibres heated at 265° C for various durations.

252° C) and I-0.7-7.3 (draw ratio = 7.3 in hot water)*, having approximately the same total draw ratio and denier per filament but quite different morphological parameters, were selected to study the influence of orientational and lateral order in the precursor fibres on stabilization.

3.3. Progression of stabilization

3.3.1. Morphological parameters

X-ray diffraction and sonic modulus measurements were made for studying the changes in morphological parameters as a function of stabilization time. Fig. 1 shows a plot of the diffraction intensities against 2θ in a WAXD scan of HTD precursor I fibres heated under constant length conditions at 265° C for various durations. The average size and orientation of the laterally ordered phase in these fibres were estimated as a function of heating time (Figs 2 and 3). The trends are the same as observed before in 3 × and 6 × drawn fibres [5] except that the initial increase in the orientation of the ordered phase is absent in the HTD fibres. Also, the large differences in the crystal size and orientation present in the HTD and HWD fibres diminish as stabilization progresses. The absence of initial increase in orientation of the HTD fibres (Fig. 3) is due to the very high orientation and lateral order that is already present in these precursor fibres.

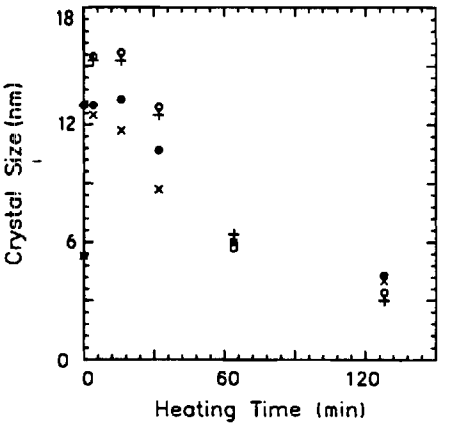

Figure 2 Crystal size of CL and FL batch stabilized fibres. (○) CL, HTD fibres, (●) CL, HWD fibres, (+) FL, HTD fibres, (×) FL, HWD fibres. Heating temperature = 265° C.

Orientation of the ordered as well as the disordered phase of the precursor fibres can be inferred from their sonic modulus. High sonic modulus of HTD fibres suggests that there is a high orientation of the ordered and disordered phases along the fibre axis direction. A continuous decrease in this orientation in HTD fibres is observed during their stabilization (Fig. 4), even when no macroscopic shrinkage is allowed. This behaviour is different from the response of the HWD fibres, where an initial increase in sonic modulus at short heating times, followed by a continuous decrease at longer times, is observed. The absence of any further increase in order in HTD fibres could be attributed again to the already high overall orientation present in these fibres. Possible relaxation of some segments in the disordered phase which are

TABLE IV Properties of precursor II fibres

Sample	Denier/ filament	Tenacity (g/denier)	Elong. (%)	Young's modulus (g/denier)	Sonic modulus (g/denier)	Orientation function, f_c	Crystal size (nm)	Density ($g cm^{-3}$)	Moisture content (%)
Boiling water drawn fibres									
II-1.2-3	2.2	2.1	11.1	78	95	0.67	7.3	1.180	2.1
II-0.7-5	2.2	3.1	11.8	90	149	0.78	7.5	1.175	2.0
II-0.7-2.5	3.9	1.8	11.4	64	105	0.61	6.5	–	–
High-temperature drawn fibres									
II-0.7-2.5-O-228-1.8	2.2	3.4	9.7	114	150	0.83	11.3	1.175	1.8
II-0.7-2.5-G-160-1.8	2.2	3.5	8.6	117	147	0.77	8.8	1.175	1.7
II-0.7-2.5-O-224-2.5	1.6	4.4	8.7	132	182	0.87	11.0	1.180	2.1
II-0.7-2.5-G-190-2.7	1.5	4.4	7.6	144	207	0.84	12.8	1.185	1.6

*Referred to as HTD and HWD fibres, respectively, in all subsequent discussions.

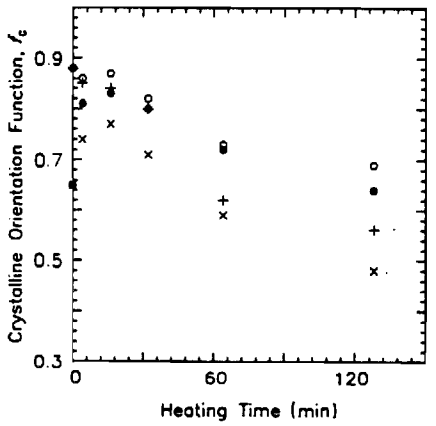

Figure 3 Crystalline orientation function, f_c, of CL and FL batch stabilized fibres. (○) CL, HTD fibres, (●) CL, HWD fibres, (+) FL, HTD fibres, (×) FL, HWD fibres. Heating temperature = 265° C.

not anchored effectively in the ordered phase may contribute to a decrease in the sonic modulus even at short heating times in these fibres. This partial relaxation of orientation in the disordered phase is also suggested by the shrinkage force experiments discussed in Section 3.3.3 (a part of the initial stress developed relaxes almost instantaneously). In HWD fibres, an increase in the sonic modulus is observed at short heating times in spite of probable partial relaxation in the less ordered phase, because of the simultaneous large increase in the crystalline orientation (Fig. 3). The decrease in sonic modulus at longer heating periods is due to the change in the intrinsic properties of the precursor fibres as a result of stabilization reactions. As expected, the free length heated fibres show a pronounced decrease in the sonic modulus in both precursor fibres (Fig. 4), due to the extensive orientational relaxation of even the bridging segments in the disordered phase between the ordered domains. In constant tension experiments, with the applied tension being the maximum that was possible without causing filament rupture, the fibres extended by almost 10 to 12%. This extension caused an increase in orientation in both HTD and HWD fibres, as reflected by the initial increase in sonic modulus (Fig. 4). The rise in sonic modulus, as expected, is more pronounced in the case of the HWD fibres.

The sonic moduli of samples from a continuous stabilization line are plotted in Fig. 5 as a function of residence time in the oven (apparent heating time). The sampling technique has been described in the experimental section. Although continuous stabilization was carried out at the same feed and take-up speeds, it does not prevent local changes in the velocities due to compensating extension and shrinkage of the fibre inside the furnace. The fibre, as soon as it reaches a temperature above its glass transition temperature (T_g), will tend to shrink provided the shrinkage can be compensated by extension in another section of the furnace. Warner *et al.* [7] have explained this phenomenon in detail. The general trends in the sonic moduli of both HWD and HTD fibres observed in continuous stabilization are similar to those in batch stabilization at constant length (Fig. 4). The slower initial increase in the sonic modulus of HWD fibres in continuous stabilization when compared to batch stabilization is due to a slower heating to 265° C in the former as opposed to the instantaneous exposure to 265° C in the latter process.

3.3.2. Calorimetry

The DSC exotherms of samples from a continuous stabilization run, representing various apparent heating periods, are shown in Fig. 6. A simultaneous decrease in the area under the exothermic peak and increase in the peak width are observed. As stabilization progresses, the nitrile groups in the precursor fibre undergo cyclization resulting in a decrease in the extent of the exotherm. A complete disappearance of the exotherm suggests completion of the cyclization reactions. Incorporation of oxygen and cyclization of nitrile groups during the stabilization of precursor fibre alters the chemical structure originally present in these fibres. This new structure formed during the intermediate stages of stabilization modifies the course of further cyclization, as indicated by the broadening of the exothermic peak.

The results from plasticized melting studies are

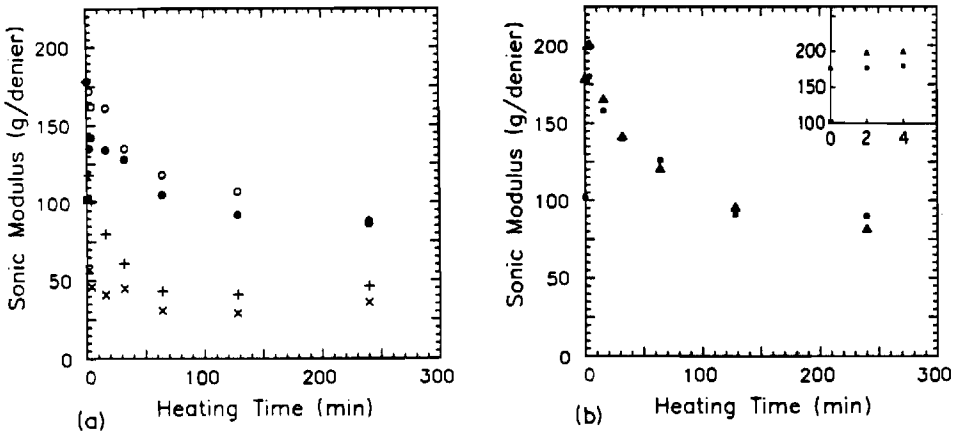

Figure 4 Sonic modulus of CL, FL and CT batch stabilized fibres. (a): (○) CL, HTD fibres, (●) CL, HWD fibres, (+) FL, HTD fibres, (×) FL, HWD fibres. (b): (■) HWD fibres, 0.1 g/denier tension; (▲) HTD fibres, 0.14 g/denier tension. (Inset: the initial response,plotted on an expanded scale.) Heating temperatures = 265° C.

TABLE V Results of plasticized melting studies

Heating time (min)	HTD fibres				HWD fibres			
	Heat of melting (cal g^{-1})	$\Delta H_m(t)/\Delta H_m(t=0)$	Heat of crystallization (cal g^{-1})	$\Delta H_c(t)/\Delta H_c(t=0)$	Heat of melting (cal g^{-1})	$\Delta H_m(t)/\Delta H_m(t=0)$	Heat of crystallization (cal g^{-1})	$\Delta H_c(t)/\Delta H_c(t=0)$
0	12.3	1.00	9.51	1.00	12.9	1.00	9.45	1.00
2	12.5	1.02	9.81	1.03	12.0	0.93	9.07	0.96
4	12.3	1.00	9.68	1.02	13.4	1.04	8.96	0.95
16	16.5	1.34	9.46	0.99	10.3	0.80	7.10	0.75
32	9.2	0.75	4.68	0.49	7.6	0.59	4.39	0.46
64	1.9	0.15	–	–	Negl.	–	Negl.	–

Temperature of heating = 265° C.

given in Table V. Depletion of the unreacted ordered phase in the later stages of the process can be seen clearly, consistent with the WAXD results reported earlier. Plasticized recrystallization results show the expected monotonic decrease in the potential of the material to crystallize with increasing time of thermal treatment. The most important aspect of these plasticized melting and recrystallization experiments is the clear observation of the characteristic enthalpy changes associated with first order transitions, establishing the presence of true crystals in the precursor fibres.

3.3.3. Shrinkage and shrinkage force

Shrinkage in acrylic fibres during their stabilization has been employed for the optimization of stabilization by previous researchers [8]. Total shrinkage during stabilization under free conditions can be divided into an almost instantaneous initial shrinkage due to the coiling-up of the oriented chains in the laterally disordered phase and a slow delayed shrinkage, also known as secondary shrinkage, which has been attributed to the chemical reaction associated with stabilization [9–11]. A plot of shrinkage against heating time, with the fibres heated at 265° C in air, is given in Fig. 7. The HTD fibres shrink instantaneously to a lower extent, 12%, compared to HWD fibres which show an instantaneous shrinkage of 17%, the difference being maintained throughout the stabilization process. The lower entropic shrinkage in HTD fibres is due to the presence of a higher fraction of the laterally ordered phase and thus a lower fraction of the oriented but laterally disordered regions which contribute to this shrinkage. The secondary shrinkage which increases with the progression of stabilization is caused by the chemical reactions associated with the stabilization. Melting of the ordered segments which takes place during the course of chemical reactions can result in continued shrinkage with the progression of stabilization. Both HWD and HTD fibres show similar rates and extents of secondary shrinkage.

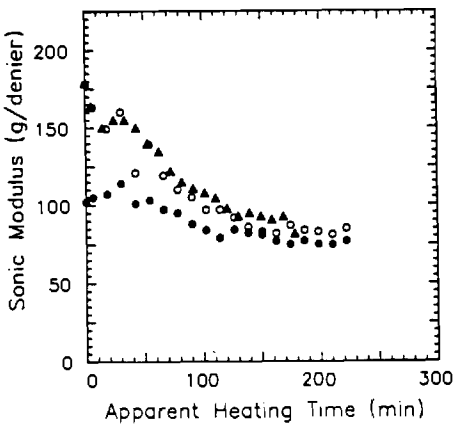

Figure 5 Change in sonic modulus during continuous stabilization at 265° C. (●) HWD fibres, 1 in. min^{-1}, (○) HTD fibres, 1 in. min^{-1}, (▲) HTD fibres, 1.25 in. min^{-1}.

When no macroscopic changes in the length of precursor fibres are allowed during heating, stress is developed due to the tendency of chains in the disordered phase to undergo entropic relaxation. This tendency of the chains to coil up is greater when their orientation is higher. Fig. 8 shows the stress or shrinkage force generated in the HTD and HWD fibres as a function of heating time. The HTD fibres have a significantly higher non-crystalline and overall orientation compared to the HWD fibres and therefore show a higher shrinkage force. Much of the initial tension decays in a relatively short period (less than 2 min) due to relaxation of some of the oriented chains in the disordered phase. The decay is slower and to a lower extent in HTD fibres compared to HWD fibres, suggesting higher connectivity between the ordered and the disordered phases. Under a macroscopically constrained state, the chains in the disordered phase of the HTD fibres cannot relax as much as the chains in HWD fibres, in spite of a larger tendency toward it.

The dependence of shrinkage force on the draw ratio is shown in Fig. 9 where the initial stresses generated in three precursor fibres having different draw ratios are plotted. An almost instantaneous and complete decay of the initial stress is observed in fibres with no high-temperature drawing, whereas fibres with high-temperature draw ratios of 1.7 and 2.3 show a larger initial stress and a slower decay, again suggesting a higher connectivity between the ordered and the disordered segments in these highly ordered fibres. The decay of initial stress is followed by a slow development of a secondary stress as a result of chemical reactions propagating to the ordered regions. As discussed earlier, these reactions are accompanid by the melting of the ordered domains which results in the development of a shrinkage force in the later stages of stabilization. Consistent with the extents of lateral order in the precursor fibres, a higher secondary stress is observed in the HTD fibres than in HWD fibres.

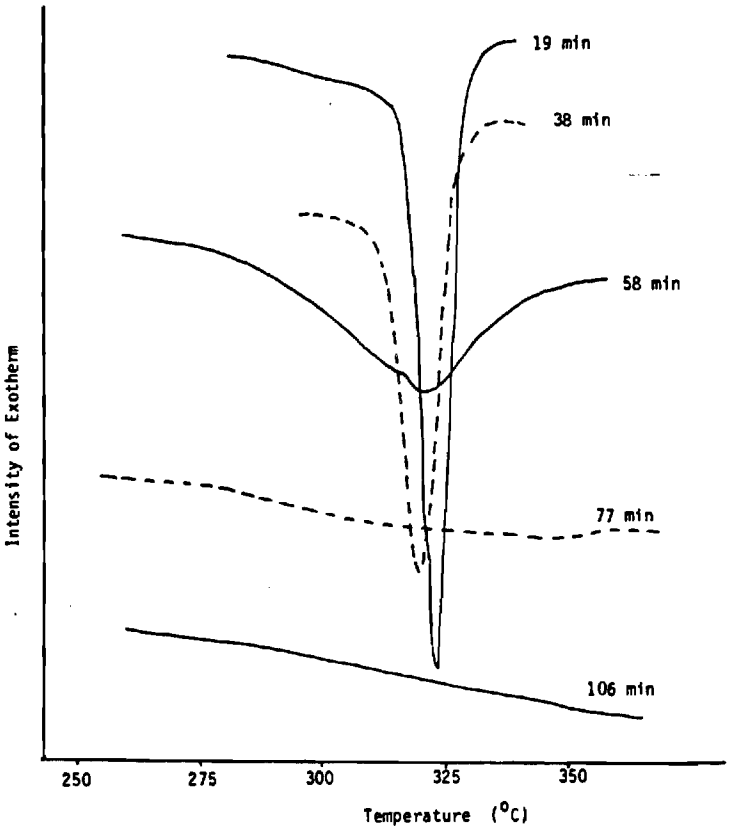

Figure 6 DSC exotherms of samples from continuous stabilization (265° C, flat profile). Various apparent heating times are shown for precursor I-0.9-3-O-252-1.7.

3.3.4. Density and oxygen pick-up

Incorporation of oxygen from the air and the denser packing of the aromatic species created during stabilization contribute to a monotonic increase in density. Both density and oxygen content have been employed in the industry as indicators of the extent of stabilization in acrylic fibres and this aspect is discussed in Part 3 [2]. The progressions of densities of the HTD and HWD precursor I fibres during batch and continuous stabilization are shown in Figs 10 and 11. Under each condition of dimensional constraint imposed during this process (FL, CL, CT or continuous), little difference is seen between the rates of change in HTD or HWD fibres. Although significant differences exist in the morphological parameters of these two precursor fibres (Table III), these differences diminish due to the rearrangements in the early stages of stabilization (Figs 2 to 5). Thus morphological contributions to the rates of solid-state reactions in stabilization, as inferred by density changes, are not likely to be revealed here. The diffusion-controlled incorporation of oxygen (Fig. 12) is also entirely consistent with the progression of density. The rate of stabilization increases with the tension (Fig. 10) in the fibres (tension in free length < in constant length < in constant tension). This, however, can not be attributed unequivocally to the higher orientations obtained at the higher tensions. The filament diameter also decreases with increase in the tension, thus raising the overall rate of diffusion-controlled reactions.

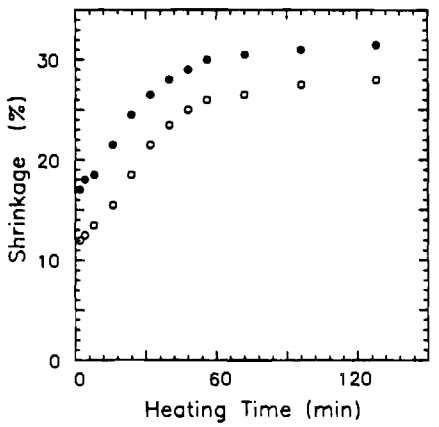

Figure 7 Shrinkage in FL batch stabilized fibres. (O) HTD fibres, (●) HWD fibres. Temperature = 265° C.

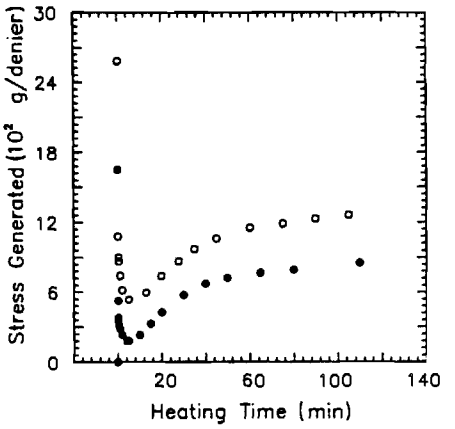

Figure 8 Shrinkage stress generated during CL batch stabilization. (O) HTD fibres, (●) HWD fibres. Temperature = 265° C.

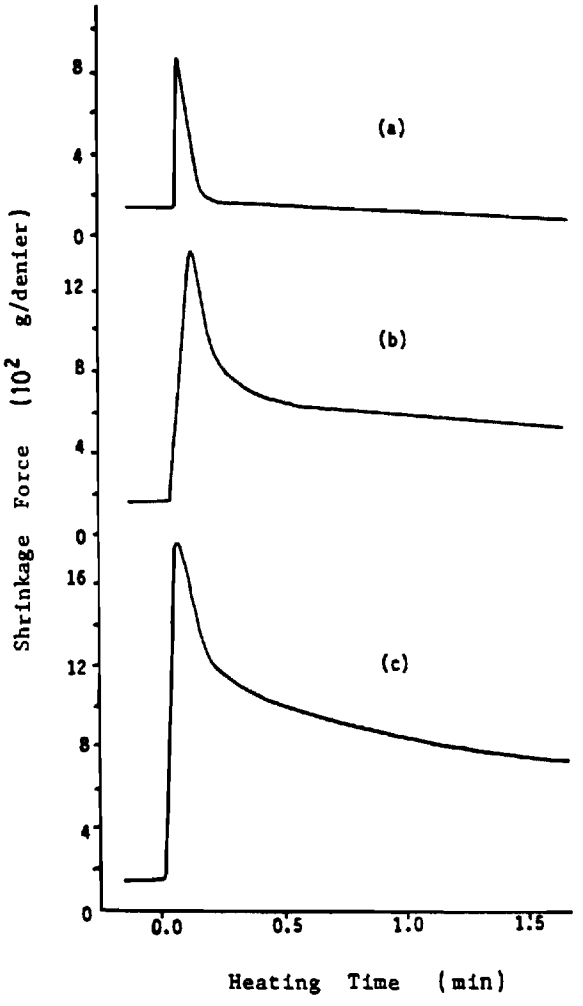

Figure 9 Shrinkage stress generation and decay in precursor I fibres. (a) I-0.9-3, (b) I-0.9-3-O-252-1.7, (c) I-0.9-3-O-252-2.3.

3.3.5. Comparison of precursors I and II

The progression of changes observed in batch and continuous stabilization of precursor II fibres, containing itaconic acid comonomer which can initiate the stabilization reactions, has the same general character as those reported here for precursor I fibres. The quantitative differences observed are due to the higher rate of stabilization in precursor II fibres. For example, the density changes (Fig. 13) for two precursor fibres (I-0.7-7.3 and II-0.7-5) show a significantly higher rate of increase in precursor II in spite of the higher denier of these filaments (2.2 denier) when compared with the denier of the precursor I filaments (1.6 denier). When these fibres are heated at constant length, the delayed shrinkage force, which indicates the propagation of stabilization reactions, also rises much faster in precursor II fibres, suggesting a higher rate of stabilization in these fibres (Fig. 14). Additional results from stabilization of this precursor are reported in Part 3 [2].

3.4. Morphology of acrylic precursor fibres

The following observations clearly show that the basic morphological unit in oriented acrylic fibres consists of a repeating sequence of oriented, laterally ordered and oriented but laterally disordered domains with a significant portion of the chain segments in the latter phase bridging the ordered domains. This model has been proposed earlier by Warner *et al.* [6]:

1. clear WAXD evidence for the presence of laterally ordered domains;
2. calorimetric evidence for the "melting of crystals" when the melting temperature is reduced through plasticization to temperatures below those of degradation reactions;
3. spontaneous shrinkage at high temperatures, *without any loss in the extent or the orientation of the ordered domains*, and the large drop in sonic modulus which accompanies this shrinkage process indicating that the ordered and disordered domains are arranged in a connected sequence along the fibre direction;
4. when thermal treatment of oriented acrylic fibres is carried out without allowance for shrinkage, the change in sonic modulus depends on the change in the extent of lateral order in the fibres. An increase in sonic modulus accompanies a significant initial increase in the extent and orientation of the laterally ordered fraction but a measurable decrease is seen when only a slight increase in lateral order occurs in those fibres which possess a high degree of initial order. These responses indicate the presence of *celia* and loose loops in the laterally disordered fraction.

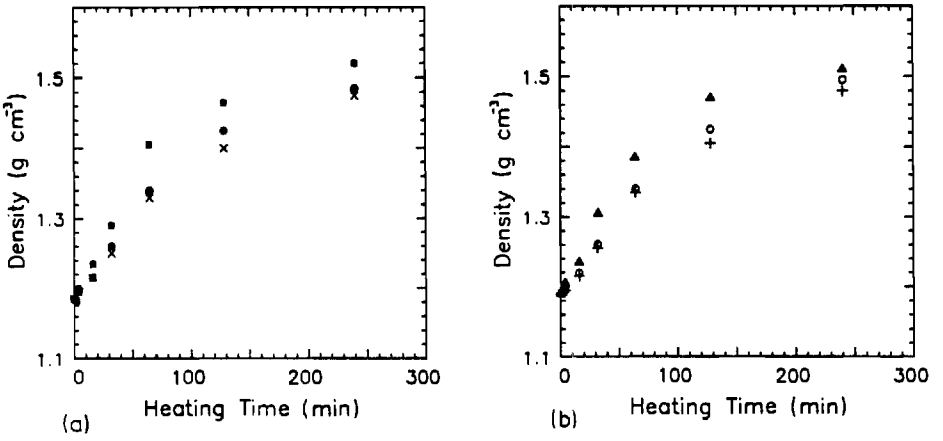

Figure 10 Effect of constraints on the density of batch stabilized HWD and HTD fibres. (a): HWD fibres, (×) FL, (●) CL, (■) 0.1 g/denier tension. (b): HTD fibres, (+) FL, (○) CL, (▲) 0.14 g/denier tension. Temperatures = 265° C.

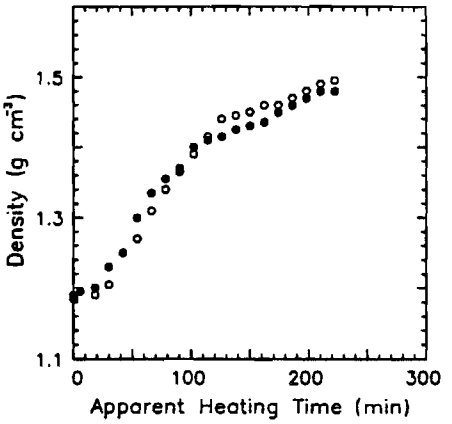

Figure 11 Change in density during continuous stabilization at 265° C. (●) HWD fibres, (○) HTD fibres.

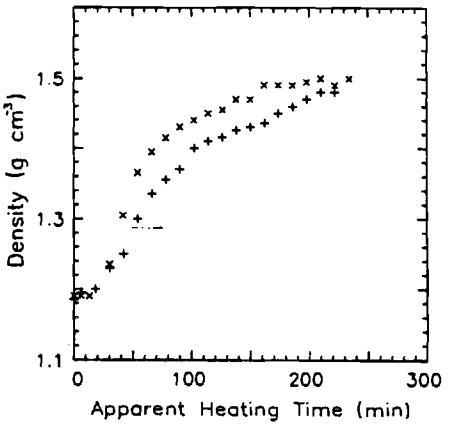

Figure 13 Change in density of precursor I and II fibres during continuous stabilization at 265° C. (+) I-0.7-7.3, (×) II-0.7-5.

The initial decrease in sonic modulus during "constant length" heating of HTD fibres is still much less than the drastic drop which accompanies "free" thermal treatment, indicating that a majority of the segments in the laterally disordered fraction act as tie chains between the laterally ordered domains;

5. acrylic fibres with demonstrably different extents of order show little difference in density, indicating that the packing densities in the laterally ordered crystals and the laterally disordered "noncrystalline" regions are essentially the same. Thus, the meridional reflection in SAXS, characteristic of the proposed two-phase oriented structure, is absent in these fibres (Fig. 15a). After heating the precursor fibres for 16 min in air, a meridional spot is observed in SAXS flat plate photographs, indicating the presence of a long period (Fig. 15b). Appearance of this meridional reflection with the onset of stabilization reactions has been presumed to be the result of their preferential occurrence in one of the two phases, thus providing indirect evidence for the proposed morphology. Confirmation of the existence of a long period in the precursor fibres is obtained by conducting SAXS studies subsequent to impregnation of these fibres with copper ions (Fig. 15c) by refluxing them in a solution of CuCl in HCl for 30 min. The electron density of the disordered phase is increased by the dispersion of copper salt in this phase, resulting in the appearance of the meridional reflection in SAXS studies.

4. Conclusions

A number of significant results have been obtained through the research on oxidative stabilization of acrylic precursors for carbon fibres reported here. These results and the inferences from them regarding needed additional research are summarized below.

1. Through a combination of evidence from thermomechanical response, thermal stress development, calorimetry, wide-angle and small-angle X-ray scattering, and sonic modulus studies of fibres through the course of an oxidative stabilization process, and small-angle X-ray scattering studies of precursor fibres impregnated with copper, the basic morphological unit in oriented acrylic fibres has been shown to have laterally ordered domains connected along the fibre axis direction through domains in which such order is absent. Our observations confirm this important aspect of the morphological model proposed by Warner *et al.* [6]. The other major aspect of their model, fibrillar geometry of this morphological unit, is being examined through small- and wide-angle X-ray

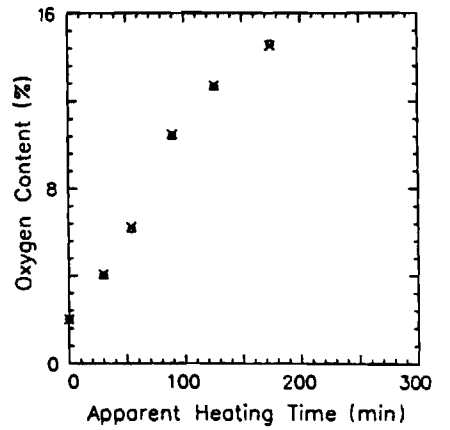

Figure 12 Oxygen incorporation during continuous stabilization of precursor I fibres at 265° C. (×) HWD fibres, (○) HTD fibres.

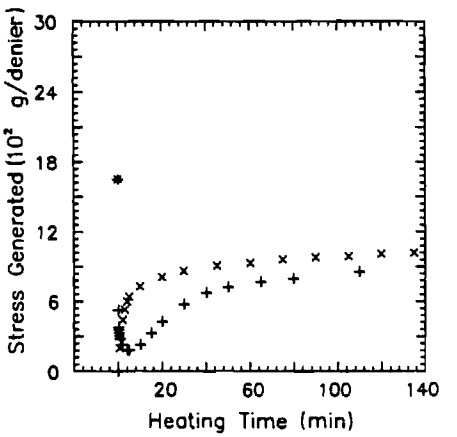

Figure 14 Shrinkage stress developed in precursor I and II fibres 265° C. (+) I-0.7-7.3, (×) II-0.7-5.

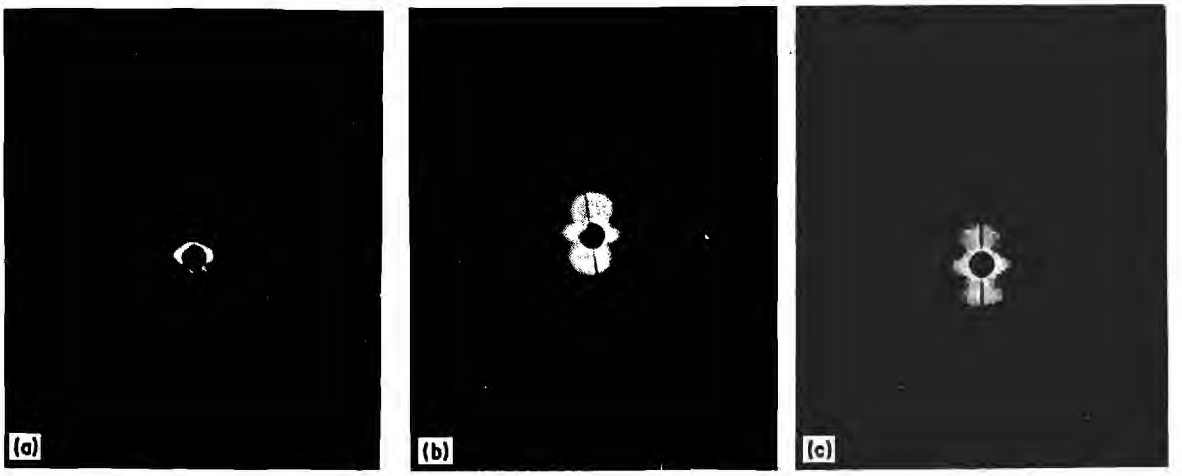

Figure 15 Small-angle flat plate photographs: (a) precursor, (b) 16 min CL stabilized, (c) copper impregnated.

scattering studies of oriented acrylic fibres after swelling them in DMF.

2. The ordered fraction and the overall orientational order in acrylic precursor fibres can be increased markedly through a process which involves plastic stretching at high temperatures of a fibre which has been only partially stretched in a conventional wet spinning process.

3. When acrylic precursor fibres are heated to the temperatures involved in the oxidative stabilization step of the process for carbon fibre formation, the physical changes that precede the onset of a significant level of stabilization reactions depend on the externally imposed dimensional constraints. The present study shows clearly that whether dimensional constraints are imposed or not, a significant tendency for increase in perfection and the extent of the laterally ordered domains occurs in the early stages of this step. The extent of this increase diminishes with increasing order initially present in these fibres. The constraints imposed on the length have a pronounced effect on the relaxation of orientation in the laterally disordered fraction. The decrease in orientation in this phase is dramatic when no constraint against shrinkage is imposed on the fibres. The effect of the degree of orientational relaxation permitted at this stage, which can be controlled by the application of stress, on the ultimate properties of carbon fibres produced from these fibres remains to be studied.

4. The critical stress for failure and the stresses generated at any level of imposed deformation (or, conversely, the deformation at any level of imposed stress) would change throughout the course of stabilization. Since the temperature–tension/deformation–time profile that can be applied during stabilization is limited by the continuously changing critical stress, it is necessary to have the provision to control these through a multistage stabilization process so that the influence of these factors on the structure of the carbon fibres can be established. There is a clear need for separating the stabilization process into at least three independently controlled stages, i.e. an initial zone of rapid morphological rearrangements, a second zone of reactions predominantly in the disordered fraction, and the subsequent zone of reactions propagating into the ordered fraction of the fibres. A multistage stabilization line would also allow the use of different environments in the different zones. In order to realize the maximum potential of a given precursor fibre, it is important to "tailor" the conditions of oxidative stabilization to suit the rates of such reactions and the deformation characteristics of the fibres during this stage. Conducting precisely controlled experiments at this stage will help in establishing the important link between the structure of the precursor fibres and the structure and properties of the carbon fibres that can be obtained from them.

5. When the progression of stabilization is monitored with measurements such as density and oxygen pick-up, little difference is seen in the rates of stabilization with the orientation or the lateral order present initially in the fibres. This appears to be the result of the nature of morphological rearrangements during the early stages of the process, especially the increase in the extent of the ordered fraction to approximately the same levels in these fibres.

6. Among the techniques examined in the present study for the characterization of morphological parameters of the fibres, wide-angle X-ray diffraction (WAXD), sonic modulus, differential scanning calorimetry (DSC), birefringence and infrared dichroic ratio, the combination of sonic modulus, WAXD and DSC was found best suited for obtaining at least semi-quantitative measures of the degree of lateral order and orientation in the precursor fibres and the changes occurring in the early stages of stabilization. Birefringence and infrared dichroic ratio were discarded because of apparently similar polarizabilities parallel and perpendicular to the chains at the precursor stage which render them unsuitable for distinguishing differences in orientational order. The difference in intrinsic polarizabilities parallel and perpendicular to the chain direction is known to become significant when these fibres are subjected to the conditions of a stabilization process. Infrared dichroism and birefringence may prove suitable for inferring the orientational order in stabilized fibres.

7. During the early stages of a stabilization process,

at least partial relaxation of orientation occurs in the occurs in the fraction in which lateral order is absent, even when a macroscopic constraint against shrinkage is present. These disorienting segments to which macroscopic constraints are not transmitted could be one of the sources of sites of low orientational order and structural defects in carbon fibres. The degree to which it can be eliminated through increase in order in the precursor fibres and through a significant increase in the molecular weight of the precursor polymer remains to be explored.

8. Aspects related to the extent to which the stabilization reactions need to be carried out before the fibres would become suitable for carbonization are discussed in Part 3 [2].

Acknowledgements

We wish to thank Dr L. H. Peebles for many useful suggestions during the course of this work and in the inferences drawn from experimental data. Discussions with Dr W. C. Tincher and Dr F. L. Cook are gratefully acknowledged. This study was supported by the United States Office of Naval Research.

References

1. M. K. JAIN and A. S. ABHIRAMAN, *J. Mater. Sci.* 22 (1987) 278.
2. M. K. JAIN, M. BALASUBRAMANIAN and A. S. ABHIRAMAN, submitted for publication.
3. M. K. JAIN, PhD thesis, Georgia Institute of Technology, Atlanta, Georgia (1985).
4. L. E. ALEXANDER, "X-ray Diffraction Methods in Polymer Science," (Wiley-Interscience, New York, 1969).
5. M. K. JAIN and A. S. ABHIRAMAN, *J. Mater. Sci.* 18 (1983) 179.
6. S. B. WARNER, D. R. UHLMANN and L. H. PEEBLES Jr, *ibid.* 14 (1979) 1893.
7. S. B. WARNER, L. H. PEEBLES Jr and D. R. UHLMANN, *ibid.* 14 (1975) 565.
8. O. P. BAHL and L. M. MANOCHA, *Fibre Sci. Technol.* 9 (1976) 77.
9. D. J. MULLER, E. FITZER and A. K. FIEDLER, Proceedings of the International Conference on Carbon Fibres, their composites and applications, (Plastics Institute, London 1971) paper 2.
10. E. FITZER and D. J. MULLER, *Die Makromol. Chemie* 144 (1971) 117.
11. E. FITZER and M. HEYN, *Chem. Ind.* 16 (1976) 663.

Received 8 October 1985
and accepted 22 May 1986

JOURNAL OF MATERIALS SCIENCE 22 (1987) 3864–3872

Conversion of acrylonitrile-based precursors to carbon fibres

Part 3 *Thermooxidative stabilization and continuous, low temperature carbonization*

M. BALASUBRAMANIAN, M. K. JAIN, S. K. BHATTACHARYA, A. S. ABHIRAMAN*
School of Chemical Engineering, Georgia Institute of Technology, Atlanta, Georgia 30332, USA

The effects of stabilization conditions on the formation of a consolidated carbon fibre structure from two acrylonitrile-based precursor fibres, one containing itaconic acid as comonomer and the other a commercial precursor, have been studied. The progression of changes in elemental composition and properties such as sonic modulus, electrical resistance and density in a continuous, low temperature (1200° C) carbonization process are reported for the first time. A criterion based on attaining a composition dependent critical density in stabilization is proposed for avoiding the formation of a hollow core in carbon fibres processed continuously at reasonably rapid rates. Aspects related to the development of open and closed micropores in the carbon fibre structure and the possible mechanisms for the formation of a hollow core in carbonization are also discussed.

1. Introduction

Manufacture of carbon fibres from acrylonitrile-based precursor copolymers involves

(a) formation of oriented fibres, usually through solution spinning and a combination of drawing in the gel state and plastic deformation of dried fibre,

(b) low temperature (200–350° C) thermooxidative stabilization of the oriented precursor fibre to yield a structure that can maintain its cohesion during subsequent carbonization,

(c) carbonizing heat treatment (800–1600° C) in an inert atmosphere to drive off non-carbon elements, and

(d) an optional high temperature (> 2000° C) treatment to improve the mechanical properties, especially the stiffness of the fibres.

The nature of the fibres at every stage in the formation of carbon fibres depends on the conditions of processing at that stage as well as the chemical composition and the geometrical and morphological features of the material produced at the previous stage. As described in our review of the literature on the production of carbon fibres [1], numerous studies of isolated aspects have yielded extensive empirical knowledge but only a partial understanding of this complex process. We have undertaken a comprehensive experimental study in our laboratories to help expand our knowledge of the material and process contributions to the properties of the ultimate carbon fibres. The results from experiments in precursor fibre formation and batch stabilization, and from an extensive study of the rearrangements in continuous thermooxidative stabilization have been reported earlier [2, 3]. We report here additional results from continuous stabilization and initial experiments on the evolution of properties in low temperature (1200° C) continuous carbonization. The progression of carbonization was monitored through measurements of density, linear density, elemental composition, electrical resistance and sonic modulus.

2. Experimental details

2.1. Precursor fibres

Detailed descriptions of the experimental procedures are given in [3]. Two acrylic precursor fibres, II and III, were used in this study. Precursor III is a commercial precursor for carbon fibres. Precursor II fibres were produced in our laboratories from a 17.5% (w/w) solution of a copolymer of acrylonitrile (AN) and itaconic acid (IA) in the weight ratio of 97/3 (average molecular weight = 131 000 g mol^{-1}, estimated from intrinsic viscosity). The spinning conditions for precursor II, established to produced fibres of good quality, are given in Table I. The jet stretch and the draw ratio were changed to obtain fibres having different orientations. High-temperature drawing of some of the precursor fibres was performed in order to produce fibres with high orientation and morphological parameters different from those produced by drawing in boiling water. Two types of post-spinning high temperature drawing processes, i.e. over a hot godet and through a hot oven, were performed on the hot water (partially) drawn fibres. In the former type of drawing, precursor fibres were drawn directly from the heated feed-godet, whereas

*Author to whom all correspondence should be addressed.

0022–2461/87 $03.00 + .12

TABLE I Conditions of formation of precursor II fibres

	Precursor II		
Polymer solution:			
Solution concentration, % (w/w)	17.5		
Solution viscosity, poise	140		
Coagulation bath			
Coagulation bath composition, % DMF	60		
Coagulation bath temp., °C	14		
Drawing conditions:			
Jet Stretch	0.7	1.2	0.7
Draw Ratio, in boiling water	2.5	3	5
Denier/filament (dpf)	3.9	2.2	2.2

in the latter type the fibres were first annealed at a relatively low temperature (115 to 130° C) on the feed-godet and then drawn through an oven. Details of the drawing conditions are given in Table II. The first letter in the sample identification code refers to the precursor type. The second and the third terms represent the jet-stretch and the draw-ratio (in boiling water), respectively. The last three terms signify the post-spinning, high temperature plastic drawing conditions, such as type of heater (oven or godet), temperature and draw-ratio, respectively. The temperatures employed in the hot-oven drawing were the maximum possible for a smooth drawing operation without filament breakages. The mechanical properties and morphological parameters of the precursor fibres are given in Table III. It can be seen clearly that a broad range of precursor fibre properties has been achieved through the different drawing processes.

2.2. Continuous stabilization and carbonization

The fibres were stabilized in air in a continuous process with an 18-ft long linear, tubular oven. The furnace was divided into three, 6-ft zones, with each zone controlled by individual temperature controllers. Various ascending temperature profiles (Table III) were used in this process. Precursor II was processed at an input and output linear velocity of 1 inch min^{-1}. When processed at constant input and output velocities, precursor III fibres developed excessive shrinkage forces, leading to breakage of filaments and so these were run with the minimum net shrinkage (9%)

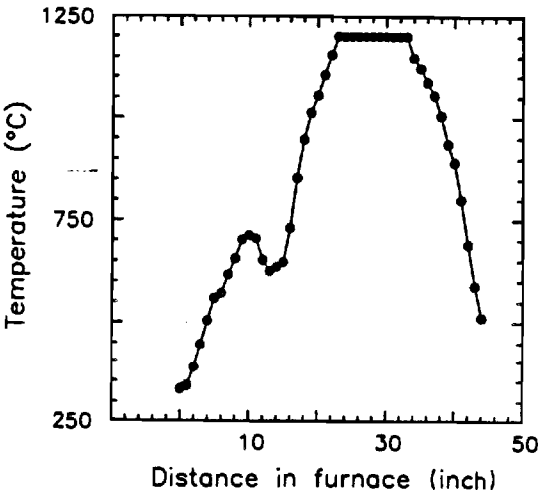

Figure 1 Temperature profile in carbonization.

required for good processing. The finer filaments in this precursor required lower residence times for stabilization when compared with Precursor II fibres and so these were processed at input and output velocities of 2.75 and 2.5 inch min^{-1}, respectively.

Carbonization of the stabilized fibres was carried out by passing them through a Lindberg furnace at 1200° C. To avoid thermal shock and allow for a gradual increase in the temperature of the filaments, two heaters were installed at the entrance to the furnace which provided two 6-inch precarbonization zones of 500 and 700° C. The temperature profile obtained in this set-up is shown in Fig. 1. The dip in the temperature profile is caused by the separation between the second preheater and the heater in the Lindberg furnace. Nitrogen was passed through both ends of the furnace to maintain an inert atmosphere.

Samples for studies of the progression of carbonization in a steady state process were obtained by cutting the fibre bundle at the delivery end and rapidly winding it on a spool at the feed end.

2.3. Properties of fibres

Measurement of velocity of sonic pulse propagation through the fibre samples was made with the sonic modulus tester PPM-5 with a refractory mount,

TABLE II Precursor II drawing conditions

Sample	Draw-ratio			Drawing godet/oven temp. (°C)	Annealing godet temp. (°C)	Denier/ filament
	B.W.*	H.T.†	Total			
II-1.2-3	3.0	–	3.0	– –	–	2.3
II-0.7-5	5.0	–	5.0	– –	–	2.2
II-0.7-2.5-O-228-1.8	2.5	1.8	4.5	228, oven	115	2.2
II-0.7-2.5-G-160-1.8	2.5	1.8	4.5	160, godet	160	2.2
II-0.7-2.5-O-224-2.5	2.5	2.5	6.2	224, oven	118	1.6
II-0.7-2.5-G-190-2.7	2.5	2.7	6.7	190, godet§	190	1.5

*Draw-ratio in boiling water.

†High-temperature draw-ratio.

§The drawn fibres were yellowish due to partial degradation/stabilization.

Sample notation: Precursor type-jet stretch-hot water draw ratio-oven/godet drawing-drawing temperature-draw ratio. e.g., II-0.7-2.5-O-228-1.8 refers to a sample with precursor II, jet stretch = 0.7, hot water draw ratio = 2.5, drawing through the oven at 228° C with draw ratio of 1.8.

TABLE III Mechanical properties and morphological parameters of precursor fibres.

Sample	Denier/ filament	Tenacity ($g\,denier^{-1}$)	Elong. (%)	Young's modulus ($g\,denier^{-1}$)	Sonic modulus ($g\,denier^{-1}$)	Orientn. function f_c	Crystal size (nm)
Boiling water drawn fibres							
II-1.2-3	2.2	2.1	11.1	78	95	0.67	7.3
II-0.7-5	2.2	3.1	11.8	90	149	0.78	7.5
II-0.7-2.5	3.9	1.8	11.4	64	105	0.61	6.5
High temperature drawn fibres							
II-0.7-2.5-O-228-1.8	2.2	3.4	9.7	114	150	0.83	11.3
II-0.7-2.5-G-160-1.8	2.2	3.5	8.6	117	147	0.77	8.8
II-0.7-2.5-O-224-2.5	1.6	4.4	8.7	132	182	0.87	11.0
II-0.7-2.5-G-190-2.7	1.5	4.4	7.6	144	207	0.84	12.8
Precursor III	0.9	5.3	8.8	127	143	0.87	

Sample notation: Precursor fibre-jet stretch-hot water draw ratio-oven/godet drawing-high temperature draw temperature-high temperature draw ratio.

(H. M. Morgan Co.). The measurement on precursor and stabilized fibres using the scanner mount is described elsewhere [3, 4]. The measurements corresponding to changes in sonic modulus with position along the carbonization line were difficult because of the drastic increase in the modulus of the fibres over a short distance in the carbonization process. The sonic modulus increases 10-fold over a distance of 15 to 20 inches. For this measurement on the filament bundle removed from the carbonization line, the transmitter was moved in 3-inch steps and the time for propagation was measured, starting with the stabilized length over lengths of 1, (1 + 3), (1 + 6) inches, etc. The average sonic velocity of each 3-inch section was obtained from the difference between the propagation times for the corresponding two successive steps.

The densities of stabilized or carbonized fibres were measured by the flotation technique. Solutions of various densities were made for this purpose by mixing the required quantities of carbon tetrachloride ($1.585\,g\,cm^{-3}$) with either toluene ($0.866\,g\,cm^{-3}$) or tetrabromoethane ($2.964\,g\,cm^{-3}$), depending on the density range required.

Moisture contents of fibres were obtained from their dried and conditioned weights. A 2-m length of fibre bundle was weighed accurately after conditioning for 24 h at standard temperature (20° C) and humidity (65% r.h.) conditions. The sample was then dried in an air circulated oven at 110° C for 8 h. The dried sample was allowed to cool in a dessicator and weighed again.

Mechanical properties of the carbon fibres were tested as a bundle after impregnation with – and curing – an epoxy resin system. These measurements were carried out with an Instron (model 1130) at an elongation rate of $0.2\,inch\,min^{-1}$ and a 12-inch gauge length.

A mini SEM by International Scientific Instruments was used to examine the surface and cross-section of the carbon fibres after coating with a thin layer of gold.

Electrical resistance measurements on the carbon fibre bundles, and on the filament bundles removed from the carbonization line, were made using two instruments, HP3456A Digital Multimeter and HP4329A High Resistance Meter, to cover the entire range of resistances of the stabilized and carbonized fibres. The fibre sample was enclosed inside a shielded metal box. The contact resistance at the point of contact between the measuring probe and the fibre bundle was minimized with silver paint.

3. Results and discussion

3.1. A criterion for sufficient stabilization

Table IV lists the various temperature profiles employed in the stabilization process for different precursor fibres. The stabilized fibres were characterized by measuring the density and moisture content which are also listed in Table IV. The densities of precursor fibres increase significantly during stabilization due to the structural rearrangements associated with stabilization reactions and the incorporation of oxygen. The stabilized fibre densities range from 1.455 to $1.535\,g\,cm^{-3}$ depending on the precursor draw ratio and the temperature profile employed for its stabilization. As expected, the densities obtained for a given precursor were higher when a higher temperature profile was employed. The fibres which were drawn to a combined draw ratio of 6.7 (II-0.7-2.5-G-190-2.7) had turned yellowish during the drawing process and show high density values ($1.52\,g\,cm^{-3}$ and higher) upon stabilization even when low temperature profiles were employed, suggesting a high rate of stabilization in these fibres. Moisture content of stabilized fibres do not show any specific trends with either the draw ratio or the temperature profile. The majority of values, however, fall in the narrow range of 9 to 10%.

One of the consequences of insufficient stabilization in a diffusion controlled stabilization process is the development of a hole in the centre of such fibres during carbonization. The holes form as a result of the incompletely stabilized core of the precursor fibres being burned off during carbonization. All the stabilized fibres listed in Table IV were carbonized with a residence time of 1 min at the maximum temperature of 1200° C and their cross-sections were examined under a scanning electron microscope. Whether a hollow core is observed to be present or not in these carbon fibres is also specified in Table IV. It appears that the stabilization of precursor II fibres is indeed a diffusion controlled process under the conditions employed for stabilization. With increasing

TABLE IV Properties of stabilized precursor II fibres

Precursor	Stabilization temperatures (T_1-T_2-T_3)*	Denier/ filament	Density ($g cm^{-3}$)	Moisture (%)	Hollow core in carbon fibres
II-1.2-3		2.25	1.180	2.0	–
	225-250-275	2.42	1.455	9.3	Yes
	250-275-275	2.39	1.475	9.3	Yes
	250-275-300	2.38	1.495	9.6	Yes
	250-275-325	2.25	1.515	9.3	Yes
	275-300-325	2.29	1.525	10.6	No
II-0.7-5		2.16	1.175	2.0	–
	250-275-275	2.34	1.515	9.2	Yes
	250-275-300	2.29	1.525	8.9	No
	250-275-325	2.25	1.535	9.7	No
II-0.7-2.5		3.86	1.180	1.9	–
II-0.7-2.5-O-228-1.8		2.22	1.175	1.8	–
	250-275-275	2.23	1.480	8.8	Yes
	250-275-300	2.19	1.495	8.9	Yes
	275-300-325	2.24	1.515	9.4	Rare
	275-300-350	2.24	1.530	9.2	No
II-0.7-2.5-G-160-1.8		2.17	1.175	1.7	–
	250-275-275	2.14	1.475	8.7	Yes
	250-300-350	2.00	1.510	9.5	Yes
	275-300-350	1.93	1.535	9.8	No
II-0.7-O-224-2.5		1.61	1.180	2.1	–
	225-250-275	1.70	1.475	8.5	Yes
	250-275-275	1.63	1.500	9.0	Yes
	250-275-300	1.66	1.515	9.6	Rare
	250-275-325	1.63	1.535	9.8	No
II-0.7-2.5-G-190-2.7		1.55	1.185	1.6	–
	250-275-275	1.62	1.525	9.4	No
	250-275-300	1.57	1.535	9.5	No

* T_1-T_2-T_3 refer to the temperatures in zones 1, 2 and 3, respectively, in the stabilization unit.

stabilization temperatures, the rate of diffusion increases, causing insufficient stabilization of the material closer to the centre of the fibre. An important observation from the data in Table IV is that when the stabilized fibres possessed a density of $1.52 g cm^{-3}$ or higher, the carbonized fibres did not show holes due to core blow out, irrespective of the precursor fibre forming conditions and the temperature profile employed in stabilization. The fact that narrow density ranges are required for optimum stabilization has been disclosed in the patent literature [5]. It should be mentioned here that under conditions of carbonization different from those mentioned above, holes in the core of carbonized fibres can result even with apparently well stabilized fibres. This aspect is discussed further in the following sections.

3.2. Progression of carbonization

Progression of carbonization using stabilized precursor II fibres (stabilized under conditions that would prevent core blow out) was followed with density, [H]/[C] and [N]/[C] ratios, electrical resistance and sonic modulus measurements. The scatter in the sonic modulus values in the high modulus range (Fig. 2) is the result of experimental limitations. As mentioned earlier, the sonic modulus values were obtained from discrete measurements of pulse propagation times. At the high modulus end, the time taken by the sonic pulse to travel three inches is only 6 to 8 μsec, and significant errors can be incurred in reading this value from the output on a chart. When the plots in Fig. 2 are compared with the temperature profile in the carbonization furnace (Fig. 1), a sharp increase in sonic modulus during heating from 700 to 1200° C can be observed. Once the fibre temperature reaches 1200° C, a much slower asymptotic increase in sonic modulus occurs with time at this temperature. The sonic moduli of the carbon fibres after 1200° C carbonization are higher with precursor fibres of higher draw ratios. Also, the carbon fibres from the high temperature drawn fibres show an increase to a higher sonic modulus compared to those from boiling water drawn fibres. The development of modulus is determined by the degree of graphitic order and the orientational order in the basal planes achieved during carbonization. The rate and the extent to which this ordering process occurs should increase with initial order in the precursor fibres.

The results from elemental analysis on samples removed from the carbonization furnace are plotted in Fig. 3. The [H]/[C] and the [N]/[C] ratios also change sharply during heating between the temperatures 700 and 1200° C, showing that both aromatization and basal plane formation occur rapidly in this temperature range. The requirement that a certain degree of aromatization has to precede the formation of basal planes is reflected clearly in the more rapid change in the [H]/[C] ratio in the early stages when compared with the [N]/[C] ratio. The progression of changes in electrical resistance through carbonization follows the

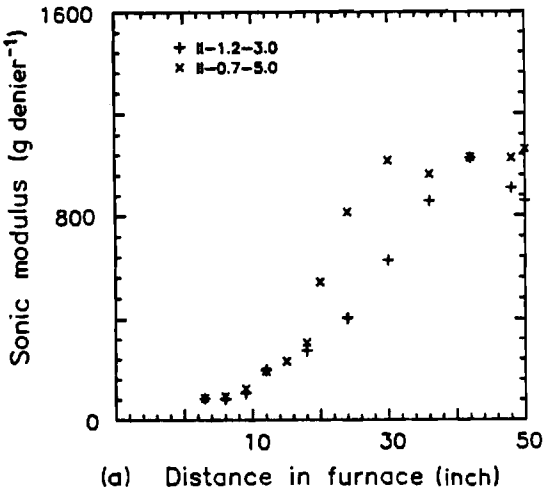

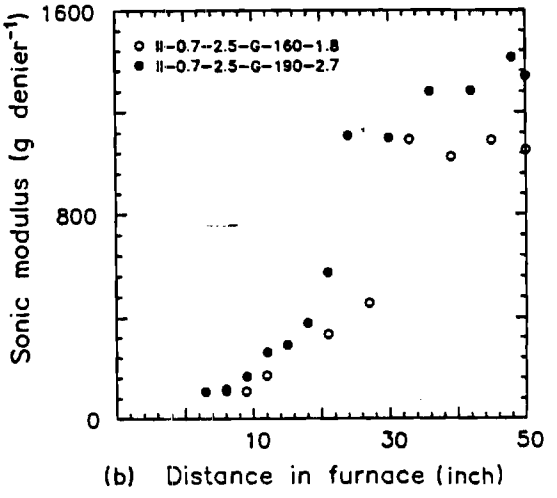

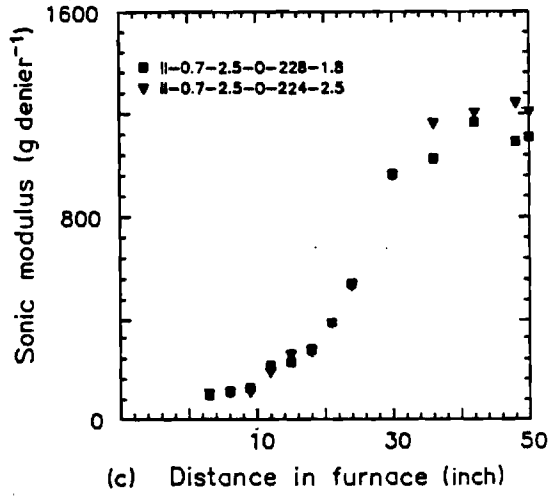

Figure 2 Change in sonic modulus during carbonization of precursor II. The fibres are drawn in (a) hot water; (b) hot water and over a hot godet; (c) hot water and through a hot oven. (The conditions of formation of the precursor fibres are given in the sample designations.)

same trend of rapid change in the 700 to 1200° C zone (Fig. 4). The resistance falls from about $10^{14}\,\Omega\,cm^{-1}$ to less than $10\,\Omega\,cm^{-1}$ when the temperature is raised to its maximum of 1200° C, after which it remains constant upon continued heating at this temperature.

The progression of density changes is plotted as a function of distance in the furnace in Fig. 5. Density increases very rapidly during the 700 to 1200° C heating, suggesting significant rearrangements leading to consolidation of structure in the fibres, but it is followed by a sharp drop before levelling off upon continued heating at 1200° C. This decrease in the measured density of the carbonized fibres is quite significant and is observed in all fibres. A plot of densities of three samples from carbonization, using II-0.7-5 fibres stabilized at 250–275–300° C, shows that the trend is very reproducible (Fig. 5d). The reason for this drop in apparent density is not very clear at this point and is being explored further. A reason for this drop in apparent density could be the conversion of open pores to closed pores, i.e. some of the pores which are initially accessible to the solvents employed for the density measurement become inaccessible, resulting in a decrease in the measured density. This suggests that consolidation of the structure occurs around the pores during the high temperature

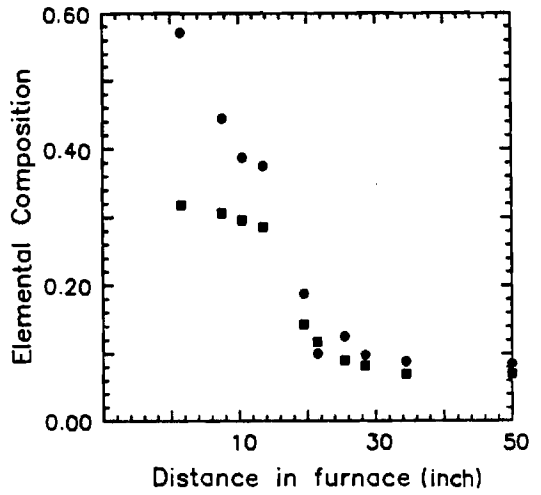

Figure 3 Change in elemental composition during carbonization of II-0.7-2.5-G-190-2.7 fibre (●) [H]/[C] ratio, (■) [N]/[C] ratio.

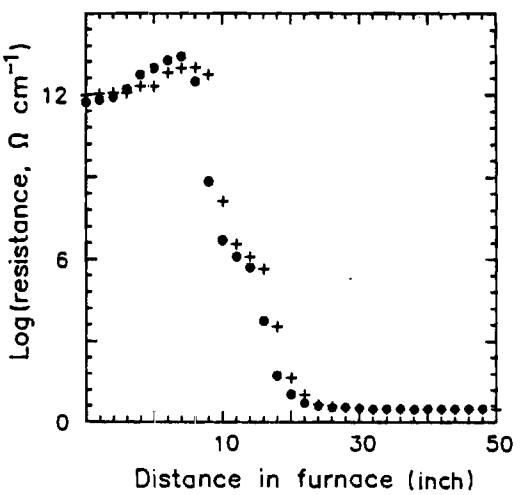

Figure 4 Change in electrical resistance during carbonization of precursor II. (+) II-0.7-5. (●) II-0.7-2.5-G-190-2.7.

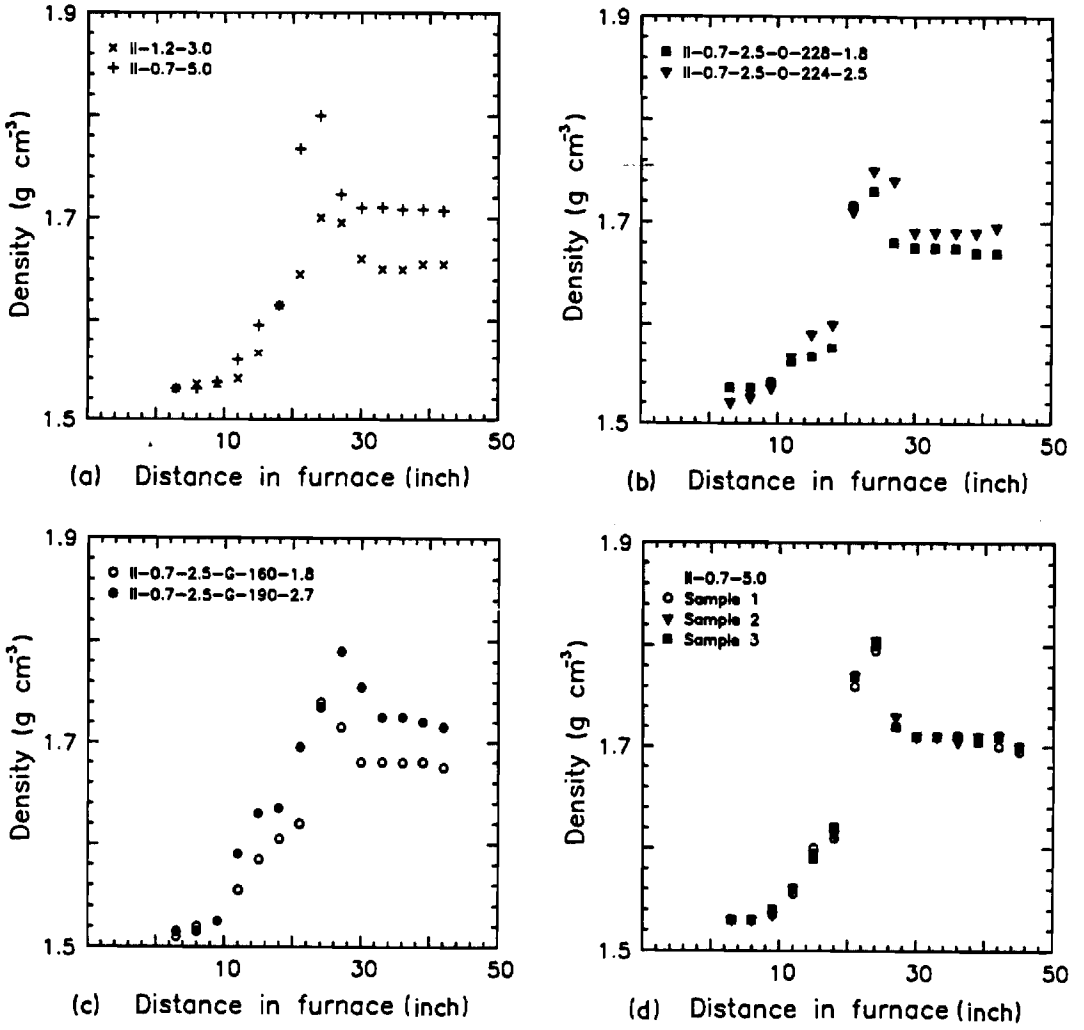

Figure 5 Change in density during carbonization of precursor II. (a) and (d) drawn in hot water; (b) drawn in hot water and hot oven; (c) drawn in hot water and hot godet. (The conditions of formation of the precursor fibres are given in the sample designations, d)

annealing in the latter stages. A similar explanation has been offered earlier by Gibson [6] for the decrease in density observed for carbon fibres produced at increasing temperatures in the range of 1000 to 2000° C.

The effect of continuous carbonization at different speeds was also explored with precursor II fibres. Sample II-0.7-5 was employed for this study and carbonization was carried out at speeds ranging from 0.5 to 3.9 ft min^{-1}, giving a residence time range of 1 to 8 min in the furnace (0.25 to 2 min in the 1200° C zone). At speeds greater than 2 ft min^{-1} very fuzzy bundles with many broken filaments were obtained. Electron microscopic examination of the cross-sections of the carbonized fibres showed holes in the centre of fibres processed at speeds of 2 ft min^{-1} and higher (Table V). From the progression of changes in carbonization discussed earlier, it is apparent that the highest temperature which the fibre experiences during carbonization is important since limits on fibre properties are dictated by this temperature. In the

TABLE V Carbonization at different speeds

Take-up speed (ft min^{-1})	Residence time at 1200° C (min)	Carbon fibres from precursor II			Carbon fibres from precursor III			
		Hollow core	Density (g cm^{-3})	Sonic modulus (g denier^{-1})	Hollow core	Density (g cm^{-3})	Sonic modulus (g denier^{-1})	Denier
0.5	2.00	No	1.715	1061	–	–	–	–
1.0	1.00	No	1.705	1049	No	1.740	1210	1650
2.0	0.50	Yes	1.665	964	Yes	1.715	1195	1761
3.0	0.33	Yes	1.660	918	Yes	1.710	1066	1818
3.9*	0.26	Yes	1.650	908	Yes	1.710	1035	1805

*Maximum speed of the take-up unit.
Temperature profile in stabilization: Precursor II-0.7-5 250-275-300° C.
Precursor III 250-275-275° C.

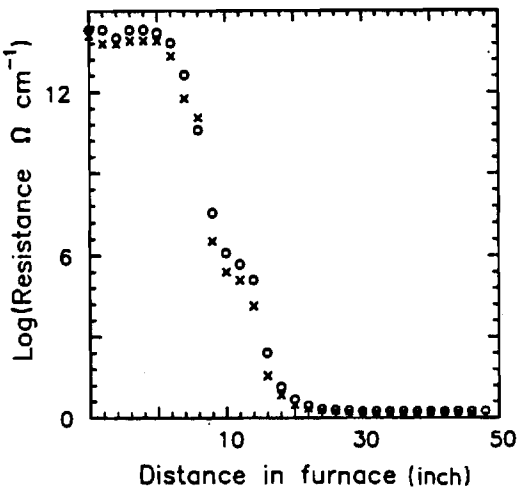

Figure 6 Change in electrical resistance during carbonization of precursor III. (o) 1 ft min^{-1}, (×) 6 inch min^{-1}.

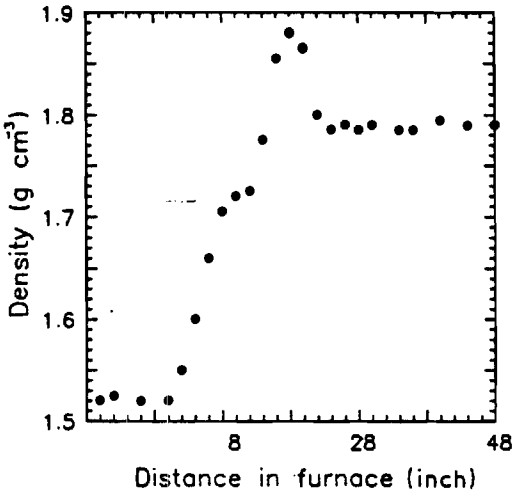

Figure 7 Change in density during carbonization of precursor III.

experiments on carbonization at different speeds, the fibre was always exposed to the maximum temperature of 1200° C, but this temperature was reached at higher rates at the higher processing speeds. The formation of a hollow core when these apparently well stabilized fibres are carbonized at higher rates of heating suggests that more than a single mechanism exists for hole formation in the core. At the higher heating rates, an outer layer of the fibre may be carbonized rapidly, with subsequent consolidation of the structure from the sheath inwards, resulting in a hollow core at the end of the process. The decrease in sonic modulus and in the apparent density of carbon fibres (Table V) produced at higher carbonization speeds reflects also poor consolidation of structure under these conditions.

The progression of changes during continuous carbonization of precursor III fibres show the same features as seen with precursor II fibres (for example, Figs 6, 7). Linear densities were also measured on these samples. These measurements reveal once again Fig. 8) simultaneous rapid loss of material and consolidation of the solid state structure in the initial zone where the temperature is raised to the maximum temperature, with little change beyond this point. When carbonization is carried out at different speeds, the development of a hollow core as well as evidence for incomplete consolidation (Table V) are seen again at processing speeds of 2 ft min^{-1} and higher.

In order to establish the validity of the two different mechanisms that have been proposed to operate under different conditions of formation of a hollow core in carbon fibres, namely,

i. "burning off" of the core material when an incompletely stabilized fibre from a diffusion controlled solid-state stabilization process is carbonized, and,

ii. propagation of the consolidated carbonized structure inwards from the skin when a well stabilized fibre is carbonized rapidly,

additional measurements were carried out in a series of carbonization experiments with incompletely and sufficiently stabilized precursor III fibres. In these experiments, the results of which are reported in Table VI, the linear densities and diameters of these fibres are compared. When the fibres are carbonized at low speeds (0.5 ft min^{-1}), the linear density of the carbon fibres from sufficiently stabilized precursor is significantly higher than that from the incompletely stabilized precursor indicating the expected loss of material in the latter through "burn off". Every filament in the latter bundle also exhibited a hollow core. When these two precursor fibres were carbonized at a higher speed (3.5 ft min^{-1}), a hollow core developed in both cases, but the linear density *and* the diameter of the sufficiently stabilized precursor were higher, consistent with the consolidation mechanism at the higher rates of carbonization proposed here. Comparison of the carbon fibres produced at different speeds from apparently well stabilized fibres shows little difference in linear densities, lending further support to the mechanism of consolidation inwards from the skin. Also, when the sufficiently stabilized precursor is carbonized repeatedly at 1.5 ft min^{-1}, a condition which yields a hollow core in about 60% of the filaments, little change in diameter is observed with

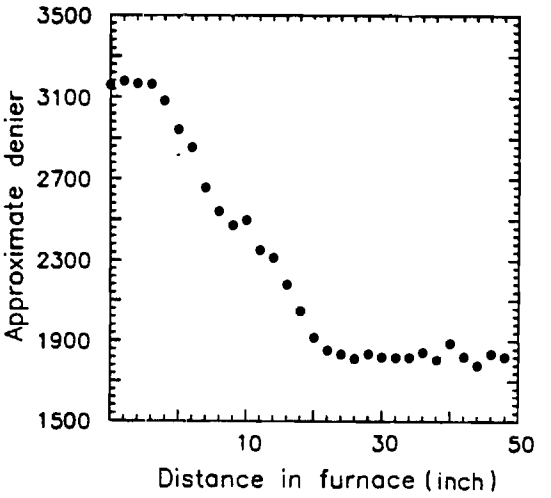

Figure 8 Change in linear density during carbonization of precursor III.

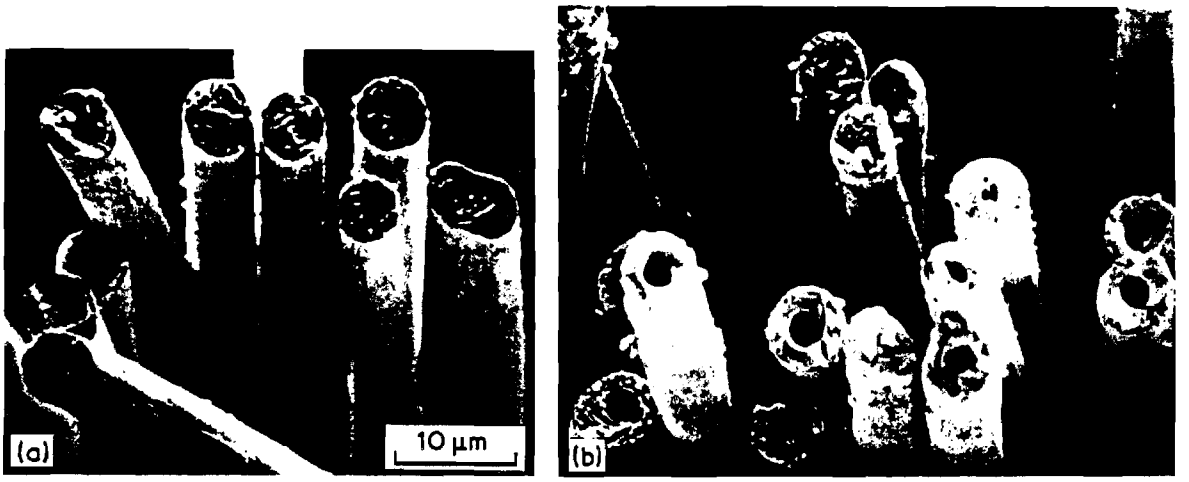

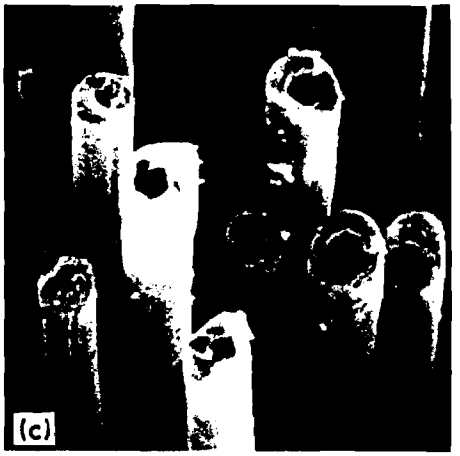

Figure 9 Typical cross-sections of carbonized fibres from precursor III. (a) Stabilized at 250–275–275, carbonized at 0.5 ft min^{-1}. (b) Stabilized at 250–275–275, carbonized at 3.5 ft min^{-1}. (c) Stabilized at 250–265–265, carbonized at 3.5 ft min^{-1}.

reconsolidation. Typical cross-sections from these experiments are shown in Fig. 9.

We see that the qualitative features of the progression of changes during the carbonization are not changed with composition (comonomer with AN) or the extent of orientational and lateral order generated in the formation of precursor fibres. Fundamental aspects of the evolution of properties revealed through the measurements in this study are thus believed to be the general characteristics of the formation of carbon fibres from acrylonitrile-based precursor fibres.

4. Conclusions

A number of significant results have been obtained through the research on continuous low temperature carbonization reported here. These findings and the inferences from them regarding needed additional research are summarized in the following.

i. It is necessary to carry out the stabilization treatment until a critical density is reached in order to avoid the formation of a hollow core in carbon fibres processed under reasonably rapid carbonization conditions. This aspect has been known in commercial practice. The dependence of this critical density on composition remains to be explored.

ii. A hollow core is also formed when apparently well stabilized fibres are carbonized at rates higher than a critical rate. This suggests that more than a single mechanism exists for hole formation in the core and that structural/chemical changes are temperature/time dependent. The influence of low stabilization and slow carbonization against high stabilization and fast carbonization on ultimate properties was not determined. It is possible that, at the higher rates of the carbonization process, an outer layer of the fibre is carbonized rapidly and that subsequent consolidation occurs from the skin inwards, resulting in a hollow core at the end of the process.

iii. Properties such as electrical conductance and sonic modulus, which depend on the extent of formation of ordered basal planes, develop rapidly initially

TABLE VI Carbonization with sufficiently (A) and incompletely (B) stabilized precursor III fibres. Stabilization temperature sequence: A (250-275-275) and B (250-265-265) in °C.

Sample	Carbonization speed (ft min^{-1})	Density (gm cm^{-3})	Denier/filament	Diameter (μm)
A-1	0.5	1.73	0.60	5.6
A-2	3.5	1.71	0.59	6.5
A-3	1.5	1.73	0.60	6.6
A-3-1*	1.5	1.73	0.58	6.5
A-3-2†	1.5	1.76	0.58	6.6
B-1	0.5	1.71	0.54	5.3
B-2	3.5	1.71	0.53	5.5

*Re-carbonization of A-3.
†Re-carbonization of A-3-1.

in the carbonization process, with a slower asymptotic increase with continued heating at the highest temperature. Both the rate and the extent of increase in sonic modulus during carbonization increase with the extent of lateral and orientational order present in the precursor fibres which should promote the ordering process during carbonization. These trends are also reflected in [H]/[C] and [N]/[C] ratios which indicate the degree of aromatization and basal plane formation.

iv. The density of fibres rises in the initial stages of carbonization but reaches a relative maximum beyond which it decreases rapidly to a lower steady value. This apparent decrease is believed to be the result of consolidation of ordered domains around some of the micropores, converting them from "open" pores to "closed" pores, inaccessible to the measuring liquid. This hypothesis needs to be confirmed with a combination of SAXS and measurements based on volume filling of accessible pores and adsorption on accessible surfaces. The combination of density and accessible surface area measurements has been used by Kipling *et al.* [7] to infer open and closed pore structures in graphitizing and non-graphitizing carbons. Additional evidence can also be obtained by combining linear density with measurements of filament diameter along the carbonization line.

v. Procedures developed in this study for monitoring the evolution of carbon fibres in a continuous process can be valuable in optimizing the carbonization set-up. It is necessary to have the provision to alter the temperature profile in carbonization so that measurements of the evolution of properties during the process can be used to advantage in tailoring the appropriate time–temperature profile.

Note

Preliminary results from current research in our laboratories indicate that while the levels of modulus that can be reached in carbonization may be dictated by the orientational order in the precursor fibres, the strength that can be obtained may be affected by both orientational and lateral crystalline order in the precursor fibres. A very high degree of crystalline order in the precursor fibres would diminish the orientational relaxation that can occur during stabilization, especially in the early stages, and thus reduce the concentration of the strength limiting misoriented crystallites in the carbon fibres produced from them. These aspects will be discussed later in this sequence.

Acknowledgements

The authors wish to thank Drs W. C. Tincher and F. L. Cook, and Mr P. Desai for valuable discussions on many aspects of this research. We wish to express our gratitude to Dr L. H. Peebles for many useful suggestions during the course of this work and in the inferences drawn from experimental data. The study was supported by the United States Office of Naval Research.

References

1. M. K. JAIN and A. S. ABHIRAMAN, *J. Mater. Sci.* **22** (1987) 278.
2. *Idem. ibid.* **18** (1983) 179.
3. M. K. JAIN, M. BALASUBRAMANIAN and A. S. ABHIRAMAN, *J. Mater. Sci.* **22** (1987) 301.
4. M. K. JAIN, PhD thesis, Georgia Institute of Technology, Atlanta, Georgia (1985).
5. US Patent 4 279 612, Great Lakes Carbon Corp., New York (1981).
6. D. W. GIBSON, *18th National SAMPE Symp.*, **18** (1973) 165.
7. J. J. KIPLING, J. N. SHERWOOD, P. V. SHOOTER and N. R. THOMPSON, *Carbon* **1** (1964) 321.

Received 8 October 1985
and accepted 15 January 1987

Carbon Vol. 26, No. 3, pp. 403–411, 1988
Printed in Great Britain.

0008-6223/88 $3.00 + .00

EXPLORATORY EXPERIMENTS IN THE CONVERSION OF PLASTICIZED MELT SPUN PAN-BASED PRECURSORS TO CARBON FIBERS

DALE GROVE, P. DESAI, and A. S. ABHIRAMAN*
School of Chemical Engineering, Georgia Institute of Technology, Atlanta, Georgia 30332, U.S.A.

(*Received* 14 *July* 1987; *accepted in revised form* 29 *October* 1987)

Abstract—Current carbon fiber production from acrylic fibers employ wet or dry spun PAN-based precursors that require expensive solvents and costly solvent recovery methods. Recently, it has been discovered that melt spun PAN-based fibers can be prepared by using water as a plasticizer to lower the viscosity and the melting point of PAN. Results from an exploratory investigation into the production of carbon fibers from experimental plasticized melt spun, PAN-based precursors are reported here.

Structural parameters based on X-ray measurements and mechanical properties of these precursors suggest that the morphology of these fibers is similar to that of wet and dry spun PAN-based precursors. However, the precursor fibers have broken filaments as well as surface defects and internal voids, all of which hinder the development of superior properties. This investigation shows, nevertheless, that carbon fibers of reasonable strength, up to an average of 15 cN/dtex (2.5 GN/m^2), and modulus, 1080–1310 cN/dtex (173–214 GN/m^2), can be produced from plasticized melt spun PAN-based precursors. Better properties may be achieved if impurities are removed from the plasticized precursor melt, surface flaws are reduced, fiber uniformity is enhanced, and the stabilization and carbonization processes are optimized for the precursors.

Keywords—Carbon fibers, PAN, melt spinning.

1. INTRODUCTION

Polyacrylonitrile (PAN)-based precursors for carbon fibers are presently wet or dry spun with expensive, environmentally harmful solvents. The spinning process becomes increasingly difficult and expensive for higher molecular weight precursors, requiring increasing amounts of solvent to lower the viscosity of the solution[1]. Since precursors of good physical properties are required in the production of carbon fibers, reasonable molecular weights are essential.

All attempts to melt spin PAN-based polymers without an additive to lower the melting point (ca. 320°C) have failed since PAN degrades before its melting point[2]. One method of lowering the melting temperature and simultaneously lowering the viscosity of the melt is to form a single fusion melt phase between a melt assistant, such as water, and the PAN-based polymer[3]. Water not only can aid the process by lowering the melt temperature and the viscosity, but it can also hinder the degradation reactions simply by blocking the nitrile groups from reacting with each other. The temperature and water composition associated with the single fusion phase are best illustrated by a phase diagram as depicted in Fig. 1. The indicated regions in the phase diagram have the following significance. Region 1 corresponds to a fluid formed by the single fusion melt of PAN and water. Region 2 contains two phases—the fusion melt and excess water. Region 3 depicts the solid fusion of PAN and water. Region 4 represents the solid fusion along with excess liquid water. The difference between regions 1 and 2 (and regions 3 and 4) is that all the water in region 1 (or region 3) is incorporated into the single fusion phase, whereas in region 2 (or region 4) it is not possible for all the water to be incorporated into the single fusion phase. The temperature and water contents identifying the boundaries of region 1, the single fusion melt region, are dependent on the nature and content of the copolymers employed. These temperatures and water concentrations may be anywhere between 140°C and 230°C, and 4% (w/w) and 45% (w/w), respectively[4].

Coxe first reported the need for replacing the expensive processes of wet and dry spinning with less expensive, nonpolluting processes such as plasticized extrusion with water[5]. He found that high pressure mixtures of PAN-based polymers (85% w/w) and water could be more readily extruded than the initial untreated polymer. However, all the filaments produced by this process showed signs of partial decomposition[5]. Early investigations by Opferkuck and Ross established a single phase melt between water and PAN-based polymers when the two were heated under autogenous pressure, but they believed that extrusion would not be possible[6]. Shortly thereafter, Bynam *et al.* used the single phase melt and excess water, region 2 in the phase diagram, to obtain a fibrillated extrudate which could be made into paper[7]. Later, Blickenstaff illustrated how the necessary water content to hydrate and uncouple nitrile

*Author to whom correspondence should be addressed.

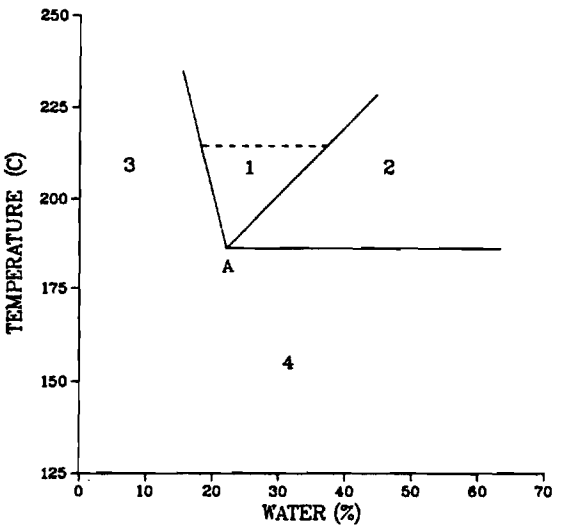

Fig. 1. Phase diagram of (100% pure) PAN and water. Adapted from [4].

groups could be estimated from differential thermal analysis (DTA) and also how the extent of nitrile hydration at a specific temperature could be detected by laser Raman spectroscopy (LRS)[8]. Blickenstaff, through the results from his characterization techniques, explained the melt fusion of water and PAN-based polymers more extensively than previous investigators. The melt spun filaments obtained by Blickenstaff had a well-defined sheath-core character. They were also full of voids and marked with longitudinal surface striations. Goodman developed a process that made reasonable PAN fibers from a mixture between a water–PAN fusion melt and another solvent[9], but the addition of a solvent works against the economy and the overall goal of the process.

Beebe[10] and Cramer[11] have described the production of plexifilaments, which consist of a roughly parallel assembly of irregularly shaped fibers that are interconnected to form a network. In the Cramer process, a dispersion of PAN and water, in region 2 of the phase diagram, is extruded at high temperatures to rapidly purge water from the ensuing plexifilament strands. In a later patent on melt spinning of PAN-based filaments, Cline still found that the newest spinning process resulted in a sheath-core definition in the cross section as well as a partially degraded extrudate[12]. Controlled diffusion of water from the ensuing solid structure was lacking in all the above processes.

By controlling the rate of water evaporation and temperature and by forcing the extrudate directly into a steam-pressurized solidification zone that is directly connected to the spinneret, Porosoff has found that the sheath-core structure could be prevented and that good physical properties could be attained[13,14]. Other refinements have been made [15–21], but Porosoff's invention appears to be the most significant.

Current steam-pressurized solidification zones are capable of drawing the PAN fibers in their "stretchable state" in several stages, with the first stretch stage generally using smaller stretch ratios, typically between 1.5 and 3.5, and subsequent stages using larger stretch ratios[4,15]. Total spin stretch ratios of at least 25 are obtained in spinning. The temperature in the solidification zone, typically between 110°C and 180°C, must be maintained between the minimum melting point on the phase diagram, point A, and the glass transition temperature. If the temperature in the solidification zone is outside this region, drawing appears to become difficult[4].

Controiled evaporation of water from the extrudate prevents drawing difficulties accompanying the formation of the sheath–core structure and maintains the stretchable state of the solidified extrudate. As a means of controlling the evaporation of water from the extrudate and, hence, the moisture content of the extrudate, 5 to 125 psig saturated steam is fed into the solidification zone[4]. Upon exiting the solidification zone, the now highly oriented fibers are dried under dry and wet bulb conditions of 100 to 150°C and 40 to 100°C, respectively, to remove the remaining water[16].

An exploratory study has been conducted in our laboratories to examine the potential of plasticized melt-spun PAN-based fibers as precursors for carbon fibers. Elementary features of these precursor fibers and their conversion to carbon fibers are revealed here and discussed in the context of typical commercial carbon fibers.

2. EXPERIMENTAL

2.1 *Plasticized/meltspun, PAN-based precursors*

The precursor fibers used in this study are experimental plasticized melt spun, PAN-based precursor fibers with spinning conditions as listed in Table 1. Samples A, B, C, and D (group 1), although different in molecular weight, are composed of the same 7% (w/w) of comonomer(s). Samples P and Q (group 2), are comprised of a 3% (w/w) comonomer composition.

2.2 *Batch and continuous stabilization*

Batch stabilization at constant length was carried out in a tubular furnace. The stress developed in the fibers was measured simultaneously. The apparatus consists of a temperature-controlled tubular heater, mounted on a platform with wheels, which can be moved rapidly over smooth rails to enclose a bundle of filaments that is attached at each end to Kevlar yarns. One of the Kevlar ends is connected to a fixed support while the other is connected to a load cell of an Instron model 1130 unit. Initially, the oven is entirely around a Kevlar end. The experiment is begun by rapidly moving the oven to completely enclose the filament bundle and recording the shrinkage force developed. The thermal response of the Kevlar fibers were negligible compared to the

Table 1. Precursor fiber characteristics

Precursor	Melt spin stretch ratio	Copolymer (wt %)	M_v (g/mole)	dtex/ filament*
A	2.0	7	2.5×10^5	1.14
B	2.0	7	1.6×10^5	1.07
C	2.0	7	0.7×10^5	2.17
D	18.5	7	1.0×10^5	1.08
P	1.8	3	1.4×10^5	1.14
Q	1.8	3	1.0×10^5	1.20

*dtex is the weight in grams of 10,000 m of the fiber.

shrinkage forces which develop in the acrylic fibers. The time period required to develop the ultimate stress varies from several hours at low temperatures to less than 5 min (leading to fiber failure) at higher stabilization temperatures.

Continuous stabilization was carried out in a tubular furnace that was divided into three six-foot zones with individual temperature controllers for each zone. Smooth transition from one zone to another and uniformity of temperature throughout a zone were ensured by a metal tube placed between the heaters and the inner glass tube. The temperature profile inside the furnace was determined with thermocouple probes placed 18 in. apart. Two air pumps, one at each end of the glass tube, provided enough air circulation. Two independently driven feed and delivery godets provided the desired dimensional control. Samples for the study of progression of continuous stabilization ("on-line" samples) were obtained after steady state was achieved by cutting the yarn at the delivery end and rapidly withdrawing it from the feed end. Samples A through D were stabilized at constant length with a 220°, 250°, and 270°C profile, while samples P and Q were stabilized with 10% and 13% shrinkage, respectively, with a 260°, 280°, and 290°C profile. All samples were stabilized for 2 h with the exception of the higher linear density specimen, sample C, which required a stabilization time of 4 h.

2.3 *Carbonization*

Carbonization was achieved by passing the stabilized fiber through two 6-in. preheaters at 500° and 700°C followed by a Lindberg furnace at 1200°C. The temperature profile for the entire unit is shown in Fig. 2. The dip in the profile is caused by the separation between the second preheater and the heater in the Lindberg furnace. To maintain an inert atmosphere, nitrogen flow into the furnace was maintained at both ends. Dimensional control was exerted by independently driven feed and delivery godets. All stabilized samples were subjected to the same carbonization conditions. The takeup speed was maintained at 1 foot/min (30.5 cm/min), while the input speed was adjusted to generate a 20-g tension during carbonization.

2.4 *Structural parameters and properties*

A Du Pont DSC model 990 was employed to determine the temperatures at which the precursor fibers undergo exothermic reactions. The preparation of the samples and the experimental procedure employed were standard except that holes were punched in the precursor sample holder to permit the evolution of gases. A heating rate of 20°C was employed with Indium as a calibration standard.

Flat plate wide-angle X-ray diffraction (WAXD) photographs of the precursor fibers were obtained with a Philips X-ray unit 4100. Equatorial and azimuthal scans were obtained using a Philips diffractometer to determine the average lateral size of the precursor's ordered domains (the average "crystal size", L_c) and to estimate the orientation of chain segments in the ordered phase with respect to the fiber axis, f_c. Samples were prepared by carefully wrapping fibers as a parallel array on the sample holder.

The Scherrer equation[22] was used to calculate the average crystal size:

$$L_c = K\lambda/(B_0 \cos\theta) \tag{1}$$

where λ is the wavelength, B_0 is the full width at half the maximum intensity (FWHM) in radians, and the constant K is commonly assigned a value of unity. The FWHM was estimated from the (100) peak at $2\theta = 17°$. No corrections were included to account for crystal imperfection or instrumental broadening and consequently the estimates obtained here are lower bounds.

Hermans crystalline orientation function, f_c, is calculated as follows[22,23]:

$$f_c = -2f_e = 1 - 3 < \cos^2\phi >_{100} \tag{2}$$

where

$$<\cos^2\phi>_{100} = \frac{\int_0^{\pi/2} I_{100}(\phi) \sin\phi \cos^2\phi \, d\phi}{\int_0^{\pi/2} I_{100}(\phi) \sin\phi \, d\phi} \tag{3}$$

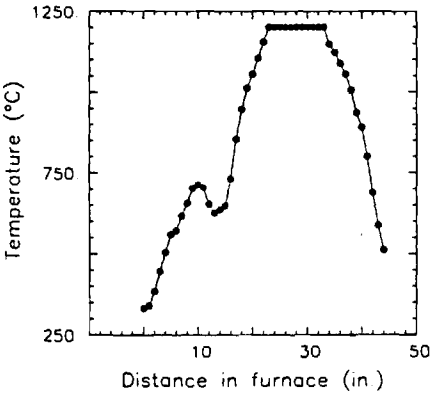

Fig. 2. Temperature profile in the carbonization furnace.

and where $I_{100}(\phi)$ is the intensity of the (100) diffraction peak and ϕ is the azimuthal angle with respect to the fiber axis.

Small angle X-ray scattering (SAXS) flat-plate photographs of the precursor and of partially stabilized fibers were taken with a Rigaku Denki generator with a sample to film distance of 196 mm and an exposure time of 16 h. It was carried out to provide a qualitative insight into the macroscopic arrangement of the ordered and the disordered regions in the fibers.

A Cambridge Merk model II scanning electron microscope was used to examine the cross-sections of carbon fibers after sputter coating with a thin layer of gold.

Densities of the precursor, stabilized, and carbonized fibers were measured by the flotation technique. Toluene (0.866 g/cm³) and CCl_4 (1.585 g/cm³) were mixed in different proportions to form mixtures in the range of 1.11 g/cm³ to 1.58 g/cm³. For solutions with density in the range of 1.59 to 2.00 g/cm³, tetrabromomethane (2.964 g/cm³) and CCl_4 were employed.

All sonic modulus tests employed a PPM-5 Sonic Modulus Tester from the H. M. Morgan Company. Measurements on precursor and stabilized fibers were conducted with the scanner mount and is described elsewhere[23]. For measurements with carbon fibers, due to their much higher sonic modulus compared to precursor and stabilized fibers, a longer distance between the transmitter and the receiver was necessary. These measurements were made with the refractory mount[24].

Tensile tests on precursor fiber bundles were performed using a mini-Instron, model 1130 unit, at a gauge length of 10 in. (25.4 cm) and an elongation rate of 50%/min. Hard, rubber-faced, pressurized grips were used to hold the bundle in place, without slippage. Due to the presence of a number of broken filaments in the carbon fiber bundles, mechanical testing of a composite carbon fiber bundle was not performed. Instead, single-filament tests were performed, using a computerized mechanical tester[25]. The fiber to be tested was fixed on a paper support that was cut after mounting in the tester. A ramp-up force function of 0.08 g/s was used for all but one of the carbon fibers. Carbon fiber C, because of its larger denier, was tested with a ramp function of 0.12 g/s. The tests employed a 2-cm gauge length. A minimum of 20 tests were carried out on each carbon fiber sample to estimate the average strength of the carbon fibers.

Viscosity average molecular weights were determined by dilute solution viscometry using DMF as the solvent. Viscosity average molecular weight was estimated by the Mark–Houwink–Sakurada equation[26].

$$[\eta] = (2.43 \times 10^{-4}) M_v^{0.75} \quad (4)$$

The above parameters are correct strictly for PAN at 25°C. Therefore, the parameters for the samples in this study, which contain 3% to 7% (w/w) unspecified comonomer, are expected to differ slightly from the parameters cited above, but no corrections were made.

3. RESULTS AND DISCUSSION

Various properties of the experimental melt spun, PAN-based precursor fibers are listed in Table 2. All the precursors had densities equal to 1.15 g/cm³. Since the total spin stretch ratio is roughly the same in precursors A through C and precursors P and Q, it is expected that higher strengths will be exhibited by larger molecular weight precursors of the same copolymer content. Precursor D with its associated higher total spin stretch ratio is expected to display a higher modulus and strength than a precursor prepared with a lower spin stretch ratio. These expectations, for the most part, appear to be valid (Table 2).

Precursors A and B had the highest strength of 3.6 cN/dtex (0.42 GN/m²) with viscosity-average molecular weights of 250,000 and 160,000, respectively. Precursor C with a 70,000 average molecular

Table 2. Mechanical properties of precursor fibers

Precursor	Strength cN/dtex (MN/m²)	Modulus cN/dtex (GN/m²)	Extension (%)	Sonic modulus cN/dtex (GN/m²)
A	3.6 ± 0.5	97 ± 18	8.0 ± 0.3	143 ± 7
	(416 ± 61)	(11.2 ± 2.0)		(16.4 ± 0.8)
B	3.6 ± 0.3	115 ± 18	7.5 ± 0.5	128 ± 8
	(416 ± 30)	(13.2 ± 2.0)		(14.7 ± 0.9)
C	2.6 ± 0.2	78 ± 10	8.7 ± 0.5	103 ± 3
	(294 ± 20)	(9.0 ± 1.1)		(11.9 ± 0.3)
D	3.4 ± 0.3	112 ± 7	7.1 ± 0.3	168 ± 26
	(396 ± 30)	(12.9 ± 0.8)		(19.3 ± 3.0)
P	3.3 ± 0.2	106 ± 18	7.0 ± 0.3	109 ± 14
	(386 ± 20)	(12.2 ± 2.0)		(12.6 ± 1.6)
Q	3.3 ± 0.3	101 ± 11	7.1 ± 0.5	95 ± 9
	(375 ± 30)	(11.6 ± 1.3)		(11.0 ± 1.0)

*Density = 1.15 g/cm³. Standard deviations reported.

Fig. 3. WAXD photograph of plasticized melt spun PAN precursors.

weight had a significantly lower strength, 2.6 cN/dtex (0.29 GN/m²). Precursors P and Q displayed similar trends. Precursor D, due to its higher spin stretch ratio, has a higher strength, 3.4 cN/dtex (0.40 GN/m²), for a 100,000 viscosity-average molecular weight than what would be predicted by a linear interpolation between precursors B and C.

Sonic modulus is an indicator of the overall orientation of the chains with respect to the fiber axis. The sonic modulus ranges from 168 cN/dtex (19.3 GN/m²) in precursor D to 95 cN/dtex (11.0 GN/m²) in precursor Q, as shown in Table 2. The sonic modulus data clearly show a relationship to the viscosity-average molecular weight in precursors with the same spin stretch ratio.

3.1 *X-ray diffraction*

Wide angle X-ray diffraction photographs of the melt spun precursor fibers are shown in Fig. 3. The diffraction pattern is similar to that observed for wet spun PAN-based precursor fibers, consisting of a set of peaks on the equator, indicating the presence of a laterally ordered domain, and no off-equator peaks, indicating the absence of true three-dimensional order. The second order equatorial peak (200) is often not observed in wet spun PAN fibers.

The average lateral dimensions of crystals, calculated using the Scherrer equation, are in a narrow range from 4.4 nm (precursor B) to 3.9 nm (precursor D). The orientation function of the chain segments in the ordered phase relative to the fiber axis ranges from 0.81 (precursor A) to 0.87 (precursor D), as shown in Table 3. The orientation of the ordered phase as estimated by the X-ray analysis is

Table 3. Wide-angle X-ray diffraction data of precursor fibers

Precursor	Orientation function f_c	L_c (nm)
A	0.81 ± 0.01	4.34
B	0.86 ± 0.03	4.43
C	0.84 ± 0.01	4.38
D	0.86 ± 0.02	3.92
P	0.87 ± 0.02	4.33
Q	0.86 ± 0.02	4.13

roughly the same in all the precursors. Since the sonic modulus of precursor D is higher than all of the other precursors, the laterally disordered phase in precursor D must be oriented to a greater degree than the laterally disordered phases in the other precursors.

The precursor PAN fibers used in this study have demonstrably different extents of order (Tables 2 and 3), but show no difference in density, indicating that the densities of the laterally ordered and the laterally disordered phases are essentially the same. Thus, the meridional reflection in SAXS is absent in these fibers (Fig. 4). After heating the precursor fibers for 16 min in air at stabilization temperatures at constant length, a meridional reflection is observed in SAXS (Fig. 4). Appearance of this reflection is presumably the result of the preferential occurrence of stabilization reactions in one of the two phases, resulting in a difference in electron densities between the two phases which manifests as a meridional reflection in SAXS. This feature is also characteristic of wet spun PAN precursor fibers[23]. The combination of wide and small angle X-ray analysis

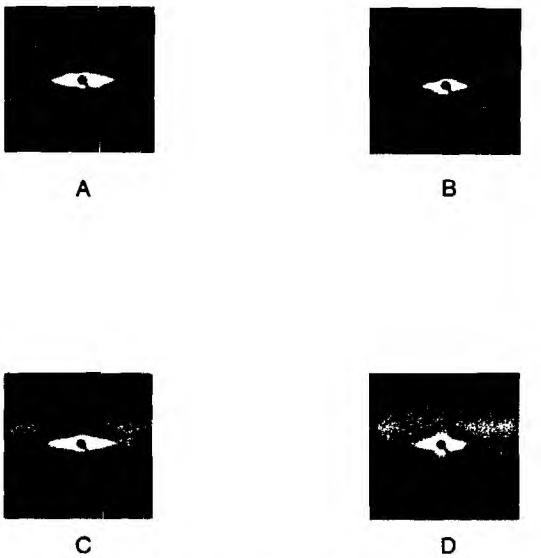

Fig. 4. Small angle X-ray scattering (SAXS) photographs of PAN precursors before and after annealing. (a) precursor A, (b) precursor A annealed for 16 min in air at 220°C, (c) precursor P, (d) precursor D annealed for 16 min in air at 260°C.

Table 4. Differential scanning calorimetry data of precursor fibers

Precursor	Scan rate (°C/min)	Initiation temperature (°C)	Heat evolved (kcal/g)
A	20	240	0.28 ± 0.04
	5	214	
B	20	240	0.26 ± 0.02
C	20	240	0.24 ± 0.07
D	20	240	0.26 ± 0.04
P	20	260	0.38 ± 0.02
	5	247	
Q	20	260	0.38 ± 0.01

results indicate that the plasticized melt spun PAN fibers possess a morphology similar to wet and dry spun PAN precursor fibers.

3.2 *Thermal analysis*

Thermal analysis (DSC) was conducted on the precursors in air to determine the lowest practical stabilization temperature. As shown in Table 4, samples A, B, C, and D had roughly the same initiation temperature and total exothermic heat of reaction, while samples P and Q each exhibited a higher initiation temperature and total exothermic heat of reaction. Precursors A through D, with a comonomer concentration of 7% (w/w), are characterized by a 20°C lower initiation temperature and by a broader DSC exotherm, than precursors P and Q containing a 3% comonomer concentration. These results are in total agreement with previous DSC investigations[27], which have shown that higher initiator comonomer concentrations result in lower initiation temperatures and broader DSC exotherms. The results of this analysis also suggest that samples within each group behave similarly.

Batch stabilization studies on precursors A and P revealed lower practical initiation temperatures than previously found in the 20°C/min thermal analysis. The analysis was, therefore, repeated at a slower rate of 5°C/min, which resulted in initiation temperatures of 214 and 247°C for precursors A and P, respectively.

3.3 *Batch stabilization at constant length*

In order to assess the shrinkage forces occurring in stabilization and to determine whether the fibers could withstand forces that develop at different temperatures, constant length batch stabilization experiments were conducted on precursors A and D. The profile of stress development during this process can be used to infer the limits on some of the conditions in continuous stabilization. For example, if excessive growth of stress leading to failure of filaments in the batch process is observed, it may indicate the need for allowing a net shrinkage in a continuous process at similar temperatures. Typical results are shown in Figs. 5 and 6.

For fibers that remain intact throughout this experiment, a typical stress versus time curve at a given constant temperature consists of three characteristic zones in succession: a rapid short-lived rise in stress, followed by a decay in stress that occurs over a period of a few minutes, with the duration of this stress decay decreasing with increasing temperature of stabilization, and finally a gradual increase in the stress level to a maximum at long times. If the fiber breaks during this test, the stress vs. time curve exhibits the rapid rise in stress followed by a decay and an abrupt break at the initial stages of the secondary increase in stress (Fig. 6).

It is widely accepted that the initial rapid rise and the subsequent decay in stress level are associated

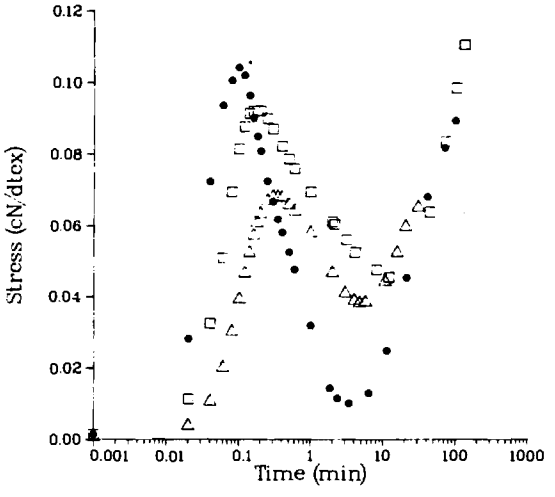

Fig. 5. Constant length batch stabilization of precursor A at different temperatures. (□) 220°C, (△) 240°C, (●) 260°C.

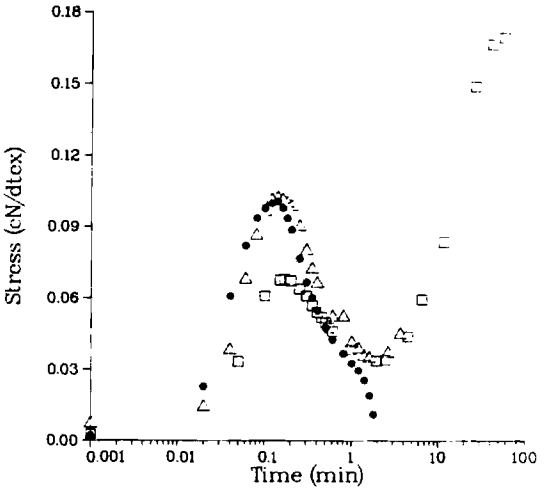

Fig. 6. Constant length batch stabilization of precursor P at different temperatures. (□) 280°C, (△) 290°C, (●) 300°C. Samples at 290 and 300°C broke after the last plotted value.

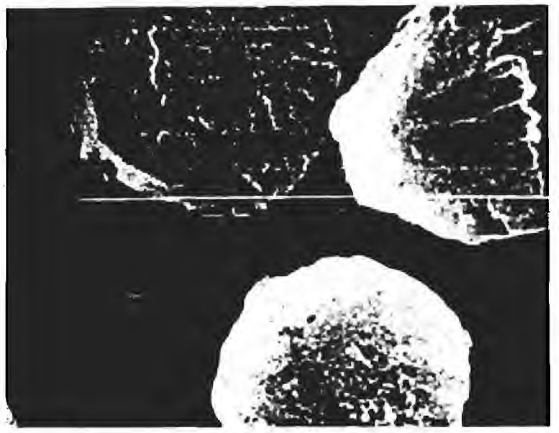

Fig. 7. Scanning electron micrographs of fully stabilized DMF etched precursor P fibers (sample taken 10 ft into stabilization line).

with entropic relaxations in the noncrystalline fraction, affected by the morphology and, thus, the physical history of the sample. The rise and decay are explained through the entropic retractive forces developing in the amorphous phase above the glass transition temperature of PAN and the subsequent relaxation of some of the oriented chains in this disordered phase. The relaxation of the chains will occur more rapidly at a higher temperature. There is still considerable disagreement over how the stabilization reactions cause the second gradual rise in the stress level. It has been interpreted in two separate ways: (1) stabilization reactions cause the linear structure of PAN to cyclize and crosslink to shorter contour lengths of chain segments. As the extent of stabilization increases, the system will become more and more stressed due to the local strains that develop in the cyclized segments and (2) a shrinkage force brought about by the "melting" of the ordered segments. A gradual "melting" of the crystals is necessary for the controlled intermolecular propagation reactions associated with stabilization. Once melted, the highly oriented chains will tend to undergo entropic recovery, causing the gradual buildup of a shrinkage stress in the later stages of stabilization. The relative extent of contributions to the shrinkage force from the two processes is yet to be resolved.

3.4 *Continuous oxidative stabilization*

In an attempt to follow the progression of stabilization, segments of fiber samples pulled out of the continuous stabilization line were immersed in hot-DMF (100°C) for approximately 5 min and their cross sections were observed using a scanning electron microscope. It was anticipated that incompletely stabilized fibers would reveal a central hole under SEM examination due to dissolution of the unstabilized core in DMF. However, instead of retaining the original structure about the holes, the fiber cross section collapses. The totally stabilized, DMF-etched sample appeared essentially the same as the totally carbonized sample under SEM examination as shown in Fig. 7.

The bulk and linear densities of stabilized fibers are given in Table 5. Due to the incorporation of oxygen into the stabilizing fiber structure and the relatively small amount of vaporizing gases leaving the structure, an increase in density and a slight increase in linear density are anticipated in the stabilized fiber when compared to the precursor.

3.5 *Properties of carbon fibers*

A distribution of microholes have been found scattered about the cross section of the carbon fibers under SEM inspection. These are seen easily at magnifications exceeding 5000X (Fig. 8). Possible sources for the microvoids are impurities (including regions of high water concentration) in the precursor fiber. DMF-etched stabilized fibers also contained microvoids indicating that some of the impurities leave the structure during the stabilization process itself (Fig. 7). Examination with SEM also revealed small pits along the surface of the carbon fibers as shown in Fig. 9. The poor surface quality and significant numbers of broken filaments in the carbon fiber bundles, particularly in precursor D, could be traced back to the melt spun precursor. The existence of an equatorial streak in SAXS photographs is also indicative of the porosity in these fibers (Fig. 4). Carbon fibers

Table 5. Properties of stabilized fibers

Precursor	dtex/ filament	Density (g/cm^3)	Sonic modulus	
			cN/dtex	(GN/m^2)
A	1.14 ± 0.01	1.370	61 ± 7	(8.3 ± 1.0)
B	1.08 ± 0.03	1.370	72 ± 4	(9.9 ± 0.5)
C*	2.20 ± 0.04	1.395	65 ± 4	(9.1 ± 0.6)
C†	2.19 ± 0.03	1.385	64 ± 4	(8.8 ± 0.5)
D	1.09 ± 0.04	1.360	74 ± 2	(10.1 ± 0.2)
P	1.32 ± 0.04	1.395	67 ± 4	(9.4 ± 0.6)
Q	1.27 ± 0.06	1.390	74 ± 7	(10.3 ± 1.0)

*4-h stabilized sample C.
†3-h stabilized sample C.

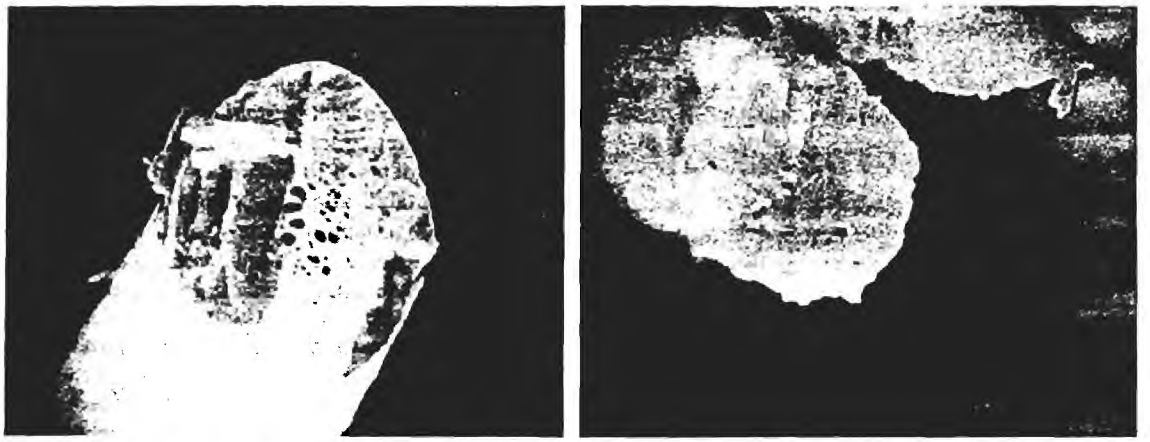

Fig. 8. Scanning electron micrographs of microvoids in carbon fibers. (a) Carbon fibers from precursor B. (b) Carbon fibers from precursor P.

with better properties than those obtained in the present study would be produced by a melt spinning process that eliminates these defects in the precursor fibers. Aspects related to phase separation should be examined carefully in developing the necessary modifications for improving the precursor fiber formation process.

All noncarbon elements are driven away and a two-dimensionally ordered structure that is oriented parallel to the fiber axis develops during the carbonization process. Since roughly 50% of the stabilized mass is removed during carbonization and carbonization is typically subject to 15% shrinkage or less, the linear density is expected to decrease. The density, on the other hand, increases primarily due to consolidation of the structure with a higher average atomic mass. The data shown in Table 6 are consistent with these well-known consequences of carbonization.

Determination of the sonic modulus of the carbon fibers was difficult because of the significant number of broken filaments in the long length (1–3 m) of carbon fiber bundles that is required to obtain a reasonable measurement. Consequently, the sonic moduli reported here should be regarded as rough estimates and not exact averages of the sonic moduli of the individual filaments. The values obtained (Table 6) are well within the sonic modulus range of typical PAN-based carbon fibers.

Single filament tensile test results are given in Table 6. Strength of these filaments ranged from an average of 15 cN/dtex (2.5 GN/m²) in sample B to 11 cN/dtex (1.7 GN/m²) in sample D, while Young's modulus ranged from 1310 cN/dtex (214 GN/m²) in sample A to 1080 cN/dtex (173 GN/m²) in sample C. These values demonstrate clearly that plasticized melt spinning for the formation of acrylonitrile-based carbon fiber precursors has the potential to produce precursors for carbon fibers with properties in the range of commercial interest. Optimization of the process by reducing defects and by selecting the best conditions for stabilization and carbonization should lead to carbon fibers with superior mechanical properties than those obtained in the present study.

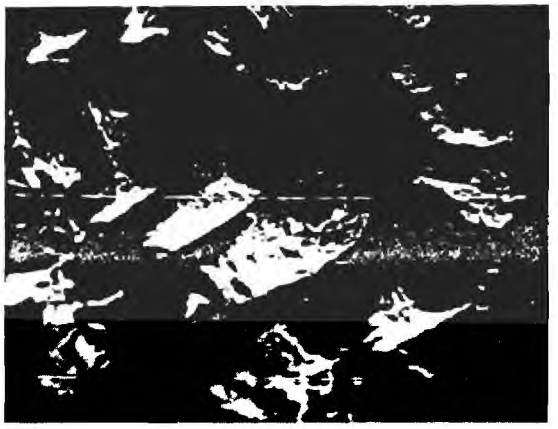

Fig. 9. Scanning electron micrographs of surface flaws on carbon fibers from precursor A.

4. CONCLUDING REMARKS

Carbon fibers of reasonable strength, up to an average of 15 cN/dtex (2.5 GN/m²), Young's modulus, 1080 to 1310 cN/dtex (173–214 GN/m²), and sonic moduli in excess of 1000 cN/dtex have been produced from experimental acrylonitrile-based, plasticized melt spun precursors. These properties have been obtained in spite of numerous surface and internal flaws, indicating that the overall process has the potential to yield fibers with commercially useful mechanical properties, if the quality of the precursor fibers can be upgraded.

Structural parameters based on X-ray analysis and mechanical properties suggest that the morphology and properties of the experimental precursor fibers used in this study are similar to wet and dry spun acrylic precursors. However, these fibers also contain numerous surface flaws and broken filaments.

Table 6. Mechanical properties of carbonized fibers

Sample	dtex/ filament	Density (g/cm^3)	Strength cN/dtex (GN/m^2)	Modulus cN/dtex (GN/m^2)	Extension (%)	Sonic modulus cN/dtex (GN/m^2)
A	0.67 ± 0.02	1.64	14 ± 4 (2.3 ± .6)	1310 ± 220 (214 ± 36)	1.1 ± 0.2	1100 ± 260 (181 ± 43)
B	0.60 ± 0.03	1.64	15 ± 4 (2.5 ± .6)	1280 ± 160 (210 ± 26)	1.2 ± 0.2	1170 ± 13 (193 ± 2)
C	1.16 ± 0.03	1.61	12 ± 3 (2.0 ± .4)	1080 ± 150 (173 ± 24)	1.2 ± 0.3	1480 (239)
D	0.63 ± 0.04	1.595	11 ± 3 (1.7 ± .4)	1090 ± 160 (173 ± 25)	1.0 ± 0.2	1140 ± 26 (182 ± 4)
P	0.73 ± 0.03	1.56	13 ± 3 (2.1 ± .4)	1160 ± 150 (182 ± 23)	1.2 ± 0.2	1000 ± 21 (156 ± 3)
Q	0.69 ± 0.04	1.56	14 ± 4 (2.2 ± .5)	1230 ± 200 (191 ± 32)	1.2 ± 0.2	1290 (202)

Microholes were observed frequently in SEM examination of cross sections of both DMF-etched stabilized fibers and carbon fibers, suggesting the presence of impurities in the precursor fibers. Surface flaws and impurities will have to be reduced for these melt spun, PAN-based precursor fibers to become a viable alternative to current wet or dry spun, acrylic precursors.

Acknowledgment—This research was supported by a grant from the Office of Naval Research and by graduate fellowships from the Alcoa Foundation and the Phillips Petroleum Foundation.

REFERENCES

1. U.S. Patent 4,271,056, American Cyanamid Company (1981).
2. U.S. Patent 4,108,818, du Pont (1978).
3. U.S. Patent 3,991,153, American Cyanamid Company (1976).
4. U.S. Patent 4,301,107, American Cyanamid Company (1981).
5. U.S. Patent 2,585,444, du Pont (1948).
6. U.S. Patent 3,388,202, Monsanto (1968).
7. U.S. Patent 3,402,231, Monsanto (1968).
8. U.S. Patent 3,984,601, du Pont (1976).
9. U.S. Patent 3,896,204, du Pont (1975).
10. U.S. Patent 4,166,091, du Pont (1979).
11. U.S. Patent 4,238,441, du Pont (1980).
12. U.S. Patent 4,238,442, du Pont (1980).
13. Fed. Rep. of Germany Patent 2,403,947, American Cyanamid Company (1974).
14. U.S. Patent 4,163,770, American Cyanamid Company (1979).
15. U.S. Patent 4,303,607, American Cyanamid Company (1981).
16. U.S. Patent 4,271,056, American Cyanamid Company (1981).
17. U.S. Patent 3,991,153, American Cyanamid Company (1976).
18. U.S. Patent 4,226,817, American Cyanamid Company (1980).
19. U.S. Patent 4,283,365, American Cyanamid Company (1981).
20. U.S. Patent 4,379,113, American Cyanamid Company (1983).
21. U.S. Patent 4,461,739, American Cyanamid Company (1983).
22. L. E. Alexander, *X-ray Diffraction Methods in Polymer Science*, p. 423. Wiley Interscience, New York (1969).
23. M. K. Jain, M. Balasubramanian, P. Desai, and A. S. Abhiraman, *J. Material Sci.* **22**, 301 (1987).
24. M. K. Jain, M. Balasubramanian, S. K. Bhattacharya, and A. S. Abhiraman, *J. Material Sci.* **22**, 3864 (1987).
25. B. R. Livesay, Private communication.
26. R. L. Cleland and W. H. Stockmayer, *J. Polym. Sci.* **17**, 473 (1955).
27. R. C. Rowe, NTIS Report AD-755427. National Technical Information Service, Springfield, VA (1972).

16th BIENNIAL CONFERENCE ON CARBON

EXTENDED ABSTRACTS and PROGRAM

July 18–22, 1983
University of California, San Diego
San Diego, California

Sponsored by

american carbon society

HIGH TEMPERATURE DEFORMATIONS IN CONVERSION OF ACRYLIC FIBERS TO CARBON FIBERS

M. Balasubramanian, W. C. Tincher and A. S. Abhiraman

Introduction

In the manufacture of carbon fibers from polyacrylonitrile-based precursor fibers, the properties of the final carbon fibers are significantly affected by the chemical composition and morphology of the acrylic fiber and chemical and morphological changes occurring during oxidative stabilization and carbonization. A comprehensive study is being carried out in our laboratories to establish the material and process interactions with the properties of the ultimate carbon fiber. Results from a study of the morphology of the fibers have shown that significant mobility and consequent reordering of structure occurs in the two phase fibrillar morphology of the precursor fibers during the stabilization stage. The changes occur before; and as a consequence of the onset of the chemical reactions at this stage. These observations suggested a high temperature pre-stabilization drawing process to produce precursor fibers of high orientational and lateral order. We present here the results from a study of the morphological changes during oxidative stabilization of these high temperature drawn (HTD) fibers. Preliminary studies have also been conducted in our laboratories on the deformation of "stabilized" fibers prior to carbonization which indicate the possibility of a plastic stretch at temperatures significantly above that of stabilization. Work is currently being carried out to determine the effect of such pre-stabilization (HTD) and post-stabilization (VHTD) high temperature drawing on the properties of carbon fibers produced from such precursors. The results from this study will be presented at the 16th Carbon Conference.

Experimentation

The experiments were done on fibers spun by redissolving commercial acrylic fibers, viz. type 43 orlon supplied by DuPont (Precursor I) and another containing methyl acrylate and acrylic acid as comonomers (Precursor II). The spinning conditions are given in reference 1.

High temperature pre-stabilization drawing of precursor I was carried out continuously by drawing the fibers between two godets. Thermal annealing experiments were conducted in an air-circulated oven, preheated to the required temperature before the sample was introduced. These experiments were conducted with free allowance for fiber shrinkage (FLA) and under conditions where such shrinkage is prevented by holding the fiber at constant length (CLA).

Continuous oxidative stabilization was carried out in an 18-foot oven. These experiments were conducted at 265°C and at the same feed and delivery rates. After steady state was achieved, the yarn was cut at the delivery end and rapidly pulled from the feed end. This sample was cut into 1 foot lengths for subsequent measurements. An apparent residence time for each section was calculated as (distance from oven entrance/feed yarn velocity).

The combination of sonic modulus and wide angle x-ray diffraction (WAXD) measurements were made on fibers annealed for different times and on the sections made from the 'on-line' samples in continuous stabilization. Hermans' orientation function of the chains in the laterally ordered regions, f_c, was calculated from azimuthal scan of the 100 reflection in WAXD measurements.

Results and Discussion

The morphological parameters of the as spun and the HTD samples of Precursor I are given in Table 1. It is seen clearly that fibers of significantly higher order can be obtained from drawing at high temperatures. The high crystalline orientation and sonic modulus obtained without a significant drop in elongation indicates that a more homogeneous structure is developed by such drawing.

The results from morphological measurements on the fibers from oven-annealing and 'on-line' stabilization are shown in Figures 1, 2 and 3. The relatively high orientational order developed in the HTD precursors persists through the oxidative stabilization stage. The cumulative shrinkage increases monotonically with annealing time over the normal duration of oxidative stabilization stage (Figure 4). The need for dimensional constraint during stabilization is seen from the significantly reduced overall orientational order in the FLA fibers compared with the CLA fibers.

The possibility of drawing a "stabilized" fiber at higher temperatures (VHTD) was explored with a commercially stabilized fiber from Precursor II. It was possible to draw this fiber through an oven at 600°C at a draw ratio of approximately 1.20. Experiments are being conducted to establish the role of stabilization conditions, and the rate and temperature of this VHTD process in determining the extent to which the fiber can be drawn. The results from these studies and from carbonization of such fibers will be discussed at the 16th Conference on Carbon.

Acknowledgements

The authors express their appreciation to Dr. F. L. Cook for many useful discussions concerning this work and to Dr. R. A. Young for making this X-ray diffraction facilities available to us.

REFERENCE

1. Muskesh K. Jain, Prashant Desai and A. S. Abhiraman, Paper Presented at this Conference.

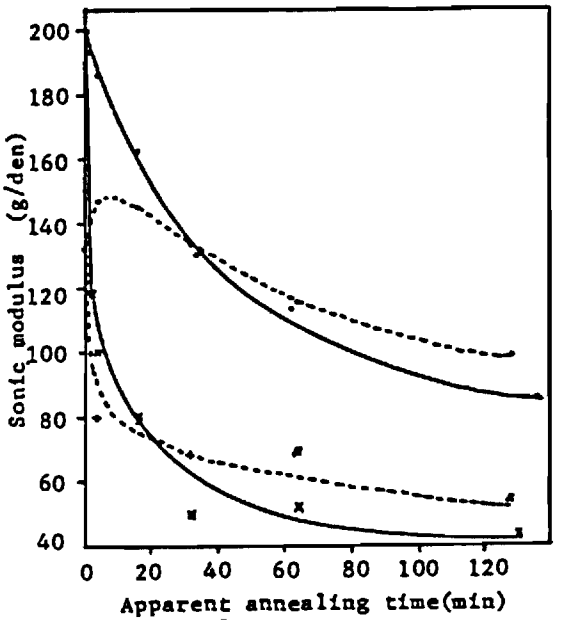

Fig.1. Sonic modulus of Precursor I fibers annealed at 270°C (—— DR=3, HTDR =2.3; ---- DR=6).

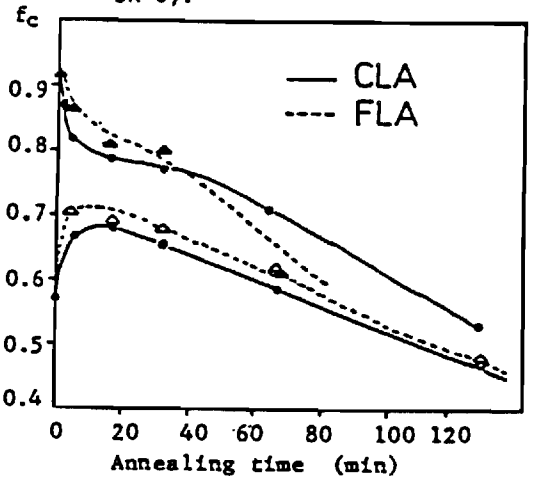

Fig.3. Hermans' Orientation Function, f_c, of Precursor I fibers annealed at 270°C (●▲ DR=3, HTDR=2.3; ○△ DR=6).

Table 1: High Temperature Drawing of Precursor I

Spinning DR	HTD DR	HTD Temp(°C)	Sonic modulus (gpd)	f_c
3	-	-	95	0.54
6	-	-	133	0.63
6	1.0	240	145	0.75
6	1.2	240	176	0.79
6	1.4	240	190	0.81
6	2.3	252	200	0.92

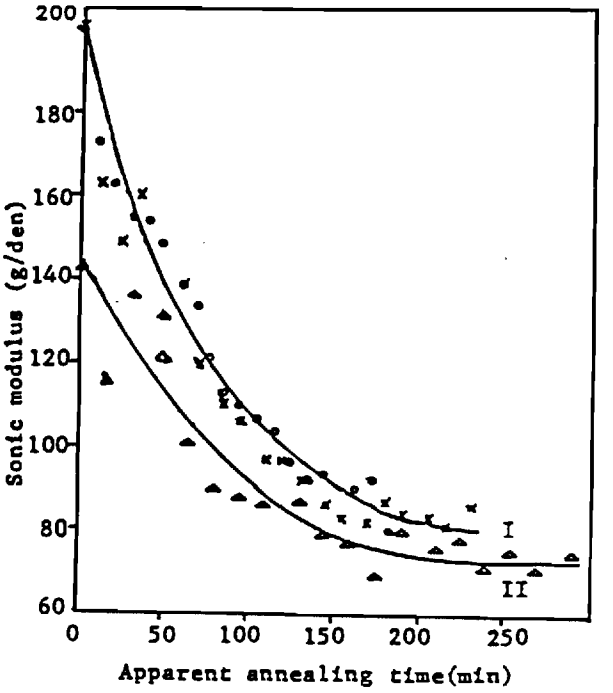

Fig.2. Sonic modulus at different stages of stabilization (Yarn velocity, inch/min; ○ 1.25; x 1.0; △ 0.75).

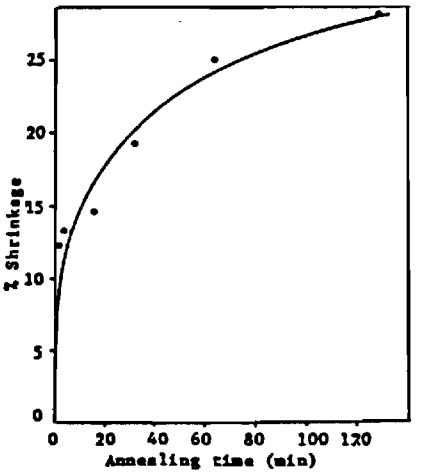

Fig.4. Shrinkage of Precursor I fibers at 270°C (DR=3, HTDR=2.3).

MORPHOLOGICAL REARRANGEMENTS IN CONVERSION OF ACRYLIC FIBERS TO CARBON FIBERS: OXIDATIVE STABILIZATION

Mukesh K. Jain, Prashant Desai and A. S. Abhiraman*

Introduction and Experimentation

Thermal annealing studies on precursor fibers have been carried out to help in identifying an appropriate morphological model for the precursor and in determining the changes that occur during oxidative stabilization. The relevance of such studies to practical stabilization processes is shown by comparison with measurements on fibers removed from a stabilization process.

The experiments were done on fibers spun by redissolving commercial acrylic fibers, viz., Type 43 Orlon, supplied by DuPont (Precursor I) and another containing methyl acrylate and acrylic acid as comonomers (Precursor II). The spinning conditions are given in Table I.

Thermal annealing experiments were conducted in an air-circulated oven, with free allowance for fiber shrinkage (FLA) or under conditions where such shrinkage is prevented by holding the fibers at constant length (CLA). Experimental details are given in reference 1.

Results and Discussion

The results from short time annealing at 230°C are given in Table II and show clearly that the orientation of the ordered fraction in the material as well as the overall orientation (inferred from sonic modulus) show a significant increase when a constraint against shrinkage is imposed on the fibers. Annealing the precursor under free conditions, however, results in considerable decrease in the overall orientation but simultaneously shows an increase in the orientation in the ordered phase. Significant shrinkage in FLA without decrease in the orientation of the ordered phase implies that the less ordered morphological units link successive oriented crystals along the fiber direction.

In order to follow the progressive changes in morphology brought about by high-temperature treatment, measurements were made with precursor fibers that were thermally annealed for various times (Figures 1 and 2). The data show clearly that the orientational changes of the ordered phase are a direct consequence of the initial association of segments into these domains followed by the "lateral order - lateral disorder" transformation caused by the stabilization reactions. The latter causes a gradual decrease in the average size of these domains. The trend in sonic modulus data (Figure 3) is a combination of the morphological rearrangements preceeding chemical reactions at the initial stages and the change in the intrinsic material caused by the reactions at the later stages.

Significant morphological rearrangements take place in acrylic precursor fibers at temperatures comparable to those in a stabilization process. These changes, which occur both prior to and after the onset of detectable chemical reactions, depend to a large extent on the dimensional constraints imposed during annealing. Annealing in the absence of dimensional constraints causes a significant shrinkage and a decrease in overall orientation, but the orientation of the ordered phase increases.

Small angle X-ray scattering patterns of the initial fiber and after annealing at constant length for 16 minutes are shown in Figure 4. The absence of a long period in the initial fiber and its appearance after annealing for a time period at which the laterally ordered domain persists to their maximum shows clearly that the reactions occur initially in the disordered domains. The gradual destruction of lateral order by chemical reactions at long times is also revealed by the monotonic increase in shrinkage (Figure 5). The responses to thermal treatments of the acrylic fibers confirm the presence of at least two phases, one laterally ordered and the other a less ordered phase which contains segments that tend to be mobile at high temperatures. The latter segments are anchored in the ordered phase and macroscopic constraints are transmitted via the ordered phase to these segments, preventing significant orientational relaxation in them. The well established fibrillar morphology of drawn acrylic fibers, coupled with the mechanical response and changes in morphological parameters during annealing support the two-phase fibril model. Relaxation of orientation in the disordered regions should lead to a significant decrease in the sonic modulus but without a decrease in the orientation of the ordered regions. The results from FLA experiments (Figures 2 and 3) support this contention.

The data from continuous CLA and drawing are given in Table 2. The morphological rearrangements are seen to occur on a very short time scale (the residence time is 4 sec.). The overall orientation can be increased significantly by drawing under these conditions where considerable mobility exists for allowing rearrangements along with a natural tendency towards ordering.

Additional results from carbonization of these fibers will be presented at the conference.

REFERENCE

1. Muskesh K. Jain, and A. S. Abhiraman, J. Mater. Sci., 18 (1983), 179.

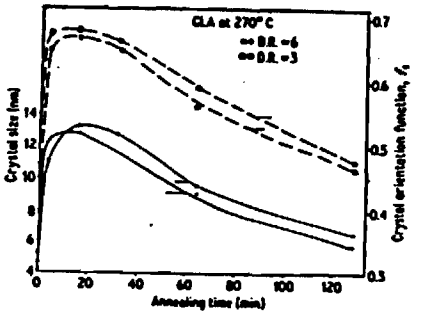

Fig.1. Hermans' Orientation Function, f_c, and crystal size of PrecursorI, CLA at 270°C

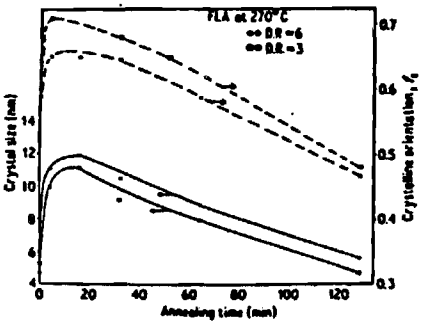

Fig.2. Same as fig.1, except FLA

Table 1. Spinning Conditions

	Precursor I	Precursor II
Spinneret	100 holes,76μm dia.	300 holes, 100μm dia.
Solution	20% w/w in DMF	16% w/w in DMAc
Coagulation bath: Composition	60:40(DMF:H_2O)	30:70(DMAc:MeOH)
Temperature	25°C	20°C
Draw ratio	3 or 6 in boiling water	6 in boiling water

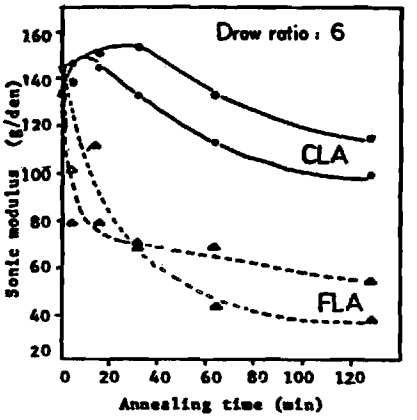

Fig.3. Sonic modulus of annealed fibers (●▲:Precursor I, 270°C;○△:Precursor II, 270°C)

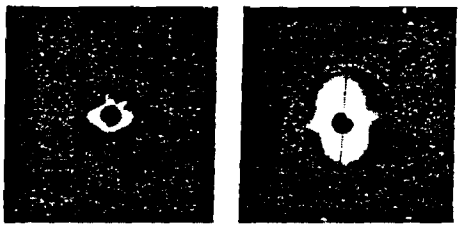

A B

Fig.4. SAXS patterns from Precursor I, DR=6 (A: as spun; B: CLA at 270°C for 16 min)

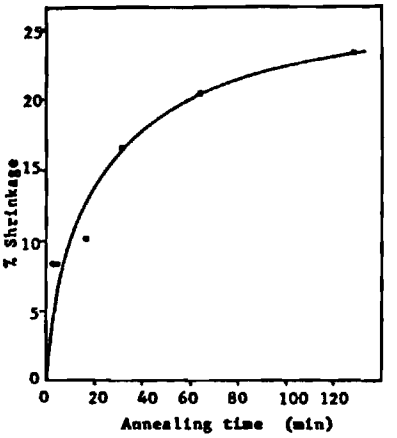

Fig.5. Shrinkage of Precursor II, FLA at 265°C

Table 2. Short Time Annealing Experiments at 230°C for 2 min.

Precursor D.R	Treatment Condition	Shrinkage (%)	Initial Modulus(g/den)	Breaking Elongation(%)	Sonic Modulus(g/den)	fc	Crystal size(nm)
3	Orig.	-	61	13	95	0.54	5.4
3	CLA	-	70	16	120	0.69	8.9
3	FLA	16	43	23	57	0.59	8.9
6	Orig.	-	73	9	130	0.63	4.7
6	CLA	-	85	13	145	0.75	8.1
6	FLA	16	57	14	78	0.63	8.5

17th BIENNIAL CONFERENCE ON CARBON

EXTENDED ABSTRACTS AND PROGRAM

June 16-21, 1985
University of Kentucky
Lexington, Kentucky

Co-sponsored by

american carbon society

university of kentucky

Morphology and Oxidative Stabilization of Acrylic Precursor Fibers

M.K.Jain, M.Balasubramanian, P.Desai and A.S.Abhiraman*
Georgia Institute of Technology, Atlanta GA. 30332

We have shown earlier that the mechanical response and the changes in morphological parameters of acrylic fibers during a batch oxidative stabilization process support the morphological model proposed by Warner, et al. namely, connected alternating regions of lateral order and disorder in a fibrillar structure[1,2]. We describe here the results from additional experiments pertaining to the morphology of acrylic precursors and the progression of chemical and morphological changes during batch and continuous oxidative stabilization processes.

Experimental

The results reported here are from experiments conducted with fibers spun in our laboratory by redissolving a commercial acrylic fiber, Orlon-43, supplied by Du Pont. Fibers of different orientations and extents of lateral order were obtained through different combinations of drawing in a hot water bath(HWD) and through a high temperature tubular oven(HTD) (Table I). Results similar to those reported here have also been obtained with two other acrylic precursor fibers. The batch stabilization experiments were conducted in an air circulated oven at 265°C. Continuous stabilization was carried out in an 18-foot tubular oven at the same input and output velocities and with a flat temperature profile (265°C). The progression of changes here were monitored through measurement on a "process sample" obtained by cutting the filament bundle at the delivery end and rapidly pulling the sample out from the feed end.

Results and Discussion

1. Progression of Stabilization

The sonic modulus and WAXD data reveal clearly the presence of a higher overall orientation and lateral order in the HTD fibers than in the fibers drawn to the same extent in hot water(HWD) (table I). However, when the progression of stabilization is monitored through measurements of density and elemental composition (figs.1,2), little difference is seen between the responses in the two fibers.

When acrylic precursor fibers are heated to the temperatures involved in oxidative stabilization, whether dimensional constraints are imposed or not, a tendency toward increase in perfection and extent of the laterally ordered domains occurs in the early stages (fig.3), the extent of this increase decreasing with increasing order initially present in these fibers. The dramatic difference seen in the initial changes in sonic modulus (fig.4) between the presence and absence of dimensional constraints, with a pronounced drop in the absence of constraints indicates clearly the presence of an oriented but less ordered fraction, in which a majority of chain segments are connected to the ordered domains. The initial drop in the sonic modulus of HTD fibers (fig.4) and the rapid initial relaxation of shrinkage stress in both fibers (fig.5) reflect that some of the less ordered fractions do not bridge the ordered domains. The higher level of shrinkage stress but the lower shrinkage of HTD fibers (fig.6) is consistent with the higher orientational as well as crystalline order seen in these fibers.

The relative extents of the ordered fraction present at different stages of stabilization has been seen in the enthalpy of melting obtained through plasticization of the fiber with water. The monotonic build-up of shrinkage stress and shrinkage in the later stages of constrained and free heating respectively, and the results from WAXD measurements reflect this melting of ordered domains.

2. Morphology of Acrylic Precursor Fibers.

The following observations clearly show that the basic morphological unit in oriented acrylic fibers consists of a repeating sequence of oriented, laterally ordered and oriented but laterally disordered domains with a significant portion of the chain segments in the latter phase bridging the ordered domains.

(i) Clear WAXD evidence for the presence of laterally ordered domains.

(ii) Calorimetric evidence for "melting of crystals" when the melting is induced, through plasticization, at temperatures below those of degradation reactions.

(iii) Spontaneous shrinkage at high temperatures, without any loss of the extent of the orientation of the ordered domains.

Acrylic fibers with demonstrably different extents of order show little difference in density, indicating that the packing densities in the laterally ordered crystals and the laterally disordered "non-crystalline" regions are essentially the same. Confirmation of the existence of a long period in the precursor fibers has been obtained through SAXS studies of precursor fibers subsequent to impregnation with CuCl from a solution. Selective diffusion of CuCl into the disordered phase produces the electron density difference with the ordered domain, resulting in the appearance of the evidence for long period in SAXS.

References

1. M.K.Jain and A.S.Abhiraman, J.Mater.Sci., 18, 179, 1983.
2. S.B.Warner, D.R.Uhlmann and L.H.Peebles Jr, J.Mater.Sci., 14, 1893, 1979.

Table I. High Temperature Drawn Fiber Properties.

DRAW RATIO			DPF	SONIC MODULUS GPD	Fc	CRYSTAL SIZE A
HOT WATER	HOT OVEN	TOTAL				
3	-	3	3.	90	0.54	54
3	2.3	6.9	1.4	200	0.92	130
7.3	-	7.3	1.6	120	0.70	54

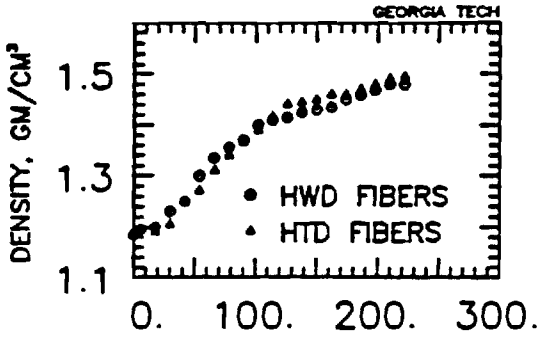

Figure 1. Density and continuous stabilization

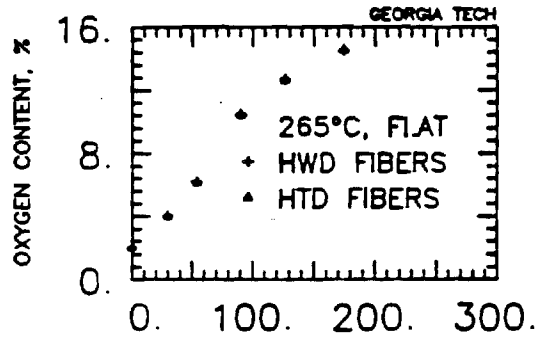

Figure 2. Oxygen pick-up in continuous stabilization

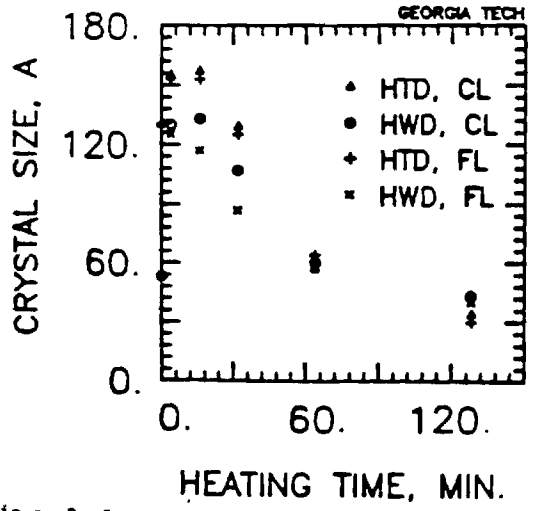

Figure 3. Crystal Size of batch stabilized fibers

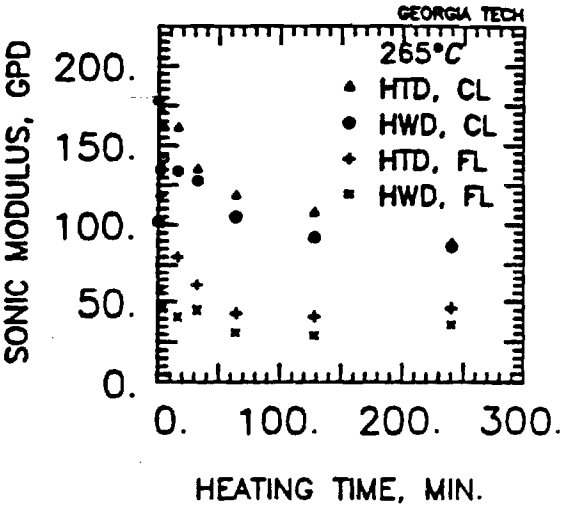

Figure 4. Sonic Modulus of batch Stabilized fibers

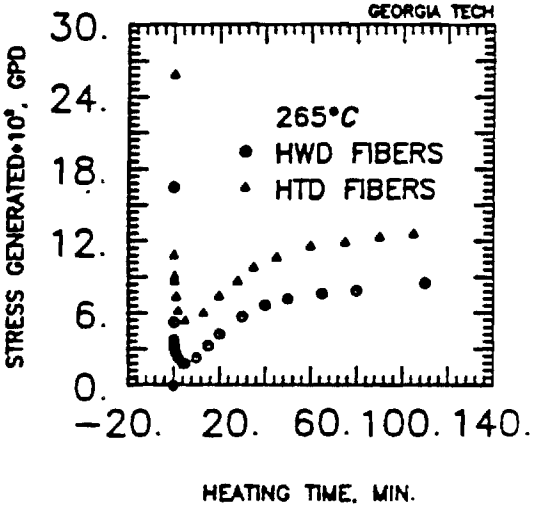

Figure 5. Shrinkage Stress in CL batch Stabilization

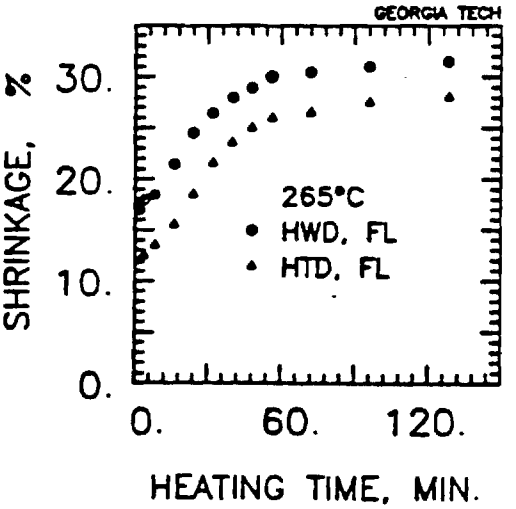

Figure 6. Shrinkage in FL batch Stabilization

Evolution of Structure and Properties in Continuous Carbon Fiber Formation

M. Balasubramanian, M.K. Jain and A.S. Abhiraman*
Georgia Institute of Technology, Atlanta, GA, 30318

A comprehensive study of the evolution of structure and properties in the formation of carbon fibers from acrylonitrile based precursors is being conducted in our laboratories. We report here some of the results regarding the effects of stabilization conditions on the formation of a consolidated carbon fiber structure. Results from a study of progression of carbonization in a continuous process are also described.

Experimental

Two precusor fibers were used in this study, one that was spun in our laboratories from a copolymer of acrylonitrile with 3% itaconic acid (precursor I) and other a commercial precursor. Different levels of orientational and lateral orders were obtained through various combinations of drawing through a hot water bath (HWD) and a high temperature tubular oven (HTD) (Table 1). Continuous oxidative stabilization was carried out in an 18-foot linear oven with various ascending temperature profiles (Table 2). The results reported here are from a continuous carbonization process with the temperature profile as shown in figure 1.

Table 1. Precursor I Drawing Conditions.

Sample	Draw Ratio B.W.	Draw Ratio High Temp	Total draw ratio	Final dpf
IA	3.0	-	3.0	2.25
IB	5.0	-	5.0	2.16
IC	2.5	1.8	4.5	2.22
ID	2.5	2.7	6.7	1.55

Table 2. Properties of Stabilized Precursor I Fibers.

SAMPLE	TEMPERATURE Profile(°C)	DPF	DENSITY gm/cc	HOLLOW CORE
IB	250-275-275	2.34	1.515	Yes
	250-275-300	2.29	1.525	No
	250-275-325	2.25	1.535	No
IC	250-275-300	2.19	1.495	Yes
	275-300-325	2.24	1.515	Rare
	275-300-350	2.24	1.530	No
ID	250-275-275	1.62	1.525	No
	250-275-300	1.57	1.535	No

Results and Discussion

The results from the SEM observations of cross sections of carbon fibers produced by continuous carbonization at 1 foot/min. of precursor I fibers stabilized with different temperature profiles are given in table 2.

A hollow core is seen from the carbon fibers when the fibers are incompletely stabilized as a result of lower stabilization temperatures, especially with the higher denier filaments. Extensive study with this precursor show that it is necessary to carry out the stabilization treatment until a critical density of 1.52 gm/cc. is reached in this precursor to avoid the formation of a hollow core in the carbon fibers. A hollow core develops in the carbon fibers also when the speed of the carbonization process is increased with apparently well stabilized fibers (Table 3). The formation of a hollow core can be caused by burning-off of an incompletely stabilized core as

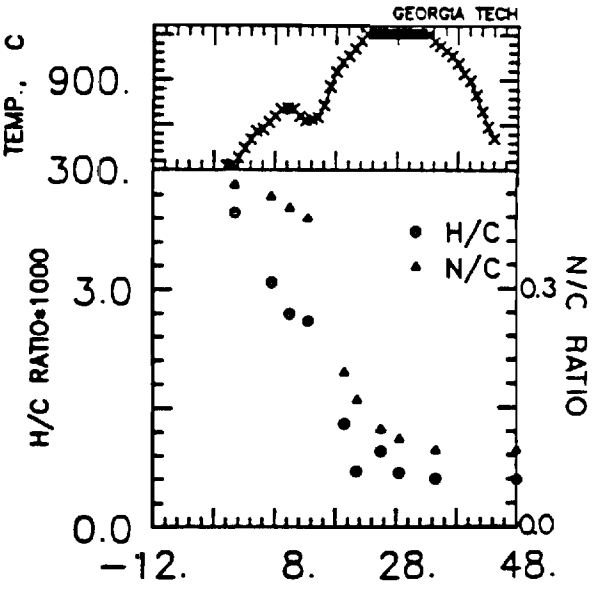

Figure 1. Elemental Composition and Progression of Carbonization.

Table 3. Carbonization at Different Speeds.

TAKE-UP SPEED ft/min.	RES. TIME AT 1200°C min.	HOLLOW CORE (SEM)	DENSITY gm/cc	SONIC MODULUS gpd
0.5	2.00	No	1.715	1061
1.0	1.00	No	1.705	1049
2.0	0.50	Yes	1.665	964
3.0	0.33	Yes	1.660	918

well as the rapid developement of a rigid skin and the subsequent developement of the carbon fiber structure inwards from the skin. These two aspects are being studied currently in our laboratories.

Higher orientational order as well as lower denier per filament in the precursor lead to superior mechanical properties of the carbon fibers (Table 4). However, the highest tensile strengths obtained from precursor I were still lower than the fibers from the commercial precursor II. The surface of carbon fibers made from precursor I displayed defects in the form of pits, presumably resulting from contamination during the formation of these precursor fibers.

Elemental composition and properties such as sonic modulus and electrical resistance change rapidly in the carbonization process, reaching their final values almost immediately upon reaching the highest temperature (figures1-3). The apparent density of carbon fibers also increases rapidly in carbonization but it reaches a relative maximum as soon as the maximum temperature is reached, with a significant drop upon continued heating at the highest temperature (figure 4). The drop in density which occurs without a change in sonic velocity and electrical resistance, is probably due to the conversion of some of the micropores from the accessible to inaccessible ones. This aspect will be studied with BET isotherms and mercury porosity measurements and the results will be presented at the conference, along with additional results from carbonization at 1600°C.

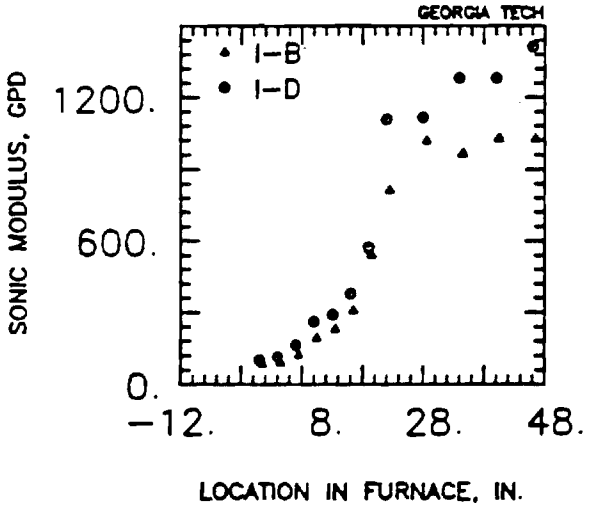

Figure 2. Sonic Modulus and Progression of Carbonization.

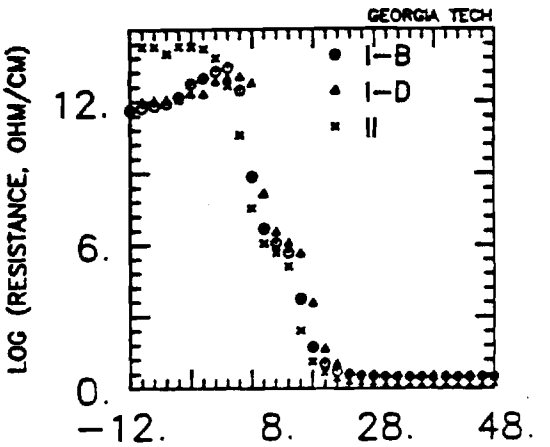

Figure 3. Electrical Resistance and Progression of Carbonization.

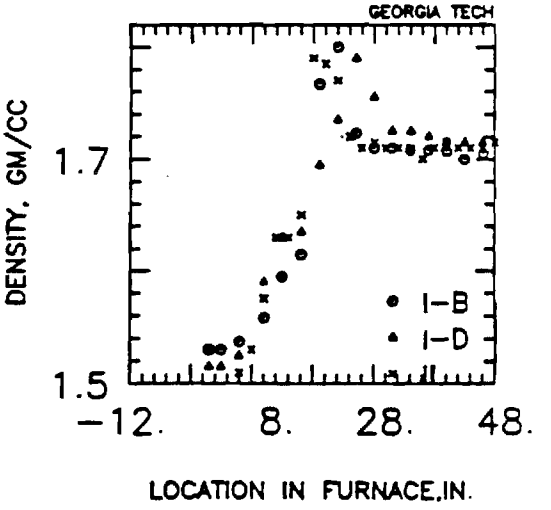

Figure 4. Density and Progression of Carbonization

Table 4. Properties of Precursors and Carbon Fibers.

SAMPLE	PRECURSOR FIBER					CARBON FIBER			
	DENSITY gm/cc	DPF	TENACITY gpd	ELASTIC MODULUS gpd	STABILIZATION TEMPERATURE (°C)	DENSITY gm/cc	DPF	TENACITY gpd	SONIC MODULUS gpd
IA	1.180	2.25	2.1	78	275-300-325	1.660	1.16	4.5	857
IB	1.175	2.16	3.1	90	250-275-300	1.705	1.13	6.3	1060
IC	1.175	2.22	3.4	114	275-300-350	1.670	1.10	7.4	1109
ID	1.185	1.55	4.4	144	250-275-275	1.715	0.83	8.1	1339
II	-	0.92	5.3	127	250-275-275	1.710	0.57	18.6	1210

SOCIETY FOR THE ADVANCEMENT OF
MATERIAL AND PROCESS ENGINEERING

32ND INTERNATIONAL SAMPE SYMPOSIUM
AND EXHIBITION

VOLUME 32

ADVANCED MATERIALS TECHNOLOGY '87

EDITED BY
Ralph Carson
Martin Burg
Kendall J. Kjoller
Frank J. Riel

Anaheim Convention Center
Anaheim, California
April 6-9, 1987

32nd International SAMPE Symposium
April 6-9, 1987

FROM PAN-BASED PRECURSOR POLYMERS TO CARBON FIBERS: EVOLUTION OF STRUCTURE AND PROPERTIES

A. S. Abhiraman
School of Chemical Engineering
Georgia Institute of Technology
Atlanta, GA 30332

Abstract

The structure and properties of carbon fibers are determined by the nature of the precursor polymers and the evolution of morphology through the three major stages of processing, viz., precursor fiber formation, oxidative stabilization and carbonization. Critical interactions exist between the processing conditions and the physico-chemical changes that occur at each stage. This presentation will attempt to provide a comprehensive view of the PAN-based carbon fiber process which includes

1. Morphology and relevant morphological parameters in PAN-based precursor fibers.
2. Stress-Environment-Material interactions during oxidative stabilization.
3. A mathematical model of the kinetics of oxidative stabilization.
4. Evolution of structure and properties in carbonization.

Methods by which high lateral and orientational order can be obtained in the precursor and the processing conditions which can minimize orientational relaxation during stabilization will be presented. Prospects for new PAN-based precursor materials and fiber formation processes will also be discussed.

Carbon/graphite fiber-reinforced composites have emerged as the most important among advanced structural materials, with physical and mechanical properties to meet a variety of highly specialized needs. Among the major commercial precursors for these fibers, cellulose-, pitch- and polyacrylonitrile (PAN)-based, the PAN-based precursor fibers have assumed a dominant position. Recent fundamental investigations pertaining to the technology of precursor fiber formation have yielded acrylic fibers of significantly higher order which are being converted to carbon fibers of superior mechanical properties in commercial processes.

Many isolated aspects of the conversion of acrylonitrile based precursors to carbon fibers have been studied and reported in the literature (1). However, a high degree of empiricism exists still in relating various material and process contributions to the structure and properties of carbon fibers. The research effort in our laboratories is aimed at minimizing empiricism and improving fundamental knowledge of the evolution of structure and properties of these critical high performance fibers.

The primary objective in our research is to provide rational directions for advance in precursor structures and process configurations to extend the range of properties which can be obtained in polyacrylonitrile-based carbon fibers. The emphasis is on the chemical and morphological evolution from precursor polymers, through fiber formation, drawing and oxidative stabilization, to carbonization. Recent research in our laboratories has yielded a number of significant results pertaining to the morphology of acrylic precursor fibers, enhancement of precursor order and chemical and morphological changes through solid state oxidative stabilization and low temperature carbonization (2-10). These results are summarized in the following.*

1. Model for Precursor Morphology

A comprehensive set of evidence (Table 1) based on x-ray scattering (WAXD and SAXS), thermal analysis, thermal deformation and stress responses, and sonic pulse propagation points clearly to the presence of a connected sequence of oriented laterally ordered and oriented but laterally disordered domains, which is the structure proposed by Warner, et al. (11) for fibrils in oriented acrylic fibers.

2. High Order Through High Temperature Deformation

When precursor acrylic fibers are exposed rapidly to temperatures in the stabilization range, significant morphological rearrangements and changes in mechanical properties are observed well before the onset of reactions, in less than 10 seconds. The rearrangements reveal a spontaneous tendency toward increase in lateral order. In the absence of a significant level of tensile stress, it is also accompanied by large scale disorientation of the laterally disordered fraction. Based on the segmental mobility and the tendency toward increase in lateral order, a high temperature deformation process has been proposed to generate highly ordered precursor fibers. For example, the data in

* Experimental details and extensive data will be presented at the conference.

Table 2 show clearly the significantly higher orientational and lateral order which can be obtained by deformation through a high temperature oven of a fiber which has been only partially drawn through a hot water bath. The high temperature deformation step proposed by us has been utilized in commercial production to yield carbon fibers of significantly superior mechanical properties.

3. Multi-Zone Oxidation

Based on chemical as well as morphological considerations, multi-zone oxidation with independent control of stress and environment in each zone has been proposed by us for maximizing the translation of orientational order from precursor fibers to carbon fibers through the stabilization step. Initial batch experiments indicated clearly that a higher level of orientational order and mechanical properties could be retained with higher levels of tensile stress in stabilization (see, for example, figure 1). Also, the maximum stress level which can be applied advantageously changes during the course of stabilization, suggesting the need for a multi-zone process with independent control of stress in each zone. It may also be advantageous to provide a sequence of inert and oxidizing atmospheres during the course of stabilization. With the combination of internally initiated reactions and those initiated by the species arising from diffusion-controlled incorporation of oxygen, an inhomogeneous shrinkage stress distribution will result in the fiber cross-section. Also the maximum extent to which ladder sequences can be formed through intramolecular nitrile polymerization can be shown to decrease with incorporation of oxygen before nitrile polymerization is completed. Such inhomogeneities can be reduced through nitrile polymerization under inert atmosphere in the initial stages, followed by stabilization in air.

A four-zone stabilization line, with computer control of stress/deformation in each zone, has been constructed to facilitate experimental investigation of multi-stress, multi-environment stabilization (Figure 2).

4. Mathematical Model of Oxidative Stabilization

Developing a mathematical model of solid-state oxidative stabilization of PAN-based precursors is extremely complex because of the multitude of events that occur in this process. Among the factors to be considered in this process are (i) initiation reactions by different species in the precursor polymer, such as comonomers and defect structures, (ii) reactions initiated by species from reaction of oxygen with the backbone, (iii) multiple options for reaction paths, (iv) intra- and

inter-molecular reactions between similar species, (v) transport of species such as O_2, *OH, etc., and (vi) morphological changes and constraints on molecular mobility accompanying the reactions, which should alter the rate constants for diffusion reactions. If all of the possibilities are considered, it leads to a large number (>30) of coupled partial differential equations, with the associated boundary conditions and material constants (9). We have reduced this general set of equations to five equations by lumping similar reactions together and developed a numerical procedure for solving them. Trial solutions of this simplified set have been obtained with estimates of rate constants from published information. The predicted responses have been of the same order of magnitude as those observed in stabilization processes. Experiments are being conducted to compare theoretical predictions with global and, if possible, local concentrations of major reaction species. It is hoped that this procedure would lead ultimately to elimination of the essentially trial and error methods used currently for establishing stabilization conditions.

5. Continuous Low-temperature (1200°C) Carbonization

Several aspects pertaining to the evolution of structure and properties in low temperature (1200°C) carbonization have been studied. These are

(i) Two different mechanisms have been recognized for the hollow core which can occur in carbonization. One is through burning-off an incompletely stabilized core due to inadequate combination of time and temperature in diffusion-controlled stabilization. The other can be due to consolidation of structure inwards from the skin when a well stabilized fiber is raised rapidly to carbonization temperatures. Whether such dual mechanisms are operational at carbonization temperatures higher than 1200°C remains to be explored (8,10).

(ii) Among the parameters which may be examined as criteria for adequate stabilization, density has been observed to be a consistent parameter which can also be measured easily. Attaining a composition-dependent critical density, independent of precursor filament size and morphological parameters, appears to be necessary in order to avoid core blow-out in carbonization (8,10).

(iii) By analyzing filaments which are withdrawn rapidly from the feed end of a continuous carbonization process, the paths for evolution of the chemical and morphological structures in carbon fibers have been studied (8,10). For example, results from low temperature carbonization indicate "aromatization

(inferred from H/C ratio) - basal plane formation (from N/C ratio) - development of strength and stiffness" to be the sequence in the evolution of structure and properties.

(iv) Apparent bulk density, measured by immersion techniques, increases rapidly to a maximum through the initial stages of carbonization, but then decreases rapidly to a lower asymptotic value (see, for example, figure 3). This drop is not accompanied by corresponding changes in linear density and diameter through the course of carbonization. The mechanism for the apparent drop in density appears to be related to conversion of some of the open or accessible pores to closed ones through consolidation of the carbonized structure around them.

REFERENCES

1. Jain, M.K., and Abhiraman, A.S. J. Mater. Sci. (in press).
2. Jain, M.K., and Abhiraman, A.S. J. Mater. Sci. 18, 179 (1983).
3. Abhiraman, A.S., Balasubramanian, M., and Tincher, W.C., Proceedings of the XVI Biennial Conference on Carbon, 497 (1983).
4. Jain, M.K., Desai, P., and Abhiraman, A.S., p 517 of ref. 3.
5. Jain, M.K., et al., Proceedings of the XVII Biennial Conference on Carbon, 310 (1985).
6. Balasubramanian, M., Jain, M.K., and Abhiraman, A.S., p. 312 of ref. 5.
7. Jain, M.K., et al., J. Mater. Sci., (in press).
8. Balasubramanian, M., et al., (to be published).
9. Grove, D., Mathematical model of solid state thermo-oxidative stabilization of acrylonitrile-based precursors to carbon fibers, M.S. Thesis, Georgia Institute of Technology (1986).
10. Jain, M.K., Physical and morphological changes during the conversion of acrylonitrile-based precursors to carbon fibers, PhD Thesis, Georgia Institute of Technology (1985).
11. Warner, S.B., Uhlmann, D.R., and Peebles, L.H., Jr., J. Mater. Sci. 14, 1983 (1979).

Biography

Professor A. S. Abhiraman was granted his PhD in Fiber and Polymer Science from N.C. State University in 1975. He worked in American Enka Co. till 1979 when he joined Georgia Institute of Technology. His current fields of interest are formation of high performance fibers, especially carbon, graphite and ceramic fibers, thermodynamics and kinetics of crystallization in polymers, fiber formation, polymer rheology, fiber-matrix interaction in composites, etc.

Acknowledgements

The study was supported by the Office of Naval Research.

TABLE 1. MORPHOLOGICAL MODEL AND DRAWN PRECURSOR FIBER

OBSERVATIONS	INFERENCES
1. WAXD Pattern	Presence of an Oriented Laterally Ordered Phase
2. Enthalpy Changes in Plasticized Heating	The Laterally Ordered Phase Consists of "True" Crystals i.e., Products of First Order Transition
3. Spontaneous Shrinkage upon Free Annealing Without Loss of Orientation in the Laterally Ordered Phase	Presence of an Oriented but Less Ordered Phase with Chain Segments Bridging the Laterally Ordered Crystals Along the Fiber Direction
4. Development of Thermal Stress Upon Constrained Annealing	
5. Large Spontaneous drop in Sonic Modulus ONLY when Shrinkage is Allowed During Annealing	
6. Constant Density of Fibers with Different Extents of Lateral Order	Ordered and Disordered Phases of the Same Density (?)
7. SAXS after Diffusion of Electron-dense Molecules	Repeating Sequence of Oriented Laterally Ordered (LO) and Laterally Disordered (LD) Phases

TABLE 2. HIGH TEMPERATURE DRAWING AND PROPERTIES OF PRECURSOR FIBERS

	HWD	HTD
Jet Stretch	0.7	0.9
Draw Ratio (Hot Water)	7.1	3.0
Draw Ratio (High Temperature)	—	2.3
Oven Temperature (°C)	—	252
Denier/filament	1.6	1.4
Sonic Modulus (g/denier)	120	180
Crystal Orientation function	0.7	0.92
Average Crystal Size (nm)	5.4	13.0

HWD : Drawing in Boiling Water
HTD : High Temperature Drawing

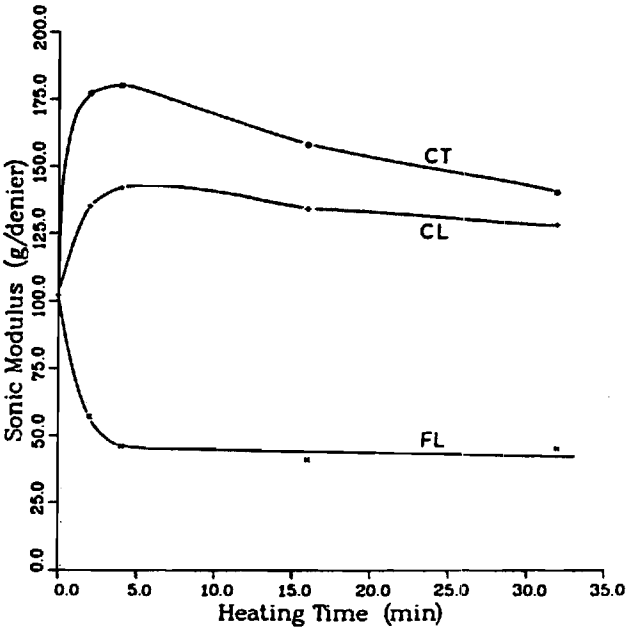

Figure 1. Progression of Sonic Modulus during stabilization at 265°C (FL-free length; CL - Constant length; CT - Constant tension of 0.1 g/denier)

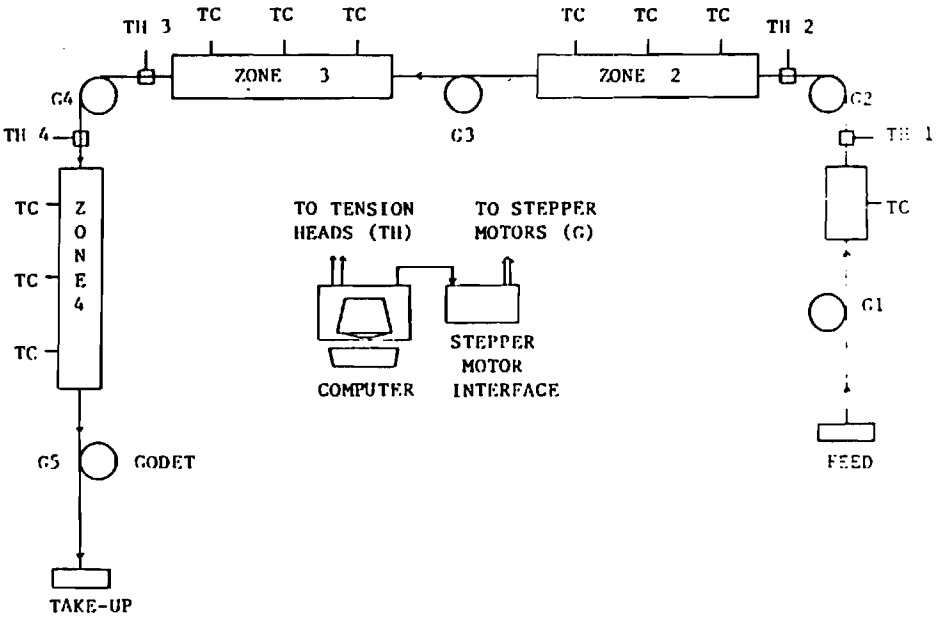

Figure 2. Schematic of Multi-Stage Stabilization Line.

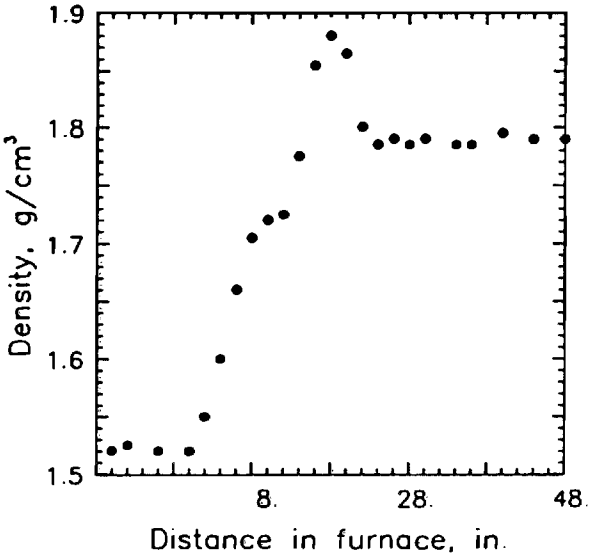

Figure 3. Progression of Density during Carbonization.

ORDER ENHANCING DEFORMATION OF PAN-BASED PRECURSORS

S. K. Bhattacharya, G. Bhat, V. Daga and A. S. Abhiraman

GEORGIA INSTITUTE OF TECHNOLOGY
Atlanta, Georgia 30332

When acrylic precursor fibers for carbon fibers are exposed rapidly to temperatures in the stabilization range, significant morphological rearrangements and changes in mechanical properties are observed well before the onset of reactions - in less than 10 seconds.[1] The rearrangements reveal a spontaneous tendency towards increase in lateral order. In the absence of a significant level of tensile stress, it is also accompanied by a large scale disorientation of the laterally disordered fraction. Based on the segmental mobility and the spontaneous tendency towards increase in lateral order, a high temperature deformation process has been proposed to generate highly ordered precursor fibers. For example, the data in table 1 show clearly the significantly higher orientational and lateral order which can be obtained by deformation, through a high temperature oven, of a fiber which has been only partially drawn through a hot water bath. Such high temperature deformation has been utilized recently in commercial production to yield carbon fibers of significantly superior mechanical properties. The high lateral order achieved in the precursor could reduce orientational relaxations in subsequent processes, especially in the early stages of oxidative stabilization, thus minimizing a source for the formation of strength-limiting misoriented crystals in carbon fibers.

The extent to which deformation can be effected in a precursor fiber is a function of rate of deformation, temperature, and the order which exists prior to the deformation process. High levels of drawing can be achieved through slow deformation or sequential drawing at successively higher temperatures.

Results will be presented at the conference from current experiments pertaining to the following aspects:

(i) Incorporation of slow deformation in conjunction with stabilization in a multi-zone stabilization process.

(ii) The role of temperature on the extent of deformation and the order which can be obtained.

(iii) High temperature relaxation, followed by drawing.

(iv) Properties of carbon fibers from continuous low temperature (1200°C) carbonization.

REFERENCES

1. M. K. Jain, A. S. Abhiraman, J. Mater. Sci., 18, 179-188 (1983)

Table 1. High Temperature Drawing and Properties of Precursor Fibers.

	HWD	HTD
Jet Stretch	0.7	0.9
Draw Ratio (Hot Water)	7.1	3.0
Draw Ratio (High Temperature)	---	2.3
Oven Temperature (°C)	---	252
Denier/filament	1.6	1.4
Sonic Modulus (g/denier)	120	180
Crystal Orientation function	0.7	0.92
Average Crystal Size (nm)	5.4	13.0

HWD : Drawing in Boiling Water
HTD : High Temperature Drawing

MATHEMATICAL MODEL OF SOLID STATE THERMO-OXIDATIVE STABILIZATION OF ACRYLIC PRECURSORS FOR CARBON FIBERS

Dale Grove and A. S. Abhiraman

GEORGIA INSTITUTE OF TECHNOLOGY
Atlanta, Georgia 30332

Oxidative stabilization constitutes an important intermediate step in the formation of carbon/graphite fibers from acrylic precursors, since an improperly stabilized fiber can not be cohesively processed at the high temperatures of carbonization into good quality carbon fibers. It is also the rate determining step of the overall process, taking anywhere from 30 minutes to several hours to achieve proper stabilization.

The chemistry of oxidative stabilization of acrylic fibers is not completely understood. The complexities arise from the combination of (i) a wide range of possible reactions, initiated by species in the acrylic copolymers and by the reaction of oxygen diffusing into the system, and (ii) a solid state structure which changes as a result of the segmental mobility and chemical conversion during the stabilization process. Any reasonable mathematical model of this solid state conversion process should account for the transport processes as well as the chemical reactions in a continually changing solid-state structure.

The mathematical model developed here is for batch stabilization occurring in an inert or oxidizing environment based on low temperature processing of PAN-based precursor fibers. The results of this model can be extended to a continuous process because the axial transport processes can be neglected in these extremely slow processes. Low temperature stabilization which eliminates rapid exothermic reactions permits the assumptions of isothermal conditions throughout the fiber and negligible evolution of NH_3 and HCN.

Following a review of the proposed stabilization reactions, a general mathematical model is developed gradually. The well established as well as theorized reactions here have been modeled in all of their complexity, and a simplified model has been deduced from this overall mathematical model with the necessary justifications. The simplification is necessary to avoid costly and time consuming computer runs, and to allow future experimental verification.

The model monitors the conversion of chemical groups such as -CN, free oxygen, oxygen reacted onto the backbone (which is known to be an important process parameter), comonomer concentration, etc. Although certain reaction orders and rate constants are assumed in obtaining sample solutions, the mathematical description and the computer simulation are general enough to allow refinements in rate constants and reaction orders.

Examples of the results, generated on a VAX computer with approximately 30 minutes of CPU time, are shown in figures 1-5. The lines represent linear interpolations between the theoretically predicted points in these figures. In run 2, the ratio of rate of reaction of oxygen with the polymer to the rate of its diffusion through the polymer is higher than in run 1.

The trends observed in the simplified numerical model are entirely consistent with the trends observed in practice. Although the material parameters in the numerical model have not been fitted with appropriate experimental values, a fitted numerical method of optimizing stabilization can be obtained from the present scheme to replace the trial and error method in current practice. The model requires precise information regarding the composition of the initial material and estimates of rate constants from experiments in inert and oxidizing environments.

The major problem of the overall mathematical model is that it relies too heavily on proposed, but not proven, stabilization reaction mechanisms. Until analytical methods are developed for quantitative analysis of all the stabilization reactions, there will always be doubt regarding the validity of the reaction mechanisms and, hence, the overall mathematical model. For this reason, and computer time consideration, a numerical simulation of the overall mathematical model is not recommended. The simplified numerical model is recommended in its place. Experimental studies on the local concentration of -CN and oxygen-bonded species as a function of temperature, copolymers and surroun-

ding environment are necessary to establish the material constants in the simplified model. With such information the model may be used to predict the responses with changes in material compositions and process parameters. The importance of this work lies in its potential predictive capabilities and in its fitting of the reaction constants and orders to the actual process of stabilization.

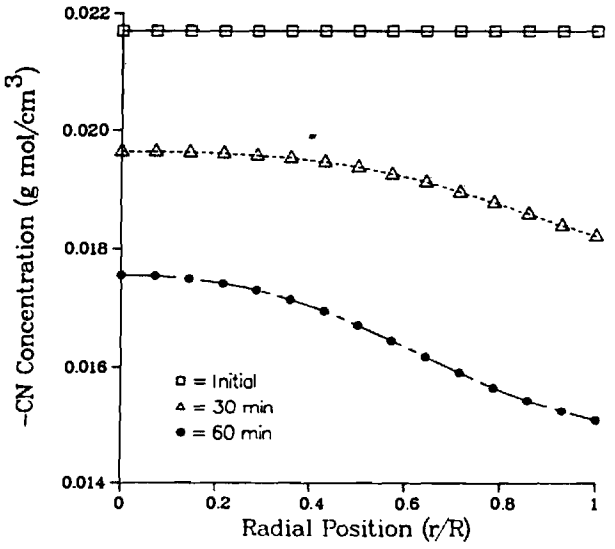

Figure 1. -CN Concentration profiles for Run 1.

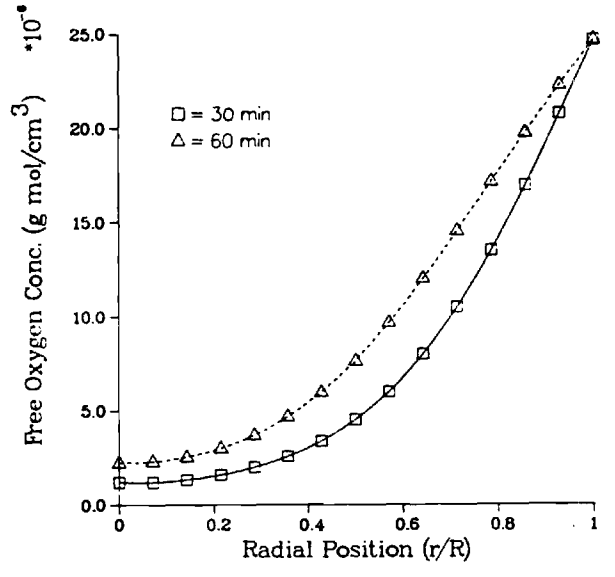

Figure 2. Free Oxygen Profiles for Run 1.

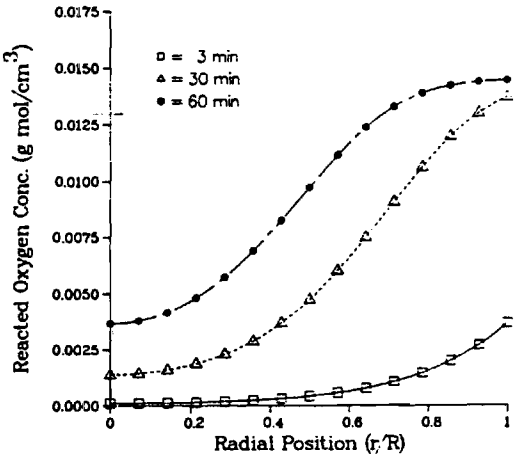

Figure 3. Reacted Oxygen Concentration Profiles for Run 1.

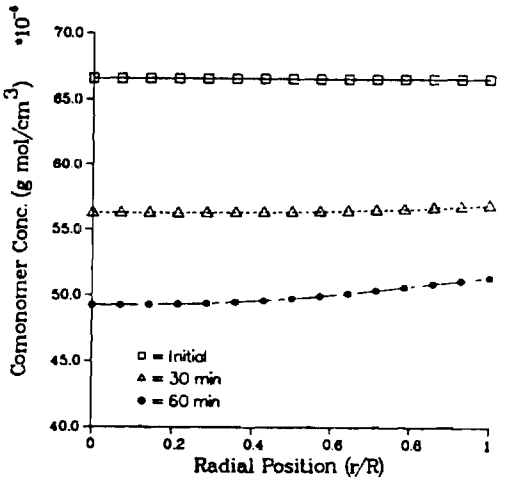

Figure 4. Comonomer Concentration Profiles for Run 1.

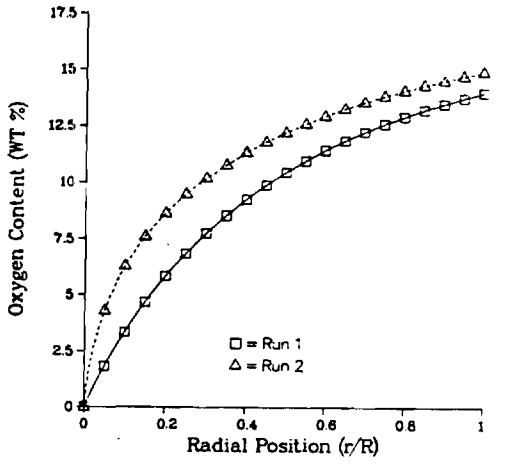

Figure 5. Comparison of Oxygen Content between Runs 1 and 2.

CONTINUOUS, MULTI-ZONE STABILIZATION IN A PAN-BASED CARBON FIBER PROCESS

G. Bhat, P. Desai and A. S. Abhiraman

GEORGIA INSTITUTE OF TECHNOLOGY
Atlanta, Georgia 30332

When acrylic precursor fibers are heated to the temperatures involved in the oxidative stabilization step of the process for carbon fiber formation, the physical changes that precede the onset of a significant level of reactions depend on the externally imposed constraints.[1] Whether dimensional constraints are imposed or not, a significant tendency for increase in perfection and in the extent of laterally ordered domains occurs in the early stages of this step, but these constraints have a pronounced effect on the relaxation of orientation in the laterally disordered fraction. The decrease in orientation in this phase is dramatic when no constraint against shrinkage is imposed on the fibers. A higher level of orientational order and mechanical properties could be retained with higher levels of tensile stress in stabilization. An example of this aspect can be seen in figure 1 which shows the progression of sonic modulus in isothermal batch stabilization of an acrylic precursor in air under three conditions (i) FL - free length, (ii) CL - constant length, and (iii) CT - at a constant tension of 0.1 g/denier.

The critical stress for failure and the stress generated at any level of imposed deformation (or, conversely, the deformation at any level of imposed stress) would change throughout the course of stabilization. Since the temperature-tension/deformation-time profile that can be applied during stabilization is limited by the continuously changing critical stress, it may be necessary to have the provision to control these through a multi-stage stabilization process, so that the influence of these factors on the carbon fibers can be established. The stabilization process may be separated into at least three independently controlled stages, viz., an initial zone of rapid morphological rearrangements, a second zone of reactions predominantly in the disordered fraction, and a third zone of reactions propagating into the ordered fraction of the fibers.

A multi-zone stabilization line also allows the use of different environments in the different zones. In order to realize the maximum potential of a given precursor fiber, it may be important to tailor the conditions (temperature, environment) of oxidative stabilization to optimize the rates of such reactions and the deformation characteristics during this stage.

A four-zone stabilization line, with computer control of stress/deformation in each zone, has been constructed to facilitate experimental investigations of multi-stress, multi-environment stabilization (figure 2). Results from exploratory experiments with two commercial precursors regarding the effects of environment and stress on the progression of chemical changes and orientational relaxation during this process, and on the properties of carbon fibers, will be presented.

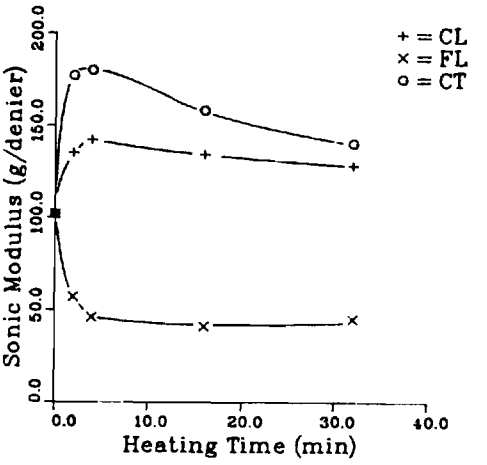

Figure 1. Progression of Sonic Modulus during Isothermal Stabilization at 265°C.

REFERENCES

1. M. K. Jain, M. Balasubramanian, P. Desai, A. S. Abhiraman, J. Mater. Sci., 22, 301-312 (1987).

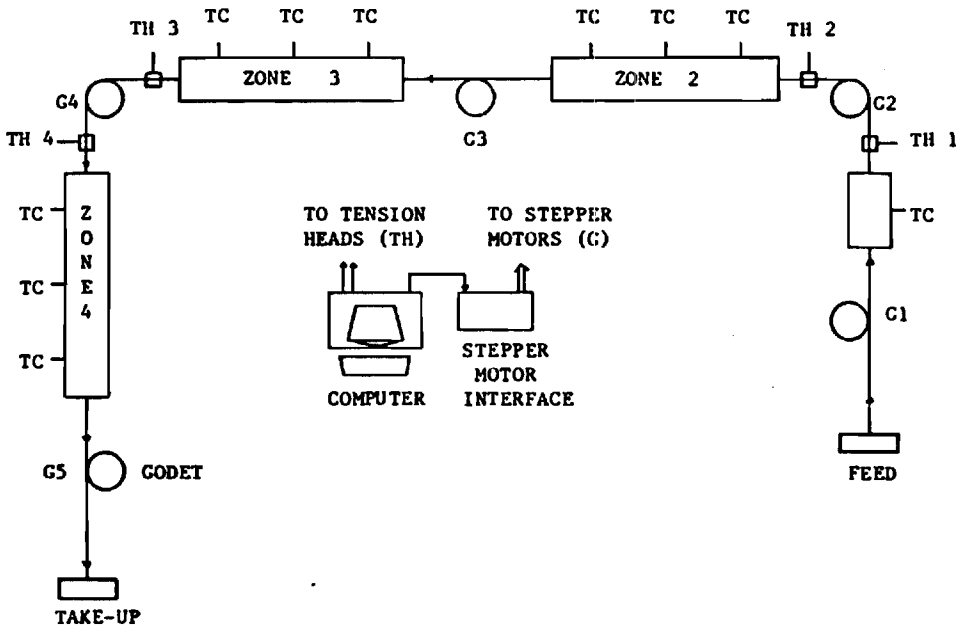

Figure 2. Schematic of Multi-Stage Stabilization line. TC - Temperature Controllers; TH - Tension Heads; G - Stepper Motor Driven Godets

Nineteenth Biennial Conference on Carbon

June 25–30, 1989

Extended Abstracts and Program

cosponsored by the
American Carbon Society

PENNSTATE

University Park
Campus

MULTI-ZONE DEFORMATION AND STABILIZATION OF ACRYLIC PRECURSORS FOR CARBON FIBERS

Gajanan S. Bhat, Vijay Daga and A. S. Abhiraman
Graduate Polymer Program, Georgia Institute of Technology
Atlanta, GA 30332

INTRODUCTION

We had observed in earlier studies (1-3) that when PAN-based precursor fibers are rapidly exposed to temperatures in the stabilization range, significant morphological rearrangements and changes in mechanical properties occur before the onset of reactions. The rearrangements showed a spontaneous tendency towards an increase in lateral order. It was also observed that the constraints imposed had a pronounced effect on the relaxation of orientation in the laterally disordered fraction, with a large decrease in orientation in this phase when no constraint against shrinkage was applied. Based on segmental mobility and the spontaneous tendency towards an increase in lateral order, a high temperature deformation process (4) was proposed to generate highly ordered precursors to yield carbon fibers of significantly superior mechanical properties.

In the present study, a multi-zone stabilization unit (5) has been used to determine if the high temperature drawing process can be coupled advantageously with stabilization in a continuous fashion. While deforming during stabilization in air, the combination of internally initiated reactions and those initiated by species arising from diffusion controlled incorporation of oxygen is expected to result in an inhomogeneous stress distribution across the fiber cross section. It is believed that the inhomogeneities may be reduced through stabilization in an inert environment to effect nitrile polymerization in the initial stages, followed by thermo-oxidative stabilization in air. In order to explore this aspect, high temperature deformation in an inert environment (nitrogen) has also been studied.

An experimental precursor with methyl acrylate and itaconic acid as comonomers, supplied by a commercial producer was used in this study and all the drawing and stabilization were carried out on the multi-zone stabilization unit. Stabilized fibers were carbonized using Lindberg furnaces. Change in morphology and mechanical properties of the fiber were studied by techniques such as, WAXD, plasticized DSC, microscopy, sonic modulus, and tensile testing.

RESULTS AND DISCUSSION

The fibers were drawn at a range of temperatures at speeds comparable to stabilization speeds (1 to 4 in/min). It was observed that the fibers could be drawn to a considerable extent both in air (Table 1) and in nitrogen (Table 2). The data in the tables is a comparison between the fibers that were drawn with those which went through the same thermal history under constant length. It is evident from the data that drawing results in increased orientation and improved mechanical properties of the fibers. The extent to which these fibers could be drawn depends on temperature. Higher draw ratios are possible with increasing temperature. However, because orientational relaxations also occur at higher rates with increase in temperature, the increase in maximum draw ratio at higher temperatures does not necessarily produce the best results in the drawn fibers. At higher temperatures, there is considerable change in color of the fibers indicating that stabilization reactions have taken place.

Table 1
High Temperature Drawing in Air (Stage I)

Temperature of Drawing (°C)	Draw Ratio	Sonic Modulus (cN/dTex)	Tenacity (cN/dTex)	f_c
220	1.00	177	3.5	.79
220	1.13	193	3.8	.83
240	1.00	146	2.7	.80
240	1.46	193	3.5	.79

Table 2
High Temperature Drawing in Nitrogen (Stage I)

Temperature of Drawing (°C)	Draw Ratio	Sonic Modulus (cN/dTex)	Tenacity (cN/dTex)	f_c
200	1.00	157	3.8	.83
200	1.11	210	4.0	.85
240	1.00	176	3.6	.86
240	1.25	191	4.1	.88

Fibers which gave best properties on deformation were selected and were drawn at a higher temperature in the second stage. As can be seen from Table 3, the fibers which were already stretched could be drawn again to a considerable extent. This drawing also shows a definite increase in the orientational order of the samples. However, the overall mechanical properties start deteriorating due to the change in structure of the fiber as the stabilization proceeds. Figure 1 shows the representative stress strain plots, where one can clearly see the improvement in strength and modulus of the fibers on drawing. As expected, stabilized fibers show poor mechanical properties.

Although the differences in properties of the stabilized fibers are not significant, final carbon fiber properties show distinctly the effect of drawing (Table4). Fibers drawn in air showed maximum improvement in strength, whereas fibers drawn in nitrogen showed very little or no improvement in strength. Our original hypothesis that a more homogeneous (and thus benefecial) structure would result from drawing in nitrogen is not supported by this data. Microscopic examination of the carbon fibers revealed that very highly drawn precursors had surface cracks compared to those drawn to a lower extent which had smooth surface.

From this study it becomes evident that one can combine deformation with stabilization and drawing at early stages leads to improved carbon fiber properties. Although the fibers can be drawn to higher extents at higher temperatures, excess drawing can lead to surface defects, in turn reducing the strength of the fibers inspite of increase in modulus due to the higher orientation achieved by drawing.

ACKNOWLEDGEMENTS

The authors express their appreciation to Dr. Prashant Desai for his help during all stages of this work. Financial support by the United States Office of Naval Research is greatly acknowledged.

REFERENCES

1 M. K. Jain, Ph.D. Thesis, Georgia Institute of Technology, USA (1984)
2 M. K. Jain, P. Desai and A. S. Abhiraman, 16th Biennial Conf. on Carbon, 517 (1983)
3 M. K. Jain, M. Balasubramanian, P. Desai ans A. S. Abhiraman, 17th Biennial Conf. on Carbon, 312 (1985)
4 S. K. Bhattacharya, G. Bhat, V. Daga and A. S. Abhiraman, 18th Biennial Conf. on Carbon, 13 (1987)
5 G. Bhat, P. Desai and A. S. Abhiraman, Ibid, 217 (1987)

Table 3
High Temperature Drawing in air (Stage II)
(previously drawn at 210°C)

Temperature of Drawing (°C)	Draw Ratio	Sonic Modulus (cN/dTex)	Tenacity (cN/dTex)
230	1.00	169	3.1
230	1.18	194	3.4
250	1.00	142	2.3
250	1.44	191	2.9

Table 4.
Properties of Carbon Fibers
(carbonized at 1525° C at 1°/min)

Sample	Tenacity (cN/dTex)	Initial Mod. (cN/dTex)	Sonic Mod. (cN/dTex)
Control (D. R. =1.0)	12.0	1250	1356
Drawn in Air*	21.1	2043	1495
Drawn in N_2#	12.1	1685	1897

* - 220° C - 1.13 and 250° C -1.44
\# - 200° C - 1.11 and 260° C -1.33

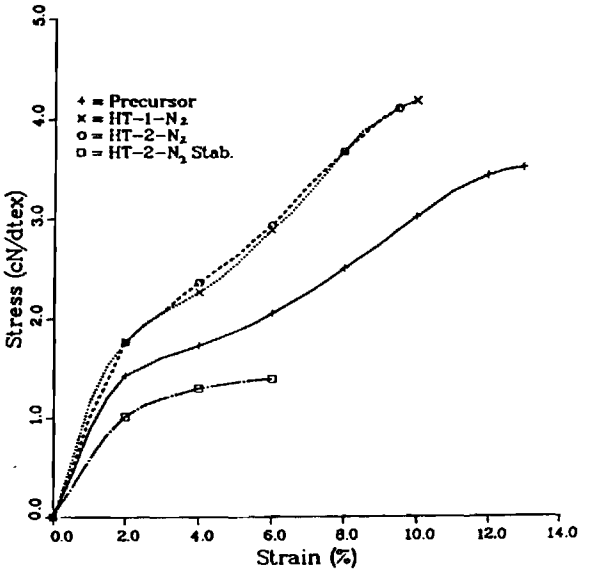

Fig.1 Typical Stress-Strain curves for (a) precursor, (b) drawn in nitrogen 1st stage, (c) drawn in nitrogen 2nd stage and (d) stabilized fibers.

2nd TOPICAL CONFERENCE ON EMERGING TECHNOLOGIES IN MATERIALS

San Francisco, California November 6-9, 1989

BIOMATERIALS • CERAMICS • COMPOSITES • ELECTRONICS MATERIALS • POLYMERS

Program and ABSTRACTS OF PAPERS

CO-SPONSORING SOCIETIES

The American Ceramic Society, Inc.
American Chemical Society
- Division of Polymer Chemistry
- Division of Polymeric Materials: Science and Engineering

American Physical Society
American Society for Testing and Materials
American Society of Composites
The Federation of Materials Societies
National Association of Corrosion Engineers
Society of Plastics Engineers
- Composites Division
- Engineering Properties and Structure Division
- Plastics Analysis Division

Conference Chairmen

John L. Kardos
Materials Research Laboratory
Washington University
St. Louis, MO 63130

Lee L. Blyler, Jr.
AT&T Bell Laboratories
Murray Hill, NJ 07974

NEW ASPECTS IN THE CONVERSION OF ACRYLIC PRECURSORS TO HIGH PERFORMANCE CARBON FIBERS

G. S. Bhat, S. Damodaran, P. Desai, L. H. Peebles, Jr.* and A. S. Abhiraman
Polymer Education and Research Center, Georgia Tech, Atlanta, GA 30332

Manufacture of carbon fibers from acrylonitrile-(AN)-based copolymers consists of precursor fiber formation followed by thermo-oxidative stabilization and carbonization. Creating high order in the precursor fiber, maximizing its transfer through the stabilization stage and optimizing the evolution of structure in carbonization are crucial to the development of wide mechanical performance in carbon fibers. We present here the results pertaining to these aspects from a comprehensive study of the evolution of structure and properties from PAN-based precursors to carbon fibers.

1. **HIGH TEMPERATURE DEFORMATION OF PRECURSOR FIBERS:** We had reported earlier that acrylic precursor fibers of high orientational and lateral order could be obtained through drawing at high temperatures, near the range used for stabilization [1]. These deformation studies are carried out in air. It is well known that diffusion and reaction of oxygen under these conditions could create a heterogeneous sheath-core structure. We have conducted a study of high temperature deformation in an "inert" (nitrogen) environment to explore the possible advantages of maintaining a relatively more homogeneous reaction environment in the fiber cross section during this process. The results from drawing, stabilization and carbonization reveal, however, that a higher extent of drawing and, consequently, higher mechanical properties are obtained through drawing in air than in nitrogen (see Table 1). Possible reasons for this will be discussed at the conference.

2. **OXIDATIVE STABILIZATION ENVIRONMENT:** Stabilization is necessary to convert the precursor polymer to an infusible structure suitable for producing a densified structure in carbonization. Use of inert environments in the early stages of this process has been suggested to yield a more homogeneous structure [2]. Peebles et al., observed that the exotherm in thermal analysis, which is believed to arise from cyclization reaction disappears faster in the presence of ammonia [3].

Table 1

Properties of Fibers carbonized at 1525°C after drawing in two stages (in air or nitrogen) and stabilizing in air

Sample	Drawing Temp. °C	Total Draw Ratio	Tenacity cN/dtex	Initial Modulus cN/dtex
Control	210 & 220	1.00	12.0	1250
**Drawn in Air	210 & 250	1.63	21.1	2043
**Drawn in N_2	210 & 260	1.51	10.9	1478

** - the conditions shown correspond to maximum extents of drawing

* Office of Naval Research, Arlington, VA 22217

Besides the advantages of faster rates of stabilization, any reduction in the temperature of stabilization by incorporating ammonia in the stabilization environment would also reduce orientational relaxations at this stage. Our studies in this regard have yielded the following results.

(i) Stabilized structure is achieved in shorter times in the presence of air and ammonia

(ii) In the absence of oxygen, ammonia does not lead to complete stabilization

(iii) Stabilization can be achieved at relatively low temperatures in the presence of ammonia

(iv) About 5 to 10 per cent ammonia in air leads to significant acceleration of stabilization

(v) Effect of ammonia is suppressed if acid comonomers are present in the precursor.

3. **EVOLUTION OF STRUCTURE IN CARBONIZATION:** Knowledge of the continuous evolution of structure and properties in carbonization can be useful in engineering the process to yield the desired combination of properties. Filaments which have been removed from a steady state carbonization process are being analyzed to determine the progression of changes in composition, morphology and mechanical properties in tension as well as compression. Results of this study will be presented at the conference.

Acknowledgements: The study presented here has been supported by the Office of Naval Research and the Air Force Office of Scientific Research.

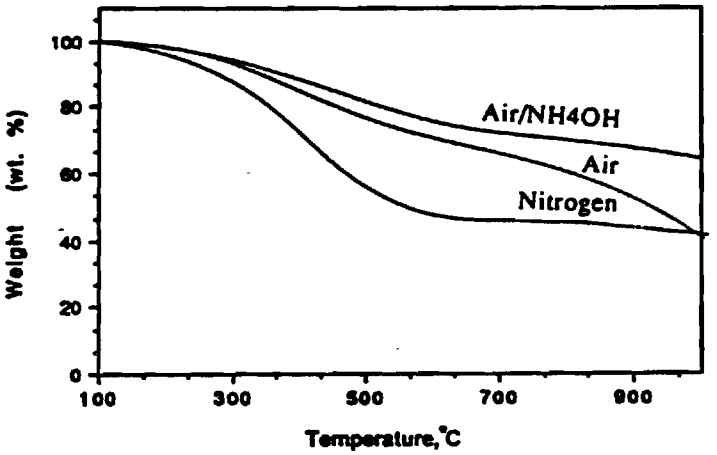

Figure 1. Thermogravimetric Analysis of samples stabilized at 260°C for 32 minutes in different environments

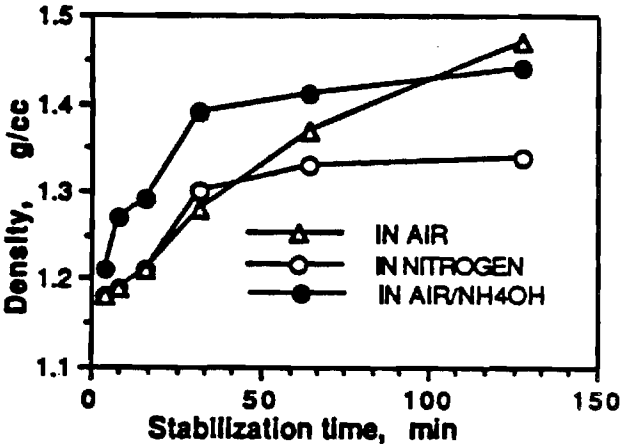

Figure 2. Density change during stabilization at 260°C in different environments

REFERENCES

1 S. K. Bhattacharya, G. Bhat, P. Desai and A. S. Abhiraman, 18th Biennial Conference on Carbon, 13 (1987)

2 J. P. Riggs, U. S. Patent 3 961 888 (1976)

3 L. H. Peebles et al., to be published